Chiral four dimensional field theory from superstring and higher dimensional super Yang-Mills theory

Hiroshi Ohki*

Department of Physics, Kyoto University, Kyoto 606-8502, Japan

*email: ohki@scphys.kyoto-u.ac.jp

Abstract

We study four dimensional field theory from higher dimensional super Yang-Mills theory based on the low-energy effective theory of Type I, II or heterotic string theories. Chiral fermions in four dimensions are obtained by several mechanisms. Especially, the background flux is one of the most interesting mechanisms for obtaining four dimensional chiral theories. Compactified extra dimensions with magnetic flux cause the gauge symmetry breaking and non-trivial boundary conditions for charged fields. Chiral matter fields have localized wavefunctions on extra dimensions. We discuss about the relations between background flux and low-energy spectra which are counted by their zero-mode. We also study the low-energy constants and these moduli dependence. They are calculated by usual dimensional reductions of super Yang-Mills theory or supergravity theory. Yukawa couplings are free parameters in the standard model and may be related to the underlying physics. In the string theory or its low-energy limit, they are determined by overlap integral of wavefunctions on extra dimensions. We specify the simple compactifications, i.e. torus and compute the overlap integral of three wavefunctions which correspond to Yukawa interactions. We also study the higher order couplings based on the field theoretical approach. From the analysis of generic n-point couplings, we can discuss about flavor structures. We find that in such a construction some discrete flavor symmetries appear in the four dimensional effective theory. Their phenomenological implications are discussed. Furthermore we extend these constructions to orbifold background. Magnetic flux still plays an important role in this background and leads to various types of low-energy spectra different from that of toroidal compactifications. The orbifold models with heterotic string are also investigated. There are some discrete symmetries on orbifolds which reflect certain geometrical symmetries of internal spaces. We use path integral methods to derive the anomaly in discrete symmetries and show the anomaly coefficients for mixed gauge or gravitational anomaly in heterotic orbifold models and higher dimensional field theory. We apply these mechanisms to realize the semi realistic model and study phenomenological implications of these models.

Contents

1 Introduction 6

2 Super Yang-Mills theory on higher dimensions 12

2.1 Toroidal wavefunctions . . . 13

2.1.1 $U(1)$ gauge theory on magnetized torus T^2 . . . 13

2.1.2 $U(N)$ gauge theory on magnetized torus T^2 . . . 15

2.1.3 $U(N)$ gauge theory on $(T^2)^3$ . . . 16

2.2 General flux and non-abelian Wilson line . . . 19

2.2.1 Matter fields . . . 21

2.2.2 $n_a = n_b$ . . . 22

2.2.3 $n_a \neq n_b$ . . . 23

2.2.4 Continuous Wilson line . . . 25

2.3 Pati-Salam model . . . 28

2.4 Exceptional gauge groups . . . 30

2.4.1 E_6 model . . . 31

2.4.2 E_7 and E_8 models . . . 33

3 Calculation of Yukawa interaction and higher order couplings 36

3.1 Low-energy effective action . . . 36

3.2 General setup . . . 37

3.3 Three-point coupling . . . 39

3.4 Higher order coupling . . . 41

3.4.1 Four-point coupling . . . 41

3.4.2 Generic L-point coupling . . . 44

3.5 Intersecting D-brane models . . . 48

3.6 Flavor symmetries . . . 51

3.7 Non-Abelian Wilson line . . . 53

3.8 Comments on soft supersymmetry breaking terms and moduli stabilization 56

4 Non-Abelian flavor symmetries 59

4.1 Generic case . . . 59

4.1.1 $g = 2$ case . . . 60

4.1.2 $g = 3$ case . . . 61

4.2 Cases without Continuous Wilson lines . . . 63

4.2.1 $g = 2$ case . . . 63

4.2.2 $g = 3$ case . . . 64

4.3 Cases with non-Abelian Wilson lines . . . 66

4.3.1 The case with $M_i \neq 1$ and $k_i = 1$ . . . 66

4.3.2 The case with $M_i = 1$ and $k \neq 1$ . . . 68

4.3.3 Illustrating examples . . . 69

4.4 Phenomenological model construction . . . 72

5 Magnetized orbifold models **78**
5.1 $U(1)$ gauge theory on magnetized orbifold T^2/Z_2 78
5.2 $U(N)$ gauge theory on magnetized orbifold T^2/Z_2 79
5.3 $U(N)$ gauge theory on magnetized orbifolds T^6/Z_2 and $T^6/(Z_2 \times Z_2')$ . . . 80
5.3.1 Discrete flavor symmetry for orbifold models 82
5.4 Three generation magnetized orbifold models 85
5.4.1 Yukawa couplings in three generation models 89
5.4.2 An illustrating example: 7-7-14 model 91
5.4.3 Numerical examples in 7-7-14 model 92
5.5 Orbifold background with non-Abelian Wilson line 94
5.6 Further direction to orbifold 95

6 Anomalies for field theory and string theory **102**
6.1 General formula for anomalies 102
6.2 Discrete flavor symmetry anomalies 104
6.3 Other anomalies in string models 108
6.3.1 Discrete R-symmetries 110
6.3.2 Discrete R-anomalies 112
6.3.3 Relation with beta-function 114
6.3.4 Relation with T-duality anomaly 115
6.3.5 Symmetry breaking of the discrete R-symmetries 117
6.3.6 Constraints on low-energy beta-functions 119

7 Conclusion **121**

A Dimensional reduction and the low-energy effective action **123**

B Models **126**

C Possible patterns of Yukawa matrices **127**
C.1 (Even-Even-Even) wavefunctions 128
C.1.1 4-4-8 model 128
C.1.2 4-5-9 model 128
C.1.3 4-5-1 model 129
C.1.4 5-5-10 model 130
C.2 (Even-Odd-Odd) wavefunctions 130
C.2.1 4-7-11 model 131
C.2.2 4-7-3 model 131
C.2.3 4-8-12 model 132
C.2.4 4-8-4 model 133
C.2.5 5-7-12 model 133
C.2.6 5-8-13 model 134
C.2.7 5-8-3 model 135
C.3 (Odd-Odd-Even) wavefunctions 136

C.3.1 7-7-14 model 136
C.3.2 7-8-15 model 136
C.3.3 7-8-1 model 137
C.3.4 8-8-16 model 138

D Non-Abelian discrete symmetries **139**
D.1 D_4 139
D.2 $\Delta(27)$ 140
D.3 $\Delta(54)$ 142

1 Introduction

The theoretical particle physics has succeeded in explaining the physics of the elementary particles based on the quantum mechanism and its extension to the relativistic field theory. It reached to the so-called standard model (SM) of particle physics, which contains the $SU(3)\times SU(2)\times U(1)$ gauge groups coupled to fundamental particles i.e. three generations of the quarks, leptons and Higgs scalar. Although the SM can explain a lot of independent high energy experimental data, it may not be accepted as the fundamental physics of the world. This is because there are many free parameters which we only fix posteriorly by the experiments, that is, the matter fields with three replica and the masses of the matters in each of generations and mixing in the quark and lepton sectors. That is the so-called flavor problem. Indeed, most of free parameters in the SM are originated from the flavor sector, that is, Yukawa couplings. In addition, the reason why the strong interactions do not break CP but weak interactions do is not explained. These issues are accomplished by one specific choice of the infinite classes of possible quantum filed theory of the SM. Beyond these issues, there are more intrinsic problems in the SM. We refer to the naturalness problems of Higgs scalar and quantum field theory of the gravity. The former problem is related to the quantum corrections to the Higgs scalar mass and may be solved by introducing the supersymmetry. The supersymmetric quantum field theory may become the extention of the SM. In its minimal extension (MSSM), it has a superpartner for each of elementary particles with different spin-statistics. The corresponding scalar partners of quarks and leptons are squarks and sleptons and the Higgs scalar also has the partner i.e. Higgisino and gauge boson has its fermionic partner as a gaugino. However the latter issue still remains.

The Superstring theory successfully unifies the concepts of quantum field theory and general relativity. This is the most promising approach to overcome these issues. In order to claim that it incorporates a unification of all forces observed in nature, one has to prove the existence of string models reproducing SM particle physics. The best way to prove its existence consists in the construction of explicit models since that allows also to investigate phenomenological implications of string theory.

Perhaps the most traditional, attempt of identifying realistic string models is given by heterotic orbifold constructions [1, 2]. In more recent years, this line of research was boosted by the observation that phenomenological properties can be connected to geometrical properties of the orbifold [3, 4, 5, 6, 7, 8, 9]. Examples for quantities which are directly tied to geometry are the Kähler potential for twisted sector states as well as Yukawa couplings [10, 11, 12, 13]. (For interesting applications see e.g. Ref. [14].) The Calabi-Yau compactifications are also interesting as compactified six dimensional spaces preserving $\mathcal{N}=1$ supersymmetry. The background metric is non-trivial and there are many kinds of six dimensional Calabi-Yau manifolds. The concrete models for heterotic orbifold can be regarded as the singular limit of the smooth Calabi-Yau compactifiactions. In a parallel development, semi realistic models have been obtained in the free fermionic formulation of heterotic strings [15, 16]. Although there are some indications [17] that these models are related to $\mathbb{Z}_2\times\mathbb{Z}_2$ orbifolds a precise connection has not been worked

out in general. Hence a geometric picture is missing for many free fermionic models.

The possibilities of the model building from type II string theory have been enriched by the discovory of the D-branes [18]. The open strings have their end points on certain D-branes. Their lowest modes give rise to massless gauge fields and their fermionic partners. Then n-stack of the D-branes have naturally n^2 number of massless gauge bosons and they have $U(n)$ gauge symmetry in low-energy. It is shown that these D-brane backgrounds give rise to realistic string compatifications. The first attempt to obtain the chiral matter fields is considered by two D-branes which are intersected each others. The chiral matter fields can appear in their localized intersecting points as bi-fundamental gauge representaions. The number of zero-modes i.e. the generation number is given by the intersection number in internal spaces. This model contruction has an advantage that the geometrical interpretation is easy as well as heterotic orbifold models. The specific examples for this type of models are discussed in type IIA string models with D6-branes [19, 20, 21, 22, 23, 24, 25].

Their T-dual models i.e. magnetized D-brane models also have been investigated. In the language of T-duality, the intersecting angle of two D-branes in the type IIA side is interpreted as the magnetic flux inside two internal spaces in the type IIB picture. There is no localized mode in the internal spaces and their low-energy effective theory can be discrebed higher dimensional super Yang-Mills theory with magnetic flux. The background magnetic fluxes cause a breaking of gauge groups and chiral matter fields can be obtained by solving the zero-mode solutions. From the T-dual of T^6 toroidal compactification of intersecting D6-brane models, corresponding chiral matter fields are calculated explicitly from a simple factorizable $T^2 \times T^2 \times T^2$ toroidal compactifications with constant magnetic flux. The resulting solutions are represented by the products of Jacobi theta functions. The bosonic mode, for example Higgs scalar or scalar partners, are also calculated by solving Laplace operator with flux background. These results can be applied for lower dimensions $D = 6, 8$ and lead to various types of models.

Concerning about the flavor problems explained above, one has to know Yukawa couplings. In the string theory computation, Yukawa couplings are calculated by string amplitude of corresponding three vertex operators by using CFT technique. Taking into accout the classical contributions of the amplitude, Yukawa couplings are represented by a sum over worldsheet instanton effects. The magnitude of the Yukawa couplings is affected by the localization points for three matter fields. When their localization points are far away each other, the exponetially surppressed Yukawa couplings are obtained. Thus Yukawa couplings are geometrically determined. On the other hand, in the T-dual picture, the calculations of the Yukawa couplings are purely field theoretical. Yukawa interactions can be calculated by overlap integrals over internal spaces with three wavefunctions as the following forms

$$Y = \int dy^6 \psi_i(y)\psi_j(y)\phi(y) \tag{1}$$

where $\psi_{i,j}(y)$ correspond to the internal wavefunctions of chiral matter fields and $\phi(y)$ is the internal wavefunctions of Higgs scalar fields. The explicit calculations of the overlap

integrals can tell us the form of the Yukawa couplings. It is found that two different approaches of stringy and field theory calculations lead to the consistent results of the Yukawa couplings after proper transformation of moduli parameters [52]. Furthermore the method using the field theoretical approach can tell us the other constants like the normalization constants or higher order couplings. For example, the former contribution is related to the Kahler moduli. In order to obtain those in the intersecting D-brane side, it needs quantum effects of stringy correlators. These results are also consistent each other up to higher order corrections to the normalization factors.

A rather bottom-up approach to understand the realistic quark/lepton mass hierarchy and mixing angles is the flavor symmetry. Symmetries play an important role in particle physics. As long time ago it was suggested that the $U(1)$ symmetries can be applied to obtain the hierarchical quark mass structure as called by Froggatt-Nielsen mechanism [27]. More recently non-abelian discrete symmetries are investigated to address the above flavor issue in particular in explanation of the large mixing of lepton flavor. It is plausible that such non-abelian discrete flavor symmetries are originated from extra dimensional theories, because non-abelian symmetries are symmetries of geometrical solids. Indeed, it has been shown that certain types of non-abelian discrete flavor symmetries such as D_4 and $\Delta(54)$ can appear in four-dimensional effective field theories derived from heterotic string theory with orbifold background [6, 28]. (See also [29].) In those analyses, the important ingredients to derive the non-abelian discrete flavor symmetry are geometrical symmetries of the compact space and stringy coupling selection rules. To investigate the flavor symmetry, it is important to investigate the higher order couplings. In the field theoretical approach, the higher order couplings are also calculable in principle. For toroidal compactification T^2 case, the generic n-point couplings are also represented analytically and have same properties as CFT calculations. The main ingredient is stressed that the generic n-point couplings are given by the products of three point couplings. Then one can analyze the flavor symmetries and find that there are several types of discrete flavor symmetries in the model with magnetized/intersecting D-brane models and a certain relation between the number of generations and the flavor symmetries. Although in the normalization factor there is a small discrepancy in the stringy and field theoretical calculations, this does not affect in the structures of the flavor since it is only determined by the number of generations i.e. the index number. Therefore it would be helpful to understand the flavor symmetries for considering the flavor problems.

Recently the wavefunction profiles have been studied in some of non-trivial background geometry, e.g. orbifold compactifications, $P^1 \times P^1$, P^2 geometry [30], warped compactifications [31] and flux compactifications [32] in which it is succeeded to obtain the explicit solutions of wavefunctions. Such string constructions are classified to two classes of global and local models. As mentioned above, the ten-dimensional compactification is naturally corresponding to the low-energy limit of the heterotic and type I string theory. From the view point of the field theory, one may consider less than ten dimensional field theory with gauge interactions. Global models are defined in the total compact space with certain choice of topological features. The simplest example is the heterotic string theory with Calabi-Yau compactifications. On the other hand, local models can be considered

localized modes living in a part of extra dimensions. The gauge and matter fields depend on the local internal spaces and do not depend on the details of other bulk topological features. Thus there are attractive features of local model construction which drastically simplify the structures of the geometry and it is easier to calculate the low-energy physics than that of global models. Indeed in the general Calabi-Yau compactifications, explicit metric of such a global compact space is not known. For example we can consider the possibility of the singular point in the six dimensional compact space with orbifold and then such a metric can be represented as $T^{2n} \times \mathcal{C}^{3-n}/\mathbf{Z}_N$. One may put the N stack of D($3+2n$)-brane wrapping the T^{2n} on the singular point of $\mathbf{Z}$ orbifold. Thus the low-energy effective theory is described by $\mathcal{N}=1$ $D=4+2n$ super Yang-Mills theory with proper gauge groups. In both cases, one can apply the formula of the overlap integrals and the method of Kluza-Klein decomposition. Thus the field theoretical approach is powerful method to calculate the low-energy constant including proper stringy effects and moduli fields dependence, which allow to construct the phenomenologically interesting models. In addition, these constructions are also related to the phenomenological model building within the extra dimensions. Suppose that the chiral matter fields have Gaussian profiles in the extra dimensions and each of generations is localized in different way, the hierarchical structures of the masses for generations may be obtained. Therefore one sees that D-brane model constructions give some of concrete examples for these phenomenological models. We then study these features of extra dimensional field theory for the case of exceptional gauge groups e.g.E_6, E_7 or E_8 which are regarded as phenomenological model buildings.

In recent years a renewal of the local model building has been developing, for instance, F-theory model buildings [33, 34]. In F-theory models, it naturally includes exceptional gauge groups beyond the type IIB D-brane. The flavor structures are different from that of D-branes models, there are a lot of development for phenomenological studies.

For the selection of the vacua, one should study the potential of the moduli field and supersymmetric four dimensional vacua. In the string theory, there are many fields beyond the SM particle. Some of them are called as moduli fields and their vacuum expectation values correspond to the size or shape of the compactification spaces and positions of D-brane and so on. These values are also related to the parameters like gauge coupling constant or masses for four dimensional fields. In the general Calabi-Yau compactifications, these moduli are not determined by means of minimalizing the potential of moduli. To solve this problem, several mechanisms have been proposed [35, 36]. In the string theory, they contain the anti-symmetric tensor fields as C_p. Their field strengths are also appearing as $F_{p+1} = dC_p$ and have non-vanishing background expectation values so called three form flux. This flux affects in the low-energy potential in the moduli sectors. Thus some of these moduli fields are stabilized in a flux compactification. Furthermore in type IIB theory, Kahler moduli T are stabilized by non-perturbative effects such as gaugino condensation. In the supergravity potential, this minimum is supersymmetric and anti-de Sitter vacuum. The anti-D3 brane is introduced in order to uplift the vacuum energy and realize the de Sitter or Minkowski vacuum. This shifts the position of the potential minimum and breaks the supersymmetry in a controllable way. This is so called

KKLT scenario [37]. In addition, a new calculable method of moduli stabilization was proposed, using the internal magnetic fields. This method can be used in simple toroidal compactifications, stabilizing the geometric moduli in a supersymmetric vacuum that is within a perturbative string description. Once if we have a mechanism to break low-energy supersymmetry, the relevant soft supersymmetry breaking terms are also related to the magnetic flux. Thus these approaches using the magnetic flux or KKLT scenario can obtain the moduli parameters in a certain level so that we can analyze the low-energy spectrum including the super particle.

Discrete symmetries play an important role in model building of particle physics. For example, abelian and non-abelian discrete flavor symmetries are useful to derive realistic quark/lepton masses and their mixing [38]. Discrete non-abelian flavor symmetries can also be used to suppress flavor changing neutral current processes in supersymmetric models [39, 40]. Furthermore, discrete symmetries can be introduced to forbid unfavorable couplings such as those leading to fast proton decay [41, 42]. It is widely assumed that superstring theory leads to anomaly-free effective theories. In fact the anomalous $U(1)$ symmetries are restored by the Green-Schwarz (GS) mechanism [43, 44, 45]. For this mechanism to work, the mixed anomalies between the anomalous $U(1)$ and other continuous gauge symmetries have to satisfy a certain set of conditions, the GS conditions, at the field theory level. In particular, in heterotic string theory the mixed anomalies between the anomalous $U(1)$ symmetries and other continuous gauge symmetries must be universal for different gauge groups up to their Kac-Moody levels [46, 47]. A well-known discrete symmetry in heterotic string theory is T-duality symmetry, and its effective theory has T-duality anomalies [48]. It has been shown that the mixed anomalies between T-duality symmetry and continuous gauge symmetries are universal except for the sector containing an $N = 2$ subsector and are exactly canceled by the GS mechanism [49]. That has phenomenologically interesting consequences which have been studied in early 90's [49, 50, 51].

For the above purposes, in this thesis, we study the phenomenological aspects of the higher dimensional super Yang-Mills theory with various dimensions as the best motivated theory for effective field theory of string theory and study the low-energy physics related to the extension of the SM. The contents of this thesis are as follows. In section 2 we first study the higher dimensional $U(N)$ super Yang-Mills theory on the torus background with magnetic fluxes using the usual Kluza-Klein dimensional reductions for obtaining the chiral matter fields. We also solve the wavefunctions explicitly in the toroidal compactifications with and without toron configurations of twisted boundary conditions [52, 53, 54]. We see the mechanism for obtaining the chiral fermion and the number of generations. Furthermore we extend this analysis to the exceptional gauge groups in a similar way [55]. In section 3 we consider about calculation of the three point couplings which can appear in the off-diagonal components for different three gauge groups [52]. These analysis can extend to the generic n-point couplings in which we see the structures of the n-point couplings are related to the product of three point couplings [56]. We also discuss about the T-dual picture, i.e. results from intersecting D-brane model.

In section 4 we analyze the flavor structures based on the field theoretical approach.

Then we show that the discrete flavor symmetries can appear in these types of models [57], which are phenomenologically interesting for the realistic patterns of the lepton mixings. The corresponding representations for each generation are classified. The role of the Wilson line parameters in flavor symmetry are shown and its phenomenological implications with symmetry breaking are also discussed.

In section 5 we study the orbifold compactifications with magnetic background [58, 59]. We will see that a possible orbifold projection on T^2 is restricted only Z_2 orbifold. Therefore the remaining matter field after orbifold projections are consist of either even or odd wave functions. They are obtained from linear combination of the wavefunctions on the torus. The zero-mode spectra are different from that of toroidal compactifications. We classify the phenomenologically interesting models with three generations of chiral matters and analyze the Yukawa couplings. We also discuss the phenomenological model building with magnetized extra-dimensions.

The question is whether discrete anomalous symmetries can appear in string-derived models. The discrete symmetries on orbifolds reflect certain geometrical symmetries of internal space. Since the geometrical operations are embedded into the gauge group, one might suspect that the discrete anomalies are related to gauge anomalies. In section 6 we use path integral methods to derive the anomaly of discrete symmetries including non-Abelian discrete symmetries and show the anomaly coefficient for mixed gauge or gravitational anomaly. We also briefly review the discrete anomalies focusing on the discrete flavor symmetries appearing in heterotic orbifold models and higher dimensional field theory. Next, we define discrete R-charges, which is defined in heterotic orbifold models and calculate the mixed anomalies between the discrete R-symmetries and the continuous gauge symmetries in concrete models. We also study the relations of R-anomalies with one-loop beta-function coefficients and T-duality anomalies. Phenomenological implications of our results are also discussed.

Finally section 7 is devoted to conclusion and discussion. In order to obtain the low-energy Lagrangian, we specify the functions of Kahler potential and super potential. In appendix A we perform the Kaluza-Klein reductions of ten dimensional super Yang-Mills theory and give a procedure for obtaining the scalar component of the chiral matter field and calculation of the Kahler potential. For toroidal compactifications the moduli dependence for Yukawa and Kahler potential is obtained. In appendix B, C, we classify the orbifold models with three generation and show the results of Yukawa couplings. In appendix D, we give a short introduction of the properties of discrete symmetries used in the thesis.

2 Super Yang-Mills theory on higher dimensions

Understanding the structure of the SM is one of the fundamental problems of theoretical particle physics. In particular, one of most outstanding puzzles of the SM of particle physics is the structure of the Yukawa couplings between the Higgs field and the SM fermions. A correct description of the observed masses and mixing of quarks and leptons seems to require very different values for the Yukawa coupling constants for the different generations.

In recent years the idea that there could be more than four dimensions has been pursued intensively, particularly due to the study of string theory which is naturally defined in 10 or 11 dimensions. In fact extra dimensional field theories, in particular string-derived extra dimensional field theories, play an important role in particle physics as well as cosmology. There is a possibility of computing the Yukawa coupling in terms of the extra-dimensional geography. Starting from d+4 dimensional compactified theory one may obtain the massless modes with factorized wavefunctions. Gauge bosons in the extra dimensional component become scalars at low-energy and its fermionic component may give rise to the matters. Yukawa couplings can appear from the higher dimensional gauge interactions $A_i\bar{\Psi}\Gamma_i\Psi$. Yukawa coupling constant is calculated in principle from the overlap integrals over extra dimensions. Our aim is to study such theories of potential phenomenological interest. We consider our starting point ten dimensional super Yang-Mills theory since it appears in the low-energy limit of the Type I, IIB and heterotic string theories.

However when we start with extra dimensional theories, how to realize chiral theory is one of important issues from the viewpoint of particle physics. Introducing magnetic fluxes in extra dimensions is one way to realize chiral fermions in field theories and superstring theories [60, 61, 52, 62]. In particular, magnetized D-brane models are T-duals of intersecting D-brane models and several interesting models have been constructed within the framework of intersecting D-brane models [19, 20, 21, 23, 24, 25].[1]

In this section we introduce the $\mathcal{N}=1$ supersymmetric Yang-Mills theory with various dimensions. We use the Kluza-Klein dimensional reductions for obtaining the internal wavefunctions. The internal wavefunctions are chosen to be eigenstates of the internal Laplace and Dirac operators. We show that the chiral fermion can be obtain from the non-trivial solutions of wavefunctions due to the internal background flux. The low-energy physics is described by those of zero-mode wavefunctions. Zero-modes are quasi-localized on the torus with the magnetic flux. The number of zero-modes, which corresponds to the generation number, is determined by the value of the magnetic flux in the same way as that the generation number is determined by the intersecting number in intersecting D-brane models. Furthermore we extend this analysis to other backgrounds and other gauge groups. In such a case, we also obtain the explicit wavefunctions and calculate the spectra within a field theoretical way.

[1] See for a review [22] and references therein.

2.1 Toroidal wavefunctions

Let us consider $N = 1$ super Yang-Mills theory in $D = 4+2n$ dimensions. Its Lagrangian density is given by

$$\mathcal{L} = -\frac{1}{4g^2}\mathrm{Tr}\left(F^{MN}F_{MN}\right) + \frac{i}{2g^2}\mathrm{Tr}\left(\bar{\lambda}\Gamma^M D_M\lambda\right), \tag{2}$$

where $M, N = 0, \cdots, (D-1)$. Here, λ denotes gaugino fields, Γ^M is the gamma matrix for D dimensions and the covariant derivative D_M is given as

$$D_M\lambda = \partial_M\lambda - i[A_M, \lambda], \tag{3}$$

where A_M is the vector field. Furthermore, the field strength F_{MN} is given by

$$F_{MN} = \partial_M A_N - \partial_N A_M - i[A_M, A_N]. \tag{4}$$

We consider the torus $(T^2)^n$ as the extra dimensional compact space, whose coordinates are denoted by y_m ($m = 4, \cdots, 2n+3$), while the coordinates of four-dimensional uncompact space $R^{3,1}$ are denoted by x_μ ($\mu = 0, \cdots, 3$). We use orthogonal coordinates and choose the torus metric such that y_m is identified by $y_m + n_m$ with n_m = integer. The gaugino fields λ and the vector fields A_m corresponding to the compact directions are decomposed as

$$\lambda(x,y) = \sum_n \chi_n(x) \otimes \psi_n(y), \tag{5}$$

$$A_m(x,y) = \sum_n \varphi_{n,m}(x) \otimes \phi_{n,m}(y). \tag{6}$$

2.1.1 $U(1)$ gauge theory on magnetized torus T^2

First, let us consider $U(1)$ gauge theory on T^2 with the coordinates (y_4, y_5). We study the non-vanishing constant magnetic flux $F_{45} = 2\pi M$. We use the following gauge,

$$A_4 = -2\pi M y_5, \qquad A_5 = 0. \tag{7}$$

Then, their boundary conditions can be written as

$$\begin{aligned} A_m(y_4+1, y_5) &= A_m(y_4, y_5) + \partial_m\chi_4, \qquad \chi_4 = 0, \\ A_m(y_4, y_5+1) &= A_m(y_4, y_5) + \partial_m\chi_5, \qquad \chi_5 = -2\pi M y_4. \end{aligned} \tag{8}$$

Now, we study the spinor field $\psi(y)$ with the $U(1)$ charge $q = \pm 1$ on T^2, which corresponds to the compact part in the decomposition (5). The zero-mode satisfies the following equation,

$$\tilde{\Gamma}^m(\partial_m - iqA_m)\psi(y) = 0, \tag{9}$$

for $m = 4, 5$, where $\tilde{\Gamma}^m$ corresponds to the gamma matrix for the two-dimensional torus T^2, e.g.

$$\tilde{\Gamma}^4 = \begin{pmatrix} 0 & 1 \\ 1 & 0 \end{pmatrix}, \qquad \tilde{\Gamma}^5 = \begin{pmatrix} 0 & -i \\ i & 0 \end{pmatrix}, \tag{10}$$

and $\psi(y)$ is the two component spinor,

$$\psi = \begin{pmatrix} \psi_+ \\ \psi_- \end{pmatrix}. \tag{11}$$

Because of (8), the spinor field satisfies the following boundary condition,

$$\psi(y_4 + 1, y_5) = e^{iq\chi_4}\psi(y_4, y_5) = \psi(y_4, y_5), \tag{12}$$

$$\psi(y_4, y_5 + 1) = e^{iq\chi_5}\psi(y_4, y_5) = e^{-2\pi iqMy_4}\psi(y_4, y_5). \tag{13}$$

The consistency for the contractible loop, i.e. $(y_4, y_5) \to (y_4 + 1, y_5) \to (y_4 + 1, y_5 + 1)$, $\to (y_4, y_5 + 1) \to (y_4 + 1, y_5 + 1)$, requires $M =$ integer.

Because of the periodicity along y_5, $\psi_\pm$ can be written by

$$\psi_\pm(y_4, y_5) = \sum_n c_{\pm,n}(y_4)e^{2\pi iny_5}. \tag{14}$$

Suppose that $qM > 0$. Then, the solution for the zero-mode equation of ψ_+ is given by

$$c_{+,n}(y_4) = k_{+,n}e^{-\pi qMy_4^2 - 2\pi ny_4}, \tag{15}$$

where $k_{+,n}$ is a constant. Furthermore the boundary condition requires

$$k_{+,n} = a_n e^{-\pi n^2/(qM)}, \tag{16}$$

and a_{n+qM} is equal to a_n, i.e. $a_{n+qM} = a_n$. Thus, there are $|M|$ independent zero-modes of ψ_+, which have normalizable wavefunctions,

$$\Theta^j(y_4, y_5) = N_j e^{-M\pi y_5^2}\vartheta\begin{bmatrix} j/M \\ 0 \end{bmatrix}(M(y_4 + iy_5), Mi), \tag{17}$$

for $j = 0, \cdots, M-1$, where N_j is a normalization constant and

$$\vartheta\begin{bmatrix} j/M \\ 0 \end{bmatrix}(M(y_4 + iy_5), Mi) = \sum_n e^{-M\pi(n+j/M)^2 + 2\pi(n+j/M)M(y_4+iy_5)}, \tag{18}$$

that is, the Jacobi theta-function. We can introduce the complex structure modulus τ by replacing the above Jacobi theta-function as

$$\vartheta\begin{bmatrix} j/M \\ 0 \end{bmatrix}(M(y_4 + iy_5), Mi) \to \vartheta\begin{bmatrix} j/M \\ 0 \end{bmatrix}(M(y_4 + \tau y_5), M\tau). \tag{19}$$

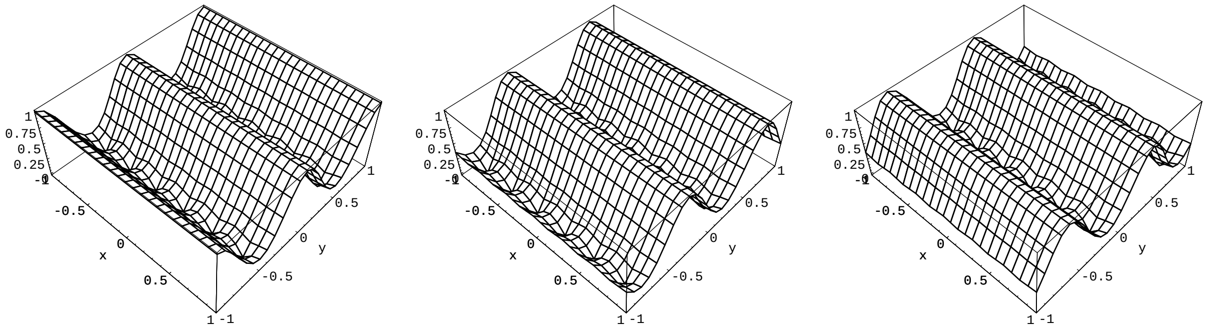

Figure 1: The wavefunction profiles of $|\Theta^j(x,y)|$ for $M=3$.

Thus, zero-mode wavefunctions depend on only the complex structure modulus, but not the overall size of T^2. Furthermore, there is the degree of freedom to shift $y_m \to y_m + d_m$ with constants d_m. They correspond to constant Wilson lines. Their localization points of zero-mode profiles are different each other and depend on the index j and constants. Their wavefunction profiles for $M=3$ are shown in the Figure 1

On the other hand, the zero-mode equation for ψ_- can be solved in a similar way, but their wavefunctions are unnormalizable. Hence, we can derive chiral theory by introducing magnetic fluxes. When $qM<0$, ψ_- has $|M|$ independent zero-modes with normalizable wavefunctions, while zero-modes for ψ_+ have unnormalizable wavefunctions. Bosonic fields are analyzed in a similar way. (See e.g. [52].)

2.1.2 $U(N)$ gauge theory on magnetized torus T^2

Here, we study $U(N)$ gauge theory on T^2. Let us consider the following form of (abelian) magnetic flux

$$F_{45} = 2\pi \begin{pmatrix} M_1 \mathbf{1}_{N_1\times N_1} & & 0 \\ & \ddots & \\ 0 & & M_n \mathbf{1}_{N_n\times N_n} \end{pmatrix}, \tag{20}$$

where $\mathbf{1}_{N_a\times N_a}$ denotes $(N_a\times N_a)$ identity matrix. This abelian magnetic flux breaks the gauge group as $U(N)\to \prod_{a=1}^n U(N_a)$ with $N=\sum_a N_a$. The rank is not reduced by the abelian magnetic flux. When we consider non-abelian magnetic flux, i.e. the toron background [63], the rank can be reduced.[2] However, here we restrict ourselves to the abelian flux.

Now, let us study gaugino fields on this background. We focus on the block including only $U(N_a)\times U(N_b)$ and such a block has the following magnetic flux,

$$F_{45} = 2\pi \begin{pmatrix} M_a \mathbf{1}_{N_a\times N_a} & 0 \\ 0 & M_b \mathbf{1}_{N_b\times N_b} \end{pmatrix}. \tag{21}$$

[2] See e.g. [64, 65] and references therein.

We use the same gauge as (7), i.e.

$$A_4 = -F_{45} y_5, \qquad A_5 = 0. \tag{22}$$

Similarly, the gaugino fields λ in $R^{3,1} \times T^2$ are decomposed as

$$\lambda(x,y) = \begin{pmatrix} \lambda^{aa}(x,y) & \lambda^{ab}(x,y) \\ \lambda^{ba}(x,y) & \lambda^{bb}(x,y) \end{pmatrix}. \tag{23}$$

Furthermore these gaugino fields are decomposed as (5),

$$\begin{aligned} \lambda^{aa}(x,y) &= \sum_n \chi_n^{aa}(x) \otimes \psi_n^{aa}(y), \quad \lambda^{ab}(x,y) = \sum_n \chi_n^{ab}(x) \otimes \psi_n^{ab}(y), \\ \lambda^{ba}(x,y) &= \sum_n \chi_n^{ba}(x) \otimes \psi_n^{ba}(y), \quad \lambda^{bb}(x,y) = \sum_n \chi_n^{bb}(x) \otimes \psi_n^{bb}(y). \end{aligned} \tag{24}$$

Each of ψ^{aa}, ψ^{ab}, ψ^{ba} and ψ^{bb} is a two-component spinor $(\psi_+, \psi_-)^T$. Their zero-modes satisfy

$$\begin{pmatrix} \bar\partial \psi_+^{aa} & [\bar\partial + 2\pi i (M_a - M_b) y_5] \psi_+^{ab} \\ [\bar\partial + 2\pi i (M_b - M_a) y_5] \psi_+^{ba} & \bar\partial \psi_+^{bb} \end{pmatrix} = 0, \tag{25}$$

$$\begin{pmatrix} \partial \psi_-^{aa} & [\partial - 2\pi i (M_a - M_b) y_5] \psi_-^{ab} \\ [\partial - 2\pi i (M_b - M_a) y_5] \psi_-^{ba} & \partial \psi_-^{bb} \end{pmatrix} = 0, \tag{26}$$

where $\bar\partial = \partial_4 + i\partial_5$ and $\partial = \partial_4 - i\partial_5$.

The zero-modes of ψ^{aa} and ψ^{bb} correspond to four-dimensional massless gauginos for the unbroken gauge group $U(N_a) \times U(N_b)$. Dirac equations of $\psi^{aa}(y)$ and $\psi^{bb}(y)$ in (25) and (26) do not include any magnetic fluxes. That is, both of $\psi_\pm$ have the same zero-modes as those on T^2 without magnetic fluxes.

Next, we study spinor fields, λ^{ab} and λ^{ba}, which correspond to bi-fundamental matter fields, $(N_a, \bar N_b)$ and $(\bar N_a, N_b)$ for the unbroken gauge group $U(N_a) \times U(N_b)$. When $M_a - M_b > 0$, λ_+^{ab} and λ_-^{ba} have $(M_a - M_b)$ zero-modes with normalizable wavefunctions, i.e. $\Theta^j(y_4, y_5)$ for $j = 0, \cdots, (M_a - M_b - 1)$ as (17), but zero-mode wavefunctions of λ_-^{ab} and λ_+^{ba} are unnormalizable. On the other hand, when $M_a - M_b < 0$, λ_-^{ab} and λ_+^{ba} have $(M_b - M_a)$ normalizable zero-modes. Hence, we obtain chiral theory.

Similarly, we can analyze bosonic fields A_m. In general, introduction of non-vanishing magnetic fluxes on T^2 breaks supersymmetry completely.

2.1.3 $U(N)$ gauge theory on $(T^2)^3$

Here, we extend the previous analysis to $U(N)$ gauge theory on $(T^2)^3$. We consider the magnetic background, where only F_{45}, F_{67} and F_{89} are non-vanishing, but the others of

F_{mn} are vanishing. Furthermore, F_{45}, F_{67} and F_{89} are given by

$$
\begin{aligned}
F_{45} &= 2\pi \begin{pmatrix} M_1^{(1)} \mathbf{1}_{N_1 \times N_1} & & 0 \\ & \ddots & \\ 0 & & M_n^{(1)} \mathbf{1}_{N_n \times N_n} \end{pmatrix}, \\
F_{67} &= 2\pi \begin{pmatrix} M_1^{(2)} \mathbf{1}_{N_1 \times N_1} & & 0 \\ & \ddots & \\ 0 & & M_n^{(2)} \mathbf{1}_{N_n \times N_n} \end{pmatrix}, \\
F_{89} &= 2\pi \begin{pmatrix} M_1^{(3)} \mathbf{1}_{N_1 \times N_1} & & 0 \\ & \ddots & \\ 0 & & M_n^{(3)} \mathbf{1}_{N_n \times N_n} \end{pmatrix}.
\end{aligned} \tag{27}
$$

This background breaks the gauge group $U(N)$ as $U(N) \to \prod_{a=1}^{n} U(N_a)$ with $N = \sum_a N_a$.

We can study gaugino fields on this background as a simple extension of the previous section 2.3. That is, we focus on the block including only $U(N_a) \times U(N_b)$ and such a block has the following magnetic flux as (21),

$$
F_{2i+2,2i+3} = 2\pi \begin{pmatrix} M_a^{(i)} \mathbf{1}_{N_a \times N_a} & 0 \\ 0 & M_b^{(i)} \mathbf{1}_{N_b \times N_b} \end{pmatrix}, \tag{28}
$$

and we use the following gauge

$$
A_{2i+2} = -y_{2i+3} F_{2i+2,2i+3}, \qquad A_{2i+3} = 0, \tag{29}
$$

for $i = 1, 2, 3$. Then, we decompose the gaugino fields $\lambda(x, y)$ as (5), i.e. the four-dimensional part $\chi(x)$ and the i-th T^2 part $\psi_{(i)}(y_{2i+2}, y_{2i+3})$, whose zero-modes satisfy

$$
\begin{aligned}
\begin{pmatrix} \bar{\partial}_i \psi_{(i)+}^{aa} & [\bar{\partial}_i + 2\pi i (M_a^{(i)} - M_b^{(i)}) y_{2i+3}] \psi_{(i)+}^{ab} \\ [\bar{\partial}_i + 2\pi i (M_b^{(i)} - M_a^{(i)}) y_{2i+3}] \psi_{(i)+}^{ba} & \bar{\partial}_i \psi_{(i)+}^{bb} \end{pmatrix} &= 0, \\
\begin{pmatrix} \partial_i \psi_{(i)-}^{aa} & [\partial_i - 2\pi i (M_a^{(i)} - M_b^{(i)}) y_{2i+3}] \psi_{(i)-}^{ab} \\ [\partial_i - 2\pi i (M_b^{(i)} - M_a^{(i)}) y_{2i+3}] \psi_{(i)-}^{ba} & \partial_i \psi_{(i)-}^{bb} \end{pmatrix} &= 0,
\end{aligned} \tag{30}
$$

where $\bar{\partial}_i = \partial_{2i+2} + i\partial_{2i+3}$ and $\partial_i = \partial_{2i+2} - i\partial_{2i+3}$.

The gaugino fields, ψ^{aa} and ψ^{bb}, for the unbroken gauge symmetry have no effect from magnetic fluxes in their Dirac equations. Hence, they have the same zero-modes as those on $(T^2)^3$ without magnetic fluxes. On the other hand, ψ^{ab} and ψ^{ba} correspond to bi-fundamental matter fields, $(N_a, \bar{N}_b)$ and $(\bar{N}_a, N_b)$. For the i-th T^2 with $M_a^{(i)} - M_b^{(i)} > 0$, $\psi_{(i)+}^{ab}$ and $\psi_{(i)-}^{ba}$ have $|M_a^{(i)} - M_b^{(i)}|$ normalizable zero-modes, while $\psi_{(i)-}^{ab}$ and

$\psi^{ba}_{(i)+}$ have no normalizable zero-modes. When $M_a^{(i)} - M_b^{(i)} < 0$, $\psi^{ab}_{(i)-}$ and $\psi^{ba}_{(i)+}$ have $|M_a^{(i)} - M_b^{(i)}|$ normalizable zero-modes. Then, the total number of bi-fundamental zero-modes is given by $\prod_{i=1}^3 |M_a^{(i)} - M_b^{(i)}|$ and all of them have the same six-dimensional chirality sign $\left[\prod_{i=1}^3 (M_a^{(i)} - M_b^{(i)})\right]$. Since the ten-dimensional chirality of gaugino fields is fixed, bi-fundamental zero-modes for either $(N_a, \bar{N}_b)$ or $(\bar{N}_a, N_b)$ appear with a fixed four-dimensional chirality. To summarize, the total number of bi-fundamental zero-modes for $(N_a, \bar{N}_b)$ is equal to

$$I_{ab} = \prod_{i=1}^{3} (M_a^{(i)} - M_b^{(i)}), \tag{31}$$

and their wavefunctions are given by a product of two-dimensional parts, i.e.

$$\Theta^{i_1,i_2,i_3}(y) = \Theta^{i_1}(y_4, y_5)\Theta^{i_2}(y_6, y_7)\Theta^{i_3}(y_8, y_9), \tag{32}$$

for $i_1 = 0, \cdots, (M_a^{(1)} - M_b^{(1)} - 1)$, $i_2 = 0, \cdots, (M_a^{(2)} - M_b^{(2)} - 1)$ and $i_3 = 0, \cdots, (M_a^{(3)} - M_b^{(3)} - 1)$. For $I_{ab} < 0$, this means that there appear $|I_{ab}|$ independent zero-modes for $(\bar{N}_a, N_b)$. It is also convenient to introduce the notation, $I^i_{ab} \equiv M_a^{(i)} - M_b^{(i)}$.

Similarly, we can analyze bosonic fields corresponding to A_m for $m = 4, \cdots, 9$. For generic values of magnetic fluxes, supersymmetry is broken completely. However, when they satisfy the following condition [62, 52],

$$\sum_{i=1}^{3} \pm \frac{M_a^{(i)} - M_b^{(i)}}{\mathcal{A}^{(i)}} = 0, \tag{33}$$

for one combination of signs, where $\mathcal{A}^{(i)}$ denotes the area of the i-th torus, there appear massless scalar modes as well as massive modes and four-dimensional N=1 supersymmetry remains unbroken at least in the $a-b$ sector. When we consider $\mathcal{A}^{(i)}$ as free parameters, we can realize the above supersymmetric condition (33) for most cases by choosing proper values of $\mathcal{A}^{(i)}$. For the case with the universal area, $\mathcal{A}^{(1)} = \mathcal{A}^{(2)} = \mathcal{A}^{(3)}$, the above condition (33) reduces to

$$\sum_{i=1}^{3} \pm (M_a^{(i)} - M_b^{(i)}) = 0. \tag{34}$$

In addition to (33), when one of them is vanishing, i.e. $(M_a^{(i)} - M_b^{(i)}) = 0$ and

$$\sum_{j \neq i} \pm \frac{M_a^{(j)} - M_b^{(j)}}{\mathcal{A}^{(j)}} = 0, \tag{35}$$

four-dimensional N=2 supersymmetry is unbroken. In these supersymmetric models, zero-mode profiles of bosonic fields are the same as their superpartners, that is, zero-mode profiles of fermionic fields.

2.2 General flux and non-abelian Wilson line

Here, we consider T^2 of $(T^2)^n$, whose coordinates are denoted as (y_4, y_5) with twisted boundary conditions. As a $U(N)$ gauge background, we introduce the following form of (abelian) magnetic flux,

$$F_{45} = 2\pi \begin{pmatrix} f_a \mathbf{1}_{N_a} & 0 \\ 0 & 0 \end{pmatrix}, \tag{36}$$

where $\mathbf{1}_{N_a}$ denotes $(N_a \times N_a)$ identity matrix. For example, we use the following gauge,

$$A_4 = -F_{45} y_5, \qquad A_5 = 0. \tag{37}$$

Then, their boundary conditions can be written as

$$\begin{aligned} A_m(y_4+1, y_5) &= A_m(y_4, y_5) + \partial_m \chi_4, \qquad \chi_4 = 0, \\ A_m(y_4, y_5+1) &= A_m(y_4, y_5) + \partial_m \chi_5, \qquad \chi_5 = -2\pi f_a y_4. \end{aligned} \tag{38}$$

This background breaks the gauge group $U(N)$ to $U(N_a) \times U(N-N_a)$. The zero-mode $\psi(y)$ corresponding to the gaugino is also decomposed as

$$\psi = \begin{pmatrix} A & B \\ C & D \end{pmatrix}, \tag{39}$$

depending on their $U(N_a) \times U(N-N_a)$ charges. That is, A and D correspond to the gaugino fields of unbroken symmetries, $U(N_a)$ and $U(N-N_a)$, respectively, while B and C correspond to bi-fundamental representations, $(N_a, \overline{N-N_a})$ and $(\overline{N_a}, N-N_a)$, respectively. The zero-mode satisfies the following equation,

$$\tilde{\Gamma}^m (\partial_m - iqA_m)\psi(y) = 0, \tag{40}$$

for $m = 4, 5$, where $\tilde{\Gamma}^m$ corresponds to the gamma matrix for the two-dimensional torus T^2 and $\psi(y)$ is the two component spinor. That is, A, B, C and D also have two components, $A_\pm, B_\pm, C_\pm$ and $D_\pm$. Here, q denotes the charge of ψ under the gauge background A_m. Since only the $U(1)$ part of $U(N_a)$ has the non-trivial background, its charge is relevant, that is, A, B, C and D have charges $q = 0, 1, -1$ and 0, respectively.

Because of (38), the spinor field satisfies the following boundary condition,

$$\psi(y_4+1, y_5) = e^{iq\chi_4} \psi(y_4, y_5), \tag{41}$$
$$\psi(y_4, y_5+1) = e^{iq\chi_5} \psi(y_4, y_5). \tag{42}$$

We write

$$\psi(y_4+1, y_5) = \Omega_4(y_4, y_5) \psi(y_4, y_5), \tag{43}$$
$$\psi(y_4, y_5+1) = \Omega_5(y_4, y_5) \psi(y_4, y_5). \tag{44}$$

Then, the consistency for the contractible loop, i.e. $(y_4, y_5) \to (y_4+1, y_5) \to (y_4+1, y_5+1) \to (y_4, y_5+1) \to (y_4, y_5)$ requires

$$\left(\Omega_5^{-1}(y_4, y_5+1)\Omega_4^{-1}(y_4+1, y_5+1)\Omega_5(y_4+1, y_5)\Omega_4(y_4, y_5)\right) \psi(y_4, y_5) = \psi(y_4, y_5), \tag{45}$$

for $\psi = A, B, C, D$. The left hand side reduces to $e^{-2\pi i q f_a}\psi(y_4, y_5)$ in the above background. Although that is trivial for $\psi = A$ and D, this condition for $\psi = B$ and C leads to the quantization condition of the magnetic flux f_a. That is, the magnetic flux f_a should be quantized such that $f_a = \text{integer}$.

When we introduce non-trivial background for the $SU(N_a)$ part of $U(N_a)$, the situation changes. Now, let us impose the following boundary conditions for $\psi = B$,

$$B(y_4 + 1, y_5) = \Omega_4(y_4, y_5)B(y_4, y_5) = e^{i\chi_4}\omega_4 B(y_4, y_5), \tag{46}$$

$$B(y_4, y_5 + 1) = \Omega_5(y_4, y_5)B(y_4, y_5) = e^{i\chi_5}\omega_5 B(y_4, y_5), \tag{47}$$

where ω_m are constant elements of $SU(N_a)$. Then, the consistency condition (45) reduces to

$$\omega_5^{-1}\omega_4^{-1}\omega_5\omega_4 e^{-2\pi i f_a} = \mathbf{1}_{N_a}. \tag{48}$$

If ω_4 and ω_5 commute each other, that would require gain $e^{-2\pi i f_a} = 1$. Thus, it is interesting that ω_4 and ω_5 do not commute each other, that is, non-Abelian Wilson lines. In particular, we consider the case that $\omega_5^{-1}\omega_4^{-1}\omega_5\omega_4$ corresponds to the center of $SU(N_a)$, that is,

$$\omega_5^{-1}\omega_4^{-1}\omega_5\omega_4 = e^{2\pi i M_a/N_a}\mathbf{1}_{N_a}, \tag{49}$$

where M_a is an integer. In this case, the consistency condition (48) requires that the magnetic flux should satisfy $f_a = M_a/N_a \pmod 1$.

We denote $P_a = \text{g.c.d.}(M_a, N_a)$, $m_a = M_a/P_a$ and $n_a = N_a/P_a$.[3] A solution of Eq. (49) is given as

$$\omega_4 = P, \qquad \omega_5 = Q^{-m_a}, \tag{50}$$

where

$$P = \begin{pmatrix} 0 & \mathbf{1}_{P_a} & 0 & 0 \\ 0 & 0 & \mathbf{1}_{P_a} & 0 \\ \cdots & & & \\ \mathbf{1}_{P_a} & 0 & 0 & 0 \end{pmatrix}, \quad Q = \begin{pmatrix} \mathbf{1}_{P_a} & 0 & 0 & 0 \\ 0 & \rho\mathbf{1}_{P_a} & 0 & 0 \\ \cdots & & & \\ 0 & 0 & 0 & \rho^{n_a-1}\mathbf{1}_{P_a} \end{pmatrix}, \tag{51}$$

with $\rho \equiv e^{2\pi i/n_a}$.

These non-Abelian Wilson lines break the gauge group $U(N_a)$ further. The following condition on the $U(N_a)$ gauge field,

$$A_\mu = w_4 A_\mu \omega_4^{-1} = w_5 A_\mu \omega_5^{-1}, \tag{52}$$

is required. Then, the gauge group $U(N_a)$ breaks to $U(P_a)$.

[3] Here, g.c.d. denotes the greatest common divisor.

2.2.1 Matter fields

Here, we consider the following form of $U(N)$ magnetic fluxes,

$$F_{45} = 2\pi \begin{pmatrix} f_1 \mathbf{1}_{N_1} & & 0 \\ & \ddots & \\ 0 & & f_n \mathbf{1}_{N_n} \end{pmatrix}. \tag{53}$$

This form of magnetic fluxes breaks $U(N)$ to $\prod_i U(N_i)$ for $f_i =$ integer. Furthermore, the gauge group is broken to $\prod_i U(P_i)$ when we choose $f_i = M_i/N_i$ with $P_i = \text{g.c.d.}(M_i, N_i)$ and non-Abelian Wilson lines such that they satisfy the consistency condition like Eq. (45).

Now, let us focus on the $(N_a + N_b) \times (N_a + N_b)$ block in $U(N)$, which has the magnetic flux,

$$F = 2\pi \begin{pmatrix} \frac{m_a}{n_a} \mathbf{1}_{N_a} & \\ & \frac{m_b}{n_b} \mathbf{1}_{N_b} \end{pmatrix}. \tag{54}$$

We use the same gauge as Eq. (37), i.e.

$$A_4 = -2\pi \begin{pmatrix} \frac{m_a}{n_a} \mathbf{1}_{N_a} & \\ & \frac{m_b}{n_b} \mathbf{1}_{N_b} \end{pmatrix} y_5, \qquad A_5 = 0. \tag{55}$$

Similarly to Eq. (8), we denote their boundary conditions as

$$\begin{aligned} A_m(y_4 + 1, y_5) &= A_m(y_4, y_5) + \begin{pmatrix} \partial_m \chi_4^a & 0 \\ 0 & \partial_m \chi_4^b \end{pmatrix}, \\ A_m(y_4, y_5 + 1) &= A_m(y_4, y_5) + \begin{pmatrix} \partial_m \chi_5^a & 0 \\ 0 & \partial_m \chi_5^b \end{pmatrix}, \end{aligned} \tag{56}$$

where

$$\chi_4^a = 0, \quad \chi_5^a = -2\pi \frac{m_a}{n_a} y_4, \quad \chi_4^b = 0, \quad \chi_5^b = -2\pi \frac{m_b}{n_b} y_4. \tag{57}$$

We decompose the gaugino fields of this block in a way similar to Eq. (39). That is, A and D correspond to adjoint matter fields of $U(N_a)$ and $U(N_b)$, respectively, while B and C correspond to bi-fundamental representations, $(N_a, \overline{N_b})$ and $(\overline{N_a}, N_b)$, respectively. Among them, we concentrate on the field B, which satisfies the boundary conditions,

$$\begin{aligned} B(y_4 + 1, y_5) &= \Omega_4^a B(y_4, y_5) (\Omega_4^b)^\dagger = e^{i(\chi_4^a - \chi_4^b)} \omega_4^a B(y_4, y_5) (\omega_4^b)^\dagger, \\ B(y_4, y_5 + 1) &= \Omega_5^a B(y_4, y_5) (\Omega_5^b)^\dagger = e^{i(\chi_5^a - \chi_5^b)} \omega_5^a B(y_4, y_5) (\omega_5^b)^\dagger. \end{aligned} \tag{58}$$

Here, $\omega_{4,5}^{a,b}$ are non-Abelian Wilson lines, which are given as Eqs. (50) and (51). Then, the gauge symmetry is broken to $U(P_a)$ and $U(P_b)$. We study zero-mode profiles of B fields in what follows.

Here, we study zero-mode profiles in the models with fractional magnetic fluxes and non-Abelian Wilson lines.

2.2.2 $n_a = n_b$

First, let us study the magnetic flux (54) for $n = n_a = n_b$. In this case, the non-Abelian Wilson lines break the gauge group $U(N_a) \times U(N_b)$ to $U(P_a) \times U(P_b)$, where $P_a = N_a/n$ and $P_b = N_b/n$. Following this breaking pattern, we decompose the fields B as

$$B = \begin{pmatrix} B_{00} & B_{01} & \cdots & \\ B_{10} & B_{11} & \cdots & \\ \cdots & & & \\ B_{n-1,0} & B_{n-1,1} & \cdots & B_{n-1,n-1} \end{pmatrix}. \tag{59}$$

Each of $B_{p,q}$ components is $(P_a \times P_b)$ matrix-valued fields, which correspond to bi-fundamental $(P_a, \bar{P}_b)$ fields under $U(P_a) \times U(P_b)$. The boundary condition (58) due to the non-Abelian Wilson lines is written as

$$\begin{aligned} B_{pq}(y_4 + 1, y_5) &= B_{p+1,q+1}(y_4, y_5), \\ B_{pq}(y_4, y_5 + 1) &= \rho^{-(m_a p - m_b q)} e^{-\frac{2\pi i m}{n} y_4} B_{p,q}(y_4, y_5), \end{aligned} \tag{60}$$

where m is used as $m = m_a - m_b$. That leads to the boundary condition,

$$\begin{aligned} B_{pq}(y_4 + n, y_5) &= B_{pq}(y_4, y_5), \\ B_{pq}(y_4, y_5 + n) &= e^{-2\pi i m y_4} B_{pq}(y_4, y_5). \end{aligned} \tag{61}$$

Suppose that $mn > 0$. Then, similar to section 2.1.1, the B_+ component for $B_{p,q}$ has nm independent solutions for the zero-mode Dirac equation (40) with the above condition (61). These solutions are given by

$$\begin{aligned} \Theta^j(y_4, y_5) &= \sum_l e^{-nm\pi(l + \frac{j}{nm})^2 + 2\pi i m(l + \frac{j}{nm}) y_4 - \frac{\pi m}{n} y_5^2 - 2\pi m (l + \frac{j}{nm}) y_5} \\ &= e^{-\frac{\pi m}{n} y_5^2} \, \vartheta \begin{bmatrix} \frac{j}{nm} \\ 0 \end{bmatrix} (mz, nm\tau), \end{aligned} \tag{62}$$

where $j = 0, 1, \cdots, nm - 1$ and $\tau = i$. On the other hand, the B_- component has no normalizable zero-modes. One finds that these solutions satisfy the boundary conditions,

$$\begin{aligned} \Theta^j(y_4 + 1, y_5) &= e^{\frac{2\pi i j}{n}} \Theta^j(y_4, y_5), \\ \Theta^j(y_4, y_5 + 1) &= e^{-\frac{2\pi i m}{n} y_4} \Theta^{j+m}(y_4, y_5). \end{aligned} \tag{63}$$

Thus, the zero-mode solutions with the boundary conditions (60) due to non-Abelian Wilson lines can be written in terms of Θ^j as

$$B^j_{pq}(y_4, y_5) = c^j_{pq} \sum_{r=0}^{n-1} e^{2\pi i (m_a p - m_b q) \frac{r}{n}} \Theta^{j+mr}, \tag{64}$$

where $j = 0, 1, ..., m - 1$. Here, c^j_{pq} is a constant normalization, which can be determined by the boundary conditions.

We have concentrated on the B_+ fields. Similarly, when $mn > 0$, the C_- fields have the same solutions as B_+. However, the B_- and C_+ have no normalizable zero-modes for $mn > 0$. On the other hand, when $mn < 0$ the B_- and C_+ have normalizable zero-modes with the same wavefunctions as the above, while B_+ and C_- have normalizable zero-modes.

We have considered the zero-modes profiles of fermionic fields. If 4D N=1 supersymmetry is preserved, the scalar mode has the same zero-mode profiles as its fermionic superpartner.

2.2.3 $n_a \neq n_b$

Next, we study the model with $n_a \neq n_b$. In this case, the non-Abelian Wilson lines break the gauge group $U(N_a) \times U(N_b)$ to $U(P_a) \times U(P_b)$, where $P_a = N_a/n_a$ and $P_b = N_b/n_b$. Similar to the previous subsection, we decompose the fields B as

$$B = \begin{pmatrix} B_{00} & B_{01} & \cdots & B_{0,n_b-1} \\ B_{10} & B_{11} & \cdots & \\ \cdots & & & \\ B_{n_a-1,0} & B_{n_a-1,1} & \cdots & B_{n_a-1,n_b-1} \end{pmatrix}. \tag{65}$$

Each of $B_{p,q}$ components is $(P_a \times P_b)$ matrix-valued fields. The boundary condition (58) due to the non-Abelian Wilson lines is written as

$$\begin{aligned} B_{pq}(y_4+1, y_5) &= B_{p+1,q+1}(y_4, y_5), \\ B_{pq}(y_4, y_5+1) &= e^{-2\pi i(\frac{m_a}{n_a}-\frac{m_b}{n_b})y_4} e^{2\pi i(\frac{m_a}{n_a}p-\frac{m_b}{n_a}q)} B_{p,q}(y_4, y_5). \end{aligned} \tag{66}$$

That leads to the boundary condition,

$$\begin{aligned} B_{pq}(y_4+Q_{ab}, y_5) &= B_{pq}(y_4, y_5), \\ B_{pq}(y_4, y_5+Q_{ab}) &= e^{-\frac{2\pi i}{k_{ab}}I_{ab}y_4} B_{p,q}(y_4, y_5), \end{aligned} \tag{67}$$

where $I_{ab} = n_b m_a - n_a m_b$ and Q_{ab} is defined by $Q_{ab} = \text{l.c.m.}(n_a, n_b)$.[4] In addition, we define $k_{ab} = \text{g.c.d.}(n_a, n_b)$, which is related with Q_{ab} as $Q_{ab} = \frac{n_a n_b}{k_{ab}}$. There are $S_{ab} = \frac{n_a n_b}{k_{ab}^2} I_{ab}$ independent zero-mode profiles, which satisfy the boundary condition (67). Those functions are obtained as

$$\begin{aligned} \Theta^j(y_4, y_5) &= \sum_n e^{-\pi S_{ab}(n+\frac{j}{S_{ab}})^2 + \frac{2\pi i S_{ab}}{Q_{ab}}(n+\frac{j}{S_{ab}})y_4 - \frac{\pi S_{ab}}{Q_{ab}^2}y_5^2 - 2\pi\frac{S_{ab}}{Q_{ab}}(n+\frac{j}{S_{ab}})y_5} \\ &= e^{-\frac{\pi S_{ab}}{Q_{ab}^2}y_5^2} \vartheta \begin{bmatrix} \frac{j}{S_{ab}} \\ 0 \end{bmatrix} ((S_{ab}/Q_{ab})z, S_{ab}\tau), \end{aligned} \tag{68}$$

where $\tau = i$. These wavefunctions satisfy the following boundary conditions,

$$\begin{aligned} \Theta^j(y_4+1, y_5) &= e^{2\pi i \frac{k_{ab}}{n_a n_b} j} \Theta^j(y_4, y_5), \\ \Theta^j(y_4, y_5+1) &= e^{2\pi i(\frac{m_a}{n_a}-\frac{m_b}{n_b})y_4} \Theta^{j-\frac{I_{ab}}{k_{ab}}}(y_4, y_5). \end{aligned} \tag{69}$$

[4] Here, l.c.m. denotes the least common multiple.

Thus, the zero-mode wavefunctions, which satisfy the boundary conditions (66), are obtained as

$$B^j_{pq}(y_4, y_5) = c^j_{pq} \sum_{r=0}^{Q_{ab}-1} e^{2\pi i(\frac{m_a}{n_a}p - \frac{m_b}{n_b}q)r} \Theta^{j+\frac{I_{ab}}{k_{ab}}r}(y_4, y_5), \tag{70}$$

where $j = 0, 1, \cdots, \frac{I_{ab}}{k_{ab}} - 1$.

As an illustrating example, we consider the model with $n_a = 2, n_b = 4$ and $m_a = m_b = 3$. Then, we have $k_{ab} = \text{g.c.d.}(n_a, n_b) = 2 \neq 1$ and $I_{ab} = 6$. We decompose the bi-fundamental fields B with the 2×4 matrix entries as

$$B = \begin{pmatrix} B_{00} & B_{01} & B_{02} & B_{03} \\ B_{00} & B_{11} & B_{12} & B_{13} \end{pmatrix}. \tag{71}$$

From the wavefunction formula in Eq. (70), one obtains the three independent solutions labeled by $j = 0, 1, 2$ for each component of B_{pq} and these are represented by linear combination of Θ^i, for example B_{00} and B_{01} are

$$\begin{aligned} B^j_{00} &= \Theta^j + \Theta^{j+3} + \Theta^{j+6} + \Theta^{j+9}, \\ B^j_{01} &= \Theta^j + e^{-\frac{3\pi i}{2}}\Theta^{j+3} + e^{-3\pi i}\Theta^{j+6} + e^{-\frac{9\pi i}{2}}\Theta^{j+9}. \end{aligned} \tag{72}$$

Obviously, the y_4-direction boundary condition can connect some of components of B as follows

$$B_{00} \to B_{11} \to B_{02} \to B_{13} \to B_{00} \tag{73}$$

$$B_{01} \to B_{12} \to B_{03} \to B_{14} \to B_{01}. \tag{74}$$

Hence, there are 6 zero-mode solutions in this background.

- Another representation of solutions

In the previous section, we have presented solutions in terms of the Θ^j functions. However, by using the properties of the theta function, one can represent the wavefunctions (64) and (70) as a single theta function as

$$B^j_{pq}(y_4, y_5) = C^j_{p,q} e^{-\pi \tilde{I}_{ab} y_5^2} \times \vartheta \begin{bmatrix} \frac{j}{M_{ab}} \\ 0 \end{bmatrix} \left(\tilde{I}_{ab} z + \left(\frac{m_a}{n_a}p - \frac{m_b}{n_b}q \right), \tilde{I}_{ab}\tau \right), \tag{75}$$

where $\tilde{I}_{ab} = I_{ab}/n_a n_b$. The constant $C^j_{p,q}$ can be determined by the boundary conditions. The net number of zero-mode multiplicity is given by $M_{ab} = I_{ab}/k_{ab}$. Therefore the wavefunctions $B^{j'}_{pq}(y_4, y_5)$ with $j' = j + M_{ab}$ should be equal to $B^j_{pq}(y_4, y_5)$. Furthermore we impose the $B^j_{p+n_a,q}, B^j_{p,q+n_b} = B^j_{p,q}$ and we have twist boundary condition $B^j_{pq}(y_4+1, y_5) = B^j_{p+1,q+1}(y_4, y_5)$. Then these conditions imply the following constraint for the coefficients of C^j_{pq} as

$$e^{2\pi i j \frac{m_a}{M_{ab}}} C^j_{p+n_a,q} = e^{-2\pi i j \frac{m_b}{M_{ab}}} C^j_{p,q+n_b} = C^j_{pq}, \tag{76}$$

$$C^j_{p+1,q+1} = C^j_{p,q}, \quad C^{j+M_{ab}}_{p,q} = C^j_{p,q}. \tag{77}$$

In general, their solutions should not be determined uniquely. We find that a simple solutions is

$$C^j_{pq} = e^{2\pi i j \frac{L}{M_{ab}}(p-q)}, \tag{78}$$

where L is a certain integer given by

$$L = \frac{M_{ab} l_a - m_a}{n_a} = -\frac{M_{ab} l_b + m_b}{n_b}, \tag{79}$$

where l_a and l_b are also integers. Then the forms of wavefunctions become simple as

$$B^j_{pq}(y_4, y_5) \;=\; N_j e^{2\pi i j \frac{L}{M_{ab}}(p-q)} e^{-\pi \tilde{I}_{ab} y_5^2} \times \vartheta \begin{bmatrix} \frac{j}{M_{ab}} \\ 0 \end{bmatrix} \left(\tilde{I}_{ab} z + \left(\frac{m_a}{n_a} p - \frac{m_b}{n_b} q \right), \tilde{I}_{ab} \tau \right). \tag{80}$$

However this expression is only valid if there exists such an integer L satisfying the relations. Furthermore, when $\frac{m_a}{M_{ab}} = \frac{m_b}{M_{ab}} =$ integer, C^j_{pq} is reduced to $C^j_{pq} =$ const.

2.2.4 Continuous Wilson line

So far, we have considered the simple T^2, where y_4 and y_5 are identified as $y_4 \sim y_4 + 1$ and $y_5 \sim y_5 + 1$. Similarly, we can study the torus compactification with arbitrary value of the complex structure modulus τ, although we have fixed $\tau = i$ in the above analysis. Then, we obtain the same zero-mode wavefunctions for arbitrary value of τ as Eq. (75) except replacing $z = y_4 + i y_5$ in the theta function by $z = y_4 + \tau y_5$. In this section, we also discuss about the effect of the constant gauge potential called by Wilson line on the gauge group and wavefunctions. It is useful to use the holomorphic basis of z and gauge potential. In order for this reason, we take the following form of magnetic flux on T^2,

$$F = \frac{\pi i}{\mathrm{Im}\tau} m \; (dz \wedge d\bar{z}), \tag{81}$$

where m is an integer [66]. We also take the following gauge of vector potential

$$A(z) = \frac{\pi m}{\mathrm{Im}\tau} \mathrm{Im}(\bar{z}\; dz). \tag{82}$$

This form of the vector potential satisfies the following relations,

$$A(z+1) \;=\; A(z) + \frac{\pi m}{\mathrm{Im}\tau} \mathrm{Im}(dz), \tag{83}$$

$$A(z+\tau) \;=\; A(z) + \frac{\pi m}{\mathrm{Im}\tau} \mathrm{Im}(\bar{\tau}\; dz). \tag{84}$$

The Dirac equations of the zero-modes are modified by the Wilson line background, $\xi = \xi_4 + \tau \xi_5$ as

$$\left(\bar{\partial} + \frac{\pi q}{2\mathrm{Im}(\tau)} (m z + \xi) \right) \psi_+(z, \bar{z}) = 0, \tag{85}$$

$$\left(\partial - \frac{\pi q}{2\mathrm{Im}(\tau)} (m \bar{z} + \bar{\xi}) \right) \psi_-(z, \bar{z}) = 0, \tag{86}$$

where ξ_4 and ξ_5 are real constants. That is, we can introduce the Wilson line background, $\xi = \xi_1 + \tau\xi_2$ by replacing χ_i in as [52]

$$\chi_4 = \frac{\pi}{\mathrm{Im}\tau}\mathrm{Im}(mz+\xi), \qquad \chi_5 = \frac{\pi}{\mathrm{Im}\tau}\mathrm{Im}(\bar{\tau}(mz+\xi)). \tag{87}$$

Because of this Wilson line, the number of zero-modes does not change, but their wavefunctions are replaced as

$$\Theta^{j,M}(z) \to \Theta^{j,M}(z+\xi/m). \tag{88}$$

It would be useful to consider $U(1)_a \times U(1)_b$ theory from the phenomenological viewpoint. We consider the fermion field $\lambda(x,z)$ with $U(1)_a \times U(1)_b$ charges, (q_a, q_b). We assume the following form of $U(1)_a$ magnetic flux on T^2,

$$F^a_{z\bar{z}} = \frac{\pi i}{\mathrm{Im}\tau} m_a, \tag{89}$$

where m_a is integer, but there is no magnetic flux in $U(1)_b$. On top of that, we introduce Wilson lines ξ^a and ξ^b for $U(1)_a$ and $U(1)_b$, respectively. The zero-mode equations are written as

$$\left(\bar{\partial} + \frac{\pi}{2\mathrm{Im}(\tau)}(q_a(m_a z + \xi^a) + q_b\xi^b)\right)\psi_+(z,\bar{z}) = 0, \tag{90}$$

$$\left(\partial - \frac{\pi}{2\mathrm{Im}(\tau)}(q_a(m_a \bar{z} + \bar{\xi}^a) + q_b\bar{\xi}^b)\right)\psi_-(z,\bar{z}) = 0. \tag{91}$$

Then, the number of zero-modes is obtained as $M = q_a m_a$ and their wavefunctions are written as

$$\Theta^{j,M}(z+\xi/m_a), \tag{92}$$

where $\xi = \xi^a + \xi^b q_b/q_a$. Here we give a few comments. All of modes with $q_a = 0$ become massive and there do not appear zero-modes with $q_a = 0$. For $q_a \neq 0$, zero-modes with $q_b = 0$ appear and the number of zero-modes is independent of q_b. Obviously, when we introduce Wilson lines ξ^a and/or ξ^b without magnetic flux F^a, zero-modes do not appear. The shift of wavefunctions depends on $1/m_a$ and the charge q_b. Note that although $F^b = 0$, Wilson lines ξ_b and charges q_b for $U(1)_b$ are also important [5].

The above aspects of magnetic fluxes and Wilson lines are phenomenologically interesting. We consider 6D super Yang-Mills theory with non-Abelian gauge group G. We introduce a magnetic flux F^a along a Cartan direction of G. Then, the gauge group breaks to $G' \times U(1)_a$ without reducing the rank. Furthermore, there appear the massless fermion fields λ' , which correspond to the gaugino fields for the broken gauge group part and have the fundamental representation of G' and non-vanishing $U(1)_a$ charge. Furthermore, we

[5] Wilson lines ξ_b and charges q_b for $U(1)_b$ are in a sense more important than Wilson lines ξ_a and charges q_a for $U(1)_a$, because the shift of wavefunctions (92) depends on q_b.

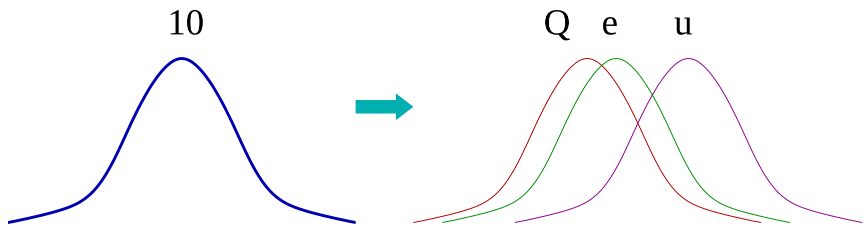

Figure 2: Wavefunction splitting by Wilson lines

introduce a Wilson line along a Cartan direction of G'. Then, the gauge group is broken to $G'' \times U(1)_a \times U(1)_b$ without reducing the rank. The gaugino fields corresponding to the broken gauge part in G' do not remain as massless modes, but they gain masses due to the Wilson line $U(1)_b$. However, the fermion fields λ' remain still massless with the same degeneracy.

Let us explain more on this aspect. Suppose that we introduce magnetic fluxes in a model with a larger group G such that they break G to a GUT group like $SU(5)$ and this model includes three families of matter fields like 10 and $\bar{5}$. Their Yukawa couplings are computed by the overlap integral of three zero-mode profiles. We obtain the GUT relation among Yukawa coupling matrices when wavefunction profiles of matter fields in 10 ($\bar{5}$) are degenerate. Then, we introduce a Wilson line along $U(1)_Y$, which breaks $SU(5)$ to $SU(3) \times SU(2) \times U(1)_Y$. Because of Wilson lines, $SU(5)$ gauge bosons except the $SU(3) \times SU(2) \times U(1)_Y$ gauge bosons become massive and the corresponding gaugino fields become massive. However, three families of 10 and $\bar{5}$ matter fields remain massless. Importantly, this Wilson line resolves the degeneracy of wavefunction profiles of left-handed quarks, right-handed up-sector quarks and right-handed charged leptons in 10 and right-handed down-sector quarks and left-handed charged leptons in $\bar{5}$ as Figure 2. That is, the GUT relation among Yukawa coupling matrices is deformed. As an illustrating model, we study the Pati-Salam model in the next subsection.

Here we study effects due to discrete values of Wilson lines such as $\xi = k\tau$ with $k =$ integer. We find

$$\Theta^{j,M}(z + k\tau/M) = e^{\pi i k \mathrm{Im}(\bar{\tau} z)/\mathrm{Im}(\tau)} \Theta^{j+k,M}(z). \qquad (93)$$

Thus, the effect of discrete Wilson lines $\xi = k\tau$ is to replace the j-th zero-mode by the $(j+k)$-th zero-mode up to $e^{\pi i k \mathrm{Im}(\bar{\tau} z)/\mathrm{Im}(\tau)}$. However, when we consider 3-point and higher order couplings, the gauge invariance requires that the sum of Wilson lines of matter fields should vanish, that is, $\sum_i k_i = 0$ for allowed n-point couplings. Thus, the part $e^{\pi i k \mathrm{Im}(\bar{\tau} z)/\mathrm{Im}(\tau)}$ is irrelevant to 4D effective theory and the resultant 4D effective theory is the equivalent even when we introduce $\xi = k\tau$. Similarly, introducing the Wilson lines $\xi = k$ with $k =$ integer leads to the equivalent 4D effective theory.

2.3 Pati-Salam model

As an illustrating model, we consider the Pati-Salam model. We start with 10D N=1 $U(8)$ super Yang-Mills theory. We compactify the extra 6 dimensions on $T_1^2 \times T_2^2 \times T_3^2$, and we denote the complex coordinate for the d-th T_d^2 by z^d, where $d = 1, 2, 3$. Then, we introduce the following form of magnetic fluxes,

$$F_{z^d\bar{z}^d} = \frac{\pi i}{\mathrm{Im}\tau_d} \begin{pmatrix} m_1^{(d)}\mathbb{1}_4 & & \\ & m_2^{(d)}\mathbb{1}_2 & \\ & & m_3^{(d)}\mathbb{1}_2 \end{pmatrix}, \quad d = 1, 2, 3, \tag{94}$$

in the gauge space, where $\mathbb{1}_N$ are the unit matrices of rank N, $m_i^{(d)}$ are integers. We assume that the above background preserves 4D N=1 supersymmetry (SUSY). Here, we denote $M_{ij}^{(d)} = m_i^{(d)} - m_j^{(d)}$ and $M_{ij} = M_{ij}^{(1)} M_{ij}^{(2)} M_{ij}^{(3)}$. This magnetic flux breaks the gauge group $U(8)$ to $U(4) \times U(2)_L \times U(2)_R$, that is the Pati-Salam gauge group up to $U(1)$ factors. The gauge sector corresponds to 4D N=4 SUSY vector multiplet, that is, there are $U(4) \times U(2)_L \times U(2)_R$ N=1 vector multiplet and three adjoint chiral multiplets. In addition, there appear bifundamental matter fields like $\lambda_{(4,2,1)}$, $\lambda_{(\bar{4},1,2)}$ and $\lambda_{(1,2,2)}$, and their numbers of zero-modes are equal to M_{12}, M_{31} and M_{23}. When M_{ij} is negative, that implies their conjugate matter fields appear with the degeneracy $|M_{ij}|$. The fields $\lambda_{(4,2,1)}$ and $\lambda_{(\bar{4},1,2)}$ correspond to left-handed and right-handed matter fields, respectively, while $\lambda_{(1,2,2)}$ corresponds to up and down Higgs (higgsino) fields. For example, we can realize three families by $M_{12}^{(d)} = (3, 1, 1)$ and $M_{31}^{(d)} = (3, 1, 1)$. That leads to $|M_{23}| = 0$ or 24. At any rate, the flavor structure is determined by the first T_1^2 in such a model. Explicitly, the zero-mode wavefunctions of both $\lambda_{(4,2,1)}$ and $\lambda_{(\bar{4},1,2)}$ are obtained as

$$\Theta^{j,3}(z^1)\Theta^{1,1}(z^2)\Theta^{1,1}(z^3). \tag{95}$$

Their Yukawa matrices are constrained by the Pati-Salam gauge symmetry, that is, up-sector quarks, down-sector quarks, charged leptons and neutrinos have the same Yukawa matrices with Higgs fields. Even with such a constraint, one could derive realistic quark/lepton masses and mixing angles, because this model has many Higgs fields and their vacuum expectation values generically break the up-down symmetry.

We introduce Wilson lines in $U(4)$ and $U(2)_R$ such that $U(4)$ breaks to $U(1) \times U(3)$ and $U(2)_R$ breaks $U(1) \times U(1)$. Then, the gauge group becomes the standard gauge group up to $U(1)$ factors. Furthermore, the profiles of left-handed quarks and leptons in $\lambda_{(4,2,1)}$ shift differently because of Wilson lines. Similarly, right-handed up-sector quarks, down-sector quarks, charged leptons and neutrinos in $\lambda_{(\bar{4},1,2)}$ shift differently. The flavor structure is determined by the first T_1^2. Thus, when we introduce Wilson lines on the second or third torus, the resultant Yukawa matrices are constrained by the $SU(4) \times SU(2)_L \times SU(2)_R$. For example, we introduce Wilson lines on T_2^2. Then, zero-mode profiles of quarks, (Q, u, d)

and leptons (L, e, ν) split as

$$\begin{array}{rcl} Q & : & \Theta^{j,3}(z^1)\Theta^{1,1}(z^2+\xi^a)\Theta^{1,1}(z^3), \\ L & : & \Theta^{j,3}(z^1)\Theta^{1,1}(z^2-3\xi^a)\Theta^{1,1}(z^3), \\ u^c & : & \Theta^{j,3}(z^1)\Theta^{1,1}(z^2-\xi^a+\xi^b)\Theta^{1,1}(z^3), \\ d^c & : & \Theta^{j,3}(z^1)\Theta^{1,1}(z^2-\xi^a-\xi^b)\Theta^{1,1}(z^3), \\ e^c & : & \Theta^{j,3}(z^1)\Theta^{1,1}(z^2+3\xi^a-\xi^b)\Theta^{1,1}(z^3), \\ \nu^c & : & \Theta^{j,3}(z^1)\Theta^{1,1}(z^2+3\xi^a+\xi^b)\Theta^{1,1}(z^3), \end{array} \tag{96}$$

where ξ^a and ξ^b are the Wilson lines to break $U(4) \to U(3) \times U(1)$ and $U(2)_R \to U(1) \times U(1)$, respectively. Those Wilson lines just change the overall factors of Yukawa matrices, but ratios among elements in one Yukawa matrix do not change. Also we can introduce Wilson lines along the same $U(1)$ directions as the magnetic fluxes, but they do not deform the up-down symmetry of Yukawa matrices, either.

On the other hand, when we introduce Wilson lines on the first T_1^2, the zero-mode wavefunctions split as

$$\begin{array}{rcl} Q & : & \Theta^{j,3}(z^1+\xi^a/3)\Theta^{1,1}(z^2)\Theta^{1,1}(z^3), \\ L & : & \Theta^{j,3}(z^1-\xi^a)\Theta^{1,1}(z^2)\Theta^{1,1}(z^3), \\ u^c & : & \Theta^{j,3}(z^1-\xi^a/3+\xi^b/3)\Theta^{1,1}(z^2)\Theta^{1,1}(z^3), \\ d^c & : & \Theta^{j,3}(z^1-\xi^a/3-\xi^b/3)\Theta^{1,1}(z^2)\Theta^{1,1}(z^3), \\ e^c & : & \Theta^{j,3}(z^1+\xi^a-\xi^b/3)\Theta^{1,1}(z^2)\Theta^{1,1}(z^3), \\ \nu^c & : & \Theta^{j,3}(z^1+\xi^a+\xi^b/3)\Theta^{1,1}(z^2)\Theta^{1,1}(z^3). \end{array} \tag{97}$$

In this case, the flavor structure is deviated from the $SU(4) \times SU(2)_L \times SU(2)_R$ relation, that is, mass ratios and mixing angles can change. Also we can introduce Wilson lines ξ^a to T_2^2 and ξ^b to T_1^2. Then we realize

$$\begin{array}{rcl} Q & : & \Theta^{j,3}(z^1)\Theta^{1,1}(z^2+\xi^a)\Theta^{1,1}(z^3), \\ L & : & \Theta^{j,3}(z^1)\Theta^{1,1}(z^2-3\xi^a)\Theta^{1,1}(z^3), \\ u^c & : & \Theta^{j,3}(z^1+\xi^b/3)\Theta^{1,1}(z^2-\xi^a)\Theta^{1,1}(z^3), \\ d^c & : & \Theta^{j,3}(z^1-\xi^b/3)\Theta^{1,1}(z^2-\xi^a)\Theta^{1,1}(z^3), \\ e^c & : & \Theta^{j,3}(z^1-\xi^b/3)\Theta^{1,1}(z^2+3\xi^a)\Theta^{1,1}(z^3), \\ \nu^c & : & \Theta^{j,3}(z^1+\xi^b/3)\Theta^{1,1}(z^2+3\xi^a)\Theta^{1,1}(z^3). \end{array} \tag{98}$$

Indeed, this behavior is well-known in the intersecting D-brane models, which are T-duals of magnetized D-brane models. In the intersecting D-brane side, introduction of Wilson lines corresponds to split D-branes. By splitting D-branes, the gauge group breaks as $U(M+N) \to U(M) \times U(N)$, but the number of massless bi-fundamental modes does not change, although they decompose because of the gauge symmetry breaking.

2.4 Exceptional gauge groups

Here we extend these analysis to the exceptional gauge symmetry. Gauge theories with the gauge groups E_6, E_7 and E_8, are quite interesting as grand unified theory in particle physics, which would lead to the standard model at low-energy. All of quarks and leptons are involved in the **16** representations of $SO(10)$ and such a **16** representation appears from the adjoint representation and **27** representation of E_6. Furthermore, these representations are included in adjoint representations of E_7 and E_8. These exceptional gauge theories can be derived in heterotic string theory, type IIB string theory with non-perturbative effects and F-theory. Indeed, interesting models have been studied e.g. in heterotic orbifold models [3, 4, 9, 8, 7] and F-theory [34, 33, 67, 68, 69, 70, 71].

We start with 10 dimensional super Yang-Mills theory with gauge group G. Introducing the magnetic flux on general gauge group G is achieved by taking the background gauge potential along the Cartan direction of gauge group G. We take this direction as $U(1)_a$.

By the magnetic flux along the $U(1)_a$ direction, all of 4D gauge vector fields A_μ, which have $U(1)_a$ charges, become massive, that is, the gauge group is broken from G to $G' \times U(1)_a$ without reducing its rank,[6] where 4D gauge fields A_μ in $G' \times U(1)_a$ have vanishing $U(1)_a$ charges and their zero-modes $\phi_\mu(z)$ have a flat profile. Since the magnetic flux has no effect on the unbroken gauge sector, 4D N=4 supersymmetry remains in the $G' \times U(1)_a$ sector, that is, there are massless four adjoint gaugino fields and six adjoint scalar fields.[7]

In addition, matter fields appear from gaugino fields corresponding to the broken gauge part, that is, they have non-trivial representations under G' and non-vanishing $U(1)_a$ charges q^a.[8] Therefore we can obtain the chiral zero-modes by using same technique even for the exceptional gauge groups.

Now, let us introduce Wilson lines along the $U(1)_b$ direction of G'. That breaks further the gauge group G' to $G'' \times U(1)_b$ without reducing its rank.[9] All of the $U(1)_b$-charged fields including 4D vector, spinor and scalar fields become massive because of the Wilson line, when they are not charged under $U(1)_a$ and their zero-mode profiles are flat. On the other hand, the matter fields with non-trivial profiles due to magnetic flux have different behavior. For matter fields with $U(1)_a$ charge q^a and $U(1)_b$ charge q^b, the Dirac equations of the zero-modes are modified by the Wilson line background, $\xi^b_d = \xi^b_{d,1} + \tau_d \xi^b_{d,2}$. That is, we can introduce Wilson lines along the $U(1)_b$ direction. Because of this Wilson line, the number of zero-modes does not change, but their wavefunctions are shifted as

$$\Theta^{j,M}(z_d) \to \Theta^{j,M}(z_d + q^b \xi^b_d/(q^a m^a_{(d)})). \tag{99}$$

Note that the shift of zero-mode profiles depend on $U(1)_b$ charges of matter fields. Simi-

[6] For example, when $G = SU(N)$, G' would correspond to $SU(N-1)$.

[7] In string terminology, these adjoint scalar fields correspond to open string moduli, that is, D-brane position moduli. How to stabilize these moduli is one of important issues.

[8] For example, when $G = SU(N)$ and $G' \times U(1)_a = SU(N-1) \times U(1)_a$, these matter fields have $(N-1)$ fundamental representation under $SU(N-1)$ and $U(1)_a$ charge $q^a = 1$ and their conjugates.

[9] For example, when $G' = SU(N-1)$, the Wilson line breaks it to $SU(N-2) \times U(1)_b$.

larly, we can introduce the Wilson line ξ^a_d along the $U(1)_a$ direction. Then, the zero-mode wavefunctions shift as

$$\Theta^{j,M}(z_d + q^b\xi^b_d/(q^a m^a_{(d)})) \to \Theta^{j,M}(z_d + \xi^a_d/m^a_{(d)} + q^b\xi^b_d/(q^a m^a_{(d)})). \tag{100}$$

However, the shift due to ξ^a_d is rather universal shift, but the shift by ξ^b_d depends on the charges q^b of matter fields. Thus, the shift by ξ^b_d would be much more important than one by ξ^a_d, in particular from the phenomenological viewpoint.

Suppose that we introduce magnetic fluxes in a model with a larger gauge group G such that they break G to a GUT group like $SO(10)$ and this model include three families of matter fields like the **16** representation, corresponding to all of quarks and leptons. Then, we assume that the $SO(10)$ gauge symmetry is broken to $SU(3) \times SU(2) \times U(1)_Y$ by some mechanism. If zero-mode profiles of quarks and leptons are degenerate even after such $SO(10)$ breaking, couplings in 4D effective field theory are constrained (at the lowest level) by the $SO(10)$ symmetry. That is, Yukawa matrices would be the same between the up-sector, the down-sector and the lepton sector. However, when we break $SO(10)$ to $SU(3) \times SU(2) \times U(1)_Y \times U(1)$ by introducing Wilson lines along the $U(1)_Y \times U(1)$ direction, these Wilson lines resolve the degeneracy of zero-mode profiles among quarks and leptons. Then, Yukawa matrices would become different from each other among the up-sector, the down-sector and the lepton sector. Similarly we can analyze 4D massless scalar modes [52]. We are assuming that 4D N=1 supersymmetry is preserved [62, 52]. Thus, the number of zero-modes and the profiles for 4D scalar fields are the same as those for their superpartners, i.e. the above spinor fields. For example, for Higgs fields, we study zero-modes and their profiles of Higgsino fields.

2.4.1 E_6 model

Here, we consider 10D super Yang-Mills theory with the E_6 gauge group.

We compactify extra six-dimensions on T^6. We introduce magnetic fluxes along the $U(1)_a$ direction, which breaks the gauge group, $E_6 \to SO(10) \times U(1)_a$. The E_6 adjoint representation is decomposed as

$$\mathbf{78} = \mathbf{45}_0 + \mathbf{1}_0 + \mathbf{16}_1 + \overline{\mathbf{16}}_{-1}, \tag{101}$$

for $SO(10) \times U(1)_a$. Here, $\mathbf{16}_1$ and $\overline{\mathbf{16}}_{-1}$ correspond to the broken part and the corresponding gaugino fields appear as matter fields.

For example, we assume magnetic fluxes,

$$m^a_{(1)} = 3, \qquad m^a_{(2)} = 1, \qquad m^a_{(3)} = 1. \tag{102}$$

Then, the chiral matter fields corresponding to $\mathbf{16}_1$ and $s_d = (+,+,+)$ have zero-modes, but there are no massless modes for $\overline{\mathbf{16}}_{-1}$. Furthermore, the number of $\mathbf{16}_1$ is equal to $m^a_{(1)}m^a_{(2)}m^a_{(3)} = 3$, that is, the model with three families of $\mathbf{16}_1$. Their wavefunctions are written as

$$\Theta^{j,3}(z_1)\Theta^{1,1}(z_2)\Theta^{1,1}(z_3). \tag{103}$$

The flavor structure is determined by the first torus T_1^2. Thus, the massless matter spectrum is realistic, although there is no Higgs fields and the gauge sector has 4D N=4 SUSY.

The $U(1)_a$ symmetry is anomalous. We assume that its gauge boson become massive by the Green-Schwarz mechanism. Hereafter, we also assume that if other $U(1)$ symmetries become anomalous they become massive by the Green-Schwarz mechanism.

Here, we break the $SO(10)$ gauge group further to the standard model gauge group up to $U(1)$ factors, i.e. $SU(3) \times SU(2) \times U(1)_Y \times U(1)_b$, by introducing Wilson lines along $U(1)_Y$ and $U(1)_b$ directions. The **16** representation of $SO(10)$ is decomposed under $SU(3) \times SU(2) \times U(1)_Y \times U(1)_b$ as

$$\mathbf{16} = (\mathbf{3},\mathbf{2})_{1,-1} + (\bar{\mathbf{3}},\mathbf{1})_{-4,-1} + (\mathbf{1},\mathbf{1})_{6,-1} + (\bar{\mathbf{3}},\mathbf{1})_{2,3} + (\mathbf{1},\mathbf{2})_{-3,3} + (\mathbf{1},\mathbf{1})_{0,-5}, \tag{104}$$

where we normalize $U(1)_Y$ and $U(1)_b$ charges, such that minimum charges satisfy $|q^Y| = 1$ and $|q^b| = 1$.

By introducing Wilson lines along $U(1)_Y$ and $U(1)_b$ directions, the generation number does not change, but the zero-mode profiles of three families of **16** split differently each other among quarks and leptons. Furthermore, their splitting behaviors depend on which torus T_d^2 we introduce Wilson lines. Recall that in this model the flavor structure is determined by the first torus T_1^2. For example, when we introduce Wilson lines along $U(1)_Y$ and $U(1)_b$ directions on the second torus T_2^2, the zero-mode profiles of quarks (Q, u, d) and leptons (L, e, ν) split as

$$\begin{aligned}
Q &: \Theta^{j,3}(z^1)\Theta^{1,1}(z^2 + \xi^Y - \xi^b)\Theta^{1,1}(z^3), \\
u^c &: \Theta^{j,3}(z^1)\Theta^{1,1}(z^2 - 4\xi^Y - \xi^b)\Theta^{1,1}(z^3), \\
d^c &: \Theta^{j,3}(z^1)\Theta^{1,1}(z^2 + 2\xi^Y + 3\xi^b)\Theta^{1,1}(z^3), \\
L &: \Theta^{j,3}(z^1)\Theta^{1,1}(z^2 - 3\xi^Y + 3\xi^b)\Theta^{1,1}(z^3), \\
e^c &: \Theta^{j,3}(z^1)\Theta^{1,1}(z^2 + 6\xi^Y - \xi^b)\Theta^{1,1}(z^3), \\
\nu^c &: \Theta^{j,3}(z^1)\Theta^{1,1}(z^2 - 5\xi^b)\Theta^{1,1}(z^3),
\end{aligned} \tag{105}$$

where ξ^Y and ξ^b are the Wilson lines along $U(1)_Y$ and $U(1)_b$ directions. On the other hand, when we introduce Wilson lines on the first torus T_1^2, the zero-mode profiles of quarks (Q, u, d) and leptons (L, e, ν) split as

$$\begin{aligned}
Q &: \Theta^{j,3}(z^1 + \xi^Y/3 - \xi^b/3)\Theta^{1,1}(z^2)\Theta^{1,1}(z^3), \\
u^c &: \Theta^{j,3}(z^1 - 4\xi^Y/3 - \xi^b/3)\Theta^{1,1}(z^2)\Theta^{1,1}(z^3), \\
d^c &: \Theta^{j,3}(z^1 + 2\xi^Y/3 + \xi^b)\Theta^{1,1}(z^2)\Theta^{1,1}(z^3), \\
L &: \Theta^{j,3}(z^1 - \xi^Y + \xi^b)\Theta^{1,1}(z^2)\Theta^{1,1}(z^3), \\
e^c &: \Theta^{j,3}(z^1 + 2\xi^Y - \xi^b/3)\Theta^{1,1}(z^2)\Theta^{1,1}(z^3), \\
\nu^c &: \Theta^{j,3}(z^1 - 5\xi^b/3)\Theta^{1,1}(z^2)\Theta^{1,1}(z^3).
\end{aligned} \tag{106}$$

Since the flavor structure is determined by the first torus T_1^2, the first case (105) preserves the $SO(10)$ flavor structure. However, such flavor structure is deformed in the second case (106) by Wilson lines.

Obviously, other configurations of Wilson lines are possible, e.g. ξ^Y on T_1^2 and ξ^b on T_2^2 and so on. In any case, the flavor structure is determined by which Wilson lines we introduce on the first T_1^2. For example, if we introduce only ξ^b on T_1^2, the resultant Yukawa matrices would have the $SU(5)$ GUT relation.

Thus, the above model is interesting. Its chiral matter spectrum is realistic and the model has the interesting flavor structure, although electro-weak Higgs fields do not appear and the gauge sector has 4D N=4 SUSY.

2.4.2 E_7 and E_8 models

Similarly, we can study E_7 and E_8 models. Their ranks are larger than E_6 and their adjoint representations include several representations. The E_8 adjoint representation **248** is decomposed under $E_7 \times U(1)_{E8}$ as

$$\mathbf{248} = \mathbf{133}_0 + \mathbf{1}_0 + \mathbf{56}_1 + \mathbf{56}_{-1} + \mathbf{1}_2 + \mathbf{1}_{-2}. \tag{107}$$

Note that we are using $U(1)$ charge normalization such that the minimum charge except vanishing charge is equal to one, $|q| = 1$. Then, the E_7 adjoint representation **133** is decomposed under $E_6 \times U(1)_{E7}$ as

$$\mathbf{133} = \mathbf{78}_0 + \mathbf{1}_0 + \mathbf{27}_{-2} + \overline{\mathbf{27}}_2, \tag{108}$$

and the **56** representation of E_7 is decomposed under $E_6 \times U(1)_{E7}$ as

$$\mathbf{56} = \mathbf{27}_1 + \overline{\mathbf{27}}_{-1} + \mathbf{1}_2 + \mathbf{1}_{-2}. \tag{109}$$

Furthermore, the **27** representation of E_6 is decomposed under $SO(10) \times U(1)_{E6}$ as

$$\mathbf{27} = \mathbf{16}_1 + \mathbf{10}_{-2} + \mathbf{1}_4. \tag{110}$$

Thus, we can construct various models from E_7 and E_8 models. Quark and lepton matter fields can be originated from several sectors, although such matter fields are originated from **16** of the E_6 adjoint sector in the models of the previous section. In addition, the E_7 and E_8 adjoint representations include exotic representations. Hence, exotic matter fields, in general, appear in 4D massless spectra. Instead of $U(1)_{E8} \times U(1)_{E7}$, we use the $U(1)_c \times U(1)_d$ basis, such that those charges are related as

$$q_c = \frac{1}{2} q_{E8} + \frac{1}{2} q_{E7}, \qquad q_d = -\frac{1}{2} q_{E8} + \frac{1}{2} q_{E7}, \tag{111}$$

where q_c, q_d, q_{E8} and q_{E7} denote $U(1)_c$, $U(1)_d$, $U(1)_{E8}$ and $U(1)_{E7}$ charges, respectively. In addition, we denote $U(1)_{E6}$ by $U(1)_a$ as in section 2.4.1. Also, as in section 2.4.1, we use the notation $U(1)_b$, which appears through the $SO(10)$ breaking as $SO(10) \to SU(5) \times U(1)_b$.

Here, we show just simple illustrating models. First of all, we can construct almost the same model as the E_6 models. For example, we start with the 10D E_7 super Yang-Mills theory. We can introduce magnetic fluxes with the same form in $U(1)_{E6}$ as (102).

Furthermore, we introduce Wilson lines such that the gauge group is broken down to $SU(3)\times SU(2)\times U(1)_Y$ up to $U(1)$ factors. Then, we realize three families of quarks and leptons under the standard model gauge group, that is, the same 4D massless spectrum as one in section 2.4.1, although the gauge sector has partly 4D N=4 SUSY and there is no Higgs fields. Similarly, the same model can be derived from the 10D E_8 super Yang-Mills theory.

Now, let us consider another illustrating model with different aspects. We start with the 10D E_8 super Yang-Mills theory. When E_8 is broken to the standard model gauge group, there are five $U(1)$'s including $U(1)_Y$, i.e., $U(1)_I$ $(I=a,b,c,d,Y)$. We introduce magnetic fluxes $m^I_{(d)}$ along these five $U(1)_I$ directions. Then, the sum of magnetic fluxes $M=\sum_I q^I m^I_{(d)}$ appears in the zero-mode Dirac equation for the matter field with charges q^I. We require that $\sum_I q^I m^I_{(d)}$ should be integer for all of matter fields, that is, the quantization condition of magnetic fluxes [66].

For example, five $(\mathbf{3},\mathbf{2})_1$ representations under $SU(3)\times SU(2)\times U(1)_Y$ as well as their conjugates appear from the **248** adjoint representation. Three of them appear from three **27** representations of **248**, i.e., Eqs. (107), (108) and (109). In the zero-mode equations of such three $(\mathbf{3},\mathbf{2})_1$ matter fields, the following sum of magnetic fluxes $\sum_I q^I m^I_{(d)}$ appears

$$\begin{aligned} m^{Q1}_{(d)} &= m^c_{(d)}+m^a_{(d)}-m^b_{(d)}+m^Y_{(d)}, \\ m^{Q2}_{(d)} &= m^d_{(d)}+m^a_{(d)}-m^b_{(d)}+m^Y_{(d)}, \\ m^{Q3}_{(d)} &= -m^c_{(d)}-m^d_{(d)}+m^a_{(d)}-m^b_{(d)}+m^Y_{(d)}. \end{aligned} \tag{112}$$

In addition, one $(\mathbf{3},\mathbf{2})_1$ representation appears from **16** of the E_6 adjoint **78** representation (101) as section 3. In the zero-mode equation of such $(\mathbf{3},\mathbf{2})_1$ matter field, the following sum of magnetic fluxes $\sum_I q^I m^I_{(d)}$ appears

$$m^{Q4}_{(d)} = -3m^a_{(d)}-m^b_{(d)}+m^Y_{(d)}. \tag{113}$$

Moreover, the $SO(10)$ adjoint **45** representation also includes a $(\mathbf{3},\mathbf{2})_1$ representation and the corresponding matter field has the sum of magnetic fluxes $\sum_I q^I m^I_{(d)}$, [10]

$$m^{Q5}_{(d)} = 4m^b_{(d)}+m^Y_{(d)}, \tag{114}$$

in the zero-mode equation. Here, we require that all of $m^{Q1}_{(d)}$, $m^{Q2}_{(d)}$, $m^{Q3}_{(d)}$, $m^{Q4}_{(d)}$ and $m^{Q5}_{(d)}$ should be integers. Similarly, we require that $\sum_I q^I m^I_{(d)}$ should be integers for all of matter fields with charges q^I, which appear from the E_8 adjoint **248** representation. By an explicit computation, it is found that the sum $\sum_I q^I m^I_{(d)}$ for any charge q^I appearing from **248** can be written as a linear combination of $m^{Q1}_{(d)}$, $m^{Q2}_{(d)}$, $m^{Q3}_{(d)}$, $m^{Q4}_{(d)}$ and $m^{Q5}_{(d)}$ with integer coefficients. Thus, when all of $m^{Q1}_{(d)}$, $m^{Q2}_{(d)}$, $m^{Q3}_{(d)}$, $m^{Q4}_{(d)}$ and $m^{Q5}_{(d)}$ are integers, the sum $\sum_I q^I m^I_{(d)}$ for any charge q^I of **248** is always integer.

[10] The $SO(10)$ adjoint **45** representation includes another $(\mathbf{3},\mathbf{2})$ representation but its $U(1)_Y$ charge is different.

Using the above notation, we introduce the magnetic fluxes such as ,

$$
\begin{array}{lll}
m^{Q1}_{(1)} = 1, & m^{Q1}_{(2)} = -1, & m^{Q1}_{(3)} = -3, \\
m^{Q2}_{(1)} = -1, & m^{Q2}_{(2)} = 0, & m^{Q2}_{(3)} = 1, \\
m^{Q3}_{(1)} = -1, & m^{Q3}_{(2)} = 0, & m^{Q3}_{(3)} = 1, \\
m^{Q4}_{(1)} = -1, & m^{Q4}_{(2)} = 0, & m^{Q4}_{(3)} = 1, \\
m^{Q5}_{(1)} = -2, & m^{Q5}_{(2)} = -1, & m^{Q5}_{(3)} = 0.
\end{array}
\tag{115}
$$

In addition, we also introduce all possible Wilson lines on each torus along five $U(1)$ directions. Then, the gauge group is $SU(3) \times SU(2) \times U(1)_Y$ with $U(1)$ factors.

The 4D massless spectrum of this model includes the following matter fields under the standard gauge group, $SU(3) \times SU(2) \times U(1)_Y$,

$$
\begin{aligned}
&3 \times \left[(\mathbf{3},\mathbf{2})_1 + (\overline{\mathbf{3}},\mathbf{1})_{-4} + (\overline{\mathbf{3}},\mathbf{1})_2 + (\mathbf{1},\mathbf{2})_{-3} + (\mathbf{1},\mathbf{1})_6\right] \\
&+8\left[(\mathbf{1},\mathbf{2})_3 + (\mathbf{1},\mathbf{2})_{-3}\right] \\
&+15 \times \left[(\mathbf{3},\mathbf{1})_4 + (\overline{\mathbf{3}},\mathbf{1})_{-4}\right] + 6 \times \left[(\mathbf{3},\mathbf{1})_{-2} + (\overline{\mathbf{3}},\mathbf{1})_2\right] + 27 \times \left[(\mathbf{1},\mathbf{1})_6 + (\mathbf{1},\mathbf{1})_{-6}\right],
\end{aligned}
\tag{116}
$$

and $SU(3)\times SU(2)$ singlets with vanishing $U(1)_Y$ charges. That is, this massless spectrum includes three families of quarks and leptons as well as eight pairs of up- and down-sectors of electroweak Higgs fields. In addition, many vector-like matter fields appear, but exotic matter fields do not appear even in vector-like form. Such exotic matter fields have (effectively) vanishing magnetic flux on one of T^2_d. Then, such fields become massive when we switch on proper Wilson lines.[11] Thus, this model has semi-realistic massless spectrum, although the gauge sector still has 4D N=4 SUSY. We can write the wavefunctions of these zero-modes. For example, the zero-mode wavefunctions of left-handed quarks are written as

$$
\Theta^{1,1}(z_1 + \xi_1)\Theta^{1,1}(z_2 + \xi_2)\Theta^{j,3}(z_3 + \xi_3/3), \tag{117}
$$

for $j = 1, 2, 3$, where ξ_d denote Wilson lines along five $U(1)$ directions. Thus, the flavor structure for the left-handed quarks is determined by the third torus. Similarly, we can write zero-mode wavefunctions of the other matter fields. The above massless spectrum includes several vector-like generations of right-handed quarks as well as right-handed leptons. These vector-like generations may gain mass terms. Thus, the flavor structure of chiral right-handed quarks depends on mass matrices of vector-like generations.

Similarly, various models can be constructed within the framework of E_7 and E_8 models with magnetic flux and Wilson line backgrounds.

[11] In the limit of vanishing Wilson lines, colored Higgs fields appear in the vector-like form, but they become massive for finite values of Wilson lines.

3 Calculation of Yukawa interaction and higher order couplings

3.1 Low-energy effective action

In this section we study the low-energy phenomenology based on the general set up of the string theory or supergravity theory. In the low-energy limit of these theories can be described as the effective action for $N = 1$ super Yang-Mills theory with chiral matter fields as far as low-energy supersymmetry exist. Their action consists of only three functions as Kahler potential, super potential and gauge kinetic functions. Furthermore such functions usually depend on the moduli fields which are corresponding the background of the higher dimensional space or tensor fields. To describe the realistic world, these moduli field should be stabilized. This can be achieved by some mechanism e.g. background flux induced super potential or non-perturbative super potential which means that moduli fields have vacuum expectation values. Therefore it is important and necessary to study the moduli field and their stabilization for understanding the dynamics of string theory or quantum field theory. For the phenomenological aspects understanding these moduli dependence is important. In such scenario the vacuum often breaks the supersymmetry. This affects on the soft supersymmetry breaking terms mediated by moduli fields. Actually we have seen the Yukawa coupling is determined by the background of the compactified space and depend on the complex structure moduli. Therefore we need to know the moduli parameters and dynamics of the mediation mechanism of supersymmetry breaking to understand low-energy phenomena.

Since these three functions are dependent on the light matter fields C_α and heavy moduli field $\mathcal{M}$, they may be represented by the expansion of the light matter fields and the general expressions for super potential $W(\mathcal{M}, C)$ and Kahler potential $K(\mathcal{M}, \bar{\mathcal{M}}, C, \bar{C})$ are given by

$$W(\mathcal{M}, C) = \sum_\alpha \xi(\mathcal{M})C_\alpha + \sum_{\alpha,\beta} \mu_{\alpha\beta}(\mathcal{M})C_\alpha C_\beta + \sum_{\alpha,\beta,\gamma} Y_{\alpha\beta\gamma}(\mathcal{M})C_\alpha C_\beta C_\gamma + \cdots , \tag{118}$$

and

$$K(\mathcal{M}, \bar{\mathcal{M}}, C, \bar{C}) = K_0(\mathcal{M}, \bar{\mathcal{M}}) + \sum_{\alpha,\beta} K_{C_\alpha C_\beta}(\mathcal{M}, \bar{\mathcal{M}})C_\alpha C_{\bar{\beta}} + \cdots . \tag{119}$$

By giving these coefficients of the moduli parameters we may obtain the low-energy constants up to higher order corrections which is denoted by ellipsis. For example, the second and third terms of the super potential give rise to the supersymmetric masses and the Yukawa couplings. We are interested in the information on the explicit form given in this expressions. There are usually two ways to obtain the effective actions. One method is to use the string S matrix calculation. This enables to compute the amplitude for massless string states at least perturbatively in α' and string coupling g_s. From the expressions we can extract the interaction terms and dependency of the moduli fields at arbitrary

order of α' and g_s in principle. Therefore this approach gives the solid results including the stringy effects. For this calculations it needs the technically higher knowledge about string vertex operators and calculation of CFT.

The second method to construct the four dimensional effective theory is easier way to start with higher dimensional field theory or DBI action which is an effective action of D-brane models and take the ordinary dimensional reductions to four dimensions. This also provides the low-energy interactions including the moduli dependence at certain accuracy. Indeed we will see such a discrepancy in the calculation of the normalization constant and Yukawa couplings in field theory which are discussed in section3.5 The explicit calculations for the dimensional reduction of toroidal compactifications are studied in appendixA.

3.2 General setup

We consider dimensional reduction of ten-dimensional $\mathcal{N}=1$ super Yang–Mills theory with $U(N)$ gauge group [72], on a six torus in Abelian magnetic flux background. We factorize the six-torus into two-tori $(T^2)^3$, each of which is specified by the complex structure τ_d and the area $A_d=(2\pi R_d)^2\ \mathrm{Im}\tau_d$ where $d=1,2,3$. We shall focus on the case with trivial background which means torus without non-abelian Wilson line. For the fractional flux case, the analysis of these couplings will be discussed later. From the periodicity of torus, the background magnetic flux is quantized as [66]

$$F_{z^d\bar{z}^d}=\frac{2\pi i}{\mathrm{Im}\tau_d}\begin{pmatrix} m_1^{(d)}\mathbb{1}_{N_1} & & \\ & \ddots & \\ & & m_n^{(d)}\mathbb{1}_{N_n}\end{pmatrix},\quad d=1,2,3, \tag{120}$$

where $\mathbb{1}_{N_a}$ are the unit matrices of rank N_a, $m_i^{(d)}$ are integers and z^d are the complex coordinates. This background breaks the gauge symmetry $U(N)\to\prod_{a=1}^n U(N_a)$ where $N=\sum_{a=1}^n N_a$. We have the $|M^{(d)}|$ zero-modes labeled by the index j. Note that the wavefunction for $j=k+M^{(d)}$ is identical to one for $j=k$. They satisfy the orthonormal condition,

$$\int d^2z^d\ \psi_d^{i,M^{(d)}}(z^d)\left(\psi_d^{j,M^{(d)}}(z^d)\right)^*=\delta_{ij}. \tag{121}$$

The important part of zero-mode wavefunctions is written in terms of the Jacobi theta function

$$\vartheta\begin{bmatrix}a\\b\end{bmatrix}(\nu,\tau)=\sum_{n=-\infty}^{\infty}\exp\left[\pi i(n+a)^2\tau+2\pi i(n+a)(\nu+b)\right]. \tag{122}$$

It transforms under the symmetry of torus lattice and has several important properties [73]. One of them is the following product rule

$$\begin{aligned}
&\vartheta \begin{bmatrix} i/M_1 \\ 0 \end{bmatrix} (z_1, \tau M_1) \cdot \vartheta \begin{bmatrix} j/M_2 \\ 0 \end{bmatrix} (z_2, \tau M_2) \\
&\qquad = \sum_{m \in \mathbf{Z}_{M_1+M_2}} \vartheta \begin{bmatrix} \frac{i+j+M_1 m}{M_1+M_2} \\ 0 \end{bmatrix} (z_1+z_2, \tau(M_1+M_2)) \\
&\qquad\quad \times \vartheta \begin{bmatrix} \frac{M_2 i - M_1 j + M_1 M_2 m}{M_1 M_2 (M_1+M_2)} \\ 0 \end{bmatrix} (z_1 M_2 - z_2 M_1, \tau M_1 M_2 (M_1+M_2)).
\end{aligned} \tag{123}$$

Here $\mathbf{Z}_M$ is the cyclic group of order $|M|$, $\mathbf{Z}_M = \{1, \ldots, |M|\}$ where every number is defined modulo M. Although this expression looks asymmetric under the exchange between i and j, it is symmetric if we take into account the summation. By using the product property (123), we can decompose a product of two zero-mode wavefunctions as follows,

$$\begin{aligned}
\psi_d^{i,M_1}(z^d)\psi_d^{j,M_2}(z^d) = &\frac{N_{M_1} N_{M_2}}{N_{M_1+M_2}} \sum_{m \in \mathbf{Z}_{M_1+M_2}} \psi_d^{i+j+M_1 m, M_1+M_2}(z^d) \\
&\times \vartheta \begin{bmatrix} \frac{M_2 i - M_1 j + M_1 M_2 m}{M_1 M_2 (M_1+M_2)} \\ 0 \end{bmatrix} (0, \tau_d M_1 M_2 (M_1+M_2)),
\end{aligned} \tag{124}$$

where the normalization factor N_M is obtained as

$$N_{M^{(d)}} = \left(\frac{2 \mathrm{Im} \tau_d |M^{(d)}|}{A_d^2} \right)^{1/4}. \tag{125}$$

In this section, we calculate the generalization of Yukawa couplings to arbitrary order L couplings

$$Y_{i_1 \ldots i_{L_\chi} i_{L_\chi+1} \cdots i_L} \chi^{i_1}(x) \cdots \chi^{i_{L_\chi}}(x) \phi^{i_{L_\chi+1}}(x) \ldots \phi^{i_L}(x), \tag{126}$$

with $L = L_\chi + L_\phi$, where χ and ϕ collectively represent four-dimensional components of fermions and bosons, respectively. The system under consideration can be understood as low-energy effective field theory of open string theory. The magnetic flux is provided by stacks of D-branes filling in the internal dimension. The leading order terms in α' are identical to ten-dimensional super-Yang–Mills theory, whose covariantized gaugino kinetic term gives the three-point coupling upon dimensional reduction [52, 74]. The higher order couplings can be read off from the effective Lagrangian of the Dirac–Born–Infeld action with supersymmetrization. The internal component of bosonic and fermionic wavefunctions is the same [52]. Therefore it suffices to calculate the wavefunction overlap in the extra dimensions

$$Y_{i_1 i_2 \ldots i_L} = g_L^{10} \int_{T^6} d^6 z \prod_{d=1}^{3} \psi_d^{i_1, M_1}(z) \psi_d^{i_2, M_2}(z) \ldots \psi_d^{i_L, M_L}(z), \tag{127}$$

where g_L^{10} denotes the coupling in ten dimensions.

3.3 Three-point coupling

In this section, we calculate the three-point coupling considering the coupling selection rule. As we see later, the three-point coupling provides a building block of higher order couplings.

The gauge group dependent part is contracted by the gauge invariance, so that the choice of three blocks m_a, m_b, m_c in (120) automatically fixes the relative magnetic fluxes

$$(m_a - m_b) + (m_b - m_c) = (m_a - m_c), \quad \text{and} \quad M_1 + M_2 = M_3, \tag{128}$$

where $M_1 = m_a - m_b$, $M_2 = m_b - m_c$ and $M_3 = m_a - m_c$. Here every M_i is assumed to be a positive integer. This relation is interpreted as the selection rule, in analogy of intersecting brane case [26, 75], to which we come back later. If it is not satisfied, there is no corresponding gauge invariant operator in ten dimensions. In terms of quantum numbers the coupling has the form $(\mathbf{N_a}, \overline{\mathbf{N}}_\mathbf{b}, \mathbf{1}) \cdot (\mathbf{1}, \mathbf{N_b}, \overline{\mathbf{N}}_\mathbf{c}) \cdot (\overline{\mathbf{N}}_\mathbf{a}, \mathbf{1}, \mathbf{N_c})$ under $U(N_a) \times U(N_b) \times U(N_c)$.

The internal part including the wavefunction integrals on the d-th T^2 gives

$$y_{ij\bar{k}} = \int d^2z \; \psi^{i,M_1}(z)\psi^{j,M_2}(z) \left(\psi^{k,M_3}(z)\right)^* . \tag{129}$$

The complete three-point coupling is the direct product of those in $d = 1, 2, 3$ and g_3^{10}. For the moment we neglect the normalization factors N_M, and consider two-dimensional wavefunctions, omitting the extra dimensional index d. By using the relation (124), we can decompose the product of the first two wavefunctions $\psi^{i,M_1}(z)\psi^{j,M_2}(z)$ in terms of $\psi^{k,M_3}(z)$ and we apply the orthogonality relation (121). Then, we obtain

$$y_{ij\bar{k}} = \sum_{m \in \mathbf{Z}_{M_3}} \delta_{i+j+M_1 m,k} \; \vartheta \begin{bmatrix} \frac{M_2 i - M_1 j + M_1 M_2 m}{M_1 M_2 M_3} \\ 0 \end{bmatrix} (0, \tau M_1 M_2 M_3), \tag{130}$$

where the numbers in the Kronecker delta is defined modulo M_3. This expression is symmetric under the exchange $(i, M_1) \leftrightarrow (j, M_2)$.

For $\gcd(M_1, M_2) = 1$, we solve the constraint from the Kronecker delta $\delta_{i+j+M_1 m,k}$,

$$i + j - k = M_3 l - M_1 m, \quad m \in \mathbf{Z}_{M_3}, l \in \mathbf{Z}_{M_1}. \tag{131}$$

Using Euclidean algorithm, it is easy to see that, in the relatively prime case $\gcd(M_1, M_2) = 1$, there is always a unique solution for given i, j, k. This situation is the same as one in intersecting D-brane models [26, 75]. The argument of the theta function in eq.(185) becomes

$$\frac{M_2 i - M_1 j + M_1 M_2 m}{M_1 M_2 (M_1 + M_2)} = \frac{M_2 k - M_3 j + M_2 M_3 l}{(M_3 - M_2) M_2 M_3}. \tag{132}$$

Therefore, the three-point coupling is written as

$$y_{ij\bar{k}}(l) = \vartheta \begin{bmatrix} \frac{M_2 k - M_3 j + M_2 M_3 l}{M_2 M_3 (M_3 - M_2)} \\ 0 \end{bmatrix} (0, \tau (M_3 - M_2) M_2 M_3), \tag{133}$$

where l is an integer related to i, j, k through (131). This is called the 2-3 picture, or the j-k picture, where the dependence on i and M_1 is only implicit.

In the case with a generic value of $\gcd(M_1, M_2) = g$, we can show

$$y_{ij\bar{k}} = \sum_{n=1}^{g} \vartheta \begin{bmatrix} \frac{M_2 k - M_3 j + M_2 M_3 l}{M_1 M_2 M_3} + \frac{n}{g} \\ 0 \end{bmatrix} (0, \tau M_1 M_2 M_3). \tag{134}$$

The point is that, for a given particular solution (i, j, k), the number of general solutions satisfying Eq. (131) is equal to g. We can use a similar argument as above, now considering $\mathbf{Z}_{M_1/g}$ and $\mathbf{Z}_{M_3/g}$ instead of the original region. There is a unique pair (l, m) in $(\mathbf{Z}_{M_1/g}, \mathbf{Z}_{M_3/g})$ satisfying the constraint (131), i.e. ,

$$\frac{i + j - k}{g} = \frac{M_3}{g} l - \frac{M_1}{g} m. \tag{135}$$

Obviously, when (l, m) is a particular solution, the following pairs,

$$\left(l + \frac{M_1}{g}, m + \frac{M_3}{g} \right) \in (\mathbf{Z}_{M_1}, \mathbf{Z}_{M_3}), \tag{136}$$

also satisfy the equation with the same right-hand side (RHS). Since $\mathbf{Z}_{M_1}$ and $\mathbf{Z}_{M_3}$ are respectively unions of g identical copies of $\mathbf{Z}_{M_1/g}, \mathbf{Z}_{M_3/g}$, there are g different solutions. This situation is the same as one in intersecting D-brane models. If we reflect the shift (136) in (132), we obtain the desired result (134).

There can be Wilson lines $\zeta \equiv \zeta_r + \tau \zeta_i$, whose effect is just a translation of each wavefunction [52]

$$\psi^{j,M}(z) \to \psi^{j,M}(z + \zeta), \qquad \text{for all } j. \tag{137}$$

Thus the corresponding product for (123) is obtained as

$$\begin{aligned} &\vartheta \begin{bmatrix} i/M_1 \\ 0 \end{bmatrix} ((z + \zeta_1) M_1, \tau M_1) \cdot \vartheta \begin{bmatrix} j/M_2 \\ 0 \end{bmatrix} ((z + \zeta_2) M_2, \tau M_2) \\ &\qquad = \sum_{m \in \mathbf{Z}_{M_1 + M_2}} \vartheta \begin{bmatrix} \frac{i + j + M_1 m}{M_1 + M_2} \\ 0 \end{bmatrix} ((M_1 + M_2)(z + \zeta_3), \tau (M_1 + M_2)) \\ &\qquad\quad \times \vartheta \begin{bmatrix} \frac{M_2 i - M_1 j + M_1 M_2 m}{M_1 M_2 (M_1 + M_2)} \\ 0 \end{bmatrix} (M_1 M_2 (\zeta_1 - \zeta_2)), \tau M_1 M_2 (M_1 + M_2)), \end{aligned} \tag{138}$$

where $M_3 = M_1 + M_2$ and $\zeta_3 M_3 = \zeta_1 M_1 + \zeta_2 M_2$.

Finally, we take into account the six internal dimensions $T^2 \times T^2 \times T^2$. Referring to (127), essentially the full coupling is the direct product of the coupling on each two-torus. The overall factor in (127) is the physical ten dimensional gauge coupling $g_3^{10} = g_{\rm YM}$, since this is obtained by dimensional reduction of super Yang–Mills theory. Collecting

the normalization factors (125) from (124), the full three-point coupling becomes

$$
\begin{aligned}
Y_{ij\bar{k}} =& g_{\mathrm{YM}} \prod_{d=1}^{3} \left(\frac{2\mathrm{Im}\tau_d}{A_d^2} \frac{M_1^{(d)} M_2^{(d)}}{M_3^{(d)}} \right)^{1/4} \\
& \times \exp \left(i\pi (M_1^{(d)} \zeta_1^{(d)} \mathrm{Im}\zeta_1^{(d)} + M_2^{(d)} \zeta_2^{(d)} \mathrm{Im}\zeta_2^{(d)} + M_3^{(d)} \zeta_3^{(d)} \mathrm{Im}\zeta_3^{(d)}) / \mathrm{Im}\tau_d \right) \\
& \times \sum_{n_d=1}^{g_d} \vartheta \begin{bmatrix} \frac{M_2^{(d)} k - M_3^{(d)} j + M_2^{(d)} M_3^{(d)} l}{M_1^{(d)} M_2^{(d)} M_3^{(d)}} + \frac{n_d}{g_d} \\ 0 \end{bmatrix} (M_2^{(d)} M_3^{(d)} (\zeta_2^{(d)} - \zeta_3^{(d)}), \tau_d M_1^{(d)} M_2^{(d)} M_3^{(d)}).
\end{aligned}
\tag{139}
$$

Here the index d indicates that the corresponding quantity is the component in d-th direction. For later use, it is useful to visualize the three-point coupling like Feynman diagram in Fig. 3.

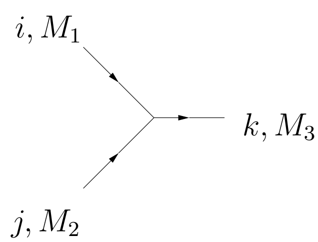

Figure 3: A three-point coupling provides a building block of higher order couplings. This diagram corresponds to the three-point coupling (139). The direction of an arrow depends on the holomorphicity of the corresponding external state.

3.4 Higher order coupling

3.4.1 Four-point coupling

We calculate the four-point coupling

$$
y_{ijk\bar{l}} \equiv \int d^2z \ \psi^{i,M_1}(z) \psi^{j,M_2}(z) \psi^{k,M_3}(z) \left(\psi^{l,M_4}(z) \right)^*, \tag{140}
$$

and represent it in various ways. The main result is that the four-point coupling can be expanded by three-point couplings. Thus by iteration, we can generalize it to higher order couplings.

We consider the case without Wilson lines, since the generalization is straightforward. The product of the first two wavefunctions $\psi^{i,M_1}(z)\psi^{j,M_2}(z)$ in (140) is the same as in (124). Again, we suppose $M_1 + M_2 + M_3 = M_4$. Then the product of the first three

wavefunctions $\psi^{i,M_1}(z)\psi^{j,M_2}(z)\psi^{k,M_3}(z)$ in (140) gives

$$\sum_{m\in\mathbf{Z}_{M_1+M_2}}\sum_{n\in\mathbf{Z}_{M_4}}\psi^{i+j+k+M_1m+(M_1+M_2)n,M_4}(z)\ \vartheta\begin{bmatrix}\frac{M_2i-M_1j+M_1M_2m}{M_1M_2(M_1+M_2)}\\ 0\end{bmatrix}(0,\tau M_1M_2(M_1+M_2))$$
$$\times\vartheta\begin{bmatrix}\frac{M_3(i+j+M_1m)-(M_1+M_2)k+(M_1+M_2)M_3n}{(M_1+M_2)M_3M_4}\\ 0\end{bmatrix}(0,\tau(M_1+M_2)M_3M_4). \tag{141}$$

Now, we product the last wavefunction $\left(\psi^{l,M_4}(z)\right)^*$ in (140), acting on the first factor in (141), yielding the Kronecker delta $\delta_{i+j+k+M_1m+(M_1+M_2)n,l}$. The relation is given modulo M_4, reflecting that i,j,k,l are defined modulo M_1,M_2,M_3,M_4, respectively. It is non-vanishing if there is r such that

$$i+j+k+M_1m+(M_1+M_2)n=l+M_4r. \tag{142}$$

We solve the constraint equation in terms of n.

For $\gcd(M_1,M_2,M_3)=1$, any coupling specified by (i,j,k,l) satisfies the constraint. For a coupling $y_{ijk\bar{l}}$ with fixed (m,r) there is always a unique n satisfying the constraint. This means that by solving the constraint equation in terms of n, we can remove the summation over n in (141). The result is

$$y_{ijk\bar{l}}=\sum_{m\in\mathbf{Z}_{M_1+M_2}}\vartheta\begin{bmatrix}\frac{M_2i-M_1j+M_1M_2m}{M_1M_2M}\\ 0\end{bmatrix}(0,\tau M_1M_2M)\cdot\vartheta\begin{bmatrix}\frac{M_3l-M_4k+M_3M_4r}{MM_3M_4}\\ 0\end{bmatrix}(0,\tau M_3M_4M), \tag{143}$$

where $M=M_1+M_2=-M_3+M_4$. This form (143) is expressed in terms of only 'external lines', i,j,k,l, and in the 'internal line' r is uniquely fixed by m from the relation (142). This is to be interpreted as expansion in terms of three-point couplings (133). From the property of the theta function, we have relations like $y_{ij\bar{k}}=y^*_{\bar{i}\bar{j}k}$, etc. Thus we can write

$$y_{ijk\bar{l}}=\sum_{m\in\mathbf{Z}_{M_1+M_2}}y_{ij\bar{m}}(m)\cdot y_{km\bar{l}}(r), \tag{144}$$

where m and r are uniquely related by the relation (142). Recall that three-point coupling can be expressed in terms of 'two external lines' depending on the 2-3 'picture.'

The result (143) can be written by arranging the summation of quantum numbers as follows,

$$y_{ijk\bar{l}}=\sum_{s\in\mathbf{Z}_{M_1+M_2}}\vartheta\begin{bmatrix}\frac{M_2s-Mj+M_2Mr}{M_1M_2M}\\ 0\end{bmatrix}(0,\tau M_1M_2M)\cdot\vartheta\begin{bmatrix}\frac{-Ml+M_4s+MM_4n}{M_3M_4M}\\ 0\end{bmatrix}(0,\tau M_3M_4M). \tag{145}$$

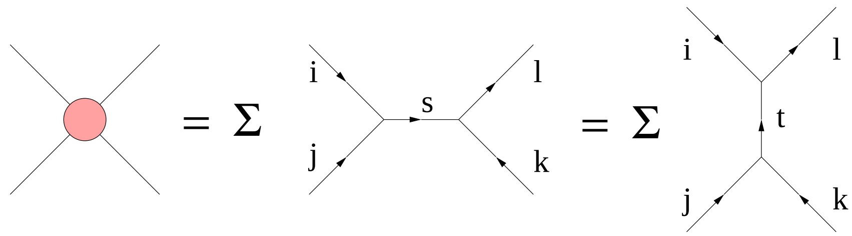

Figure 4: A four-point coupling is decomposed into products of three-point couplings. It also has 'worldsheet' duality. We have another 'u-channel' diagram.

Here, we rewrite (142)

$$\begin{aligned} i + j + M_1 m &= s + (M_1 + M_2) r, \\ -k + l + M_3 r &= s + (M_1 + M_2) n, \end{aligned} \tag{146}$$

by introducing an auxiliary label s, defined modulo $M = M_1 + M_2 = -M_3 + M_4$. This is uniquely fixed by other numbers from (142) and it can be traded with m. Thus we arrive at the second form (145), which becomes

$$y_{ijk\bar{l}} = \sum_{s \in \mathbf{Z}_{M_1+M_2}} y_{ij\bar{s}} \cdot y_{ks\bar{l}}. \tag{147}$$

The second expression (145), explicitly depends on the 'internal line' s. It is useful to track the intermediate quantum number s.

We saw that in the case $\gcd(M_1, M_2) = 1$, there is a unique solution. Since we expand higher order coupling in terms of three-point couplings, if any of them have degeneracies as in (134), i.e., $\gcd(M_i, M_j) = g_{ij} > 1$, we should take into account their effects. It is interpreted that each three-point coupling contains a flavor symmetry $\mathbf{Z}_{g_{ij}}$ [57]. For the four-point coupling with $\gcd(M_1, M_2) = g_{12}$ and $\gcd(M_3, M_4) = g_{34}$ we have also $\gcd(g_{12}, g_{34}) = g = \gcd(M_1, M_2, M_3, M_4)$, without loss of generality (see below). Employing the 'intermediate state picture', or the (j-s) $\times$ (s-l) picture, in the last expression in (145), we have

$$\begin{aligned} \sum_{p \in \mathbf{Z}_g} \sum_{s \in \mathbf{Z}_{M_1+M_2}} & \vartheta \begin{bmatrix} \frac{M_2 s - M j + M_2 M r}{(M - M_2) M_2 M} + \frac{p}{g} \\ 0 \end{bmatrix} (0, \tau (M - M_2) M_2 M) \\ & \times \vartheta \begin{bmatrix} \frac{-M l + M_4 s + M M_4 n}{M M_4 (M_4 - M)} + \frac{p}{g} \\ 0 \end{bmatrix} (0, \tau M M_4 (M_4 - M)). \end{aligned} \tag{148}$$

It shows that the two symmetries $\mathbf{Z}_{g_{12}}$ and $\mathbf{Z}_{g_{34}}$ are broken down to the largest common symmetry $\mathbf{Z}_g$, due to the constraint. Otherwise we cannot put together the vertices with the common intermediate state s.

Reminding that we are examining the overlap of four wavefunctions, and it *does not depend on the order of product*. If we change the order of the product in (140), namely

consider the product of the second and the third wavefunctions $\psi^{j,M_2}(z)\psi^{k,M_3}(z)$ first, we have differently-looking constraint relation which is equivalent to (142) undergoing the decomposition,

$$\begin{aligned} j+k+M_2m' &= t+(M_2+M_3)r', \\ -i+l+M_1r' &= t+(M_2+M_3)n'. \end{aligned} \tag{149}$$

This looks like the 't-channel' and we have

$$\begin{aligned} y_{ijk\bar{l}} &= \sum_{t\in\mathbf{Z}_{M'}} \vartheta\begin{bmatrix} \frac{M_3t-M'k+M_3M'r'}{(M'-M_3)M_3M'} \\ 0 \end{bmatrix}(0,\tau(M'-M_3)M_3M') \\ &\qquad\qquad \times\vartheta\begin{bmatrix} \frac{-M'l+M_1t+M'M_1n}{M'M_1(M_1-M')} \\ 0 \end{bmatrix}(0,\tau M'M_1(M_1-M')) \\ &= \sum_{t\in\mathbf{Z}_{M'}} y_{i\bar{l}t}\cdot y_{jk\bar{t}}, \end{aligned} \tag{150}$$

with $M'=-M_1+M_4=M_2+M_3$. The result has a behavior like 'worldsheet' *duality* in those of Veneziano and Virasoro–Shapiro [76]. This means that, in decomposing the diagram, the position of an insertion does not matter.

If we have Wilson lines, we just replace the three-point couplings by those with Wilson lines (139).

3.4.2 Generic L-point coupling

We have seen that the four point coupling is expanded in terms of three-point couplings. We can generalize the result to obtain arbitrary higher order couplings. The constraint relations and the higher order couplings are always decomposed into products of three-point couplings. It is easily calculated by Feynman-like diagram.

The decompositions (143),(145),(150) are understood as inserting the identity expanded by the complete set of orthonormal eigenfunctions $\{\psi_n^{i,M}\}$ as follows. For example, we split the integral (140) as

$$y_{ijk\bar{l}} = \int d^2z d^2z' \ \psi^{i,M_1}(z)\psi^{j,M_2}(z)\delta^2(z-z')\psi^{k,M_3}(z')\left(\psi^{l,M_4}(z')\right)^*. \tag{151}$$

Then, we use the complete set of orthonormal eigenfunctions $\{\psi_n^{i,M}\}$ of the Hamiltonian with a magnetic flux M. That is, they satisfy

$$\sum_{s,n}\left(\psi_n^{s,M}(z)\right)^*\psi_n^{s,M}(z') = \delta^2(z-z'). \tag{152}$$

We insert LHS instead of the delta function $\delta^2(z-z')$ in (151). Since $\psi^{i,M_1}(z)\psi^{j,M_2}(z)$ is decomposed in terms of $\psi_n^{s,M_1+M_2}(z)$, it is convenient to take $M=M_1+M_2$ for inserted wavefunctions $\left(\psi_n^{s,M}(z)\right)^*\psi_n^{s,M}(z')$. In such a case, only zero-modes of $\psi_n^{s,M}(z)$ appear in

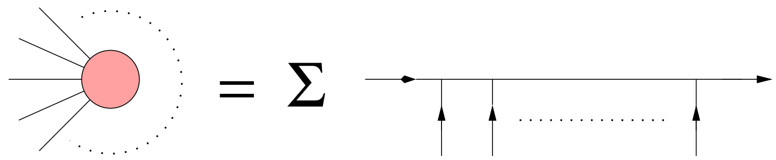

Figure 5: Likewise, any amplitude with arbitrary external lines is decomposed into product of three-point amplitudes.

this decomposition. If we take $M \neq M_1 + M_2$, higher modes of $\psi_n^{s,M}(z)$ would appear. At any rate, when we take $M = M_1 + M_2$, we can lead to the result (145) and (144). On the other hand, we can split

$$y_{ijk\bar{l}} = \int d^2z d^2z' \; \psi^{j,M_2}(z)\psi^{k,M_3}(z)\delta^2(z-z')\psi^{i,M_1}(z') \left(\psi^{l,M_4}(z')\right)^*, \tag{153}$$

and insert (152) with $M = M_2 + M_3$. Then, we can lead to (150). Furthermore, we can calculate the four-point coupling after splitting

$$y_{ijk\bar{l}} = \int d^2z d^2z' \; \psi^{i,M_1}(z)\psi^{k,M_3}(z)\delta^2(z-z')\psi^{j,M_2}(z') \left(\psi^{l,M_4}(z')\right)^*. \tag{154}$$

How to split corresponds to 's-channel', 't-channel' and 'u-channel'. Note that only zero-modes appear in 'intermediate states', when we take proper values of M because of the product property.

We have considered the four-point couplings with $M_1 + M_2 + M_3 = M_4$ for $M_i > 0$. We may consider the case with $M_1 + M_2 = M_3 + M_4$ for $M_i > 0$, which corresponds to

$$y_{ij\bar{k}\bar{l}} \equiv \int d^2z \; \psi^{i,M_1}(z)\psi^{j,M_2}(z) \left(\psi^{k,M_3}(z)\right)^* \left(\psi^{l,M_4}(z)\right)^*. \tag{155}$$

In order to consider both of this case and the previous case at the same time, we would have more symmetric expression for the four-point coupling

$$y_{ijkl} = \int d^2z \; \psi^{i_1,M_1}(\tilde{z})\psi^{i_2,M_2}(\tilde{z})\psi^{i_3,M_3}(\tilde{z})\psi^{i_4,M_4}(\tilde{z}), \tag{156}$$

by defining

$$\psi^{i,-M}(\bar{z}) \equiv \left(\psi^{i,M}(z)\right)^*, \tag{157}$$

with

$$M_1 + M_2 + M_3 + M_4 = 0,$$

where some of M_i are negative, and $\tilde{z} = z$ for $M > 0$ and $\tilde{z} = \bar{z}$ for $M < 0$.

We can extend the above calculation to the L-point coupling,

$$y_{i_1 i_2 \ldots i_L} \equiv \int d^2z \prod_{j=1}^{L} \psi^{i_j,M_j}(\tilde{z}), \tag{158}$$

with the extension as in (157). We have then the selection rule

$$\sum_{j=1}^{L} M_j = 0, \tag{159}$$

where some of M_j are negative. The constraint is given as

$$\sum_{j=1}^{L} \left(i_j + \left(\sum_{l=1}^{j} M_l \right) r_j \right) = 0. \tag{160}$$

Again, it shows the conservation of the total flavor number i_j, reflecting the fact that each i_j is defined modulo M_j. We can decompose L-point coupling into $(L-1)$ and three-point couplings

$$\begin{aligned} \sum_{j=1}^{L-3} \left(i_j + \left(\sum_{l=1}^{j} M_l \right) r_j \right) + i_{L-2} &= s - K r_{L-1}, \\ i_{L-1} + i_L + M_{L-1} r_{L-1} &= -s - K r_{L-2}, \end{aligned} \tag{161}$$

where

$$K = \sum_{k=1}^{L-2} M_i = -M_{L-1} - M_L, \tag{162}$$

is the intermediate quantum number. Therefore if $\gcd(M_1, M_2, \dots, M_L) = 1$, by induction we see that there is a unique solution by Euclidean algorithm. By iteration

$$y_{i_1 i_2 \dots i_L} = \sum_s y_{i_1 i_2 \dots i_{L-2} s} \cdot y_{\bar{s} i_{L-1} i_L}, \tag{163}$$

we can obtain the coupling including the normalization. Thus, we can obtain L-point coupling out of $(L-1)$-point coupling. Due to the independence of ordering, we can insert (or cut and glue) any node.

As an illustrating example we show the result for the five-point coupling. We employ s-channel-like insertions, by naming intermediate quantum numbers s_i as in Fig. 6. We have

$$\begin{aligned} y_{i_1 i_2 i_3 i_4 i_5} &= \prod_{j=1}^{5} \vartheta \begin{bmatrix} i_j/M_j \\ 0 \end{bmatrix} (z M_i, \tau M_i) \\ &= \sum_{s_1, s_2} \vartheta \begin{bmatrix} \frac{M_2 s_1 - (M_1+M_2) i_2 + M_2 (M_1+M_2) l_1}{M_2 (M_1+M_2)(M_1+2M_2)} \\ 0 \end{bmatrix} (0, M_1 M_2 (M_1 + M_2) \tau) \\ &\quad \times \vartheta \begin{bmatrix} \frac{(M_1+M_2) i_3 - M_3 s_1 + M_3 (M_1+M_2) l_2}{M_3 (M_1+M_2)(M_1+M_2+M_3)} \\ 0 \end{bmatrix} (0, (M_1 + M_2) M_3 (M_1 + M_2 + M_3)) \\ &\quad \times \vartheta \begin{bmatrix} \frac{(M_1+M_2+M_3) i_4 - M_4 s_2 + M_4 (M_1+M_2+M_3) l_3}{M_4 (M_1+M_2+M_3)(M_1+M_2+M_3+M_4)} \\ 0 \end{bmatrix} (0, -(M_4 + M_5) M_4 M_5 \tau), \end{aligned} \tag{164}$$

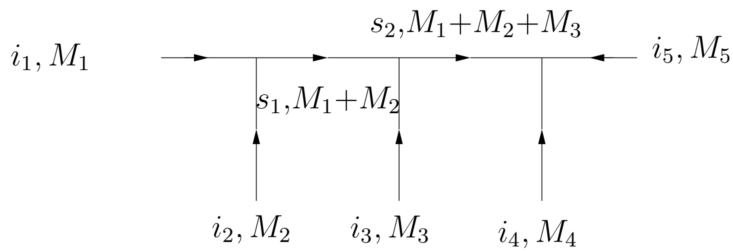

Figure 6: Five-point coupling. No more independent Feynman-like diagram for different insertion.

where

$$s_1 \in \mathbf{Z}_{M_1+M_2}, \quad s_2 \in \mathbf{Z}_{M_1+M_2+M_3}.$$

From the regular patterns of increasing orders, we can straightforwardly generalize the couplings to arbitrary order.

Now, taking into account full six internal dimensions, as in three-coupling case (139), we have various normalization factors besides the product of theta functions. Again, from the product relation of theta function (123) we have

$$\begin{aligned} & s_L g_{\rm YM}^{L-2} \alpha'^{(L-4+L_\chi/2)/2} \\ & \times \prod_{d=1}^3 \left(\frac{2{\rm Im}\tau_d}{A_d^2} \sum_{M_i^{(d)}>0} |M_i^{(d)}| \right)^{-\frac14} \left(\frac{2{\rm Im}\tau_d}{A_d^2} \sum_{M_i^{(d)}<0} |M_i^{(d)}| \right)^{-\frac14} \prod_{i=1}^L \left(\frac{2{\rm Im}\tau_d |M_i^{(d)}|}{A_d^2} \right)^{\frac14}. \end{aligned} \tag{165}$$

Recall that L_χ is the number of fermions in the couplings (126). We have $g_L^{10} = s_L g_{\rm YM}^{L-2}$ $\alpha'^{(L-4+L_\chi/2)/2}$ in (127), where symmetric factor s_L comes from higher order expansions of lower-level completion of Yang–Mills theory, having also an expansion parameter α'. In open string theory, it is the Dirac–Born–Infeld action, and it is unknown beyond the quartic order in $\alpha' F$ [77]. The dependence of ten-dimensional gauge coupling $g_{\rm YM}$ and Regge slope α' can be easily accounted by order counting [78]. Note that $g_{\rm YM}$ is dimensionful. This factor (165) is non-holomorphic in the complex structure τ and complexified Kähler modulus $\alpha' J = B + iA/4\pi^2$, where $B_{z^d \bar z^d}$ is the antisymmetric tensor field component in d-th two-torus. They are interpreted as originating from the Kähler potential [52, 74]. The product $\prod M_i^{1/4}$ is the leading order approximation of Euler beta function and its multivariable generalization, which is the property of dual amplitude.

As an example of full expressions, we show the four-point coupling among scalar fields, $Y_{ij\bar l \bar m} \phi^i \phi^j (\phi^l)^* (\phi^m)^*$, where ϕ^i and $(\phi^l)^*$ (ϕ^j and $(\phi^m)^*$) correspond to the magnetic flux $M_1^{(d)}$ ($M_2^{(d)}$). For simplicity, we consider the case with vanishing Wilson lines and $\gcd(M_1, M_2) = 1$. The full coupling $Y_{ij\bar l \bar m}$ is obtained as

$$Y_{ij\bar l \bar m} = g_{\rm YM}^2 \prod_{d=1}^3 \left(\frac{2{\rm Im}\tau_d}{A_d^2} \frac{M_1^{(d)} M_2^{(d)}}{M_3^{(d)}} \right)^{1/2} \sum_{k \in \mathbf{Z}_{M_1^{(d)}+M_2^{(d)}}} y_{ij\bar k}^{(d)} \, (y^{(d)})^*_{k \bar l \bar m}, \tag{166}$$

up to s_L, where

$$y^{(d)}_{ij\bar{k}} = \vartheta \begin{bmatrix} \frac{M_2^{(d)}k - M^{(d)}j + M_2^{(d)}M^{(d)}r}{M_1^{(d)}M_2^{(d)}M^{(d)}} \\ 0 \end{bmatrix} (0, \tau_d M_1^{(d)} M_2^{(d)} M^{(d)}). \tag{167}$$

This scalar coupling with $s_L = 1$ appears from ten-dimensional super Yang-Mills theory and satisfies the relation $Y_{ij\bar{l}\bar{m}} = Y_{ij\bar{k}}(Y)^*_{k\bar{l}\bar{m}}$ for the three-point coupling $Y_{ij\bar{k}}$ in eq. (139).

3.5 Intersecting D-brane models

Here we give comments on the relation between the results in the previous sections and higher order couplings in intersecting D-brane models, i.e. CFT-calculations.

There is well-known T-duality relation between magnetized and intersecting brane models. In intersecting brane case, the wavefunctions are highly localized around intersection points, whereas magnetized brane wavefunctions are fuzzily delocalized over the entire space.

Under the 'horizontal' duality with respect to real axis, $y_i \leftrightarrow 2\pi\alpha' A_i$. The parameter is changed as

$$\tau \leftrightarrow J, \quad \zeta \leftrightarrow \nu. \tag{168}$$

Still the translational offset ν is the Wilson line. Thus, the magnetic flux gives the slope $A^i_{\bar{z}} = -\frac{i}{2}F^i_{z\bar{z}}z = \frac{\pi}{\mathrm{Im}\tau}M_i$ and the corresponding quantum number is the 'relative angle,' for small angles,

$$\pi\theta_i = \frac{M_i}{\mathrm{Im}J}. \tag{169}$$

The selection rule due to the gauge invariance becomes

$$M_1 + M_2 = M_3 \leftrightarrow \theta_1 + \theta_2 = \theta_3. \tag{170}$$

In the intersecting brane case, as well as heterotic string case, there have been CFT calculation of higher order amplitude [79, 80, 81] using vertex operator insertion [10, 26, 82, 83]. There are vertex operators V_i corresponding to massless modes. We compute their L-point amplitude,

$$\langle V_1 V_2 \ldots V_L \rangle. \tag{171}$$

We have operator product expansion (OPE),

$$V_i(z)V_j(0) \sim \sum_k \frac{c_{ijk}}{z^{h_{ijk}}} V_k(0), \tag{172}$$

with $h_{ijk} = h(V_k) - h(V_i) - h(V_j)$, where $h(V_l)$ is the conformal dimension of V_l. This OPE corresponds to (124). Furthermore, the coefficients c_{ijk} correspond to the three-point couplings in four-dimensional effective field theory. In Ref. [52], it is shown that the above three-point coupling c_{ijk} in intersecting D-brane models corresponds to the T-dual of the three-point couplings Y_{ijk} in magnetized D-brane models.

Now, let us consider the L-point amplitude $\langle \prod_i V_i(z_i) \rangle$. We use the OPE (172) to write the L-point amplitude in terms of $(L-1)$ point amplitudes. Such a procedure is similar to one in the previous sections, where we write L-point couplings in terms of three-point couplings.

For example, the CFT calculations for the four-point couplings c_{ijkl} in the intersecting D-brane models would lead

$$c_{ijkl} \sim \sum_s c_{ij\bar{s}} c_{skl}, \tag{173}$$

and

$$c_{ijkl} \sim \sum_t c_{ik\bar{t}} c_{tjl}, \tag{174}$$

depending on the order of OPE's, i.e. s-channel or t-channel. Thus, the form of the four-point couplings as well as L-point couplings ($L > 4$) is almost the same as the results in the previous sections. Note that in eq.(124), a product of two wavefunctions is decomposed in terms of only the lowest modes. On the other hand, in RHS of Eq. (172), higher modes as well as lowest modes may appear. However, dominant contribution due to the lowest modes are the same, because c_{ijk} for the lowest modes (i, j, k) corresponds exactly to Y_{ijk} for the lowest modes.

Let us examine the correspondence of couplings between magnetized models and intersecting D-brane models by using concrete formulae. In the intersecting D-brane models, the amplitude (171) is decomposed into the classical and the quantum parts,

$$\langle V_1 V_2 \dots V_L \rangle = \mathcal{Z}_{\rm qu} \cdot \mathcal{Z}_{\rm cl} = \mathcal{Z}_{\rm qu} \cdot \sum_{\{X_{\rm cl}\}} \exp(-S_{\rm cl}), \tag{175}$$

where $X_{\rm cl}$ is the solution to the classical equation of motion. The classical part is formally characterized as decomposable part and physically gives instanton of worldsheet nature, via the exchange of intermediate string. That gives intuitive understanding via the 'area rule', where the area corresponds to one, which intermediate string sweeps.

In the three-point amplitude, the summation of the classical action $\sum_{\{X_{\rm cl}\}} \exp(-S_{\rm cl})$ becomes the theta function [26], where $S_{\rm cl}$ corresponds to the triangle area. When we exchange τ and J as (168) in the magnetized models, the Yukawa coupling (133) corresponds to the following expansion

$$\begin{aligned} y_{ij\bar{k}} &= \vartheta \begin{bmatrix} \frac{M_2 k - M_3 j + M_2 M_3 l}{M_1 M_2 M_3} \\ 0 \end{bmatrix} \left(0, i M_1 M_2 M_3 A/(4\pi^2 \alpha')\right) \\ &= \sum_{n \in \mathbf{Z}} \exp\left[-\frac{M_1 M_2 M_3 A}{4\pi\alpha'} \left(\frac{M_2 k - M_3 j + M_2 M_3 l}{M_1 M_2 M_3} + n \right)^2 \right], \end{aligned} \tag{176}$$

by using the definition (122). We have neglected the antisymmetric tensor component B. The exponent corresponds to the area (divided by $4\pi\alpha'$) of possible formation of triangles and the one with $n = 0$ corresponds to the minimal triangle. Recall that the theta function part depends on only τ and J in magnetized and intersecting D-brane models, respectively.

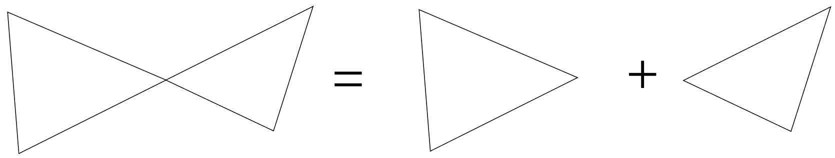

Figure 7: Area of polygon, responsible for the classical part exponent, is decomposed in terms of those of three point functions.

We have omitted the normalization factor, corresponding to the quantum part $\mathcal{Z}_{\rm qu}$. It is obtained by comparing the coupling (176) with (139). We find the factor

$$2^{-9/4}\pi^{-3}e^{\phi_4/2}\prod_{d=1}^{3}\left(\mathrm{Im}\tau_d\frac{M_1^{(d)}M_2^{(d)}}{M_3^{(d)}}\right)^{1/4}, \tag{177}$$

in the magnetized brane side corresponds to

$$\mathcal{Z}_{\rm qu}=(2\pi)^{-9/4}e^{\phi_4/2}\prod_{d=1}^{3}\left((\mathrm{Im}J_d)^2\frac{\theta_1^{(d)}\theta_2^{(d)}}{\theta_3^{(d)}}\right)^{1/4}, \tag{178}$$

in the intersecting brane side. We obtain the four dimensional dilaton $\phi_4=\phi_{10}-\ln|\mathrm{Im}\tau_1\mathrm{Im}\tau_2\mathrm{Im}\tau_3|$ from the ten dimensional one ϕ_{10}, which is related with $g_{\rm YM}$ as $g_{\rm YM}=e^{\phi_{10}/2}\alpha'^{3/2}$. The vacuum expectation value of the dilaton gives gauge coupling $e^{\langle\phi_4\rangle/2}=g$. In this case, the factor containing the angles is a leading order approximation of the ratio of Gamma function

$$\frac{\Gamma(1-\theta_1)\Gamma(1-\theta_2)\Gamma(\theta_3)}{\Gamma(\theta_1)\Gamma(\theta_2)\Gamma(1-\theta_3)}\simeq\frac{\theta_1\theta_2}{\theta_3}, \tag{179}$$

valid for small angles. Therefore, the three-point couplings coincide each other between magnetized and intersecting D-brane models. That is the observation of [52].

Now, let us consider the four-point coupling of intersecting D-brane model corresponding to the left figure of Fig. 7. The four-point amplitude is written as (175), where the classical action corresponds to the area of the left figure. However, that can be decomposed into two triangles like the right figure, that is, the classical part can be decomposed into two parts, each of which corresponds to the classical part of three-point amplitude, i.e.

$$\exp(-S_{\rm cl}^{(4)})=\exp(-S_{\rm cl}^{(3)})\exp(-S'^{(3)}_{\rm cl}), \tag{180}$$

where $S_{\rm cl}^{(4)}$ corresponds to the area of the left figure of Fig. 7 and $S_{\rm cl}^{(3)}$ and $S'^{(3)}_{\rm cl}$ correspond to the triangle areas of the right figure.

On the other hand, our results in the previous sections show that the four-point coupling in the magnetized model is also expanded as (145). Each of theta functions in (145) corresponds to the classical parts of the three-point couplings in the intersecting D-brane models. This relation corresponds to the above decomposition (180). Thus, the

theta function parts of the four-point couplings, i.e. the classical part, coincide each other between magnetized and intersecting D-brane models. That means that the holomorphic complex structure, τ, dependence of the four-point couplings in the magnetized brane models is the same as the holomorphic Kähler moduli J dependence in the intersecting D-brane models, since the theta function part in the magnetized (intersecting) D-brane models depends only on τ (J). The other part in the magnetized brane models corresponds to normalization factors N_M. When we take a proper normalization, these factors also coincide.

3.6 Flavor symmetries

We study order L couplings including the three point couplings $L = 3$ in four-dimensional effective theory, i.e.,

$$Y_{i_1 \ldots i_{L_\chi} i_{L_\chi+1} \cdots i_L} \chi^{i_1}(x) \cdots \chi^{i_{L_\chi}}(x) \phi^{i_{L_\chi+1}}(x) \ldots \phi^{i_L}(x), \tag{181}$$

with $L = L_\chi + L_\phi$, where χ and ϕ collectively represent four-dimensional components of fermions and bosons, respectively. In particular, the selection rule for allowed couplings is important. The three-point couplings can appear from the dimensional reduction of ten-dimensional super-Yang–Mills theory and higher order coupling terms can be read off from the effective Lagrangian of the Dirac–Born–Infeld action with supersymmetrization. The internal component of bosonic and fermionic wavefunctions is the same [52]. Thus, the couplings are determined by the wavefunction overlap in the extra dimensions,

$$Y_{i_1 i_2 \ldots i_L} = g_L^{10} \int_{T^6} d^6 z \prod_{d=1}^{3} \psi_d^{i_1, M_1}(z) \psi_d^{i_2, M_2}(z) \ldots \psi_d^{i_L, M_L}(z), \tag{182}$$

where g_L^{10} denotes the coupling in ten dimensions. Here, as mentioned in the previous section, we concentrate on the two-dimensional T^2 part of the overlap integral of wavefunctions,

$$y_{i_1 i_2 \ldots i_L} = \int_{T^2} d^2 z \; \psi^{i_1, M_1}(z) \psi^{i_2, M_2}(z) \ldots \psi^{i_L, M_L}(z), \tag{183}$$

where we have omitted the subscript d, again.

For example, we calculate the three-point couplings,

$$y_{i_1 i_2 \bar{i}_3} = \int d^2 z \; \psi^{i_1, M_1}(z) \psi^{i_2, M_2}(z) \left(\psi^{i_3, M_3}(z)\right)^* . \tag{184}$$

For the moment, we consider the case with vanishing Wilson lines. The gauge invariance requires that $M_1 + M_2 = M_3$ and that the wavefunction $\left(\psi^{i_3, M_3}(z)\right)^*$ but not $\psi^{i_3, M_3}(z)$ appears in the allowed three-point couplings. If these are not satisfied, there is not corresponding operators in the ten dimensions, i.e. $g_3^{10} = 0$. The results are obtained as [52]

$$y_{i_1 i_2 \bar{i}_3} = \sum_{m \in Z_{M_3}} \delta_{i_1 + i_2 + M_1 m, i_3} \; \vartheta \begin{bmatrix} \frac{M_2 i_1 - M_1 i_2 + M_1 M_2 m}{M_1 M_2 M_3} \\ 0 \end{bmatrix} (0, \tau M_1 M_2 M_3), \tag{185}$$

where the numbers in the Kronecker delta is defined modulo M_3. Indeed, the Kronecker delta part leads to the selection rule for allowed couplings as

$$i_1 + i_2 - i_3 = M_3 l - M_1 m, \quad m \in Z_{M_3},\ l \in Z_{M_1}. \tag{186}$$

When $\gcd(M_1, M_2, M_3) = 1$, every combination (i_1, i_2, i_3) satisfies this constraint (186) because of Euclidean algorithm. On the other hand, when $\gcd(M_1, M_2, M_3) = g$, the above constraint becomes

$$i_1 + i_2 - i_3 = 0 \qquad (\ \mathrm{mod}\ g\ ). \tag{187}$$

This implies that we can define Z_g charges from i_k for zero-modes and the allowed couplings are controlled by such Z_g symmetry. Indeed, each quantum number i_k corresponds to quantized momentum defined with the M_i modulo structure. When $\gcd(M_1, M_2, M_3) = g$, the modulo structure becomes Z_g and the conservation law of these discrete momenta corresponds to a requirement due to the Z_g invariance.

Let us consider higher order couplings. In [56], it has been shown that higher order couplings can be decomposed as productions of three-point couplings. For example, we consider the four-point coupling,

$$y_{i_1 i_2 i_3 \bar{i}_4} = \int d^2z\ \psi^{i_1,M_1}(z)\psi^{i_2,M_2}(z)\psi^{i_3,M_3}(z)\left(\psi^{i_4,M_4}(z)\right)^*. \tag{188}$$

This four-point coupling can be decomposed as

$$y_{i_1 i_2 i_3 \bar{i}_4} = \sum_{s \in Z_M} y_{i_1 i_2 \bar{s}}\ y_{s i_3 \bar{i}_4}, \tag{189}$$

where

$$\begin{aligned} y_{i_1 i_2 \bar{s}} &= \int d^2z\ \psi^{i_1,M_1}(z)\psi^{i_2,M_2}(z)\left(\psi^{s,M}(z)\right)^*, \\ y_{s i_3 \bar{i}_4} &= \int d^2z\ \psi^{s,M}(z)\psi^{i_3,M_3}(z)\left(\psi^{i_4,M_4}(z)\right)^*, \end{aligned} \tag{190}$$

with $M = M_1 + M_2 = M_4 - M_3$. Here, $\psi^{s,M}(z)$ denotes the s-th zero-mode of Dirac equation with the relative magnetic flux M, and these modes correspond to intermediate states in the above decomposition. Each of $y_{i_1 i_2 \bar{s}}$ and $y_{s i_3 \bar{i}_4}$ is obtained as eq. (185). That is, the coupling selection rule is controlled by the Z_g invariance (186), i.e. the conservation law of discrete momenta, and its modulo structure is determined by $\gcd(M_1, M_2, M_3, M_4) = g$.

Similarly, higher order couplings are decomposed as products of three-point couplings [56]. Therefore, the above analysis is generalized to generic order L couplings. That is, the coupling selection rule is given as the Z_g invariance and its modulo structure is determined by $\gcd(M_1, \cdots, M_L) = g$.

So far, we have considered the model with vanishing Wilson lines. Non-vanishing Wilson lines do not affect the coupling selection rule due to the Z_g invariance, but change

values of couplings $y_{i_1 i_2 \bar{i}_3}$. For example, when we introduce Wilson lines ζ_k for $\psi^{i_k,M_k}(z)$, the three-point coupling (185) becomes

$$
\begin{aligned}
y_{i_1 i_2 \bar{i}_3} &= \sum_{m\in \mathbf{Z}_{M_3}} \delta_{i_1+i_2+M_1 m, i_3} e^{i\pi(\sum_{k=1}^3 M_k \zeta_k \mathrm{Im}\zeta_k)/\mathrm{Im}\tau} \\
& \quad \times \vartheta \begin{bmatrix} \frac{M_2 i_1 - M_1 i_2 + M_1 M_2 m}{M_1 M_2 M_3} \\ 0 \end{bmatrix} (M_2 M_3(\zeta_2 - \zeta_3), \tau M_1 M_2 M_3),
\end{aligned}
\tag{191}
$$

where Wilson lines must satisfy $\zeta_3 M_3 = \zeta_1 M_1 + \zeta_2 M_2$. Similarly, higher order couplings with non-vanishing Wilson lines can be obtained.

3.7 Non-Abelian Wilson line

In this section we calculate the Yukawa coupling with non-Abelian Wilson lines. Let us consider the following form of the magnetic fluxes,

$$
F = \begin{pmatrix} \frac{m_a}{n_a}\mathbf{1}_{N_a} & & \\ & \frac{m_b}{n_b}\mathbf{1}_{N_b} & \\ & & \frac{m_c}{n_c}\mathbf{1}_{N_c} \end{pmatrix}, \tag{192}
$$

and non-Abelian Wilson lines similar to (50). Then, there are three types of matter fields, $(N_a, \overline{N}_b)$, $(N_b, \overline{N}_c)$, $(N_c, \overline{N}_a)$ and their conjugates under $U(N_a)\times U(N_b)\times U(N_c)$, although they break to $U(P_a)\times U(P_b)\times U(P_c)$ by non-Abelian Wilson lines. We consider the case with $\frac{m_a}{n_a} - \frac{m_b}{n_b} > 0$, $\frac{m_b}{n_b} - \frac{m_c}{n_c} > 0$ and $\frac{m_a}{n_a} - \frac{m_c}{n_c} > 0$. Then, the three types of matter fields whose wavefunctions are denoted by Ψ^{j,M_1}, Ψ^{k,M_2} and $(\Psi^{l,M_3})^*$, appear in the following off-diagonal elements,

$$
\begin{pmatrix} \text{const} & \Psi^{j,M_1} & \\ & \text{const} & \Psi^{k,M_2} \\ (\Psi^{l,M_3})^* & & \text{const} \end{pmatrix}, \tag{193}
$$

where $M_1 = M_{ab}$, $M_2 = M_{bc}$ and $M_3 = M_{ac}$ for simplicity. We use the same indices for Q_{ab} and others, i.e. $Q_1 = Q_{ab}$, $Q_2 = Q_{bc}$ and $Q_3 = Q_{ac}$. As already explained, in the background with fractional fluxes and non-Abelian Wilson lines, their fields are the matrix valued wavefunctions. The Yukawa coupling can be calculated by computing the following overlap integral of zero-modes in the (y_4, y_5) compact space,

$$
y^{jkl}_{1,pqr} = \int_0^1 dy_4 \int_0^1 dy_5 \mathrm{Tr}[\Psi^{j,M_1}_{pq} \Psi^{k,M_2}_{qr} (\Psi^{l,M_3}_{pr})^*]. \tag{194}
$$

The Yukawa coupling Y^{ijk} in 4D effective theory is obtained as their products on $(T^2)^n$, i.e. $Y^{ijk}_{1,pqr} = g_D \prod_{d=1}^{n/2} y^{ijk}_d$, where $y^{ijk}_{d,pqr}$ denotes the overall integral similar to Eq. (194) for the d-th torus (T^2) and g_D is the D-dimensional gauge coupling. From this structure, one can see that the allowed couplings are restricted. In order to see it, we introduce the following parameters as $k_1 = \text{g.c.d.}(n_a, n_b)$, $k_2 = \text{g.c.d.}(n_b, n_c)$, $k_3 = \text{g.c.d.}(n_a, n_c)$

and K = g.c.d.(k_1, k_2, k_3) = g.c.d.(n_a, n_b, n_c). Then the parameter of K determines the allowed couplings of Yukawa interactions. If $K = 1$, all of possible combinations (p, q, r) appear in the above trace (194). However, if $K \neq 1$, only restricted combinations of (p, q, r) appear in Eq. (194), but not all combinations. That is, the couplings are restricted by the Z_K symmetry. Indeed, allowed combinations of (p, q, r) are controlled by the gauge invariance before the gauge symmetry breaking. This Z_K symmetry is unbroken symmetry in the original gauge symmetry.

Now, let us consider the following summation of wavefunction products,

$$\begin{aligned} I^{jkl}_{pqr} &= \Psi^j_{pq}\Psi^k_{qr}(\Psi^l_{pr})^* + \Psi^j_{p+1,q+1}\Psi^k_{q+1,r+1}(\Psi^l_{p+1,r+1})^* \\ &\quad + \cdots + \Psi^j_{p+Q-1,q+Q-1}\Psi^k_{q+Q-1,r+Q-1}(\Psi^l_{p+Q-1,r+Q-1})^*, \end{aligned}$$

where $Q = \mathrm{l.c.m.}(Q_1, Q_2, Q_3)$. One can represent Q as $Q = Q_1 q_1 = Q_2 q_2 = Q_3 q_3$. To compute the integral it is useful to represent the wavefunctions as follows

$$\begin{aligned} \tilde{\Psi}^{j',M'_1}(y_4, y_5)_{pq} &= C^{j'}_{pq} e^{-\pi \frac{M'_1}{Q} y_5^2} \vartheta \begin{bmatrix} \frac{j'}{M'_1} \\ 0 \end{bmatrix} \left(\frac{M'_1}{Q} z + \left(\frac{m_a}{n_a} p - \frac{m_b}{n_b} q \right), \frac{M'_1}{Q} \tau \right), \\ \tilde{\Psi}^{k',M'_2}(y_4, y_5)_{qr} &= C^{k'}_{qr} e^{-\pi \frac{M'_2}{Q} y_5^2} \vartheta \begin{bmatrix} \frac{k'}{M'_2} \\ 0 \end{bmatrix} \left(\frac{M'_2}{Q} z + \left(\frac{m_b}{n_b} q - \frac{m_c}{n_c} r \right), \frac{M'_2}{Q} \tau \right), \\ \tilde{\Psi}^{l',M'_3}(y_4, y_5)_{pr} &= C^{l'}_{pr} e^{-\pi \frac{M'_3}{Q} y_5^2} \vartheta \begin{bmatrix} \frac{l'}{M'_3} \\ 0 \end{bmatrix} \left(\frac{M'_3}{Q} z + \left(\frac{m_a}{n_a} p - \frac{m_c}{n_c} r \right), \frac{M'_3}{Q} \tau \right), \end{aligned} \qquad (195)$$

where $j' = q_1 j$ $k' = q_2 k$, $l' = q_3 l$ and $M'_i = q_i M_i$, $(i = 1, 2, 3)$. Here the relation $M'_1 + M'_2 = M'_3$ holds. By using the production property of the theta function, the product of $\Psi^{j,M_1}\Psi^{k,M_2}$ is represented by the sum of the theta functions as

$$\begin{aligned} \tilde{\Psi}^{j,M_1}_{pq}\tilde{\Psi}^{k,M_2}_{qr} = C^{j'}_{pq} C^{k'}_{qr} e^{\pi \frac{M'_3}{Q} y_5^2} \sum_{m \in Z_{M'_3}} \vartheta \left[\frac{j' + k' + M'_1 m}{M'_3} \right] \left(\frac{M'_3}{Q} z + \left(\frac{m_a}{n_a} p - \frac{m_c}{n_c} r \right), \frac{M'_3}{Q} \tau \right) \\ \times \vartheta \left[\frac{M'_2 j' - M'_1 k' + M'_1 M'_2 m}{M'_1 M'_2 M'_3} \right] \left(\frac{m_a}{n_a} M'_2 p - \frac{m_b}{n_b} M'_2 q - \frac{m_b}{n_b} M'_1 q + \frac{m_c}{n_c} M'_1 r, \frac{M'_1 M'_2 M'_3}{Q} \tau \right). \end{aligned} \qquad (196)$$

Here one can use the properties of boundary conditions for non-Abelian Wilson lines. Using the property of $\Psi_{p,q}(y_4 + 1, y_5) = \Psi_{p+1,q+1}(y_4, y_5)$ the overlap integral reduces to the following integral

$$\int_0^1 dy_4 \int_0^1 dy_5 I^{ijk}_{pqr} = \int_0^Q dy_4 \int_0^1 dy_5 \Psi^i_{pq} \Psi^j_{qr} (\Psi^k_{rp})^* \qquad (197)$$

where Q is again defined by $Q = \mathrm{l.c.m.}(Q_1, Q_2, Q_3)$. Therefore we can obtain the analytic form of Yukawa couplings and similar flavor structures to the case with Abelian Wilson lines. By using the orthogonal condition for the matrix valued wavefunctions as

$$\int_0^Q dy_4 \int_0^1 dy_5 \Psi^{j,M_1}_{pq} (\Psi^{k,M_1}_{pq})^\dagger = \delta_{j,k}, \qquad (198)$$

one can lead the following form of Yukawa couplings

$$\int_0^Q dy_4 \int_0^1 dy_5 \Psi^i_{pq}\Psi^j_{qr}(\Psi^k_{rp})^* = N_{M_1}N_{M_2}N^*_{M_3}C^j_{pq}C^k_{qr}(C^l_{pr})^* Q\sqrt{\frac{Q}{2M'_3}} \sum_{m\in Z_{M'_3}} \delta_{j'+k'+M'_1m,\ l'(\mathrm{mod}M'_3)}$$

$$\times\vartheta\begin{bmatrix}\frac{M'_2j'-M'_1k'+M'_1M'_2m}{M'_1M'_2(M'_3)}\\ 0\end{bmatrix}\left(Q\left(\frac{m_a}{n_a}\tilde{I}_{bc}p+\frac{m_b}{n_b}\tilde{I}_{ca}q+\frac{m_c}{n_c}\tilde{I}_{ab}r\right),\frac{M'_1M'_2M'_3}{Q}\tau\right) \quad (199)$$

Here, the Kronecker delta $\delta_{j'+k'+M'_1m,\ l'(\mathrm{mod}M'_3)}$ leads to the coupling selection rule

$$j'+k'+M'_1m = l' \mod M'_3, \quad (200)$$

where $m = 0,1,...,M'_3-1$. When $g = \text{g.c.d.}(M'_1,M'_2,M'_3) = \text{g.c.d.}(M_1,M_2,M_3)$, the coupling selection rule is given by

$$j'+k' = l' \mod g. \quad (201)$$

That means that we can assign Z_g charges to all of zero-modes.[12]

Here we study again the Z_K symmetry, which we showed. The total number of multiplicity of Ψ_{ab} is nothing but $|I_{ab}|$, and it is represented by two parameters of k_{ab} and M_{ab} as $I_{ab} = k_{ab}M_{ab}$. If $K = \text{g.c.d.}(k_{ab},k_{bc},k_{ca}) \neq 1$, they are divided to K types of zero-modes and distinguished by labeling the component of each matrix. We introduce such a kind of flavor indices as $\tilde{j},\tilde{k}$ and $\tilde{l}$ for *ab*-, *bc*-, *ca*-sectors, respectively. We define the relation between the flavor labeled by $\tilde{j}$ and the component of matrix p,q as $\tilde{j} = p-q \mod k_1$. Similarly the other sectors are also defined as $\tilde{k} = q-r \mod k_2$ and $\tilde{l} = p-r \mod k_3$. Since the allowed couplings must be gauge invariance, there is the coupling selection rule for this kind of flavor indices, which is given by

$$\tilde{j}+\tilde{k} = \tilde{l} \mod K. \quad (202)$$

This is because the Yukawa couplings are restricted in the trace of the matrix. Therefore we find two types of coupling selection rules, i.e. the Z_g and Z_K symmetries.

We can extend the computation of 3-point couplings to higher order couplings. For example, we show the computation of 4-point couplings. We assume that $\tilde{I}_{ab}$, $\tilde{I}_{bc}$, $\tilde{I}_{cd} > 0$ and $\tilde{I}_{da} < 0$. Four zero-mode wavefunctions are written as

$$\begin{aligned}
\psi^{j,M_1}_{pq} &= C_{pq}e^{-\pi\frac{M'_1}{Q}y_5^2}\vartheta\begin{bmatrix}j'/M'_1\\0\end{bmatrix}\left(\frac{M'_1}{Q}z+(\frac{m_a}{n_a}p-\frac{m_b}{n_b}q),\frac{M'_1}{Q}\tau\right),\\
\psi^{k,M_2}_{qr} &= C_{qr}e^{-\pi\frac{M'_2}{Q}y_5^2}\vartheta\begin{bmatrix}k'/M'_2\\0\end{bmatrix}\left(\frac{M'_2}{Q}z+(\frac{m_b}{n_b}q-\frac{m_c}{n_c}r),\frac{M'_2}{Q}\tau\right),\\
\psi^{l,M_3}_{rs} &= C_{rs}e^{-\pi\frac{M'_3}{Q}y_5^2}\vartheta\begin{bmatrix}l'/M'_3\\0\end{bmatrix}\left(\frac{M'_3}{Q}z+(\frac{m_c}{n_c}r-\frac{m_d}{n_d}s),\frac{M'_3}{Q}\tau\right),\\
\psi^{t,M_4}_{ps} &= C_{ps}e^{-\pi\frac{M'_4}{Q}y_5^2}\vartheta\begin{bmatrix}t'/M'_4\\0\end{bmatrix}\left(\frac{M'_4}{Q}z+(\frac{m_a}{n_a}p-\frac{m_d}{n_b}s),\frac{M'_4}{Q}\tau\right),
\end{aligned}$$

[12]See Refs. [26, 75] for a similar selection rule in intersecting D-brane models.

where Q is defined as $Q = \text{l.c.m.}(n_a, n_b, n_c, n_d)$. First, the product of ψ_{pq}^{j,M_1} and ψ_{qr}^{k,M_2} becomes

$$\psi_{pq}^{j,M_1}\psi_{qr}^{k,M_2} = C_{pq}C_{qr}e^{-\pi\frac{M'}{Q}y_5^2}\sum_{m\in Z_{M'}}\vartheta\begin{bmatrix}\frac{j'+k'+M_1'm}{M'}\\0\end{bmatrix}\left(\frac{M'}{Q}z+(\frac{m_a}{n_a}p-\frac{m_c}{n_c}r),\frac{M'}{Q}\tau\right)$$
$$\times\vartheta\begin{bmatrix}\frac{M_2'j'-M_1'k'+M_1'M_2'm}{M_1'M_2'M'}\end{bmatrix}\left(M_2'(\frac{m_a}{n_a}p-\frac{m_b}{n_b}q)-M_1'(\frac{m_b}{n_b}q-\frac{m_c}{n_c}r),\frac{M_1'M_2'M'}{Q}\tau\right) \quad (203)$$

where $M' = M_1' + M_2'$. Then we repeat this product for ψ_{rs}^{l,M_3} and use the orthogonal condition for the M_4' sector because $M_1' + M_2' + M_3' = M' + M_3' = M_4'$ hold by definition. Finally we obtain the overlap integral for four wavefunctions as

$$Y_{pqrs}^{jklt} = C_{pq}^{j}C_{qr}^{k}C_{rs}^{l}(C_{ps}^{t})^*Q\sqrt{\frac{M_4'}{Q}}\sum_{m\in Z_{M'}}\sum_{n\in Z_{M_4'}}\delta_{j'+k'+M_1'm+l'+M'n,t' (\mod M_4')}$$
$$\times\vartheta\begin{bmatrix}\frac{M_2'j'-M_1'k'+M_1'M_2'm}{M_1'M_2'M'}\end{bmatrix}\left(M_2'(\frac{m_a}{n_a}p-\frac{m_b}{n_b}q)-M_1'(\frac{m_b}{n_b}q-\frac{m_c}{n_c}r),\frac{M_1'M_2'M'}{Q}\tau\right) \quad (204)$$
$$\times\vartheta\begin{bmatrix}\frac{M_3'(j'+k'+M_1'm)-M'l'+M'M_4'n}{M_3'M_4'M'}\end{bmatrix}\left(M_3'(\frac{m_a}{n_a}p-\frac{m_c}{n_c}r)-M'(\frac{m_c}{n_c}r-\frac{m_d}{n_d}s),\frac{M'M_3'M_4'}{Q}\tau\right).$$

This result is just the product of two theta functions. By solving the Kronecker delta, we obtain the sum of two theta functions like $\sum_m y^{j'k'm}y^{l't'm'}$. Therefore even including the non-Abelian Wilson lines we obtain results which are similar to Ref. [56] for general four point couplings.

3.8 Comments on soft supersymmetry breaking terms and moduli stabilization

In this section we discuss about the relation between moduli parameters and low-energy supersymmetry breaking effects. If these low-energy physics describe our world, the supersymmetry must be broken softly. In the MSSM or its extension, supersymmetry breaking is parameterized by a set of soft supersymmetry breaking terms. However the MSSM can not tell the microscopic origin of the soft supersymmetry breaking terms. They are generally free parameters and it needs some new physics mechanism for the supersymmetry breaking from the underlying theory such as string theory constructions. A method to obtain the soft supersymmetry breaking terms of the MSSM is to calculate the couplings of the matter sectors in the MSSM and moduli fields. The spontaneous supersymmetry breaking can be induced by the non-vanishing F and D terms of some moduli fields. The super potential are already given in Eq.118 and the F-term contribution of the tree-level scalar potential is given by

$$V_F(\mathcal{M},\bar{\mathcal{M}}) = e^G(G_MK^{MN}G_N-3), \quad (205)$$

then supersymmetry is broken if some of them have non-zero VEVs which are the SM gauge singlet scalar fields like as dilaton, or some geometric moduli as Kahler moduli and complex structure moduli. We have seen that dimensional reduction scheme can give a key observation about such moduli field dependence about matter sectors as well as low-energy phenomena like chiral spectrums or generation number. The soft supersymmetry breaking terms can be triggered by the spurious field methods [85] as

$$\begin{aligned} m_a &= \frac{1}{2\mathrm{Ref_a}}(F^M \partial_M f_a) \\ m^2_{\alpha\beta} &= (m^2_{3/2} + V_F) - \bar{F}^{\bar{M}} F^N \partial_{\bar{M}} \partial_N \log (K_{\alpha\beta}), \\ A_{\alpha\beta\gamma} &= F^M (K_M + \partial_M \log (Y_{\alpha\beta\gamma}) - \partial \log (K_{\alpha\beta} K_{\beta\gamma} K_{\gamma\alpha})) \end{aligned} \tag{206}$$

where m_a, $m^2_{\alpha\beta}$ and $A_{\alpha\beta\gamma}$ are corresponding to the soft supersymmetry breaking terms for gaugino masses and scalar masses and A-terms. Therefore these scenario enable to carry out the model independent analysis for the low-energy physics.

We have some comment on the moduli stabilization and low-energy spectra. First of all, these formulae for the soft terms are depending on the Yukawa couplings. For instance as shown in section3.5, Yukawa coupling in magnetized D-brane side is represented by

$$\begin{aligned} Y_{IIB} =& 2^{-9/4} \pi^{-3} e^{\phi_4/2} \prod_{d=1}^{3} \left(\mathrm{Im}\tau_d \frac{M_1^{(d)} M_2^{(d)}}{M_3^{(d)}} \right)^{1/4} \\ & \times \vartheta \begin{bmatrix} \frac{M_2^{(d)} k - M_3^{(d)} j + M_2^{(d)} M_3^{(d)} l}{M_1^{(d)} M_2^{(d)} M_3^{(d)}} \\ 0 \end{bmatrix} (0, \tau_d M_1^{(d)} M_2^{(d)} M_3^{(d)}). \end{aligned} \tag{207}$$

Therefore these supersymmetry breaking terms may affect on the low-energy phenomena. The flavor dependent part only come from the theta functions. This structure has dependence of the parameters of complex structure moduli, on the contrary, in the type IIA sides, flavor dependence is a function of Kahler moduli. As well known, there are some experimental constraint on the soft supersymmetry breaking terms. The crucial constraint is the limitation of the flavor changing neutral currents (FCNC) which suggests the universal squark mass for all generations. The simplest way to avoid the dangerous soft breaking terms is the scenario with dilaton moduli dominated scenario where it is assumed that the F-terms contributions of the moduli fields are dominated by dilaton moduli F^s. Then the soft supersymmetry breaking terms are universal for all the flavors and that is nicely acceptable for the experimental constraint. Furthermore from the expression of the Yukawa couplings in the scenario, the flavor dependence of the physical Yukawa couplings can only appear as the parameters of the complex structure moduli. Therefore the scenario with the dilaton and Kahler moduli dominant may not affect the low-energy spectrum. For generic case, we analyze carefully the soft supersymmetry breaking terms mediated by those dilaton, Kahler and complex structure moduli by using the formula in Eq. (206).

In order to specify the scenario to be selected it is necessary to study the moduli stabilization mechanism, because these F-term as F^U, F^S and F^K are usually proportional

to its vacuum expectation values. There are several ways for stabilization mechanism in the string theory. The dilaton and moduli stabilization mechanism using the three form flux are very well studied in which these moduli are stabilized at the Planck scale VEVs of the background fluxes. The KKLT scenario can provide the novel way to stabilize the overall Kahler moduli by non-perturbative super potential. The gauge flux can also stabilize some of Kahler moduli by F flatness conditions like in Eq.33. If we use the oblique flux for gauge, its generalized supersymmetry conditions are obtained. This type of model constructions are explored in globally defined toroidal compactifications [86, 87] with stabilized geometric moduli in a supersymmetric vacuum within a perturbative string description. Combining the three form flux and magnetic flux may stabilize all the geometric moduli. These scenario would give the moduli VEVs of the same magnitude of the scale. They may occur some unwanted FCNC process by induced soft supersymmetry breaking terms. However once we obtain the realistic patterns of Yukawa couplings, the characteristic patterns of the sparticle spectrum may be predicted. Therefore analysis for the relations between low-energy spectrum and moduli breaking parameters is important issue.

4 Non-Abelian flavor symmetries

Here we study more presicely the flavor structures by using the analysis on the coupling selection rule in the previous section.

4.1 Generic case

First we study generic case with non-vanishing Wilson lines. For simplicity, we restrict on the case with trivial torus background (integer flux). The case with fractional flux will be discussed later. We consider the model with zero-modes ψ^{i_k,M_k} for $k = 1, \cdots, L$. We denote $\gcd(M_1, \cdots, M_L) = g$. As studied in the previous section, these modes have Z_g charges and their couplings are controlled by the Z_g invariance. For simplicity, suppose that $M_1 = g$. Then, there are g zero-modes of ψ^{i_1,M_1}. The above Z_g transformation acts on $\psi^{i_1,g}$ as $Z\psi^{i_1,g}$, where

$$Z = \begin{pmatrix} 1 & & & & \\ & \rho & & & \\ & & \rho^2 & & \\ & & & \ddots & \\ & & & & \rho^{g-1} \end{pmatrix}, \tag{208}$$

and $\rho = e^{2\pi i/g}$.

In addition to this Z_g symmetry, the effective theory has another symmetry. That is, the effective theory must be invariant under cyclic permutations

$$\psi^{i_1,g} \to \psi^{i_1+n,g}, \tag{209}$$

with a universal integer n for i_1. That is nothing but a change of ordering and also has a geometrical meaning as a discrete shift of the origin, $z = 0 \to z = -\frac{n}{g}$. This symmetry also generates another Z_g symmetry, which we denote by $Z_g^{(C)}$ and its generator is represented as

$$C = \begin{pmatrix} 0 & 1 & 0 & 0 & \cdots & 0 \\ 0 & 0 & 1 & 0 & \cdots & 0 \\ & & & & \ddots & \\ 1 & 0 & 0 & & \cdots & 0 \end{pmatrix}, \tag{210}$$

on $\psi^{i_1,g}$. That is, the above permutation (210) is represented as $C^n\psi^{i_1,g}$. These generators, Z and C, do not commute each other, i.e.,

$$CZ = \rho ZC. \tag{211}$$

Then, the flavor symmetry corresponds to the closed algebra including Z and C. Diagonal matrices in this closed algebra are written as $Z^n(Z')^m$, where Z' is the generator of another

Z'_g and written as

$$Z' = \begin{pmatrix} \rho & & \\ & \ddots & \\ & & \rho \end{pmatrix}, \tag{212}$$

on $\psi^{i_1,g}$. Hence, these would generate the non-abelian flavor symmetry $(Z_g \times Z'_g) \rtimes Z_g^{(C)}$, since $Z_g \times Z'_g$ is a normal subgroup. These discrete flavor groups would include g^3 elements totally.

Let us study actions of Z and C on other zero-modes, ψ^{i_k,M_k}, with $M_k = gn_k$, where n_k is an integer. First, the generator C acts as

$$\psi^{i,gn_k} \to \psi^{i+n_k,gn_k}, \tag{213}$$

because the above discrete shift of the origin $z = 0 \to z = -\frac{n}{g}$ can be written as $z = 0 \to z = -\frac{nn_k}{gn_k}$ for these zero-modes. Thus, the generator C is represented as the same as (210) on the basis

$$\begin{pmatrix} \psi^{p,gn_k} \\ \psi^{p+n_k,gn_k} \\ \vdots \\ \psi^{p+(g-1)n_k,gn_k} \end{pmatrix}, \tag{214}$$

where p is an integer. Note that ψ^{p+gn_k,gn_k} is identical to ψ^{p,gn_k}. Furthermore, the generator Z is represented on this basis (214) as

$$Z = \rho^p \begin{pmatrix} 1 & & & & \\ & \rho^{n_k} & & & \\ & & \rho^{2n_k} & & \\ & & & \ddots & \\ & & & & \rho^{(g-1)n_k} \end{pmatrix}. \tag{215}$$

Thus, the zero-modes ψ^{i_k,gn_k} include n_k g-plet representations of the symmetry $(Z_g \times Z'_g) \rtimes Z_g^{(C)}$ and some of them may be reducible g-plet representations. For example, when we consider the zero-modes corresponding to $n_k = g$, i.e. $M_k = g^2$, the generator Z is represented as $\rho^p \mathbb{1}_g$ on the above g-plet (214), where $\mathbb{1}_g$ is the $(g \times g)$ unit matrix. In such a case, the generator C can also be diagonalized. Then, these zero-modes correspond to g singlets of $(Z_g \times Z'_g) \rtimes Z_g^{(C)}$ including trivial and non-trivial singlets.

As illustrating examples, we consider the models with $g = 2, 3$ in the next subsections and study more concretely about non-abelian discrete flavor symmetries.

4.1.1 $g = 2$ case

Here we consider the model with $g = 2$, that is, all of relative magnetic fluxes M_k are even. Its flavor symmetry is given as the closed algebra of Z_2, Z'_2 and $Z_2^{(C)}$, and all of

these elements are written as

$$\pm\begin{pmatrix} 1 & 0 \\ 0 & 1 \end{pmatrix}, \quad \pm\begin{pmatrix} 0 & 1 \\ 1 & 0 \end{pmatrix}, \quad \pm\begin{pmatrix} 0 & 1 \\ -1 & 0 \end{pmatrix}, \quad \pm\begin{pmatrix} 1 & 0 \\ 0 & -1 \end{pmatrix}. \tag{216}$$

That is, the flavor symmetry is D_4. The zero-modes with the relative magnetic flux $M = 2$,

$$\begin{pmatrix} \psi^{0,2} \\ \psi^{1,2} \end{pmatrix}, \tag{217}$$

correspond to the doublet representation $\mathbf{2}$ of D_4. This result is the same as the non-abelian flavor symmetry appearing from heterotic orbifold models with S^1/Z_2, where twisted modes on two fixed points of S^1/Z_2 correspond to the D_4 doublet [6, 28].

Next, we consider the zero-modes corresponding to the relative magnetic flux $M = 4$, $\psi^{i,4}$ $(0 = 0, 1, 2, 3)$. As discussed in the previous subsection, in order to represent C, it may be convenient to decompose them into the g-plets (214)

$$\begin{pmatrix} \psi^{0,4} \\ \psi^{2,4} \end{pmatrix}, \qquad \begin{pmatrix} \psi^{1,4} \\ \psi^{3,4} \end{pmatrix}. \tag{218}$$

However, they are reducible representations as follows. Note that both $\psi^{0,4}$ and $\psi^{2,4}$ have even Z_2 charges, and that both $\psi^{1,4}$ and $\psi^{3,4}$ have odd Z_2 charges. That is, the generator Z is represented in the form $\pm\mathbf{1}_2$, where $\mathbf{1}_2$ is the 2×2 identity matrix. Thus, the generator C can be diagonalized and such a diagonalizing basis is obtained as

$$\begin{aligned} &\mathbf{1}_{++}: \ (\psi^{0,4} + \psi^{2,4}), \qquad \mathbf{1}_{+-}: \ (\psi^{0,4} - \psi^{2,4}), \\ &\mathbf{1}_{-+}: \ (\psi^{1,4} + \psi^{3,4}), \qquad \mathbf{1}_{--}: \ (\psi^{1,4} - \psi^{3,4}), \end{aligned} \tag{219}$$

up to normalization factors. Obviously, these correspond to four D_4 singlets, $\mathbf{1}_{++}$, $\mathbf{1}_{+-}$, $\mathbf{1}_{-+}$ and $\mathbf{1}_{--}$. The first subscript of two denotes Z_2 charges for Z and the second one denotes Z_2 charges for C. Hence, all of irreducible representations of D_4 appear from $\psi^{i,2}$ and $\psi^{i,4}$. New representations can not appear in zero-modes $\psi^{i,M}$ with $M > 4$. For example, we consider zero-modes corresponding to $M = 6$, i.e. $\psi^{i,6}$. They can be decomposed as

$$|\psi^6\rangle_1 = \begin{pmatrix} \psi^{0,6} \\ \psi^{3,6} \end{pmatrix}, \quad |\psi^6\rangle_2 = \begin{pmatrix} \psi^{2,6} \\ \psi^{5,6} \end{pmatrix}, \quad |\psi^6\rangle_3 = \begin{pmatrix} \psi^{4,6} \\ \psi^{1,6} \end{pmatrix}. \tag{220}$$

Each of $|\psi^6\rangle_i$ with $i = 1, 2, 3$ is nothing but the D_4 doublet. That is, we have three D_4 doublets in $\psi^{i,6}$. The above representations appear repeatedly in $\psi^{i,M}$ with larger M. These results are shown in Table 1.

4.1.2 $g = 3$ case

Here we consider the model with $g = 3$, where all of relative magnetic fluxes are equal to $M_k = 3n_k$. Its flavor symmetry is given as $(Z_3 \times Z_3) \rtimes Z_3$, that is, $\Delta(27)$ [88]. This flavor

M	Representation of D_4
2	$\mathbf{2}$
4	$\mathbf{1}_{++},\ \mathbf{1}_{+-},\ \mathbf{1}_{-+},\ \mathbf{1}_{--}$
6	$3\times\mathbf{2}$

Table 1: D_4 representations of zero-modes in the model with $g=2$.

symmetry is different from the flavor symmetry appearing from heterotic orbifold models with T^2/Z_3. Later, we will explain what makes this difference.

The zero-modes corresponding to the relative magnetic flux $M=3$,

$$|\psi^3\rangle_1 = \begin{pmatrix} \psi^{0,3} \\ \psi^{1,3} \\ \psi^{2,3} \end{pmatrix}, \tag{221}$$

correspond to the triplet representation $\mathbf{3}$ of $\Delta(27)$. Next, we consider the zero-modes corresponding to the relative magnetic flux $M=6$, i.e. $\psi^{i,6}$. Again, it may be convenient to decompose them into the g-plets (214)

$$|\psi^6\rangle_1 = \begin{pmatrix} \psi^{0,6} \\ \psi^{2,6} \\ \psi^{4,6} \end{pmatrix}, \quad |\psi^6\rangle_2 = \begin{pmatrix} \psi^{3,6} \\ \psi^{5,6} \\ \psi^{1,6} \end{pmatrix}. \tag{222}$$

The generator C is represented in the same way for $|\psi^3\rangle_1$ and $|\psi^6\rangle_i$ $(i=1,2)$. On the other hand, the representation of the generator Z for $|\psi^6\rangle_i$ $(i=1,2)$ is the complex conjugate to one for $|\psi^3\rangle_1$. Thus, both $|\psi^6\rangle_i$ $(i=1,2)$ correspond to $\bar{\mathbf{3}}$ representations of $\Delta(27)$.

Moreover, let us consider the zero-modes with the relative magnetic flux $M=9$, i.e. $\psi^{i,9}$. Then, we decompose them into the g-plets (214)

$$|\psi^9\rangle_1 = \begin{pmatrix} \psi^{0,9} \\ \psi^{3,9} \\ \psi^{6,9} \end{pmatrix}, \quad |\psi^9\rangle_\omega = \begin{pmatrix} \psi^{1,9} \\ \psi^{4,9} \\ \psi^{7,9} \end{pmatrix}, \quad |\psi^9\rangle_{\omega^2} = \begin{pmatrix} \psi^{2,9} \\ \psi^{5,9} \\ \psi^{8,9} \end{pmatrix}, \tag{223}$$

where $\omega = e^{2\pi i/3}$. These (reducible) triplets $|\psi^9\rangle_{\omega^n}$ have Z_3 charges, n and are decomposed into nine singlets,

$$\mathbf{1}_{\omega^n,\omega^m} : \psi^{n,9} + \omega^m \psi^{n+3m,9} + \omega^{2m}\psi^{n+6m,9}, \tag{224}$$

up to normalization factors, where n and m are Z_3 charges for Z and C, respectively. In zero-modes with $M>9$, new representations do not appear, but the above representations appear repeatedly. These results as well as zero-modes with $M>9$ are shown in Table 2. Similar analysis can be carried out in other models with $g>3$.

We comment on symmetries in subsectors. Suppose that our model has zero-modes ψ^{i_k,M_k} for $k=1,\cdots,L$ with $\gcd(M_1,\cdots,M_L)=g$ and they are separated into two classes, ψ^{i_l,M_l} $(l=1,\cdots,L_1)$ and ψ^{i_m,M_m} $(m=L_1,\cdots,L)$, where $\gcd(M_1,\cdots,M_{L_1})=g_1$,

M	Representation of $\Delta(27)$
3	$\mathbf{3}$
6	$2 \times \bar{\mathbf{3}}$
9	$\mathbf{1}_1,\ \mathbf{1}_2,\ \mathbf{1}_3,\ \mathbf{1}_4,\ \mathbf{1}_5,\ \mathbf{1}_6,\ \mathbf{1}_7,\ \mathbf{1}_8,\ \mathbf{1}_9$
12	$4 \times \mathbf{3}$
15	$5 \times \bar{\mathbf{3}}$
18	$2 \times \{\mathbf{1}_1,\ \mathbf{1}_2,\ \mathbf{1}_3,\ \mathbf{1}_4,\ \mathbf{1}_5,\ \mathbf{1}_6,\ \mathbf{1}_7,\ \mathbf{1}_8,\ \mathbf{1}_9\}$

Table 2: $\Delta(27)$ representations of zero-modes in the model with $g = 3$.

$\gcd(M_{L_1}, \cdots, M_L) = g_2$ and $\gcd(g_1, g_2) = g$. Coupling terms including only the first class of fields ψ^{i_l, M_l} $(l = 1, \cdots, L_1)$ in the four-dimensional effective theory have the symmetry $(Z_{g_1} \times Z_{g_1}) \rtimes Z_{g_1}$, where g_1 would be larger than g. However, such a symmetry is broken by terms including the second class of fields. Thus, we would have a larger symmetry at least at tree level for the subsectors. Such larger symmetries in the subsectors would be interesting for model building.

4.2 Cases without Continuous Wilson lines

In the section 4.1, we have considered the models with non-vanishing Wilson lines. Here, we study the models without Abelian Wilson lines. In this case, flavor symmetries are enhanced.

When Wilson lines are vanishing, all of zero-modes ψ^{0,M_k} have the peak at the same point in the extra dimensions. In the intersecting D-brane picture, this corresponds to the D-brane configuration, that all of D-branes intersect (at least) at a single point on T^2. This model has the Z_2 rotation symmetry around such a point. Here, we denote its generator as P. In general, this acts as

$$P:\ \psi^{i,M} \to \psi^{M-i,M}. \tag{225}$$

As in the previous section, we consider the models with $g = 2, 3$ as illustrating models.

4.2.1 $g = 2$ case

First, we consider the zero-modes with $M = 2$, $\psi^{i,2}$, which correspond to the D_4 doublet. For them, the generator P acts as the identity. That implies that the flavor symmetry is enhanced as $D_4 \times Z_2$ and $\psi^{i,2}$ correspond to $\mathbf{2}_+$, where the subscript denotes the Z_2 charge for P.[13]

We consider the zero-modes with $M = 4$, $\psi^{i,4}$, which are decomposed as the four D_4 singlets, $\mathbf{1}_{++}$, $\mathbf{1}_{+-}$, $\mathbf{1}_{-+}$ and $\mathbf{1}_{--}$ as (219). They have definite Z_2 charges for P and are

[13] Although this is just an enhancement by the factor Z_2, such an enhanced flavor symmetry $D_4 \times Z_2$ would be important to phenomenological model building. See e.g. [89].

M	Representation of $D_4 \times Z_2$
2	$\mathbf{2}_+$
4	$\mathbf{1}_{+++},\ \mathbf{1}_{+-+},\ \mathbf{1}_{-++},\ \mathbf{1}_{---}$
6	$2 \times \mathbf{2}_+,\ \mathbf{2}_-$
8	$\mathbf{1}_{+++},\ \mathbf{1}_{+-+},\ \mathbf{1}_{+++},\ \mathbf{1}_{+--},\ \mathbf{1}_{-++},\ \mathbf{1}_{-+-},\ \mathbf{1}_{---},\ \mathbf{1}_{--+}$
10	$3 \times \mathbf{2}_+,\ 2 \times \mathbf{2}_-$

Table 3: $D_4 \times Z_2$ representations of zero-modes in the model with $g = 2$.

represented as

$$\begin{aligned} &\mathbf{1}_{+++} : \ (\psi^{0,4} + \psi^{2,4}), \qquad \mathbf{1}_{+-+} : \ (\psi^{0,4} - \psi^{2,4}), \\ &\mathbf{1}_{-++} : \ (\psi^{1,4} + \psi^{3,4}), \qquad \mathbf{1}_{---} : \ (\psi^{1,4} - \psi^{3,4}), \end{aligned} \tag{226}$$

where the third sign in the subscripts denotes Z_2 charges for P.

Now, let us consider the zero-modes with $M = 6$, $\psi^{i,6}$, which are decomposed as three D_4 doublets (220). The doublet $|\psi^6\rangle_1$ has the even Z_2 charges for P. However, other doublets $|\psi^6\rangle_2$ and $|\psi^6\rangle_3$ transform each other under P. Thus, we take linear combinations of these two doublets as

$$|\psi^6\rangle_\pm \equiv |\psi^6\rangle_2 \pm |\psi^6\rangle_3 = \begin{pmatrix} \psi^{2,6} \\ \psi^{5,6} \end{pmatrix} \pm \begin{pmatrix} \psi^{4,6} \\ \psi^{1,6} \end{pmatrix}, \tag{227}$$

where $\pm$ also means Z_2 charge of P. As a result, these zero-modes $\psi^{i,6}$ are decomposed as two $\mathbf{2}_+$ and one $\mathbf{2}_-$.

We can repeat these analysis for larger M. For example, zero-modes with $M = 8$, $\psi^{i,8}$, are decomposed as

$$\{\mathbf{1}_{+++},\ \mathbf{1}_{+-+},\ \mathbf{1}_{+++},\ \mathbf{1}_{+--},\ \mathbf{1}_{-++},\ \mathbf{1}_{-+-},\ \mathbf{1}_{---},\ \mathbf{1}_{--+}\}, \tag{228}$$

and zero-modes with $M = 10$, $\psi^{i,10}$, are decomposed as three $\mathbf{2}_+$ and two $\mathbf{2}_-$. These results are shown in Table 3.

4.2.2 $g = 3$ case

Here, we study the model with $g = 3$. First, we consider the zero-modes with $M = 3$, $\psi^{i,3}$. They correspond to a triplet of $\Delta(27)$ with non-vanishing Wilson lines. At any rate, the generators, Z, C and P, act on $\psi^{i,3}$ as

$$Z = \begin{pmatrix} 1 & 0 & 0 \\ 0 & \omega & 0 \\ 0 & 0 & \omega^2 \end{pmatrix}, \quad C = \begin{pmatrix} 0 & 1 & 0 \\ 0 & 0 & 1 \\ 1 & 0 & 0 \end{pmatrix}, \quad P = \begin{pmatrix} 1 & 0 & 0 \\ 0 & 0 & 1 \\ 0 & 1 & 0 \end{pmatrix}. \tag{229}$$

Their closed algebra is $\Delta(54)$. Thus, the zero-modes $\psi^{i,3}$ correspond to the triplet of $\Delta(54)$, $\mathbf{3}_1$. This is the same as the flavor symmetry, which appears in heterotic orbifold

models with T^2/Z_3 [28]. Three fixed points on the orbifold T^2/Z_3 have the geometrical permutation symmetry S_3. Such symmetry is enhanced in magnetized brane models, only when Wilson lines are vanishing. Indeed, the closed algebra of generators C and P is S_3.

Similarly, we can consider the zero-modes with $M = 6$, $\psi^{i,6}$. We decompose them as (222). The generators, C and P, act on $|\psi^6\rangle_i$ $(i = 1, 2)$ in the same way as $\psi^{i,3}$, but the representation of the generator Z for $|\psi^6\rangle_i$ $(i = 1, 2)$ is the complex conjugate to one for $|\psi^3\rangle_1$. Thus, both $|\psi^6\rangle_i$ correspond to $\bar{\mathbf{3}}_1$ representations of $\Delta(54)$. Recall that $|\psi^6\rangle_i$ are $\bar{\mathbf{3}}$ representations of $\Delta(27)$.

Next, let us consider the zero-modes with $M = 9$, $\psi^{i,9}$. Recall that they correspond to nine singlets of $\Delta(27)$ as (224). The following linear combination,

$$\psi^{0,9} + \psi^{3,9} + \psi^{6,9}, \tag{230}$$

is still a singlet under $\Delta(54)$, which is a trivial singlet $\mathbf{1}_1$. However, the others in linear combinations (224) transform each other under P. Then, they correspond to four doublets of $\Delta(54)$,

$$\begin{aligned}
&\mathbf{2}_1 : \begin{pmatrix} \psi^{0,9} + \omega\psi^{3,9} + \omega^2\psi^{6,9} \\ \psi^{0,9} + \omega^2\psi^{3,9} + \omega\psi^{6,9} \end{pmatrix}, \qquad \mathbf{2}_2 : \begin{pmatrix} \psi^{1,9} + \psi^{4,9} + \psi^{7,9} \\ \psi^{2,9} + \psi^{5,9} + \psi^{8,9} \end{pmatrix}, \\
&\mathbf{2}_3 : \begin{pmatrix} \psi^{1,9} + \omega\psi^{4,9} + \omega^2\psi^{7,9} \\ \psi^{8,9} + \omega^2\psi^{5,9} + \omega\psi^{2,9} \end{pmatrix}, \qquad \mathbf{2}_4 : \begin{pmatrix} \psi^{1,9} + \omega^2\psi^{4,9} + \omega\psi^{7,9} \\ \psi^{8,9} + \omega^2\psi^{5,9} + \omega\psi^{2,9} \end{pmatrix}.
\end{aligned} \tag{231}$$

Now, let us consider the zero-modes with $M = 12$, $\psi^{i,12}$. We decompose them into g-plets (214)

$$\begin{aligned}
|\psi^{12}\rangle_1 &= \begin{pmatrix} \psi^{0,12} \\ \psi^{4,12} \\ \psi^{8,12} \end{pmatrix}, \qquad |\psi^{12}\rangle_2 = \begin{pmatrix} \psi^{6,12} \\ \psi^{10,12} \\ \psi^{2,12} \end{pmatrix}, \\
|\psi^{12}\rangle_3 &= \begin{pmatrix} \psi^{3,12} \\ \psi^{7,12} \\ \psi^{11,12} \end{pmatrix}, \qquad |\psi^{12}\rangle_4 = \begin{pmatrix} \psi^{9,12} \\ \psi^{1,12} \\ \psi^{5,12} \end{pmatrix}.
\end{aligned} \tag{232}$$

They correspond to four triplets of $\Delta(27)$. Representations of the generators, Z, C and P, on $|\psi^{12}\rangle_1$ and $|\psi^{12}\rangle_2$ are the same as those on $\psi^{i,3}$ like Eq. (229). Thus, they correspond to $\mathbf{3}_1$. On the other hand, $|\psi^{12}\rangle_3$ and $|\psi^{12}\rangle_4$ transform each other under P. Hence, we take the following linear combinations,

$$|\psi^{12}\rangle_\pm = \begin{pmatrix} \psi^{3,12} \pm \psi^{9,12} \\ \psi^{7,12} \pm \psi^{1,12} \\ \psi^{11,12} \pm \psi^{5,12} \end{pmatrix}. \tag{233}$$

Then, representations of Z, C and P on $|\psi^{12}\rangle_+$ are the same as (229), and $|\psi^{12}\rangle_+$ corresponds to $\mathbf{3}_1$. On the other hand, representations of Z and C on $|\psi^{12}\rangle_-$ are the same as

M	Representation of $\Delta(54)$
3	$\mathbf{3}_1$
6	$2 \times \bar{\mathbf{3}}_1$
9	$\mathbf{1}_1,\ \mathbf{2}_1,\ \mathbf{2}_2,\ \mathbf{2}_3,\ \mathbf{2}_4$
12	$3 \times \mathbf{3}_1,\ \mathbf{3}_2$
15	$3 \times \bar{\mathbf{3}}_1,\ 2 \times \bar{\mathbf{3}}_2$
18	$2 \times \{\mathbf{1}_1,\ \mathbf{2}_1,\ \mathbf{2}_2,\ \mathbf{2}_3,\ \mathbf{2}_4\}$

Table 4: $\Delta(54)$ representations of zero-modes in the model with $g = 3$.

(229), but the generator P is represented on $|\psi^{12}\rangle_-$ as

$$P = \begin{pmatrix} -1 & 0 & 0 \\ 0 & 0 & -1 \\ 0 & -1 & 0 \end{pmatrix}. \tag{234}$$

That is, $|\psi^{12}\rangle_-$ corresponds to another triplet of $\Delta(54)$, i.e. $\mathbf{3}_2$. Furthermore, the zero-modes with $M = 15$, $\psi^{i,15}$ correspond to

$$3 \times \bar{\mathbf{3}}_1, \quad 2 \times \bar{\mathbf{3}}_2, \tag{235}$$

and the zero-modes with $M = 18$, $\psi^{i,18}$ correspond to

$$2 \times \{\mathbf{1}_1,\ \mathbf{2}_1,\ \mathbf{2}_2,\ \mathbf{2}_3,\ \mathbf{2}_4\}. \tag{236}$$

These results are shown in Table 4. Irreducible representations of $\Delta(54)$ are two triplets $\mathbf{3}_1$, $\mathbf{3}_2$, their conjugates $\bar{\mathbf{3}}_1$ $\bar{\mathbf{3}}_2$, four doublets $\mathbf{2}_1$, $\mathbf{2}_2$, $\mathbf{2}_3$, $\mathbf{2}_4$, trivial singlet $\mathbf{1}$ and non-trivial singlet $\mathbf{1}_2$. All of them except the non-trivial singlet $\mathbf{1}_2$ can appear in this model.

Similar analysis can be carried out in other models with $g > 3$. In generic case, the Z and P satisfy

$$PZ = Z^{-1}P, \tag{237}$$

and the closed algebra of C and P is D_g. Thus, the flavor symmetry, which is generated by Z, C and P, would be written as $D_g \ltimes (Z_g \times Z_g)$. Note that $S_3 \sim D_3$ and $\Delta(54)$ is $D_3 \ltimes (Z_3 \times Z_3)$.

4.3 Cases with non-Abelian Wilson lines

Here, we study the non-Abelian flavor symmetries, which can appear in our models.

4.3.1 The case with $M_i \neq 1$ and $k_i = 1$

First, we consider the models with $k_1 = k_2 = k_3 = 1$. Then, the number of zero-modes are given by $|I_{ab}| = M_1$, $|I_{bc}| = M_2$ and $|I_{ca}| = M_3$. We consider the models

with $g = \text{g.c.d.}(M_1, M_2, M_3) \neq 1$. The Yukawa couplings do not depend on the matrix components (p, q, r), and are reduced to the following form

$$\int_0^Q dy_4 \int_0^1 dy_5 \Psi^i_{pq} \Psi^j_{qr} \Psi^k_{rp} = N_{M_1} N_{M_2} N^*_{M_3} Q \sqrt{\frac{Q}{2M'_3}} \sum_{m \in Z_{M'_3}} \delta_{j'+k'+M'_1 m, l' (\mathrm{mod M'_3})} \\ \times \vartheta \begin{bmatrix} \frac{M'_2 j' - M'_1 k' + M'_1 M'_2 m}{M'_1 M'_2 (M'_3)} \\ 0 \end{bmatrix} (0, M'_1 M'_2 M'_3 / Q\tau) \,, \qquad (238)$$

where we have taken simply $p = q = r = 0$ and the phase factor like C^j_{pq} disappears. This form is nothing but the case with integer fluxes and without non-Abelian Wilson lines. In this types of Yukawa couplings, 4D effective theory has another flavor symmetry called by the shift symmetry, which corresponds to the transformations of flavor indices as

$$\begin{aligned} j' &\to j' + M'_1/g, \\ k' &\to k' + M'_2/g, \\ l' &\to l' + M'_3/g, \end{aligned} \qquad (239)$$

simultaneously. Under this transformation, Yukawa couplings are invariant. This has also coupling selection rule as shown in the previous section given by the Z_g symmetry (201). Then, they form the non-Abelian discrete flavor symmetries as the same as the case without non-Abelian Wilson lines.

For simplicity, suppose that $M'_1 = g$. Then, there are g zero-modes of Ψ^{j', M'_1}. The selection rule (201) means that 4D effective theory is symmetric under the Z_g transformation, which acts on $\Psi^{j',g}$ as $Z\Psi^{j',g}$, where

$$Z = \begin{pmatrix} 1 & & & & \\ & \rho & & & \\ & & \rho^2 & & \\ & & & \ddots & \\ & & & & \rho^{g-1} \end{pmatrix}, \qquad (240)$$

and $\rho = e^{2\pi i/g}$. Furthermore, the effective theory has another symmetry (239). That can be written as cyclic permutations on $\Psi^{j',g}$,

$$\Psi^{j',g} \to \Psi^{j'+1,g}. \qquad (241)$$

That is nothing but a change of ordering and also has a geometrical meaning as a discrete shift of the origin, $z = 0 \to z = -\frac{1}{g}$. This symmetry also generates another Z_g symmetry, which we denote by $Z_g^{(C)}$ and its generator is represented as

$$C = \begin{pmatrix} 0 & 1 & 0 & 0 & \cdots & 0 \\ 0 & 0 & 1 & 0 & \cdots & 0 \\ & & & & \ddots & \\ 1 & 0 & 0 & & \cdots & 0 \end{pmatrix}, \qquad (242)$$

on $\Psi^{j',g}$. These generators, Z and C, do not commute each other, i.e.,

$$CZ = \rho ZC. \tag{243}$$

Then, the flavor symmetry corresponds to the closed algebra including Z and C. Diagonal matrices in this closed algebra are written as $Z^n(Z')^m$, where Z' is the generator of another Z'_g written as

$$Z' = \begin{pmatrix} \rho & & \\ & \ddots & \\ & & \rho \end{pmatrix}, \tag{244}$$

on $\Psi^{j',g}$. Hence, these would generate the non-Abelian flavor symmetry $(Z_g \times Z'_g) \rtimes Z_g^{(C)}$, since $Z_g \times Z'_g$ is a normal subgroup. These discrete flavor groups would include g^3 elements totally.

For example, for $g = 2$ and 3 these flavor symmetries are given as $Z_2 \rtimes Z_2 = D_4$ and $(Z_3 \times Z_3) \rtimes Z_3 = \Delta(27)$, respectively. Then, the fields $\Psi^{j',g}$ correspond to **2** of D_4 and **3** of $\Delta(27)$, as shown in Tables 1 and 2, respectively. When M'/g is an integer larger than 1, the $\Psi^{j',M'}$ fields correspond to other representations. For smaller values of M'/g, the corresponding representations are shown in Tables 1 and 2.

However we note that their multiplets have several types of representation under this symmetry. Because a Z_g charge of fields labeled by j is not j but $j' = qj$. Therefore even if they have same multiplicities ($M_1 = M_2$), their representations may be different from each other.

4.3.2 The case with $M_i = 1$ and $k \neq 1$

Next, we consider the models with $M_i = 1$ and $k \neq 1$. In this case, we also find similar flavor structures as well as the case without non-Abelian Wilson lines. Suppose all the components of zero-modes are given by $|I_{ab}| = k_1$, $|I_{bc}| = k_2$ and $|I_{ca}| = k_3$. Then it is possible to take phase factors for each wavefunction $C^j_{pq} = 1$. We commonly use $K = \text{g.c.d.}(k_1, k_2, k_3)$. The Yukawa couplings only depend on the indices p, q and r as a function θ_{pqr} given by

$$\begin{aligned} \theta_{pqr} &= Q\left(\frac{m_a}{n_a}\tilde{I}_{bc}p + \frac{m_b}{n_b}\tilde{I}_{ca}q + \frac{m_c}{n_c}\tilde{I}_{ab}r\right) \\ &= Q\left(\frac{m_a}{n_a}\tilde{I}_{bc}(\tilde{j} + n_1 k_1) - \frac{m_c}{n_c}\tilde{I}_{ab}(\tilde{k} + n_2 k_2)\right), \end{aligned} \tag{245}$$

where we have used the relations $p - q = n_1 k_1 + \tilde{j}$ and $l - r = n_2 k_2 + \tilde{k}$ with $n_1, n_2 \in Z$. We find that the Yukawa couplings are invariant under the following transformation as

$$\begin{aligned} \tilde{j} &\to \tilde{j} + \frac{m_c I_{ab}}{K}, \\ \tilde{k} &\to \tilde{k} + \frac{m_a I_{bc}}{K}, \\ \tilde{l} &\to \tilde{l} + \frac{m_b I_{ac}}{K}. \end{aligned} \tag{246}$$

It is obvious that this transformation is the permutation of flavor index with order K. Therefore we have two symmetries: one is the discrete Z_K symmetry comes from the coupling selection rule and another is this shift symmetry. By combining these two symmetries, it becomes the same non-Abelian discrete flavor symmetry as the case without Non-Abelian Wilson-lines. That is, these flavor symmetries are given as $Z_2 \rtimes Z_2 = D_4$ for $K = 2$, $(Z_3 \times Z_3) \rtimes Z_3 = \Delta(27)$ for $K = 3$ and $(Z_K \times Z_K) \rtimes Z_K$ for generic K.

We have two aspects of flavor structures which are characterized by the parameters M, K. In the latter case, the origin of flavor symmetry is the gauge symmetry. The background breaks the continuous gauge symmetry, but discrete symmetry remains as the flavor symmetry. In the former case, the flavor would not be directly originated from the gauge symmetry. However, T-duals of both cases would correspond to similar intersecting D-brane models, where n_a and m_a have almost the same meaning, that is, winding numbers of D-branes for different directions. Thus, these two pictures of flavor symmetries are related with each other by T-duality through the intersecting D-brane picture.

So far, we have considered the models with $M_i = 1$ and $K \neq 1$ and found the flavor symmetry $(Z_K \times Z_K) \rtimes Z_K$. Here we comment on generic case with $M \neq 1$ and $K \neq 1$. Even in such a case, the selection rules due to Z_g and Z_K symmetries hold exact. However, the general formula of Yukawa couplings depend on both the indices j and $\tilde{j}$. Then, 4D effective Lagrangian is not always invariant under the above (independent) shift transformations (239) and (246).

4.3.3 Illustrating examples

We show two illustrating examples. We concentrate on only the T^2 torus. The first example is the model with $(I_1, I_2, I_3) = (2, 4, 2)$. The background magnetic flux is taken as

$$F = 2\pi \begin{pmatrix} \frac{1}{2}\mathbf{1}_{N_a} & & \\ & \frac{3}{8}\mathbf{1}_{N_b} & \\ & & \frac{1}{4}\mathbf{1}_{N_c} \end{pmatrix}. \tag{247}$$

Then the appearing chiral matters are denoted by

$$\lambda = \begin{pmatrix} \text{const} & L_{pq}^{j,M_1=1} & \\ & \text{const} & R_{qr}^{k,M_2=1} \\ H_{rp}^{l,M_3=1} & & \text{const} \end{pmatrix}, \tag{248}$$

where p =0, 1, q =0, 1, ..., 7 and r =0, 1, 2, 3. The wavefunctions are represented by following theta functions as

$$\begin{aligned} L^j_{pq}(x,y) &= N_{M_1}e^{-\pi/8y^2}\vartheta\begin{bmatrix}0\\0\end{bmatrix}(z/8+(1/2p-3/8q),\tau/8), \\ R^k_{qr}(x,y) &= N_{M_2}e^{-\pi/8y^2}\vartheta\begin{bmatrix}0\\0\end{bmatrix}(z/8+(3/8q-1/4r),\tau/8), \\ H^l_{pr}(x,y) &= N_{M_3}e^{-\pi/4y^2}\vartheta\begin{bmatrix}0\\0\end{bmatrix}(z/4+(1/2p-1/4r),2\tau/8), \end{aligned} \tag{249}$$

where we take $j=k=l=0$. The several parameters are also given by these fluxes. We have $k_1=2$, $k_2=4$, $k_3=2$ and $K=\text{g.c.d.}(k_1,k_2,k_3)=2$. The gauge invariant 3-point couplings are divided to four types of Yukawa couplings shown below

$$\begin{aligned} \mathcal{L} &= Y_{000}+Y_{010}+Y_{001}+Y_{100}, \\ Y_{000} &= L_{00}R_{00}H^\dagger_{00}+L_{11}R_{11}H^\dagger_{11}+L_{02}R_{22}H^\dagger_{02}+L_{13}R_{33}H^\dagger_{13} \\ &\quad +L_{04}R_{40}H^\dagger_{00}+L_{15}R_{51}H^\dagger_{11}+L_{06}R_{62}H^\dagger_{02}+L_{17}R_{73}H^\dagger_{13}, \\ Y_{011} &= L_{00}R_{01}H^\dagger_{01}+L_{11}R_{12}H^\dagger_{12}+L_{02}R_{23}H^\dagger_{03}+L_{13}R_{30}H^\dagger_{10} \\ &\quad +L_{04}R_{41}H^\dagger_{01}+L_{15}R_{52}H^\dagger_{12}+L_{06}R_{63}H^\dagger_{03}+L_{17}R_{70}H^\dagger_{10}, \\ Y_{101} &= L_{10}R_{00}H^\dagger_{10}+L_{01}R_{11}H^\dagger_{01}+L_{12}R_{22}H^\dagger_{12}+L_{03}R_{33}H^\dagger_{03} \\ &\quad +L_{14}R_{40}H^\dagger_{10}+L_{05}R_{51}H^\dagger_{01}+L_{16}R_{62}H^\dagger_{12}+L_{07}R_{73}H^\dagger_{03}, \\ Y_{110} &= L_{10}R_{01}H^\dagger_{11}+L_{01}R_{12}H^\dagger_{01}+L_{12}R_{23}H^\dagger_{13}+L_{03}R_{30}H^\dagger_{00} \\ &\quad +L_{14}R_{41}H^\dagger_{11}+L_{05}R_{52}H^\dagger_{02}+L_{16}R_{63}H^\dagger_{13}+L_{07}R_{70}H^\dagger_{00}. \end{aligned}$$

As seen in these interaction terms, one finds that all the combinations (p,q,r) are not allowed. This is because it has $K=\text{g.c.d.}(2,4,2)=2$. Their fields L,R,H are divided to two classes under the discrete Z_2 charge. For instance, for R fields, the flavor index is defined by $\tilde{k}=q-r \mod 4$. We assign the Z_2 charges as

$$\begin{aligned} Z_2+ &: R^{\tilde{k}=0},R^{\tilde{k}=2}, \\ Z_2- &: R^{\tilde{k}=1},R^{\tilde{k}=3}, \end{aligned} \tag{250}$$

and other fields are also assigned the Z_2 charges as

$$\begin{aligned} Z_2+ &: L^{\tilde{k}=0},H^{\tilde{k}=0}, \\ Z_2- &: L^{\tilde{k}=1},H^{\tilde{k}=1}. \end{aligned} \tag{251}$$

That corresponds to the coupling selection rule as $\tilde{j}+\tilde{k}=\tilde{l} \mod 2$. The Yukawa couplings Y^{pqr}_{jl} are calculated by the overlap integrals as follows

$$Y^{kl}_{pqr}\propto\vartheta\begin{bmatrix}0\\0\end{bmatrix}(1/2p-3/4q+1/4r,\tau/4). \tag{252}$$

We also consider about the shift symmetry for this model, i.e.

$$\begin{aligned} \tilde{j} &\to \tilde{j} + \frac{m_c I_{ab}}{K} = \tilde{j} + 1 \mod 2, \\ \tilde{k} &\to \tilde{k} + \frac{m_a I_{ab}}{K} = \tilde{k} + 2 \mod 4, \\ \tilde{l} &\to \tilde{l} + \frac{m_b I_{ab}}{K} = \tilde{l} + 1 \mod 2. \end{aligned} \tag{253}$$

As shown in the previous section, the Yukawa couplings are invariant under this transformation. These two operators make the $D_4 = Z_2 \rtimes Z_2$ discrete flavor symmetry. One can understand the representation for each field under D_4 symmetry. As an analysis similar to the previous section, one can find that L and R correspond to doublets and H fields become four non-trivial singlets under D_4 symmetry.

As another example, we consider the model with $(I_1, I_2, I_3) = (3, 3, 3)$, which is not realized by only integer fluxes. We choose fluxes as

$$F = 2\pi \begin{pmatrix} 3\mathbf{1}_{N_a} & & \\ & \frac{3}{2}\mathbf{1}_{N_b} & \\ & & 0\mathbf{1}_{N_c} \end{pmatrix}. \tag{254}$$

Then the appearing chiral matter fields are denoted as follows,

$$\lambda = \begin{pmatrix} \text{const} & L_{0p}^{j,M_1=3} & \\ & \text{const} & R_{q0}^{k,M_2=3} \\ H_{00}^{l,M_3=3} & & \text{const} \end{pmatrix}, \tag{255}$$

where $p, q = 0, 1$. This model has $k_i = 1$ and $Q_1 = 2, Q_2 = 2, Q_1 = 1, Q = 2$ $(j' = j, k' = k, l' = 2l)$. The gauge invariant 3-point couplings are given as

$$\begin{aligned} \mathcal{L} &= \mathrm{tr} L_{pq} R_{qr} H_{pr}^{\dagger} \\ &= L_{00} R_{00} H_{00}^{\dagger} + L_{01} R_{10} H_{00}^{\dagger}. \end{aligned} \tag{256}$$

The Yukawa couplings Y_{jl}^{pqr} are calculated by overlap integrals as follows

$$\begin{aligned} Y_{pqr}^{jkl} &= \int_0^1 dy_4 \int_0^2 dy_5 L_{pq}(x,y) R_{qr}(x,y) H_{rp}(x,y)^* \\ &\propto \sum_{m \in Z_6} \delta_{j'+k'+3m,l'} \vartheta \begin{bmatrix} \frac{3j'-3k'+9m}{54} \\ 0 \end{bmatrix} (0, 27\tau), \end{aligned} \tag{257}$$

where we take $p = q = r = 0$. From the structure of Kronecker delta, one can read the selection rule as

$$\begin{aligned} & j' + k' + 3m = l' \mod 6 \\ \to \quad & j + k - 2l = 0 \mod 3 \quad . \end{aligned} \tag{258}$$

Since g is defined by $g = \text{g.c.d.}(M'_1, M'_2, M'_3) = 3$, so this model has $\Delta(27) = (Z_3 \times Z_3) \rtimes Z_3$ flavor symmetry. Here we mention that the charge assignment is different from the case with Abelian Wilson line. For the H fields, their Z_3 charges are given as $l' = 2l$, so they correspond to the multiplet of $\bar{\mathbf{3}}$ representations. Other sectors of L and R correspond to $\mathbf{3}$ representations, and they can couple in the language of flavor symmetry. Therefore the extension to the non Abelian Wilson line case causes to have more various types of representations and flavor structures.

It is possible to introduce the constant gauge potential called the Abelian Wilson line. We use the previous model with $(I_1, I_2, I_3) = (3, 3, 3)$. We assume $N_a = 4$, $N_b = 4$, $N_c = 2$. The fractional fluxes can break the rank of gauge symmetry, that is, the $U_b(4)$ gauge group breaks to $U_b(2)$ and the total gauge symmetry is $U(4) \times U(2) \times (2)$. To break the gauge symmetry to the standard-model gauge group, Abelian Wilson line is introduced. There are three types of gauge potential A_a, A_b and A_c. Their configurations are taken as follows

$$A_a = \begin{pmatrix} a_1 \mathbf{1}_3 & \\ & a_2 \mathbf{1}_1 \end{pmatrix}, \quad A_b = b\mathbf{1}_2, \quad A_c = \begin{pmatrix} c_1 \mathbf{1}_1 & \\ & c_2 \mathbf{1}_1 \end{pmatrix}. \tag{259}$$

Then the (supersymmetric) standard model with three generations is realized. Since the different Wilson line leads to different Yukawa couplings, that would lead to various flavor structures. For example, the above model leads to the $\Delta(27)$ flavor symmetry in generic values of Wilson lines as studied in the previous section. However, the flavor symmetry is enhanced to the $\Delta(54)$ symmetry when Wilson lines vanish. Thus by choosing the particular choice of Abelian Wilson lines, we could realize that the flavor symmetry is large like $\Delta(54)$ in a subsector, e.g. in the lepton sector, but the other sector, e.g. the quark sector, has the smaller flavor symmetry like $\Delta(27)$.[14] This is the explicit example which can realize the *co-existence* of the different types of the flavor symmetries from the GUT type models [57]. Furthermore in the next section we will see that this mechanism plays an important role to obtain the realistic quark/lepton mass matrices and mixings.

4.4 Phenomenological model construction

Here the flavor structures we obtained are from their effective field theoretical constructions. Therefore the effective three point couplings have common structures for each of four types of Yukawa couplings and does not depend on the gauge symmetry. Among these structures, the specific example is U(8) Pati-Salam GUT models where its matter sectors have three generations and up and down type Higgs sectors to couple through the Yukawa interactions. We assume the compactification with factorizable three T^2. Then we also assume that all the flavors are generated at one torus in order to obtain various types of Yukawa structures. We show such an example to generate three generations for quarks and leptons and up and down type Higgs fields by introducing following magnetic

[14] Indeed, non-Abelian discrete flavor symmetries such as D_4, $\Delta(27)$ and $\Delta(54)$ would lead to phenomenologically interesting models [89, 88, 90].

flux and Wilson lines which break the standard model gauge groups as

$$F_{z\bar{z}} = \frac{2\pi i}{\mathrm{Im}\tau}\begin{pmatrix} m_1\mathbf{1}_4 & & \\ & m_2\mathbf{1}_2 & \\ & & m_3\mathbf{1}_2 \end{pmatrix}, \tag{260}$$

and

$$A_{z\bar{z}} = \begin{pmatrix} \begin{pmatrix} \xi_Y\mathbf{1}_1 & \\ & \xi_C\mathbf{1}_3 \end{pmatrix} & & \\ & \xi_L\mathbf{1}_2 & \\ & & \begin{pmatrix} \xi_u & \\ & \xi_d \end{pmatrix} \end{pmatrix}, \tag{261}$$

where ξ_Y and ξ_C are the Wilson lines which should have different VEVs each other, otherwise it does not break $U(4) \to U(3) \times U(1)$. Similarly ξ_u and ξ_d are also different VEVs and the remain gauge group goes to the $U(3) \times U(2) \times U(1)^3$. Then the bi-fundamental matter fields are affected by the difference of the Wilson line parameters stratched between each gauge sectors like $A_\alpha - A_\beta$. These structures are also understood by the Intersecting D-brane models in which the positions of the two stack of D-brane are parameterized by the two different open string moduli parameters. One can show the following wavefunction profiles

$$\begin{array}{ccl} Q & : & \Theta^{j,3}(z+\xi_C-\xi_u) \\ L & : & \Theta^{j,3}(z+\xi_Y-\xi_d) \\ u & : & \Theta^{j,3}(z+\xi_C-\xi_L) \\ d & : & \Theta^{j,3}(z+\xi_C-\xi_d) \\ e & : & \Theta^{j,3}(z+\xi_Y-\xi_d) \\ \nu & : & \Theta^{j,3}(z+\xi_Y-\xi_u), \end{array} \tag{262}$$

and

$$H_u : \Theta^{j,3}(z+\xi_L-\xi_u), \qquad H_d : \Theta^{j,3}(z+\xi_L-\xi_d). \tag{263}$$

From the above constructions, up type quark and Dirac neutrino ν couple to the same Higgs fields H^u but their couplings have different Wilson lines. Therefore even in this Pati-Salam models, it allows for quark and lepton to have different types of flavor structures. Then four dimensional Yukawa interactions are expressed by the flavor indices and the parameters of Wilson line degrees of freedom as

$$\mathcal{L} = y^u_{jkl}(\xi^q_u)Q^j u^k H^l_u + y^u_{jkl}(\xi^l_u)E^j\nu^k H^l_u + y^d_{jkl}(\xi^q_d)Q^j d^k H^l_d + y^d_{jkl}(\xi^l_d)E^j e^k H^l_d \tag{264}$$

where Wilson lines ξ^q_u, ξ^l_u, ξ^q_d and ξ^l_d are generally different each other. From the previous analysis this model has flavor structures of $\Delta(27)$ discrete symmetry generally. Three

generations are corresponding to the multiplet of $\Delta(27)$, i.e. triplet $\mathbf{3}$, and 6 Higgs are two triplets. We denote these multiplets as

$$L = \begin{pmatrix} L_0 \\ L_1 \\ L_2 \end{pmatrix}, \quad R = \begin{pmatrix} R_0 \\ R_1 \\ R_2 \end{pmatrix}, \quad H_a = \begin{pmatrix} H_0 \\ H_2 \\ H_4 \end{pmatrix}, \quad H_b = \begin{pmatrix} H_3 \\ H_5 \\ H_1 \end{pmatrix}. \tag{265}$$

In order to get the quark/lepton masses and break the electro weak gauge symmetry, Higgs VEVs are needed. We consider about following typical breaking pattern of Higgs VEV

$$H \to \begin{pmatrix} v \\ 0 \\ 0 \end{pmatrix}. \tag{266}$$

Allowed Yukawa coupling are calculated by overlap integrals, one can show the all possible patterns of Yukawa matrices as

$$H_0 \begin{pmatrix} y_a & 0 & 0 \\ 0 & 0 & y_c \\ 0 & y_e & 0 \end{pmatrix}, \quad H_1 \begin{pmatrix} 0 & y_f & 0 \\ y_b & 0 & 0 \\ 0 & 0 & y_d \end{pmatrix}, \quad H_2 \begin{pmatrix} 0 & 0 & y_e \\ 0 & y_a & 0 \\ y_c & 0 & 0 \end{pmatrix},$$
$$H_3 \begin{pmatrix} y_d & 0 & 0 \\ 0 & 0 & y_f \\ 0 & y_b & 0 \end{pmatrix}, \quad H_4 \begin{pmatrix} 0 & y_c & 0 \\ y_e & 0 & 0 \\ 0 & 0 & y_a \end{pmatrix}, \quad H_5 \begin{pmatrix} 0 & 0 & y_b \\ 0 & y_d & 0 \\ y_f & 0 & 0 \end{pmatrix}.$$

There are six independent Yukawa couplings $y_a, y_b, \cdots, y_f$, these numerical values depend on the complex structure moduli ($\tau = \tau_1 + i\tau_2$) and Wilson line degrees of freedom in two internal directions ($A_1 + iA_2$). In general, one can assign these coefficients as $|y_a| \geq |y_b|, |y_f| \geq |y_c|, |y_e| \geq |y_d|$. Especially, taking $\xi = 0$ or its equivalent configurations of ξ they lead $y_b = y_f$ and $y_c = y_e$. In that case, enhancement of symmetry occurs and approximate flavor symmetry becomes $\Delta(54)$.

Here we provide semi realistic Yukawa patterns. For up type quark sector we take $\tau = 4i$ and $\xi = -4.2i$. Here we note that the moduli parameter τ must be commonly taken for down type quark sectors and lepton sectors. We take following up type Higgs VEVs as $(v_u^a)^T = (v_u\ 0\ 0)$ and $(v_u^b)^T = (0\ 0\ 0)$. Then Yukawa coefficients are $y_a = 0.77$, $y_c = 0.0033$, $y_e = 9.5 \times 10^{-6}$ and quark mass ratio $m_c/m_t = 0.0043$ and $m_u/m_c = 0.0028$. These values are roughly close to realistic ones.

Next we consider about down type quark masses. Taking the down type Higgs VEVs as $v_0^d \neq 0, v_1^d \neq 0$ and others $= 0$ has following down type quark mass matrix

$$m_d = \begin{pmatrix} y_d v_1^d & y_c v_0^d & 0 \\ y_e v_0^d & 0 & y_f v_1^d \\ 0 & y_b v_1^d & y_a v_0^d \end{pmatrix}.$$

To give the models explicitly, we provide some results by taking certain values of Wilson line. For down type quark matrix, we take $A = 0$ with $\tau = 4i$, then it has $m_c/m_b = 0.0010$,

$m_d/m_c = 0.053$, we assume that the Higgs VEVs are $v_0^d = v^d$ and $v_1^d = \frac{v_d}{4}$. It have also small quark mixing as

$$V_{CKM} = \begin{pmatrix} 0.97 & 0.23 & -0.0070 \\ 0.23 & -0.97 & 0.029 \\ 6.9 \times 10^{-6} & 0.030 & 1.0 \end{pmatrix}.$$

The details of the numerical values are shown below

$$y_a = 1, \quad y_b = 0.12, \qquad y_c = 0.00023 \quad y_d = 1.3 \times 10^{-8}$$
$$y_f = y_b, \qquad y_c = y_e.$$

For charged lepton sectors, we can take other Wilson line, it gives m_μ/m_τ =0.049, $m_e/m_\mu = 1.8 \times 10^{-5}$ with $A = -40i$ and commonly used $\tau = 4i$. It gives following charged lepton mass matrix as

$$y_a = 3.4 \times 10^{-7}, \quad y_b = 0.30 \times 10^{-3}, \quad y_c = 0.39$$
$$y_d = 0.79, \qquad y_e = 0.024, \qquad y_f = 1.2 \times 10^{-5}.$$

This matrix gives very small mixing.

For the right handed neutrino masses, it is necessary to make use of seesaw mechanism. In this model it is forbidden to have Majorana neutrino mass terms at tree level. Therefore it may be generated via higher dimensional operators and need additional vector like matter fields. It is obvious that our set up is not defined globally, we must introduce other gauge sectors beyond U(8) gauge symmetry. Even in such case, it is possible to calculate the higher order couplings in principle and these couplings obey the selection rule from the overlap integrals of localized wavefunction. We assume that the effective Majorana mass terms can also have structures similar to three point couplings, $M_{ij}(N_\nu)_i(N_\nu)_j$ and $y_{ijk}(H^u)_k E_i (N_\nu)_j$. Therefore we take the following form of the Majorana mass matrix M_{ij} as

$$M_{ij} = \begin{pmatrix} M & M' & M' \\ M' & M & M' \\ M' & M' & M \end{pmatrix}. \tag{267}$$

These structures respect the $\Delta(54)$ discrete flavor symmetries. Moreover one can construct the Dirac mass matrices simply by assuming the specific vacuum alignments. Here again we must take following up type Higgs VEVs as $(v_u^a)^T = (v_u\ 0\ 0)$ and $(v_u^b)^T = (0\ 0\ 0)$. It leads following Dirac mass matrices

$$M_D = v_u \begin{pmatrix} y_a & 0 & 0 \\ 0 & 0 & y_c \\ 0 & y_e & 0 \end{pmatrix}.$$

As shown before, these coupling y_a, y_c, y_e have generally deferent values. However taking some special combinations of Wilson lines like an enhancement point to $\Delta(54)$, one can

obtain $y_a = y_c \neq y_e$. Then Dirac mass matrices has

$$M_D = v_u \begin{pmatrix} a & 0 & 0 \\ 0 & 0 & b \\ 0 & b & 0 \end{pmatrix}.$$

Here we use the formula of the light neutrino mass formula within seesaw mechanism as $m_D = -M_D^T M_R^{-1} M_D$. That has following neutrino mass matrices as

$$m_D = -\begin{pmatrix} x & y & y \\ y & z & w \\ y & w & z \end{pmatrix},$$

where coefficients x, y, z, w are

$$\begin{aligned} x &= a^2(M + M')D, \qquad y = -abM'D \\ z &= b^2(M + M')D, \qquad w = -b^2 M'D \\ D &= \frac{v_u^2}{M^2 + MM' - 2M'^2}. \end{aligned}$$

As well known, this structure of matrix can be diagonalized by a unitary matrix U as

$$U = \begin{pmatrix} \cos\theta & \sin\theta & 0 \\ -\sin\theta\sqrt{2} & \cos\theta/\sqrt{2} & 1/\sqrt{2} \\ -\sin\theta\sqrt{2} & \cos\theta/\sqrt{2} & -1/\sqrt{2} \end{pmatrix}.$$

For realistic neutrino mixing angles it requires the constraint as $x + y - z - w = 0$ which means $M'/M = -(a + b)/a$ and this gives rise to tri-bimaximal neutrino mixing. One can calculate the tree-level analysis of the coefficient of a, b which depend on the moduli parameters. For the case $a > b$, naively one can expect that $M' \sim -M$ and for the case of $b > a$ it means that the $M'/M \sim b/a$. Since we would expect that the Majorana masses M, M' also depend on the same moduli parameters as a, b, these structures are naturally understood. In fact, if Dirac neutrino mass matrix are taken as $a = 1.0$ and $b = 0.00023$ with assuming $M' = -1.00023M \sim -M$ as a consequence of tri-bi maximal neutrino mixing. By combing two results from up and down type lepton mass matrix, we obtain the following mixing matrix

$$V_{MNS} = \begin{pmatrix} 0.81 & 0.59 & -0.012 \\ -0.41 & 0.55 & -0.72 \\ -0.42 & 0.59 & 0.69 \end{pmatrix}.$$

As shown here, we can obtain the semi-realistic values of not only lepton mixing but also quark mass mixing by shifting the Wilson line parameters. Actually these mass hierarchies in particular lowest mode (e.g. up/down quark or electron) are less than realistic ones but these results are tree-level analysis, so the higher order couplings can give small deviations which may have the large contributions to the small Yukawa sectors.

Moreover we can analyze it including the full parameter spaces of moduli fields. Then we would expect that these Yukawa structures have fully realistic structures of quark/lepton mass hierarchies and mixings. We have shown that it is useful to obtain the realistic flavor structures for the *co-existence* of the different types of flavor symmetries like $\Delta(54)$ and $\Delta(27)$. Actually they are related as the breaking of the larger flavor symmetries. Recently, many interesting discrete symmetries and its subgroups are discussed in [91] and this model is an example for such a scenario. Therefore it is also interesting to study the other different types of the flavor symmetries for quark and lepton as a bottom up approach.

5 Magnetized orbifold models

In this section, we study orbifold models with non-vanishing magnetic fluxes, in particular N=1 super Yang-Mills theory on such a background. Orbifolding the extra dimensions is another way to derive chiral theories [1]. We will show that four-dimensional effective field theories on magnetized orbifolds have a rich structure and they lead to interesting aspects, which do not appear in magnetized torus models. In particular, it will be found that a new type of flavor structures can appear. We also show semi-realistic models on magnetized orbifolds. Furthermore we study more about these backgrounds such as consistency conditions, zero-mode profiles and phenomenological aspects of 4D effective theory.

Effects of Wilson lines on the torus with magnetic fluxes are gauge symmetry breaking and shift of wavefunction profiles. For the same magnetic flux, the numbers of chiral zero-modes between the torus compactification and orbifold compactification are different from each other and zero-modes profiles are different [58, 59]. Adjoint matter fields remain massless on the torus with magnetic fluxes, those are projected out on the orbifold [15]. These differences lead to phenomenologically interesting aspects [59]. In the latter of this section we study more about Wilson line backgrounds such as consistency conditions, zero-mode profiles and phenomenological aspects of 4D effective theory [53].

5.1 $U(1)$ gauge theory on magnetized orbifold T^2/Z_2

Now, let us study $U(1)$ gauge theory on the orbifold T^2/Z_2 with the coordinates (y_4, y_5), which are transformed as

$$y_4 \to -y_4, \qquad y_5 \to -y_5, \tag{268}$$

under the Z_2 orbifold twist. Then, we introduce the same magnetic flux $F_{45} = 2\pi M$ as one in section 2.2 and use the same gauge as (7). Note that this magnetic flux is invariant under the Z_2 orbifold twist and consistent with fractional flux with non-Abelian Wilson line. In the followings we focus on the integer flux case and it is straightforward to extend to the case with non-Abelian Wilson line which is discussed later.

We study the spinor field $\psi(y)$ on the above background. The spinor field $\psi(y)$ with the $U(1)$ charge $q = \pm 1$ satisfies the same equation as one on T^2, i.e. (40). Then, we require $\psi(y)$ transform under the Z_2 twist as

$$\psi(-y_4, -y_5) = (-i)\tilde{\Gamma}^4\tilde{\Gamma}^5 P\psi(-y_4, -y_5), \tag{269}$$

where P depends on the charge q like $P = (-1)^{q+n}$ with $n =$ integer and it should satisfy $P^2 = 1$. Suppose that $qM > 0$. Then, there are M independent zero-modes for ψ when we do not take into account the Z_2 projection. However, some of them are projected out by the above Z_2 boundary condition. For example, for $(-i)\tilde{\Gamma}^4\tilde{\Gamma}^5 P = 1$, only even

[15] Within the framework of intersecting D-brane models, analogous results have been obtained by considering D6-branes wrapping rigid 3-cycles [92].

functions remain, while only odd functions remain for $(-i)\tilde{\Gamma}^4\tilde{\Gamma}^5 P = -1$. Note that

$$\Theta^j(-y_4, -y_5) = \Theta^{M-j}(y_4, y_5), \tag{270}$$

where $\Theta^M(y_4, y_5) = \Theta^0(y_4, y_5)$. That is, even and odd functions are given by

$$\Theta^j_{\rm even} = \frac{1}{\sqrt{2}}(\Theta^j + \Theta^{M-j}), \tag{271}$$

$$\Theta^j_{\rm odd} = \frac{1}{\sqrt{2}}(\Theta^j - \Theta^{M-j}), \tag{272}$$

respectively. Hence, for $M = 2k$ with $k =$ integer and $k > 0$, the number of zero-modes ψ_+ for $P = 1$ and $P = -1$ are equal to $k + 1$ and $k - 1$, respectively. On the other hand, for $M = 2k + 1$ with $k =$ integer and $k \geq 0$, the number of zero-modes ψ_+ for $P = 1$ and $P = -1$ are equal to $k + 1$ and k, respectively. It is interesting that odd functions can correspond to zero-modes in magnetized orbifold models. On the orbifold with vanishing magnetic flux $M = 0$, odd modes correspond to not zero-modes, but massive modes. However, odd modes, which would correspond to massive modes for $M = 0$, mix to lead to zero-modes in the case with $M \neq 0$. It would be convenient to write these results explicitly for later discussions. Table 5 shows the numbers of zero-modes with even and odd wavefunctions for $M \leq 10$. Note that the degree of continuous Wilson line, which we have on the torus, is ruled out on the orbifold.

M	0	1	2	3	4	5	6	7	8	9	10
even	1	1	2	2	3	3	4	4	5	5	6
odd	0	0	0	1	1	2	2	3	3	4	4

Table 5: The numbers of zero-modes with even and odd wavefunctions.

5.2 $U(N)$ gauge theory on magnetized orbifold T^2/Z_2

Now, let us study $U(N)$ gauge theory on the orbifold T^2/Z_2. We consider the same magnetic flux as (53), which breaks the gauge group $U(N) \rightarrow \prod_{a=1}^n U(N_a)$. Furthermore, we associate the Z_2 twist with the Z_2 action in the gauge space as

$$A_\mu(x, -y) = PA_\mu(x, y)P^{-1}, \qquad A_m(x, y) = -PA_m(x, y)P^{-1}. \tag{273}$$

In general, the Z_2 boundary condition breaks the gauge group $\prod_{a=1}^n U(N_a)$ further. For simplicity, here we restrict ourselves to the Z_2 action, which remains the gauge group $\prod_{a=1}^n U(N_a)$ unbroken. Thus, the Z_2 action is trivial for the unbroken gauge group, but it is not trivial for spinor fields as well as scalar fields.

Here, let us study spinor fields. We focus on the $U(N_a) \times U(N_b)$ block (21) and use the same gauge as (7), i.e. $A_4 = F_{45}y_5$ and $A_5 = 0$. We consider the spinor fields, $\lambda^{aa}_\pm$,

$\lambda_\pm^{ab}$, $\lambda_\pm^{ba}$ and $\lambda_\pm^{bb}$, where $\pm$ denotes the chirality in the extra dimension like (11). Their Z_2 boundary conditions are given by

$$\lambda_\pm(x,-y) = \pm P\lambda_\pm(x,y)P^{-1}, \tag{274}$$

for $\lambda_\pm^{aa}$, $\lambda_\pm^{ab}$, $\lambda_\pm^{ba}$ and $\lambda_\pm^{bb}$. First, we study the gaugino fields, $\lambda_\pm^{aa}$ and $\lambda_\pm^{bb}$ for the unbroken gauge group. Since the Z_2 action P is trivial for the unbroken gauge indices, the above Z_2 boundary conditions reduce to $\lambda_\pm^{aa}(x,-y) = \pm\lambda_\pm^{aa}(x,y)$ and $\lambda_\pm^{bb}(x,-y) = \pm\lambda_\pm^{bb}(x,y)$. In addition, the magnetic flux does not appear in their zero-mode equations. Thus, $\lambda_+^{aa}(x,y)$ as well as $\lambda_+^{bb}(x,y)$ has a zero-mode, but $\lambda_-^{aa}(x,y)$ and $\lambda_-^{bb}(x,y)$ are projected out by the Z_2 orbifold projection as the usual Z_2 orbifold without the magnetic flux.

Next, let us study the bi-fundamental matter fields $\lambda_\pm^{ab}$ and $\lambda_\pm^{ba}$. The magnetic flux $M_a - M_b$ appears in their zero-mode equations. Without the Z_2 projection, there are $|M_a - M_b|$ zero-modes. For example, when $M_a - M_b > 0$, λ_+^{ab} as well as λ_-^{ba} has $(M_a - M_b)$ zero-modes with the wavefunctions Θ^j for $j = 0, \cdots, (M_a - M_b - 1)$. When we consider the Z_2 projection, either even or odd modes remain. For example, when we consider the projection P such that $\lambda_+^{ab}(x,-y) = \lambda_+^{ab}(x,y)$, only zero-modes corresponding to $\Theta^j_{\rm even}$ remain and the number of zero-modes is equal to $(M_a - M_b)/2 + 1$ for $(M_a - M_b) =$ even and $(M_a - M_b + 1)/2$ for $(M_a - M_b) =$ odd. On the other hand, when we consider the projection P such that $\lambda_+^{ab}(x,-y) = -\lambda_+^{ab}(x,y)$, only zero-modes corresponding to $\Theta^j_{\rm odd}$ remain and the number of zero-modes is equal to $(M_a - M_b)/2 - 1$ for $(M_a - M_b) =$ even and $(M_a - M_b - 1)/2$ for $(M_a - M_b) =$ odd. The same holds true for λ_-^{ba}. Furthermore, when $M_a - M_b < 0$, the situation is the same except replacing $(M_a - M_b)$, λ_+^{ab} and λ_-^{ba} by $|M_a - M_b|$, λ_-^{ab} and λ_+^{ba}, respectively.

The 3-point couplings among modes corresponding to the wavefunctions, $\Theta^i_{\rm even,odd}$, $\Theta^j_{\rm even,odd}$ and $\Theta^k_{\rm even,odd}$ are given by the overlap integral like (129). Note that

$$\int dy\ \Theta^i_{\rm even}(y)\cdot\Theta^j_{\rm even}(y)\cdot\Theta^k_{\rm odd}(y) = \int dy\ \Theta^i_{\rm odd}(y)\cdot\Theta^j_{\rm odd}(y)\cdot\Theta^k_{\rm odd}(y) = 0, \tag{275}$$

while $\int dy\ \Theta^i_{\rm even}(y)\cdot\Theta^j_{\rm odd}(y)\cdot\Theta^k_{\rm odd}(y)$ and $\int dy\ \Theta^i_{\rm even}(y)\cdot\Theta^j_{\rm even}(y)\cdot\Theta^k_{\rm even}(y)$ are nonvanishing.

5.3 $U(N)$ gauge theory on magnetized orbifolds T^6/Z_2 and $T^6/(Z_2\times Z_2')$

Here, we can extend the previous analysis on the two-dimensional orbifold T^2/Z_2 to the $U(N)$ gauge theory on the six-dimensional orbifolds T^6/Z_2 and $T^6/(Z_2\times Z_2')$. We consider two types of six-dimensional orbifolds, T^6/Z_2 and $T^6/(Z_2\times Z_2')$. For the orbifold T^6/Z_2, the Z_2 twist acts on the six-dimensional coordinates y_m $(m = 4, \cdots, 9)$ as

$$y_m \to -y_m \ \ (\text{for} \ \ m = 4,5,6,7), \qquad y_n \to y_n \ \ (\text{for} \ \ n = 8,9). \tag{276}$$

In addition to this Z_2 action, we introduce another independent Z_2' action,

$$y_m \to -y_m \ \ (\text{for} \ \ m = 4,5,8,9), \qquad y_n \to y_n \ \ (\text{for} \ \ n = 6,7), \tag{277}$$

for the orbifold $T^6/(Z_2 \times Z_2')$. If magnetic flux is vanishing, we realize four-dimensional N=2 and N=1 supersymmetric gauge theories for the orbifolds, T^6/Z_2 and $T^6/(Z_2 \times Z_2')$, respectively.

Now, let us introduce the same magnetic flux as (27). The gauge group $U(N)$ is broken as $U(N) \to \prod_{a=1}^n U(N_a)$ with $N = \sum_a N_a$. This magnetic flux is invariant under both Z_2 and Z_2' actions. Furthermore, we associate the Z_2 and Z_2' twists with the Z_2 and Z_2' actions in the gauge space as

$$\begin{aligned} A_\mu(x,-y_m,y_n) &= PA_\mu(x,-y_m,y_n)P^{-1}, \\ A_m(x,-y_m,y_n) &= -PA_m(x,-y_m,y_n)P^{-1}, \\ A_n(x,-y_m,y_n) &= PA_n(x,-y_m,y_n)P^{-1}, \end{aligned} \tag{278}$$

for $m = 4,5,6,7$ and $n = 8,9$, and

$$\begin{aligned} A_\mu(x,-y_m,y_n) &= P'A_\mu(x,-y_m,y_n)P'^{-1}, \\ A_m(x,-y_m,y_n) &= -P'A_m(x,-y_m,y_n)P'^{-1}, \\ A_n(x,-y_m,y_n) &= P'A_n(x,-y_m,y_n)P'^{-1}, \end{aligned} \tag{279}$$

for $m = 4,5,8,9$ and $n = 6,7$. In general, these Z_2 boundary conditions break the gauge group $\prod_{a=1}^n U(N_a)$ further. For simplicity, here we restrict to the Z_2 and Z_2' projections, which remain the gauge group $\prod_{a=1}^n U(N_a)$ unbroken. That is, both the Z_2 and Z_2' actions are trivial for the unbroken gauge group.

Now, we study spinor fields. We focus on the $U(N_a)\times U(N_b)$ block as (28) and use the same gauge as (29). We consider the spinor fields $\lambda^{aa}_{s_1,s_2,s_3}$, $\lambda^{ab}_{s_1,s_2,s_3}$, $\lambda^{ba}_{s_1,s_2,s_3}$ and $\lambda^{bb}_{s_1,s_2,s_3}$, where s_i denotes the chirality corresponding to the i-th T^2. Their Z_2 boundary conditions are given by

$$\lambda_{s_1,s_2,s_3}(x,-y_m,y_n) = s_1 s_2 P \lambda_{s_1,s_2,s_3}(x,y_m,y_n)P^{-1}, \tag{280}$$

with $m = 4,5,6,7$ and $n = 8,9$ for $\lambda^{aa}_{s_1,s_2,s_3}$, $\lambda^{ab}_{s_1,s_2,s_3}$, $\lambda^{ba}_{s_1,s_2,s_3}$ and $\lambda^{bb}_{s_1,s_2,s_3}$. Similarly, the Z_2' boundary conditions are given by

$$\lambda_{s_1,s_2,s_3}(x,-y_m,y_n) = s_1 s_3 P' \lambda_{s_1,s_2,s_3}(x,y_m,y_n)P'^{-1}, \tag{281}$$

with $m = 4,5,8,9$ and $n = 6,7$.

First, we study the gaugino fields $\lambda^{aa}_{s_1,s_2,s_3}$ and $\lambda^{bb}_{s_1,s_2,s_3}$ for the unbroken gauge group. Their zero-mode equations have no effect due to magnetic fluxes, but only the Z_2 and Z_2' orbifold twists play a role. Since the Z_2 and Z_2' twists, P and P', are trivial for the unbroken gauge sector, the boundary conditions are given by

$$\lambda^{aa(bb)}_{s_1,s_2,s_3}(x,-y_m,y_n) = s_1 s_2 \lambda^{aa(bb)}_{s_1,s_2,s_3}(x,y_m,y_n) \qquad \text{for} \quad Z_2, \tag{282}$$

with $m = 4,5,6,7$ and $n = 8,9$, and

$$\lambda^{aa(bb)}_{s_1,s_2,s_3}(x,-y_m,y_n) = s_1 s_3 \lambda^{aa(bb)}_{s_1,s_2,s_3}(x,y_m,y_n) \qquad \text{for} \quad Z_2', \tag{283}$$

with $m = 4, 5, 8, 9$ and $n = 6, 7$. Hence, zero-modes of $\lambda^{aa(bb)}_{+,+,\pm}$ and $\lambda^{aa(bb)}_{-,-,\pm}$ survive on T^6/Z_2, that is, two kinds of gaugino fields with a fixed four-dimensional chirality. Furthermore, on $T^6/(Z_2 \times Z_2')$, zero-modes of $\lambda^{aa(bb)}_{+,+,+}$ and $\lambda^{aa(bb)}_{-,-,-}$ survive, that is, a single sort of gaugino fields with a fixed four-dimensional chirality.

Next, let us study the bi-fundamental matter fields, $\lambda^{ab}_{s_1,s_2,s_3}$ and $\lambda^{ba}_{s_1,s_2,s_3}$. Without the Z_2 projection, they have zero-modes, whose number is $I_{ab} = I^1_{ab} I^2_{ab} I^3_{ab}$ and wavefunctions are given by $\Theta^{j_1}(y_4, y_5)\Theta^{j_2}(y_6, y_7)\Theta^{j_3}(y_8, y_9)$ $(j_i = 0, \cdots, (I^i_{ab} - 1))$. We assume that $I^i_{ab} > 0$ for $i = 1, 2, 3$. Then, the zero-modes correspond to $\lambda^{ab}_{+,+,+}$. On T^6/Z_2, some of them are projected out. Suppose that the Z_2 boundary condition is given by

$$\lambda^{ab}_{s_1,s_2,s_3}(x, -y_m, y_n) = s_1 s_2 \lambda^{ab}_{s_1,s_2,s_3}(x, y_m, y_n), \tag{284}$$

with $m = 4, 5, 6, 7$ and $n = 8, 9$. Then, surviving zero-modes correspond to $\Theta^{j_1}_{\rm even}(y_4, y_5)\Theta^{j_2}_{\rm even}(y_6, y_7)\Theta^{j_3}(y_8, y_9)$ and $\Theta^{j_1}_{\rm odd}(y_4, y_5)\Theta^{j_2}_{\rm odd}(y_6, y_7)\Theta^{j_3}(y_8, y_9)$. Further modes are projected out on $T^6/(Z_2 \times Z_2')$. Suppose that the Z_2' boundary condition is given by

$$\lambda^{ab}_{s_1,s_2,s_3}(x, -y_m, y_n) = s_1 s_3 \lambda^{ab}_{s_1,s_2,s_3}(x, y_m, y_n), \tag{285}$$

with $m = 4, 5, 8, 9$ and $n = 6, 7$. Then, the surviving modes through the $Z_2 \times Z_2'$ projection correspond to $\Theta^{j_1}_{\rm even}(y_4, y_5)\Theta^{j_2}_{\rm even}(y_6, y_7)\Theta^{j_3}_{\rm even}(y_8, y_9)$ and $\Theta^{j_1}_{\rm odd}(y_4, y_5)\Theta^{j_2}_{\rm odd}(y_6, y_7)\Theta^{j_3}_{\rm odd}(y_8, y_9)$. Similarly, we can analyze surviving zero-modes through the $Z_2 \times Z_2'$ projection in the models with different signs of I^i_{ab} and different $Z_2 \times Z_2'$ projections. It would be convenient to introduce the notation, $I^i_{ab({\rm even})}$ and $I^i_{ab({\rm odd})}$, such that $I^i_{ab({\rm even})}$ and $I^i_{ab({\rm odd})}$ denote the number of even and odd functions, $\Theta^j_{\rm even}$ and $\Theta^j_{\rm odd}$, respectively, among $|I^i_{ab}|$ functions Θ^j for the i-th T^2. Note that $I^i_{ab({\rm even})}, I^i_{ab({\rm odd})} \geq 0$ in the above definition, while I^i_{ab} can be negative.

5.3.1 Discrete flavor symmetry for orbifold models

We have found that several non-abelian discrete flavor symmetries like D_4, $\Delta(27)$ and $\Delta(54)$ can appear. However, these exact symmetries may be rather large to explain realistic mass matrices of quarks and leptons. Their breaking would be preferable. Such symmetry breaking can happen within the framework of four-dimensional effective field theory, that is, scalar fields with non-trivial representations are assumed to develop their vacuum expectation values. On the other hand, a certain type of symmetry breaking can happen on the orbifold background, which is called magnetized orbifold models [58, 59]. Here, we discuss the flavor structure in magnetized orbifold models.

The orbifold T^2/Z_2 is constructed by dividing T^2 by the Z_2 projection $z \to -z$. Furthermore, on such an orbifold, we require periodic or anti-periodic boundary condition for matter fields as well as gauge fields,

$$\psi(-z) = \pm\, \psi(z). \tag{286}$$

Since such boundary conditions are consistent in models with vanishing Wilson lines, we consider the case without Wilson lines. Indeed, zero-mode wavefunctions in models

without Wilson lines satisfy the following relation,

$$\psi^{j,M}(-z) = \psi^{M-j,M}(z). \tag{287}$$

Thus, even and odd zero-modes are obtained as their linear combinations,

$$\psi^j_\pm(z) = \psi^{j,M}(z) \pm \psi^{M-j,M}(z), \tag{288}$$

up to a normalization factor. Which modes among even and odd modes are selected depends on how to embed the Z_2 orbifold projection into the gauge space, that is, model dependent. At any rate, either even or odd zero-modes are projected out for each kind of matter fields[16]. Note that the Z_2 orbifold parity of $\psi^j_\pm(z)$ is the same as the Z_2 charge of P. Thus, through the orbifold projection zero-modes with either even or odd Z_2 charge of P survive for each kind of matter fields.

Let us consider examples. First we study the model with $g = 2$. This model has the non-abelian flavor symmetry $D_4 \times Z_2$. The zero-modes with $M = 2$, $\psi^{i,2}$, correspond to $\mathbf{2}_+$ of $D_4 \times Z_2$. When we require the periodic boundary condition, they survive. On the other hand, they are projected out for the anti-periodic boundary condition. Similarly, the zero-modes with $M = 4$, $\psi^{i,4}$, correspond to $\mathbf{1}_{+++}$, $\mathbf{1}_{+-+}$, $\mathbf{1}_{-++}$ and $\mathbf{1}_{---}$, where the third subscript denotes the Z_2 charge of P. Thus, the zero-modes corresponding to $\mathbf{1}_{+++}$, $\mathbf{1}_{+-+}$ and $\mathbf{1}_{-++}$ survive for the periodic boundary condition, while only $\mathbf{1}_{---}$ survives for the anti-periodic boundary condition. Similarly, we can identify which modes can survive through the Z_2 orbifold projection. The number of matter fields are reduced through the Z_2 orbifold projection. However, four-dimensional effective field theory after orbifolding has the flavor symmetry $D_4 \times Z_2$. The reason why the flavor symmetry $D_4 \times Z_2$ remains unbroken is that the flavor symmetry is the direct product between D_4 and Z_2.

Next, let us consider the model with $g = 3$. This model has the flavor symmetry $\Delta(54)$. The zero-modes with $M = 3$, $\psi^{i,3}$, correspond to $\mathbf{3}_1$ of $\Delta(54)$. However, the eigenstates of Z_2 are $\psi^{0,3}$ and $\psi^{1,3} \pm \psi^{2,3}$. Hence, when we project out Z_2 even or odd modes, the triplet structure is broken, that is, the flavor symmetry $\Delta(54)$ is completely broken. However, such symmetry breaking is non-trivial, because the original theory has the $\Delta(54)$ symmetry and we project out certain modes from such a theory.[17]

Orbifold models with larger g, $g > 3$ have a similar structure on flavor symmetries. The original theory before orbifolding has a large non-abelian flavor symmetry. By orbifolding, certain matter fields are projected out and the flavor symmetry is broken although some symmetries like abelian discrete symmetries remain unbroken. However, there remains a footprint of the larger flavor symmetry in four-dimensional effective theory, that is, coupling terms are constrained.

As an illustrating example, let us consider explicitly the model with three zero-modes, which have relative magnetic fluxes, $(M_1, M_2, M_3) = (4, 4, 8)$, that is, $g = 4$. The genera-

[16]Within the framework of intersecting D-brane models, analogous results have been obtained by considering D6-branes wrapping rigid 3-cycles [92].

[17] This type of flavor symmetry breaking has been proposed in not magnetized brane models, but orbifold models [93, 94, 95].

i,j,k	L_i	R_j	H_k
0	$\psi^{0,4}$	$\psi^{0,4}$	$\psi^{0,8}$
1	$\frac{1}{\sqrt{2}}\left(\psi^{1,4}+\psi^{3,4}\right)$	$\frac{1}{\sqrt{2}}\left(\psi^{1,4}+\psi^{3,4}\right)$	$\frac{1}{\sqrt{2}}\left(\psi^{1,8}+\psi^{7,8}\right)$
2	$\psi^{2,4}$	$\psi^{2,4}$	$\frac{1}{\sqrt{2}}\left(\psi^{2,8}+\psi^{6,8}\right)$
3	-	-	$\frac{1}{\sqrt{2}}\left(\psi^{3,8}+\psi^{5,8}\right)$
4	-	-	$\psi^{4,8}$

Table 6: Wavefunctions in the orbifold model.

tors, Z, C and P, are represented on the zero-modes with $M_1 = 4$ as

$$Z = \begin{pmatrix} 1 & & & \\ & i & & \\ & & -1 & \\ & & & -i \end{pmatrix}, \quad C = \begin{pmatrix} & 1 & & \\ & & 1 & \\ & & & 1 \\ 1 & & & \end{pmatrix}, \quad P = \begin{pmatrix} 1 & & & \\ & & & 1 \\ & & 1 & \\ & 1 & & \end{pmatrix}. \tag{289}$$

Obviously, we find $[P,Z] \neq 0$ and $[C,P] \neq 0$. Thus, eigenstates of P are not eigenstates for Z or C. Since eigenstates with $P = 1$ or $P = -1$ are projected out by orbifolding, the flavor symmetry is broken. However, one can find that $[P,Z^2] = [P,C^2] = 0$. The symmetry generated by Z^2, C^2 and P remains unbroken after orbifolding. Thus, the flavor symmetry is reduced to $Z_2 \times Z_2 \times Z_2$. The first two Z_2 factors are originally subgroups of $Z_4 \ltimes (Z_4 \times Z_4)$ generated by Z and C algebra and they are abelian groups.

For concreteness, let us consider the following Z_2 boundary conditions,

$$\psi^{i_1,M_1}(-z) = \psi^{i_1,M_1}(z), \quad \psi^{i_2,M_2}(-z) = \psi^{i_2,M_2}(z), \quad \psi^{i_3,M_3}(-z) = \psi^{i_3,M_3}(z), \tag{290}$$

for three types of zero-modes. Then, we assign the first and second modes with left-handed and right-handed fermions, L_i and R_j, while the third is assigned with Higgs fields H_k. There are three Z_2 even modes for $M_1 = M_2 = 4$, that is, the three generation model [58, 59], while there are five Z_2 even modes for $M_3 = 8$. Their wavefunctions are shown in Table 6.

After orbifold projection, Yukawa couplings $Y_{ijk}L_iR_jH_k$ in this model are given by [59]

$$Y_{ijk}H_k = \begin{pmatrix} y_aH_0 + y_eH_4 & y_fH_3 + y_bH_1 & y_cH_2 \\ y_fH_3 + y_bH_1 & \frac{1}{\sqrt{2}}(y_a + y_e)H_2 + y_c(H_0 + H_4) & y_bH_3 + y_dH_1 \\ y_cH_2 & y_bH_3 + y_dH_1 & y_eH_0 + y_aH_4 \end{pmatrix}. \tag{291}$$

Here, Yukawa coupling strengths, $y_a, y_b, \cdots, y_f$, are written as functions of moduli and they are, in general, different from each other.

We can take the basis of L_i, R_j, H_k as eigenstates of Z^2 and C^2. Such a basis is shown in Table 7. Thus, if this effective theory has only $Z_4 \times Z_2 \times Z_2$ symmetry, the following

L_i	Z^2	C^2	R_j	Z^2	C^2	H_k	Z^2	C^2
$\frac{1}{\sqrt{2}}(L^0+L^2)$	1	1	$\frac{1}{\sqrt{2}}(R^0+R^2)$	1	1	$\frac{1}{\sqrt{2}}(H^0+H^4)$	1	1
$\frac{1}{\sqrt{2}}(L^0-L^2)$	1	–1	$\frac{1}{\sqrt{2}}(R^0-R^2)$	1	–1	$\frac{1}{\sqrt{2}}(H^0-H^4)$	1	–1
L_1	–1	1	R_1	–1	1	$\frac{1}{\sqrt{2}}(H^1+H^3)$	–1	1
–	–	–	–	–	–	$\frac{1}{\sqrt{2}}(H^1-H^3)$	–1	–1
–	–	–	–	–	–	H_2	1	1

Table 7: Eigenstates of Z^2 and C^2

couplings would be allowed,

$$Y_{ijk}H_k = \begin{pmatrix} y_1H_0+y_2H_2+y_3H_4 & y_4H_1+y_5H_3 & y_6H_0+y_7H_2+y_8H_4 \\ y'_4H_1+y'_5H^3 & y_9(H_0+H_4)+y_{10}H_2 & y'_5H_1+y'_4H_3 \\ y_8H_0+y_7H_2+y_6H_4 & y_5H_1+y_4H_3 & y_3H_0+y_2H_2+y_1H_4 \end{pmatrix} \quad (292)$$

where coupling strengths like y_1,y_2, etc. are independent parameters. For example, the $Z_4\times Z_2\times Z_2$ symmetry allows non-vanishing couplings of y_2, y_6 and y_8. However, these couplings are forbidden by the symmetry $Z_4 \ltimes (Z_4\times Z_4)$ and such couplings do not appear in Eq. (291). Thus, Yukawa couplings derived from orbifolding are constrained more compared with the model, which has only the $Z_4\times Z_2\times Z_2$ flavor symmetry.

Similarly, other orbifold models have more constraints at least at tree level compared with unbroken symmetry as a footprint of larger flavor symmetries before orbifolding. Such a structure would be useful for phenomenological applications.

Finally let us consider generic situation of unbroken flavor symmetry. Here we use the properties of the algebra for the discrete symmetries. All the elements h are represented by $h=\omega^tZ^rC^s$, $(r,s,t=0,1,\cdots,g-1)$. The remain generator with respect to unbroken symmetry should commute with generator P. Using the following properties

$$\begin{aligned} Z^g = C^g = \omega^g = 1, \quad CZ = \omega ZC, \\ PC = C^{-1}P, \quad PZ = Z^{-1}P \end{aligned} \quad (293)$$

elements satisfying the conditions ($2r=0 \mod g$ and $2s=0 \mod g$) only remain as unbroken symmetry. Obviously the case with $g=$ odd has trivial discrete symmetries as Z_g. Cases with $g=$ even are divided two possibilities as $g=2m$ or $g=2m+2$, $(m\in\mathcal{Z})$. For the former case all the elements are commutable, remain symmetry is $Z_g\times Z_2\times Z_2$. On the other hand, in the latter case one find two elements $C^{g/2}$ and $Z^{g/2}$ have $C^{g/2}Z^{g/2}=-Z^{g/2}C^{g/2}$. Therefore the remain symmetry is non-Abelian discrete symmetry $Z_2\ltimes(Z_g\times Z_2)$.

5.4 Three generation magnetized orbifold models

In this section, we consider the $U(N_a)\times U(N_b)\times U(N_c)$ models, which lead to three families of bi-fundamental matter fields, $(N_a,\bar{N}_b)$ and $(\bar{N}_a,N_c)$. Such a gauge group is derived by

starting with the $U(N)$ group and introducing the following form of the magnetic flux,

$$
\begin{aligned}
F_{45} &= 2\pi \begin{pmatrix} M_a^{(1)}\mathbf{1}_{N_a\times N_a} & & 0 \\ & M_b^{(1)}\mathbf{1}_{N_b\times N_b} & \\ 0 & & M_c^{(1)}\mathbf{1}_{N_c\times N_c} \end{pmatrix}, \\
F_{67} &= 2\pi \begin{pmatrix} M_a^{(2)}\mathbf{1}_{N_a\times N_a} & & 0 \\ & M_b^{(2)}\mathbf{1}_{N_b\times N_b} & \\ 0 & & M_c^{(2)}\mathbf{1}_{N_c\times N_c} \end{pmatrix}, \\
F_{89} &= 2\pi \begin{pmatrix} M_a^{(3)}\mathbf{1}_{N_a\times N_a} & & 0 \\ & M_b^{(3)}\mathbf{1}_{N_b\times N_b} & \\ 0 & & M_c^{(3)}\mathbf{1}_{N_c\times N_c} \end{pmatrix},
\end{aligned}
$$

where $N = N_a + N_b + N_c$. For $N_a = 4, N_b = 2$ and $N_c = 2$, we can realize the Pati-Salam gauge group up to $U(1)$ factors, some of which may be anomalous and become massive by the Green-Schwarz mechanism. Then, the bi-fundamental matter fields, $(N_a, \bar{N}_b)$ and $(\bar{N}_a, N_c)$ correspond to left-handed and right-handed matter fields. In addition, the bi-fundamental matter fields $(N_b, \bar{N}_c)$ correspond to higgsino fields. We assume that supersymmetry is preserved at least locally at the $a-b$ sector, $b-c$ sector and $c-a$ sector.[18] Then, the number of Higgs scalar fields are the same as the number of higgsino fields. There are no tachyonic modes at the tree level. Indeed, in intersecting D-brane models it would be one of convenient ways towards realistic models to derive the Pati-Salam model at some stage and to break the gauge group to the group $SU(3) \times SU(2)_L \times U(1)$. (See e.g. Ref. [25, 96] and references therein.)[19] At the end of this section, we give a comment on breaking of $SU(4) \times SU(2)_L \times SU(2)_R$ to $SU(3) \times SU(2)_L \times U(1)$.

In both cases with and without orbifolding, the total number of chiral matter fields is a product of the numbers of zero-modes corresponding to the i-th T^2 for $i = 1, 2, 3$. That is, the three generations are realized in the models, where the i-th T^2 has three zero-modes while each of the other tori has a single zero-mode. Thus, there are two types of flavor structures. That is, in one type the three zero-modes corresponding to both left-handed matter fields $(N_a, \bar{N}_b)$ and right-handed matter fields $(\bar{N}_a, N_c)$ appear in the same i-th T^2, while each of the other tori has a single zero-mode for $(N_a, \bar{N}_b)$ as well as $(\bar{N}_a, N_c)$. In the other type, three zero-modes of $(N_a, \bar{N}_b)$ and $(\bar{N}_a, N_c)$ are originated from different tori. The Yukawa coupling for 4D effective field theory is evaluated by the following overlap integral of zero-mode wavefunctions [97]

$$
Y_{ij} = \int d^6y \psi_{Li}(y)\psi_{Rj}(y)\phi_H(y),
$$

[18] See for the supersymmetric conditions e.g. Ref. [52, 62].

[19] See for the Pati-Salam model in heterotic orbifold models e.g. Ref. [3], where $SU(4) \times SU(2)_L \times SU(2)_R$ is broken to the standard gauge group by vacuum expectation values of scalar fields, $(4, 1, 2)$ and $(\bar{4}, 1, 2)$, while in the intersecting D-brane models $SU(4) \times SU(2)_L \times SU(2)_R$ is broken by splitting D-branes, that is, vacuum expectation values of adjoint scalar fields.

	λ^{ab}	λ^{ca}	λ^{bc}
I	even	even	even
II	even	odd	odd
II'	odd	even	odd
III	odd	odd	even

Table 8: Possible patterns of wavefunctions with non-vanishing Yukawa couplings for the first torus.

where $\psi_L(y)$, $\psi_R(y)$ and $\phi_H(y)$ denote zero-mode wave-functions of the left-handed, right-handed matter fields and Higgs field, respectively. Note that the integral corresponding to each torus is factorized in the Yukawa coupling. In the second type of flavor structure, one obtains the following form of Yukawa matrices,

$$Y_{ij} \quad = \quad a_i b_j,$$

at the tree-level, because the flavor structure of left-handed and right-handed matter fields are originated from different tori. This matrix, Y_{ij}, has rank one and that is not phenomenologically interesting, unless certain corrections appear. Hence, we concentrate on the first type of the flavor structure. In the first type, the flavor structure is originated from the single torus, where both three zero-modes of $(N_a, \bar{N}_b)$ and $(\bar{N}_a, N_c)$ appear. We assign this torus with the first torus. On the other hand, the other tori, the second and third tori, do not lead to flavor-dependent aspects. That is, Yukawa matrices are obtained as the following form,

$$Y_{ij} \quad = \quad a^{(2)} a^{(3)} a^{(1)}_{ij},$$

where the structure of $a^{(1)}_{ij}$ is determined by only the first torus corresponding to three zero-modes $(N_a, \bar{N}_b)$ and $(\bar{N}_a, N_c)$ while the other tori contribute to overall factors $a^{(2)}$ and $a^{(3)}$. Thus, we concentrate on the single torus, where both of three zero-modes $(N_a, \bar{N}_b)$ and $(\bar{N}_a, N_c)$ appear, i.e. the first torus.

Zero-mode wavefunctions are classified into even and odd modes under the Z_2 twist. Only even or odd modes remain through the orbifold projection. Furthermore, the 4D Yukawa couplings are non-vanishing for combinations among (even, even, even) wavefunctions and (even, odd, odd) wavefunctions, while Yukawa couplings vanish for combinations among (even, even, odd) wavefunctions and (odd, odd, odd) wavefunctions. Thus, we study only the former case with non-vanishing Yukawa couplings, that is, the combinations among (even, even, even) wavefunctions and (even, odd, odd) wavefunctions. Hence, we are interested in four types of combinations of wavefunctions for the first torus, as shown in Table 8. The II' type of combinations is obtained by exchanging the left and right-handed matter fields in the II type. Thus, we study explicitly the three types, I, II and III.

We can realize three even zero-modes when $|I^{(1)}_{ab}| = 4, 5$, as shown in Table 5. On the other hand, three odd zero-modes can appear when $|I^{(1)}_{ab}| = 7, 8$. Furthermore, the

	$\lvert I_{ab}^{(1)}\rvert$	$\lvert I_{ca}^{(1)}\rvert$	$\lvert I_{bc}^{(1)}\rvert$	the numbers of Higgs zero-modes
I	4	4	8	5
	4	4	0	1
	4	5	9	5
	4	5	1	5
	5	5	10	6
	5	5	0	1
II	4	7	11	5
	4	7	3	1
	4	8	12	5
	4	8	4	1
	5	7	12	5
	5	7	2	0
	5	8	13	6
	5	8	3	1
III	7	7	14	8
	7	7	0	1
	7	8	15	8
	7	8	1	1
	8	8	16	9
	8	8	0	1

Table 9: The number of Higgs fields of $(T^2)^1$ with non-vanishing Yukawa couplings.

consistency condition on magnetic fluxes requires

$$|I_{bc}^{(1)}| \;\; = \;\; |I_{ab}^{(1)}| \pm |I_{ca}^{(1)}|.$$

Thus, the number of Higgs and higgsino fields are constrained. Table 9 shows all of possible magnetic fluxes for the three types, I, II and III. The fourth and fifth columns of the table show possible sizes of magnetic fluxes for $|I_{bc}^{(1)}|$ and the number of zero-modes corresponding to the Higgs fields. As a result, flavor structures of our models with Yukawa couplings are classified into 20 classes. However, the model with $(|I_{ab}^{(1)}|, |I_{ca}^{(1)}|, |I_{bc}^{(1)}|) = (5, 7, 2)$ has no zero-modes for the Higgs fields. Thus, we do not consider this case, but we will study the other 19 classes in Table 9. Therefore, we study possible flavor structures explicitly by deriving the coupling selection rule and evaluating values of Yukawa couplings in these 19 classes. That is the purpose of the next section.

Before explicit study on flavor structures of 19 classes in the next section, we give a comment on breaking of $SU(4) \times SU(2)_L \times SU(2)_R$. At any rate, we need the $SU(3) \times SU(2)_L \times U(1)$ gauge group at low-energy. When the magnetic flux and orbifold projections lead to the $SU(4) \times SU(2)_L \times SU(2)_R$ gauge group from $U(8)$ as we have discussed so far, we need further breaking of $SU(4) \times SU(2)_L \times SU(2)_R$ to $SU(3) \times SU(2)_L \times U(1)$. Such

breaking can be realized by assuming non-vanishing vacuum expectation values (VEVs) of Higgs fields like adjoint scalar fields for $SU(4)$ and $SU(2)_R$ and/or bi-fundamental scalar fields like $(4,1,2)$ and $(\bar{4},1,2)$ on fixed points. Note that our models have degree of freedom to add any modes at the fixed points from the viewpoint of point particle field theory. The above breaking may affect the structure of Yukawa matrices as higher dimensional operators. However, we will show results on Yukawa matrices without such corrections.

Alternatively, magnetic fluxes and/or orbifold projections break $U(8)$ into $U(3) \times U(1)_1 \times U(2)_L \times U(1)_2 \times U(1)_3$. The gauge group $U(3) \times U(1)_1$ would correspond to $U(4)$ and $U(1)_2 \times U(1)_3$ would correspond to $U(2)_R$. We assume that all the bi-fundamental matter fields under $U(3) \times U(1)_1$, i.e. extra colored modes, are projected out. The bi-fundamental matter fields for $U(3) \times U(1)_2$ and $U(3) \times U(1)_3$ correspond to up and down sectors of right-handed quarks, respectively. Similarly, up and down sectors of Higgs fields and right-handed charged leptons and neutrinos are obtained. In this case, the classification of this section and patterns of Yukawa matrices, which will be studied in the next section and Appendix, are available for up-sector and down-sector quarks as well as the lepton sector. However, the up sector and down sector can correspond to different classes of Table 9. On the other hand, the up sector and down sector correspond to the same class in Table 9, when the $SU(4) \times SU(2)_L \times SU(2)_R$ is broken by VEVs of Higgs fields on fixed points as discussed above.

5.4.1 Yukawa couplings in three generation models

Following [52, 74], first we show computation of Yukawa interactions on the torus with the magnetic flux. Omitting the gauge structure and spinor structure, the Yukawa coupling among left, right-handed matter fields and Higgs field corresponding to three zero-mode wavefunctions, $\Theta^{i,M_1}(z)$, $\Theta^{j,M_2}(z)$ and $(\Theta^{k,M_3}(z))^*$, is written by

$$Y_{ijk} \;=\; c\int dz d\bar{z}\,\Theta^{i,M_1}(z)\Theta^{j,M_2}(z)(\Theta^{k,M_3}(z))^*, \tag{294}$$

where $z = x_4 + \tau y_5$, $M_1 \equiv I_{ab}^{(1)}$, $M_2 \equiv I_{ca}^{(1)}$, $M_3 \equiv I_{cb}^{(1)}$ and c is a flavor-independent contribution due to the other tori. Note that $M_1 + M_2 = M_3$. Because of the gauge invariance, not the wavefunction $\Theta^{k,M_3}(z)$, but $(\Theta^{k,M_3}(z))^*$ appears in the Yukawa coupling [52].

By using the formula of the ϑ function,

$$\begin{aligned}
&\vartheta\begin{bmatrix} r/N_1 \\ 0 \end{bmatrix}(z_1, N_1\tau) \,\times\, \vartheta\begin{bmatrix} s/N_2 \\ 0 \end{bmatrix}(z_2, N_2\tau) \\
&= \sum_{m\in\mathcal{Z}_{N_1+N_2}} \vartheta\begin{bmatrix} \frac{r+s+N_1 m}{N_1+N_2} \\ 0 \end{bmatrix}(z_1+z_2, \tau(N_1+N_2)) \\
&\qquad\qquad \times \vartheta\begin{bmatrix} \frac{N_2 r - N_1 s + N_1 N_2 m}{N_1 N_2 (N_1+N_2)} \\ 0 \end{bmatrix}(z_1 N_2 - z_2 N_1, \tau N_1 N_2 (N_1+N_2)),
\end{aligned}$$

we can decompose $\Theta^{i,M_1}(z)\Theta^{j,M_2}(z)$ as

$$\Theta^{i,M_1}(z)\,\Theta^{j,M_2}(z) \;=\; \sum_{m\in\mathcal{Z}_{M_3}} \Theta^{i+j+M_1m,M_3}(z)\,\times\,\vartheta\begin{bmatrix}\frac{M_2i-M_1j+M_1M_2m}{M_1M_2M_3}\\ 0\end{bmatrix}(0,\tau M_1M_2M_3)\,.$$

Wavefunctions satisfy the orthogonal condition

$$\int dzd\bar{z}\,\Theta^{i,M}\,(\Theta^{j,M})^* \;=\; \delta_{ij}.$$

Then, the integral of three wavefunctions is represented by

$$\begin{aligned} Y_{ijk} &= c\int dzd\bar{z}\,\Theta^{i,M_1}\,\Theta^{j,M_2}(\Theta^{k,M_3})^* \\ &= c\sum_{m=0}^{|M_3|-1}\vartheta\begin{bmatrix}\frac{M_2i-M_1j+M_1M_2m}{M_1M_2M_3}\\ 0\end{bmatrix}(0,\tau M_1M_2M_3)\times\delta_{i+j+M_1m,\,k+M_3\ell}, \end{aligned}$$

where $\ell=$ integer.

Thus, we have the selection rule for allowed Yukawa couplings as

$$i+j=k,$$

where i,j and k are defined up to mod M_1, M_2 and M_3, respectively.[20] In addition, the Yukawa coupling Y_{ijk}, in particular its flavor-dependent part, is written by the ϑ function. When $g.c.d.(M_1,M_3)=1$, a single ϑ function appears in Y_{ijk}. When $g.c.d.(M_1,M_3)=g\neq 1$, g terms appear in Y_{ijk} as

$$Y_{ijk}=c\sum_{n=1}^{g}\vartheta\begin{bmatrix}\frac{M_2k-M_3j+M_2M_3\ell_0}{M_1M_2M_3}+\frac{n}{g}\\ 0\end{bmatrix}(0,\tau M_1M_2M_3),$$

where ℓ_0 is an integer corresponding to a particular solution of $M_3l_0=M_1m_0+i+j-k$ with integer m_0.

Zero-mode wavefunctions on the orbifold with the magnetic flux are obtained as even or odd linear combinations of wavefunctions on the torus with the magnetic flux (288). Thus, it is straightforward to extend the above computations of Yukawa couplings on the torus to Yukawa couplings on the orbifold. As a result, Yukawa couplings on the orbifold are obtained as proper linear combinations of Yukawa couplings on the torus, i.e. linear combinations of ϑ functions. Here we introduce the following short notation for the Yukawa coupling,

$$\eta_N \;=\; \vartheta\begin{bmatrix}\frac{N}{M}\\ 0\end{bmatrix}(0,\tau M)\,, \tag{295}$$

[20] See for the selection rule in intersecting D-brane models, e.g. Ref. [26, 75].

	$L_i(\lambda^{ab})$	$R_j(\lambda^{ca})$	$H_k(\lambda^{bc})$
0	$\frac{1}{\sqrt{2}}(\Theta^{1,7}-\Theta^{6,7})$	$\frac{1}{\sqrt{2}}(\Theta^{1,7}-\Theta^{6,7})$	$\Theta^{0,14}$
1	$\frac{1}{\sqrt{2}}(\Theta^{2,7}-\Theta^{5,7})$	$\frac{1}{\sqrt{2}}(\Theta^{2,7}-\Theta^{5,7})$	$\frac{1}{\sqrt{2}}(\Theta^{1,14}+\Theta^{13,14})$
2	$\frac{1}{\sqrt{2}}(\Theta^{3,7}-\Theta^{4,7})$	$\frac{1}{\sqrt{2}}(\Theta^{3,7}-\Theta^{4,7})$	$\frac{1}{\sqrt{2}}(\Theta^{2,14}+\Theta^{12,14})$
3	-	-	$\frac{1}{\sqrt{2}}(\Theta^{3,14}+\Theta^{11,14})$
4	-	-	$\frac{1}{\sqrt{2}}(\Theta^{4,14}+\Theta^{10,14})$
5	-	-	$\frac{1}{\sqrt{2}}(\Theta^{5,14}+\Theta^{9,14})$
6	-	-	$\frac{1}{\sqrt{2}}(\Theta^{6,14}+\Theta^{8,14})$
7	-	-	$\Theta^{7,14}$

Table 10: Zero-mode wavefunctions in the 7-7-14 model.

where

$$M = M_1M_2M_3.$$

Since the value of M is unique in one model, we omit the value of M as well as τ for a compact presentation of long equations.

Four models in Table 9 has $|I_{bc}^{(1)}| = 0$, where the Higgs zero-mode corresponds to the even function, that is, the constant profile. We can repeat the above calculation for this case, that is, the case where, one of wavefunctions in (294), e.g. $\Theta^{i,M_1}(z)$ is constant. As a result, the Yukawa matrix is proportional to the (3×3) unit matrix, $Y_{jk} = c'\delta_{jk}$. That is not realistic. Thus, we will not consider such models.

At any rate, we can apply the above selection rule and η_N for 20 classes of models, which have been classified in section 5.4, in order to analyze explicitly all of possible patterns of Yukawa matrices. In the next subsection, we show one example of Yukawa matrix among 20 classes of models. In Appendix C, we show all of possible Yukawa matrices for 15 classes of models in Table 9 except models with $I_{bc}^{(1)} = 0$ and the model without zero-modes for the Higgs fields.

5.4.2 An illustrating example: 7-7-14 model

Let us study the model with $(|I_{ab}^{(1)}|, |I_{ca}^{(1)}|, |I_{bc}^{(1)}|) = (7, 7, 14)$. Following Table 9, we consider the combination of zero-mode wavefunctions, where zero-modes of left and right-handed matter fields and Higgs fields correspond to odd, odd and even wavefunctions, respectively. Their wavefunctions are shown in Table 10. Hereafter, for concreteness, we denote left and right-handed matter fields and Higgs fields by L_i, R_j and H_k, respectively. This model has eight zero-modes for Higgs fields.

Then, their Yukawa couplings $Y_{ijk}L_iR_jH_k$ are written by

$$Y_{ijk}H_k = y_{ij}^0H_0 + y_{ij}^1H_1 + y_{ij}^2H_2 + y_{ij}^3H_3 + y_{ij}^4H_4 + y_{ij}^5H_5 + y_{ij}^6H_6 + y_{ij}^7H_7,$$

where

$$
\begin{aligned}
y^0_{ij} &= \begin{pmatrix} -y_c & 0 & 0 \\ 0 & -y_e & 0 \\ 0 & 0 & -y_g \end{pmatrix}, \quad y^1_{ij} = \begin{pmatrix} 0 & -\frac{1}{\sqrt{2}}y_d & 0 \\ -\frac{1}{\sqrt{2}}y_d & 0 & -\frac{1}{\sqrt{2}}y_f \\ 0 & -\frac{1}{\sqrt{2}}y_f & \frac{1}{\sqrt{2}}y_h \end{pmatrix}, \\
y^2_{ij} &= \begin{pmatrix} \frac{1}{\sqrt{2}}y_a & 0 & -\frac{1}{\sqrt{2}}y_e \\ 0 & 0 & \frac{1}{\sqrt{2}}y_g \\ -\frac{1}{\sqrt{2}}y_e & \frac{1}{\sqrt{2}}y_g & 0 \end{pmatrix}, \quad y^3_{ij} = \begin{pmatrix} 0 & \frac{1}{\sqrt{2}}y_b & \frac{1}{\sqrt{2}}y_f \\ \frac{1}{\sqrt{2}}y_b & \frac{1}{\sqrt{2}}y_h & 0 \\ \frac{1}{\sqrt{2}}y_f & 0 & 0 \end{pmatrix}, \\
y^4_{ij} &= \begin{pmatrix} 0 & \frac{1}{\sqrt{2}}y_g & \frac{1}{\sqrt{2}}y_c \\ \frac{1}{\sqrt{2}}y_g & \frac{1}{\sqrt{2}}y_a & 0 \\ \frac{1}{\sqrt{2}}y_c & 0 & 0 \end{pmatrix}, \quad y^5_{ij} = \begin{pmatrix} \frac{1}{\sqrt{2}}y_h & 0 & -\frac{1}{\sqrt{2}}y_d \\ 0 & 0 & \frac{1}{\sqrt{2}}y_b \\ -\frac{1}{\sqrt{2}}y_d & \frac{1}{\sqrt{2}}y_b & 0 \end{pmatrix}, \\
y^6_{ij} &= \begin{pmatrix} 0 & -\frac{1}{\sqrt{2}}y_e & 0 \\ -\frac{1}{\sqrt{2}}y_e & 0 & -\frac{1}{\sqrt{2}}y_c \\ 0 & -\frac{1}{\sqrt{2}}y_c & \frac{1}{\sqrt{2}}y_a \end{pmatrix}, \quad y^7_{ij} = \begin{pmatrix} -y_f & 0 & 0 \\ 0 & -y_d & 0 \\ 0 & 0 & -y_b \end{pmatrix}, \qquad (296)
\end{aligned}
$$

and

$$
\begin{aligned}
y_a &= \eta_0 + 2\eta_{98} + 2\eta_{196} + 2\eta_{294}, \\
y_b &= \eta_7 + \eta_{91} + \eta_{105} + \eta_{189} + \eta_{203} + \eta_{287} + \eta_{301}, \\
y_c &= \eta_{14} + \eta_{84} + \eta_{112} + \eta_{182} + \eta_{210} + \eta_{280} + \eta_{308}, \\
y_d &= \eta_{21} + \eta_{77} + \eta_{119} + \eta_{175} + \eta_{217} + \eta_{273} + \eta_{315}, \\
y_e &= \eta_{28} + \eta_{70} + \eta_{126} + \eta_{168} + \eta_{224} + \eta_{266} + \eta_{322}, \\
y_f &= \eta_{35} + \eta_{63} + \eta_{133} + \eta_{161} + \eta_{231} + \eta_{259} + \eta_{329}, \\
y_g &= \eta_{42} + \eta_{56} + \eta_{140} + \eta_{154} + \eta_{238} + \eta_{252} + \eta_{336}, \\
y_h &= 2\eta_{49} + 2\eta_{147} + 2\eta_{245} + \eta_{343}.
\end{aligned}
$$

Here we have used the short notation η_N defined in Eq. (295) with the omitted value $M = M_1M_2M_3 = 686$.

5.4.3 Numerical examples in 7-7-14 model

Here, we give examples of numerical studies by using the 7-7-14 model, which is discussed in the previous subsection. For such studies, the numerical values of η_N defined in Eq. (295) are useful. The N-dependence of η_N is shown in Fig. 8.

We assume that both the up-sector and the down-sector of quarks as well as their Higgs fields have the Yukawa matrix, which is led in the 7-7-14 model. Such situation is realized in the case that we start with the $U(8)$ gauge group and break it to $U(4)\times U(2)_L\times U(2)_R$ by the magnetic flux, and then the Pati-Salam gauge group is broken to the Standard gauge group by assuming VEVs of Higgs fields on fixed points. Alternatively, we break the $U(8)$ gauge group to $U(3)\times U(1)_1\times U(2)_L\times U(1)_2\times U(1)_3$ by magnetic fluxes and orbifold projections as discussed in section 3. Then, both the up-sector and down-sector of quarks

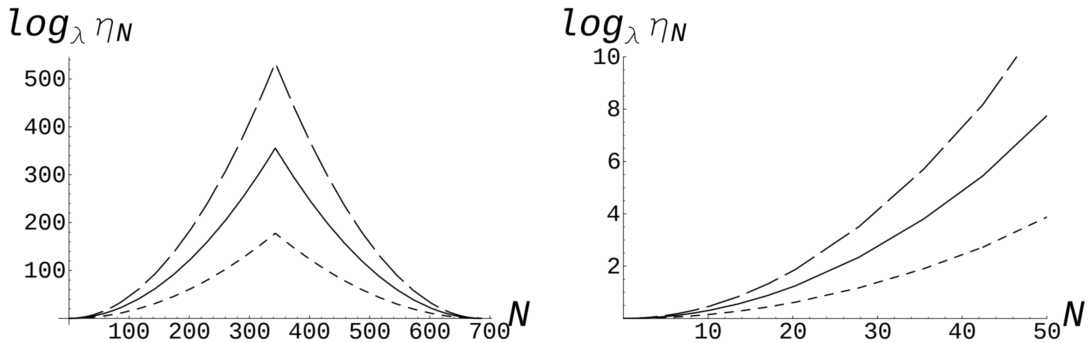

Figure 8: The N-dependence of $\log_\lambda \eta_N$ in the 7-7-14 model ($M = 686$), where $\lambda = 0.22$ is chosen to the Cabibbo angle. The solid, dashed and dotted curves correspond to $\tau = i$, $1.5i$ and $0.5i$, respectively. Note that η_N has a periodicity $\eta_{N+nM} = \eta_N$ with an integer n.

can correspond to the Yukawa matrix led in the 7-7-14 model, although the up-sector and down-sector can generically correspond to different patterns of Yukawa matrices. In both cases, VEVs of the up-sector and down-sector Higgs fields are independent.

First, we consider the case that VEVs of H_d^6, H_d^7 and H_u^0 are non-vanishing and the other VEVs vanish. In this case, the relevant Yukawa couplings are

$$
\begin{aligned}
Y_{ijk}^u H_k &= \begin{pmatrix} -y_c & & \\ & -y_e & \\ & & -y_g \end{pmatrix} H_u^0, \\
Y_{ijk}^d H_k &= \begin{pmatrix} -y_f H_d^7 & -\frac{1}{\sqrt{2}} y_e H_d^6 & 0 \\ -\frac{1}{\sqrt{2}} y_e H_d^6 & -y_d H_d^7 & -\frac{1}{\sqrt{2}} y_c H_d^6 - \\ 0 & -\frac{1}{\sqrt{2}} y_c H_d^6 & \frac{1}{\sqrt{2}} y_a H_d^6 - y_b - H_d^7 \end{pmatrix}.
\end{aligned}
$$

Let us assume $\langle H_d^6 \rangle = -\langle H_d^7 \rangle$ for their VEVs. Then, quark mass ratios are obtained from these matrices as

$$
\begin{aligned}
(m_u, m_c, m_t)/m_t &\sim (7.6 \times 10^{-4}, 6.8 \times 10^{-2}, 1.0), \\
(m_d, m_s, m_b)/m_b &\sim (7.5 \times 10^{-4}, 5.1 \times 10^{-2}, 1.0),
\end{aligned}
$$

for $\tau = i$. Furthermore, the mixing angles are obtained as

$$
|V_{CKM}| \sim \begin{pmatrix} 0.97 & 0.24 & 0.0025 \\ 0.24 & 0.95 & 0.20 \\ 0.046 & 0.19 & 0.98 \end{pmatrix}.
$$

Similarly, for $\tau = 1.5i$, quark mass ratios are obtained as

$$
\begin{aligned}
(m_u, m_c, m_t)/m_t &\sim (2.1 \times 10^{-5}, 1.8 \times 10^{-2}, 1.0), \\
(m_b, m_s, m_d)/m_b &\sim (1.4 \times 10^{-4}, 1.7 \times 10^{-2}, 1.0),
\end{aligned}
$$

and the mixing angles are obtained as

$$|V_{CKM}| \sim \begin{pmatrix} 0.99 & 0.13 & 0.00029 \\ 0.13 & 0.98 & 0.13 \\ 0.017 & 0.13 & 0.99 \end{pmatrix}.$$

Let us consider another type of VEVs. We assume that VEVs of H_u^0, H_u^2, H_d^1 and H_d^7 are non-vanishing and the other VEVs vanish. Furthermore, we consider the case with $\langle H_u^0 \rangle = -\langle H_u^2 \rangle$ and $\langle H_d^1 \rangle = \langle H_d^7 \rangle/3$. In this case, the mass ratios are given by

$$\begin{aligned}(m_u, m_c, m_t)/m_t &\sim (2.9 \times 10^{-5},\, 2.5 \times 10^{-2},\, 1.0), \\ (m_d, m_s, m_b)/m_b &\sim (4.4 \times 10^{-3},\, 0.18,\, 1.0),\end{aligned}$$

for $\tau = i$, and the mixing angles are given by

$$|V_{CKM}| \sim \begin{pmatrix} 0.98 & 0.22 & 0.018 \\ 0.22 & 0.98 & 0.0014 \\ 0.017 & 0.0052 & 1.0 \end{pmatrix}.$$

Similarly, for $\tau = 1.5i$ the mass ratios and the mixing angles are given by

$$\begin{aligned}(m_u, m_c, m_t)/m_t &\sim (5.6 \times 10^{-6},\, 4.7 \times 10^{-3},\, 1.0), \\ (m_d, m_s, m_b)/m_b &\sim (3.3 \times 10^{-3},\, 7.1 \times 10^{-2},\, 1.0),\end{aligned}$$

$$|V_{CKM}| \sim \begin{pmatrix} 0.98 & 0.22 & 0.0034 \\ 0.22 & 0.98 & 0.000081 \\ 0.0033 & 0.00081 & 1.0 \end{pmatrix}.$$

Thus, these values can realize experimental values of quark masses and mixing angles at a certain level by using a few parameters, i.e. τ and a couple of VEVs of Higgs fields. If we consider more non-vanishing VEVs of Higgs fields, we could obtain more realistic values. For example, we assume that VEVs of H_u^0, H_u^1, H_u^2, H_d^1 and H_d^7 are non-vanishing and they satisfy $-\langle H_u^0 \rangle = \langle H_u^1 \rangle = \langle H_u^2 \rangle$ and $\langle H_d^1 \rangle = -\langle H_d^7 \rangle/2$ while the other VEVs vanish. For $\tau = 1.5i$, we realize the mass ratios, $m_u/m_t \sim 2.7 \times 10^{-5}$, $m_c/m_t \sim 3.5 \times 10^{-3}$, $m_d/m_b \sim 7.3 \times 10^{-3}$ and $m_s/m_b \sim 7.5 \times 10^{-2}$, and mixing angles, $V_{us} \sim 0.2$, $V_{cb} \sim 0.03$ and $V_{ub} \sim 0.006$. When we consider more non-vanishing VEVs of Higgs fields, it is possible to derive completely realistic values. Similarly, we can study other classes of models and they have a rich flavor structure.

5.5 Orbifold background with non-Abelian Wilson line

Since we have obtained the explicit wavefunctions on the torus with non-Abelian Wilson lines, we can easily extend above analysis to the case with non-Abelian Wilson line. we study the T^2/Z_2 orbifold, which is constructed by dividing T^2 by the Z_2 projection $z \rightarrow$

$-z$. Furthermore, we require the field projection of periodic or anti-periodic boundary conditions with consistent of Z_2 orbifold,

$$\Psi(-y_4, -y_5) = P\Psi(y_4, y_5), \tag{297}$$

where P is $+1$ or -1. One can show that the matter wavefunctions satisfy the following property

$$\Psi^j_{pq}(-y_4, -y_5) = \Psi^{-j}_{-p,-q}(y_4, y_5). \tag{298}$$

Obviously, in the case with Abelian Wilson, this result reduces to $\Psi(-y_4, -y_5)^j = \Psi(y_4, y_5)^j$. For the case with $k = 1$, this relation holds, because every sector of (p, q) is related by the boundary conditions, so the labels (p, q) have no meaning. However $k \neq 1$ case, they have $k \times M$ independent zero-modes and we symbolically denote them by $\Psi^{j,\tilde{j}}$ ($j = 0, 1, ..., M-1$ and $\tilde{j} = 0, 1, ..., k-1$). For example, in the case with $n_a = n_b = 3$, we may use the following notations

$$\begin{gathered}
\Psi^j_{00},\ \Psi^j_{11},\ \Psi^j_{22} \to \Psi^{j,\tilde{j}=0}, \\
\Psi^j_{01},\ \Psi^j_{12},\ \Psi^j_{20} \to \Psi^{j,\tilde{j}=1}, \\
\Psi^j_{02},\ \Psi^j_{10},\ \Psi^j_{21} \to \Psi^{j,\tilde{j}=2}.
\end{gathered} \tag{299}$$

where $\tilde{j} = p - q \mod K$. Then, the above property (298) can be written as

$$\Psi^{j,\tilde{j}}(-y_4, -y_5) = \Psi^{-j,-\tilde{j}}(y_4, y_5). \tag{300}$$

Then the even and odd wave-functions are easily obtained. For the case with $M = 3$, there are 3×3 independent fields and they are divided into the following even and odd wavefunctions

$$\begin{array}{rcl}
\text{even} & : & \Psi^{0,0},\ \Psi^{1,0} + \Psi^{2,0},\ \Psi^{0,1} + \Psi^{0,2},\ \Psi^{1,1} + \Psi^{2,2}, \Psi^{2,1} + \Psi^{1,2}, \\
\text{odd} & : & \Psi^{1,0} - \Psi^{2,0},\ \Psi^{1,1} - \Psi^{2,2},\ \Psi^{2,1} - \Psi^{1,2}.
\end{array} \tag{301}$$

Note that these represent the wavefunctions e.g. $\Psi^1_{12} + \Psi^2_{21}$ by $\Psi^{1,1} + \Psi^{2,2}$. As examples, the zero-mode numbers of even and odd wavefunctions for smaller values of k and M are shown in Table 11.

Yukawa couplings as well as higher order couplings can be computed on the orbifold background by overlap integrals of wavefunctions in a way similar to the torus models.

5.6 Further direction to orbifold

Here, we study orbifold models with magnetic fluxes and Wilson lines. The T^2/Z_2 orbifold is constructed by identifying $z \sim -z$ on T^2. We also embed the Z_2 twist into the gauge space as P. Note that under the Z_2 twist, magnetic flux background is invariant. That

$k=1$

M	1	2	3	4	5	6
even	1	2	2	3	3	4
odd	0	0	1	1	2	2

$k=2$

M	1	2	3	4	5	6
even	2	4	4	6	6	8
odd	0	0	2	2	4	4

$k=3$

M	1	2	3	4	5	6
even	2	4	5	7	8	10
odd	1	2	4	5	7	8

$k=4$

M	1	2	3	4	5	6
even	3	6	7	10	11	14
odd	1	2	5	6	9	10

Table 11: The numbers of even and odd zero-modes

is, we have no constraint on magnetic fluxes due to orbifolding. Furthermore, zero-mode wavefunctions satisfy

$$\Theta^{j,M}(-z) = \Theta^{M-j,M}(z). \tag{302}$$

Note that $\Theta^{0,M}(z) = \Theta^{M,M}(z)$. Hence, the Z_2 eigenstates are written as [58]

$$\Theta^{j,M}_{\pm}(z) = \frac{1}{\sqrt{2}} \left(\Theta^{j,M}(z) \pm \Theta^{M-j,M}(z) \right), \tag{303}$$

for $j \neq 0, M/2, M$. The wavefunctions $\Theta^{j,M}(z)$ for $j = 0, M/2$ are the Z_2 eigenstates with the Z_2 even parity. Either of $\Theta^{j,M}_{+}(z)$ and $\Theta^{j,M}_{-}(z)$ is projected out by the orbifold projection. Odd wavefunctions can also correspond to massless modes in the magnetic flux background, although on the orbifold without magnetic flux odd modes always correspond to massive modes, but not massless modes. Before orbifolding, the number of zero-modes is equal to the magnetic flux M. For example, we have to choose $M = 3$ in order to realize the three families. On the other hand, the number of zero-modes on the orbifold also depends on the boundary conditions under the Z_2 twist, even or odd functions. For $M =$ even, the number of zero-modes with even (odd) functions are equal to $M/2 + 1$ $(M/2 - 1)$. For $M =$ odd, the number of zero-modes with even and odd functions are equal to $(M + 1)/2$ and $(M - 1)/2$, respectively.

Now, let us introduce Wilson lines [98] with some different types of gauge groups. For example, we consider $U(1)_a \times SU(2)$ theory. Then we introduce magnetic flux in $U(1)_a$ like Eq. (89). In addition, we embed the Z_2 twist P into the $SU(2)$ gauge space. For example, we consider the $SU(2)$ doublet

$$\begin{pmatrix} \lambda_{1/2} \\ \lambda_{-1/2} \end{pmatrix}, \tag{304}$$

with the $U(1)_a$ charge q_a. We embed the Z_2 twist P in the gauge space as

$$P = \begin{pmatrix} 0 & 1 \\ 1 & 0 \end{pmatrix}, \tag{305}$$

for the doublet. Obviously, we can diagonalize P as $P' = \mathrm{diag}(1, -1)$, if there is no Wilson line along the other $SU(2)$ directions. However, we introduce a Wilson line along

the Cartan direction of $SU(2)$, i.e, the following direction

$$\begin{pmatrix} 1 & 0 \\ 0 & -1 \end{pmatrix}, \tag{306}$$

in the P basis. Thus, we use the above basis for P. For the $SU(2)$ gauge sector, there is no effect due to the magnetic flux. Then, the situation is the same as one on the orbifold without magnetic flux. The $SU(2)$ gauge group is broken completely, that is, all of $SU(2)$ vector multiplets become massive.

Before orbifolding, the $SU(2)$ is not broken and both $\lambda_{1/2}$ and $\lambda_{-1/2}$ have $M = q_a m_a$ independent zero-modes, which we denote by $\Theta^{j,M}_{1/2}(z)$ and $\Theta^{j,M}_{-1/2}(z)$, respectively. Here, we have put the indices, $1/2$ and $-1/2$ in order to make it clear that they correspond to $\lambda_{1/2}$ and $\lambda_{-1/2}$, respectively. However, the form of wavefunctions are the same, i.e. $\Theta^{j,M}_{1/2}(z) = \Theta^{j,M}_{-1/2}(z)$. When we impose the orbifold boundary conditions with the above P in (305), the zero-modes on the orbifold without Wilson lines are written as

$$\frac{1}{\sqrt{2}}\left(\Theta^{j,M}_{1/2}(z) + \Theta^{M-j,M}_{-1/2}(z)\right), \tag{307}$$

for $j = 0, \cdots, M-1$. Note that there are M independent zero-modes. It may be useful to explain remaining zero-modes in the basis for P'. Before orbifolding, both $\lambda'_{1/2}$ and $\lambda'_{-1/2}$ have $M = q_a m_a$ independent zero-modes in the basis for P'. Then by orbifolding with P', even modes corresponding to $\Theta^{j,M}_{+}(z)$ remain for $\lambda'_{1/2}$, while $\lambda'_{-1/2}$ has only odd modes $\Theta^{j,M}_{-}(z)$. Their total number is equal to M.

Then, we introduce the Wilson lines along the Cartan direction in the basis for P. The corresponding zero-mode wavefunctions are shifted as

$$\frac{1}{\sqrt{2}}\left(\Theta^{j,M}_{1/2}(z + C^b/2M) + \Theta^{M-j,M}_{-1/2}(z - C^b/2M)\right), \tag{308}$$

for $j = 0, \cdots, M-1$, where C^b is a continuous parameter. Note that $\lambda_{1/2}$ and $\lambda_{-1/2}$ have opposite charges under the $SU(2)$ Cartan element. Then, their wavefunctions are shifted to opposite directions by the same Wilson lines C^b as $\Theta^{j,M}_{1/2}(z + C^b/2M)$ and $\Theta^{j,M}_{-1/2}(z - C^b/2M)$. We can also consider the Z_2 twist P in the doublet such that the following wavefunction

$$\frac{1}{\sqrt{2}}\left(\Theta^{j,M}_{1/2}(z + C^b/2M) - \Theta^{M-j,M}_{-1/2}(z - C^b/2M)\right), \tag{309}$$

remains.

The above aspect would be important to applications for particle phenomenology. We compute Yukawa couplings among two $SU(2)$ doublet fields and a singlet field. We assume that two $SU(2)$ doublet fields have $U(1)_a$ charges q^1_a and q^2_a, while the singlet field has the $U(1)_a$ charge q^3_a. We introduce the magnetic flux m_a in $U(1)_a$ and the same $SU(2)$

Wilson line as the above. Then, the zero-mode wavefunctions of two $SU(2)$ doublets and the singlet can be obtained on the orbifold as

$$\begin{aligned}
\begin{pmatrix} \lambda^1_{1/2} \\ \lambda^1_{-1/2} \end{pmatrix} &: \frac{1}{\sqrt{2}}\left(\Theta^{i,M_1}_{1/2}(z+C^b/2M_1)+\Theta^{M_1-i,M_1}_{-1/2}(z-C^b/2M_i)\right), \\
\begin{pmatrix} \lambda^2_{1/2} \\ \lambda^2_{-1/2} \end{pmatrix} &: \frac{1}{\sqrt{2}}\left(\Theta^{j,M_2}_{1/2}(z+C^b/2M_2)+\Theta^{M_2-j,M_2}_{-1/2}(z-C^b/2M_j)\right), \\
\lambda^3_0 &: \frac{1}{\sqrt{2}}\left(\Theta^{k,M_3}_{0}(z)+\Theta^{M_3-k,M_3}_{0}(z)\right)^*,
\end{aligned} \tag{310}$$

where $M_i = q^i_a m_a$. Note that the Wilson line C^b has no effect on the wavefunctions of the $SU(2)$ singlet field λ^3_0 because λ^3_0 has no $SU(2)$ charges. Here we have taken the same orbifold projection P as Eq. (305), but we can study other orbifold projections. Then, their Yukawa couplings are obtained by the following overlap integral,

$$\begin{aligned}
&\frac{1}{2\sqrt{2}}\int d^2z\{\Theta^{i,M_1}_{1/2}(z+C^b/2M_1)\Theta^{j,M_2}_{-1/2}(z-C^b/2M_2)\left(\Theta^{k,M_3}_{0}(z)+\Theta^{M_3-k,M_3}_{0}(z)\right)^* \\
&+\Theta^{M_1-i,M_1}_{-1/2}(z-C^b/2M_1)\Theta^{M_2-j,M_2}_{1/2}(z+C^b/2M_2)\left(\Theta^{k,M_3}_{0}(z)+\Theta^{M_3-k,M_3}_{0}(z)\right)^*\}.
\end{aligned} \tag{311}$$

This integral is computed as

$$\begin{aligned}
&\sum_{m\in \mathbf{Z}_{M_3}} \delta_{i+j+M_1m,k}\times\vartheta\begin{bmatrix}\frac{M_2i-M_1j+M_1M_2m}{M_1M_2M_3}\\ 0\end{bmatrix}(C^b(M_1+M_2)/2,\tau M_1M_2M_3), \\
&+\sum_{m\in \mathbf{Z}_{M_3}} \delta_{i+j+M_1m,-k}\times\vartheta\begin{bmatrix}\frac{M_2i-M_1j+M_1M_2m}{M_1M_2M_3}\\ 0\end{bmatrix}(C^b(M_1+M_2)/2,\tau M_1M_2M_3), \\
&+\sum_{m\in \mathbf{Z}_{M_3}} \delta_{-i-j+M_1m,k}\times\vartheta\begin{bmatrix}\frac{-M_2i+M_1j+M_1M_2m}{M_1M_2M_3}\\ 0\end{bmatrix}(-C^b(M_1+M_2)/2,\tau M_1M_2M_3) \\
&+\sum_{m\in \mathbf{Z}_{M_3}} \delta_{-i-j+M_1m,-k}\times\vartheta\begin{bmatrix}\frac{-M_2i+M_1j+M_1M_2m}{M_1M_2M_3}\\ 0\end{bmatrix}(-C^b(M_1+M_2)/2,\tau M_1M_2M_3),
\end{aligned} \tag{312}$$

up to the normalization factor $N_1N_2/(2\sqrt{2}N_3)$, where the Kronecker delta $\delta_{i+j+M_1m,k}$ in the first term means $i+j+M_1m = k$ mod M_3 and others have the same meaning. Obviously, the result depends non-trivially on the Wilson line C^b. Thus, the Wilson lines have important effects on the Yukawa couplings.

For comparison, we study another dimensional representations, e.g. a triplet

$$\begin{pmatrix} \lambda_1 \\ \lambda_0 \\ \lambda_{-1} \end{pmatrix}, \tag{313}$$

with the $U(1)_a$ charge q_a. Suppose that we embed the Z_2 twist P in the three dimensional gauge space as

$$P = \begin{pmatrix} 0 & 0 & 1 \\ 0 & 1 & 0 \\ 1 & 0 & 0 \end{pmatrix}, \tag{314}$$

for the triplet. Then, zero-modes on the orbifold are written as

$$\begin{aligned} &\Theta_1^{j,M}(z) + \Theta_{-1}^{M-j,M}(z), \\ &\Theta_0^{j,M}(z) + \Theta_0^{M-j,M}(z), \end{aligned} \tag{315}$$

up to the normalization factor $1/\sqrt{2}$. The former corresponds to λ_1 and λ_{-1} and there are M zero-modes. The latter corresponds to λ_0 and there are $(M/2+1)$ zero-modes and $(M+1)/2$ zero-modes when M is even and odd, respectively. When we introduce the continuous Wilson lines along the Cartan direction, the wavefunctions of these zero-modes shift as

$$\begin{aligned} &\Theta_1^{j,M}(z + C_b/M) + \Theta_{-1}^{M-j,M}(z - C_b/M), \\ &\Theta_0^{j,M}(z) + \Theta_0^{M-j,M}(z), \end{aligned} \tag{316}$$

up to the normalization factor $1/\sqrt{2}$.

Similarly to the above, here let us compute the Yukawa couplings among two $SU(2)$ doublets corresponding to Eq. (310) and the triplet $(\lambda_1^3, \lambda_0^3, \lambda_{-1}^3)$. In particular, we compute the couplings including λ_1^3 and λ_{-1}^3, whose zero-mode wavefunctions are obtained by

$$\frac{1}{2\sqrt{2}} \left(\Theta_1^{k,M_3}(z + C_b/M_3) + \Theta_{-1}^{M_3-k,M_3}(z - C_b/M_3) \right)^*, \tag{317}$$

with $M_3 = q_a^3 m_a$ after orbifolding. Their Yukawa couplings are obtained by the following overlap integral,

$$\begin{aligned} \frac{1}{2\sqrt{2}} \int d^2z \{ &\Theta_{1/2}^{i,M_1}(z + C^b/2M_1) \Theta_{1/2}^{j,M_2}(z + C^b/2M_2) \left(\Theta_{-1}^{M_3-k,M_3}(z - C_b/M_3) \right)^* \\ &+ \Theta_{-1/2}^{M_1-i,M_1}(z - C^b/2M_1) \Theta_{-1/2}^{M_2-j,M_2}(z - C^b/2M_2) \left(\Theta_1^{k,M_3}(z + C_b/M_3) \right)^* \}. \end{aligned} \tag{318}$$

This integral is computed as

$$\begin{aligned} &\sum_{m \in \mathbf{Z}_{M_3}} \delta_{i+j+M_1 m, k} \times \vartheta \begin{bmatrix} \frac{M_2 i - M_1 j + M_1 M_2 m}{M_1 M_2 M_3} \\ 0 \end{bmatrix} (C^b(M_2 - M_1)/2), \tau M_1 M_2 M_3), \\ &+ \sum_{m \in \mathbf{Z}_{M_3}} \delta_{-i-j+M_1 m, -k} \times \vartheta \begin{bmatrix} \frac{-M_2 i + M_1 j + M_1 M_2 m}{M_1 M_2 M_3} \\ 0 \end{bmatrix} (C^b(M_1 - M_2)/2), \tau M_1 M_2 M_3), \end{aligned} \tag{319}$$

up to the normalization factor $N_1N_2/(2\sqrt{2}N_3)$. This result is different from Eq. (312), in particular from the viewpoint of Wilson line dependence. Thus, the Wilson lines have phenomenologically important effects, depending on the directions of Wilson lines and the representations of matter fields.

We can extend the above analysis to larger gauge groups. Here, we show a rather simple example. We consider $U(1)_a \times SU(3)$ theory with the magnetic flux in $U(1)_a$ like Eq. (89). Then, we consider the $SU(3)$ triplet,

$$\begin{pmatrix} \lambda_0 \\ \lambda_{1/2} \\ \lambda_{-1/2} \end{pmatrix}, \tag{320}$$

with the $U(1)_a$ charge q_a, where the subscripts $(0, 1/2, -1/2)$ denote the $U(1)_b$ charge along one of $SU(3)$ Cartan directions. Now, we embed the Z_2 twist P in the gauge space as

$$P = \begin{pmatrix} 1 & 0 & 0 \\ 0 & 0 & 1 \\ 0 & 1 & 0 \end{pmatrix}, \tag{321}$$

for the triplet. In addition, we introduce the Wilson line C^b along the $U(1)_b$ direction. The gauge group is broken as $SU(3) \to U(1)$.[21] There are M zero-modes for linear combinations of $\lambda_{1/2}$ and $\lambda_{-1/2}$ with the wavefunctions,

$$\Theta^{j,M}_{1/2}(z + C^b/2M) + \Theta^{M-j,M}_{-1/2}(z - C^b/2M), \tag{322}$$

up to the normalization factor. Also, the zero-modes for λ_0 are written as

$$\Theta^{j,M}_0(z) + \Theta^{M-j,M}_0(z), \tag{323}$$

up to the normalization factor. The number of zero-modes is equal to $(M/2 + 1)$ and $(M + 1)/2$ when M is even and odd, respectively. Thus, the situation is almost the same as the above $SU(2)$ case with the triplet. Although the above example is rather simple, we can consider various types of breaking for larger groups. For example, when the gauge group includes two or more $SU(2)$ subgroups, we could embed the Z_2 twist in two of $SU(2)$'s and introduce independent Wilson lines along their Cartan directions. Similarly, we can investigate such models and other types of various embedding of P and Wilson lines.

In section 2.2, we have considered 10D theory on T^6. Also, we can consider the T^6/Z_2 orbifold, where the Z_2 twist acts e.g.

$$Z_2 \ : \ z_1 \to -z_1, \qquad z_2 \to -z_2, \qquad z_3 \to z_3. \tag{324}$$

[21] This remaining $U(1)$ symmetry might be anomalous. If so, the remaining $U(1)$ would also be broken by the Green-Schwarz mechanism.

For T_1^2 and T_2^2, we can introduce the type of Wilson lines, which we have considered in this section, while for T_3^2 we can introduce the type of Wilson lines, which are considered in the previous section. Then, we have a richer structure of models on the T^6/Z_2 orbifold. Furthermore, we could consider another independent Z_2' twist as

$$Z_2 \ : \ z_1 \to -z_1, \qquad z_2 \to z_2, \qquad z_3 \to -z_3, \tag{325}$$

on the $T^6/(Z_2 \times Z_2')$ orbifold. In this case, we can consider another independent embedding P' of Z_2' twist on the gauge space. Using these two Z_2 twist embedding and Wilson lines, we could construct various types of models. For example, when the gauge group includes two or more $SU(2)$ subgroups, we could embed P on one of $SU(2)$ and P' on other $SU(2)$ and introduce independent Wilson lines along their Cartan directions. Other various types of model building would be possible. Thus, it would be interesting to study such model building elsewhere.

6 Anomalies for field theory and string theory

In the previous section, we have seen some phenomenological interesting features of non-Abelian discrete symmetries which can appear dynamically as flavor symmetries. In general, symmetries at the tree-level can be broken by quantum effects, i.e. anomalies. Anomalies of continuous symmetries, in particular gauge symmetries, have been studied well. Here we study about anomalies of non-Abelian discrete symmetries. For our purpose, the path integral approach is convenient. Thus, we use Fujikawa's method [99, 100] to derive anomalies of discrete symmetries.

6.1 General formula for anomalies

Here we consider a gauge theory with a (non-Abelian) gauge group G_g and a set of fermions $\Psi = [\psi^{(1)}, \cdots, \psi^{(M)}]$. Then, we assume that their Lagrangian is invariant under the following chiral transformation,

$$\Psi(x) \to U\Psi(x), \tag{326}$$

with $U = exp(i\alpha P_L)$ and $\alpha = \alpha^A T_A$, where T_A denote the generators of the transformation and P_L is the left-chiral projector. It is not always necessary for above transformation to be a gauge transformation. The fermions $\Psi(x)$ are the (irreducible) M-plet representation $\boldsymbol{R}^M$. For the moment, we suppose that $\Psi(x)$ correspond to a (non-trivial) singlet under the flavor symmetry while they correspond to the $\boldsymbol{R}^M$ representation under the gauge group G_g. Since the generator T_A as well as α is represented on $\boldsymbol{R}^M$ as a $(M \times M)$ matrix, we use the notation, $T_A(\boldsymbol{R}^M)$ and $\alpha(\boldsymbol{R}^M) = \alpha^A T_A(\boldsymbol{R}^M)$.

The anomaly appears in Fujikawa's method from the transformation of the path integral measure as the Jacobian,

$$\mathcal{D}\Psi\mathcal{D}\bar{\Psi} \to J(\alpha)\mathcal{D}\Psi\mathcal{D}\bar{\Psi}, \quad J(\alpha) = \exp\left(i\int d^4x\mathcal{A}(x;\alpha)\right). \tag{327}$$

The anomaly function $\mathcal{A}$ decomposes into a gauge part and a gravitational part [101, 102, 103]

$$\mathcal{A} \;=\; \mathcal{A}_{\text{gauge}} + \mathcal{A}_{\text{grav}}\ . \tag{328}$$

The gauge part is given by

$$\mathcal{A}_{\text{gauge}}(x;\alpha) \;=\; \frac{1}{32\,\pi^2}\text{Tr}\left[\alpha(\boldsymbol{R}^M)\,F^{\mu\nu}(x)\,\widetilde{F}_{\mu\nu}(x)\right]\ , \tag{329}$$

where $F^{\mu\nu}$ denotes the field strength of the gauge fields, $F_{\mu\nu} = [D_\mu, D_\nu]$, and $\widetilde{F}_{\mu\nu}$ denotes its dual, $\widetilde{F}^{\mu\nu} = \varepsilon^{\mu\nu\rho\sigma}F_{\rho\sigma}$. The trace 'Tr' runs over all internal indices. When the transformation corresponds to a continuous symmetry, this anomaly can be calculated by the triangle diagram with external lines of two gauge bosons and one current corresponding to the symmetry for Eq. 326.

Similarly, the gravitation part is obtained as

$$\mathcal{A}_{\text{grav}} \;=\; -\,\mathcal{A}_{\text{grav}}^{\text{Weyl fermion}} \text{tr}\left[\alpha(\boldsymbol{R}^{(M)})\right] \;, \tag{330}$$

where 'tr' is the trace for the matrix $(M \times M)$ $T_A(\boldsymbol{R}^M)$. The contribution of a single Weyl fermion to the gravitational anomaly is given by

$$\mathcal{A}_{\text{grav}}^{\text{Weyl fermion}} \;=\; \frac{1}{384\pi^2}\,\frac{1}{2}\,\varepsilon^{\mu\nu\rho\sigma}\,R_{\mu\nu}{}^{\lambda\gamma}\,R_{\rho\sigma\lambda\gamma}\;. \tag{331}$$

When other sets of M_i-plet fermions Ψ_{M_i} are included in a theory, the total gauge and gravity anomalies are obtained as their summations, $\sum_{\Psi_{M_i}} \mathcal{A}_{\text{gauge}}$ and $\sum_{\Psi_{M_i}} \mathcal{A}_{\text{grav}}$.

For the evaluation of these anomalies, it is useful to recall the index theorems [101, 102], which imply

$$\int d^4x\,\frac{1}{32\pi^2}\,\varepsilon^{\mu\nu\rho\sigma}\,F^a_{\mu\nu}\,F^b_{\rho\sigma}\,\text{tr}\left[\mathsf{t}_a\,\mathsf{t}_b\right] \;\in\; \mathbb{Z}\;, \tag{332a}$$

$$\frac{1}{2}\int d^4x\,\frac{1}{384\pi^2}\,\frac{1}{2}\,\varepsilon^{\mu\nu\rho\sigma}\,R_{\mu\nu}{}^{\lambda\gamma}\,R_{\rho\sigma\lambda\gamma} \;\in\; \mathbb{Z}\;, \tag{332b}$$

where t_a are generators of G_g in the fundamental representation. We use the convention that $\text{tr}[\mathsf{t}_a\,\mathsf{t}_b] = \frac{1}{2}\delta_{ab}$. The factor $\frac{1}{2}$ in eq. (332b) follows from Rohlin's theorem [104], as discussed in [105]. Of course, these indices are independent of each other. The path integral includes all possible configurations corresponding to different index numbers.

First of all, we study anomalies of the continuous $U(1)$ symmetry. We consider a theory with a (non-Abelian) gauge symmetry G_g as well as the continuous $U(1)$ symmetry, which may be gauged. This theory include fermions with $U(1)$ charges, $q^{(f)}$ and representations $\boldsymbol{R}^{(f)}$. Those anomalies vanish if and only if the Jacobian is trivial, i.e. $J(\alpha) = 1$ for an arbitrary value of α. Using the index theorems, one can find that the anomaly-free conditions require

$$A_{\text{U(1)}-\text{G}_\text{g}-\text{G}_\text{g}} \;\equiv\; \sum_{\boldsymbol{R}^{(f)}} q^{(f)}\,T_2(\boldsymbol{R}^{(f)}) \;=\; 0, \tag{333}$$

for the mixed $U(1) - G_g - G_g$ anomaly, and

$$A_{\text{U(1)}-\text{grav}-\text{grav}} \;\equiv\; \sum_{f} q^{(f)} \;=\; 0, \tag{334}$$

the $U(1)$–gravity–gravity anomaly. Here, $T_2(\boldsymbol{R}^{(f)})$ is the Dynkin index of the $\boldsymbol{R}^f$ representation, i.e.

$$\text{tr}\left[\mathsf{t}_a\left(\boldsymbol{R}^{(f)}\right)\,\mathsf{t}_b\left(\boldsymbol{R}^{(f)}\right)\right] \;=\; \delta_{ab}T_2(\boldsymbol{R}^{(f)})\;. \tag{335}$$

6.2 Discrete flavor symmetry anomalies

Next, let us study anomalies of the abelian discrete symmetry, i.e. the Z_N symmetry. For the Z_N symmetry, we write $\alpha = 2\pi Q_N/N$, where Q_N is the Z_N charge operator and its eigenvalues are integers. Here we denote Z_N charges of fermions as $q_N^{(f)}$. Then we can evaluate the $Z_N - G_g - G_g$ and Z_N-gravity-gravity anomalies as the above $U(1)$ anomalies. However, the important difference is that α takes a discrete value. Then, the anomaly-free conditions, i.e., $J(\alpha) = 1$ for a discrete transformation, require

$$A_{Z_N-G_g-G_g} \;=\; \frac{1}{N}\sum_{\boldsymbol{R}^{(f)}} q^{(f)_N}\left(2\,T_2(\boldsymbol{R}^{(f)})\right) \in \mathbb{Z}\ , \tag{336}$$

for the $Z_N - G_g - G_g$ anomaly, and

$$A_{Z_N-\mathrm{grav}-\mathrm{grav}} \;=\; \frac{2}{N}\sum_{f} q_N^{(f)}\ \dim \boldsymbol{R}^{(f)} \in \mathbb{Z}\ , \tag{337}$$

for the Z_N-gravity-gravity anomaly. These anomaly-free conditions reduce to

$$\sum_{\boldsymbol{R}^{(f)}} q_N^{(f)}\, T_2(\boldsymbol{R}^{(f)}) \;=\; 0 \quad \mathrm{mod}\ N/2\ , \tag{338a}$$

$$\sum_{f} q_N^{(f)}\ \dim \boldsymbol{R}^{(f)} \;=\; 0 \quad \mathrm{mod}\ N/2\ . \tag{338b}$$

Note that the Z_2 symmetry is always free from the Z_2-gravity-gravity anomaly.

Finally, we study anomalies of non-Abelian discrete symmetries G. A discrete group G consists of the finite number of elements, g_i. Hence, the non-Abelian discrete symmetry is anomaly-free if and only if the Jacobian is vanishing for the transformation corresponding to each element g_i. Furthermore, recall that $(g_i)^{N_i} = 1$. That is, each element g_i in the non-Abelian discrete group generates a Z_{N_i} symmetry. Thus, the analysis on non-Abelian discrete anomalies reduces to one on Abelian discrete anomalies. One can take the field basis such that g_i is represented in a diagonal form. In such a basis, each field has a definite Z_{N_i} charge, $q_{N_i}^{(f)}$. The anomaly-free conditions for the g_i transformation are written as

$$\sum_{\boldsymbol{R}^{(f)}} q_{N_i}^{(f)}\, T_2(\boldsymbol{R}^{(f)}) \;=\; 0 \quad \mathrm{mod}\ N_i/2\ , \tag{339a}$$

$$\sum_{f} q_{N_i}^{(f)}\ \dim \boldsymbol{R}^{(f)} \;=\; 0 \quad \mathrm{mod}\ N_i/2\ . \tag{339b}$$

If these conditions are satisfied for all of $g_i \in G$, there are no anomalies of the full non-Abelian symmetry G. Otherwise, the non-Abelian symmetry is broken completely or partially to its subgroup by quantum effects.

In principle, we can investigate anomalies of non-Abelian discrete symmetries G following the above procedure. However, we give a practically simpler way to analyze those

anomalies. Here, we consider again the transformation similar to (326) for a set of fermions $\Psi = [\psi^{(1)}, \cdots, \psi^{(Md_\alpha)}]$, which correspond to the $\boldsymbol{R}^M$ irreducible representation of the gauge group G_g and the $\mathbf{r}^\alpha$ irreducible representation of the non-Abelian discrete symmetry G with the dimension d_α. Let U correspond to one of group elements $g_i \in G$, which is represented by the matrix $D_\alpha(g_i)$ on $\mathbf{r}^\alpha$. Then, the Jacobian is proportional to its determinant, $\det D(g_i)$. Thus, the representations with $\det D_\alpha(g_i) = 1$ do not contribute to anomalies. Therefore, the non-trivial Jacobian, i.e. anomalies are originated from representations with $\det D_\alpha(g_i) \neq 1$. Note that $\det D_\alpha(g_i) = \det D_\alpha(g g_i g^{-1})$ for $g \in G$, that is, the determinant is constant in a conjugacy class. Thus, it would be useful to calculate the determinants of elements on each irreducible representation. Such a determinant for the conjugacy class C_i can be written by

$$\det(C_i)_\alpha = e^{2\pi i q^\alpha_{\hat{N}_i}/\hat{N}_i}, \tag{340}$$

on the irreducible representation $\mathbf{r}^\alpha$. Note that $\hat{N}_i$ is a divisor of N_i, where N_i is the order of g_i in the conjugacy class C_i, i.e. $g^{N_i} = e$, such that $q^\alpha_{\hat{N}_i}$ are normalized to be integers for all of the irreducible representation $\mathbf{r}^\alpha$. We consider the $Z_{\hat{N}_i}$ symmetries and their anomalies. Then, we obtain the anomaly-free conditions similar to (339). That is, the anomaly-free conditions for the conjugacy classes C_i are written as

$$\sum_{\boldsymbol{r}^{(\alpha)}, \boldsymbol{R}^{(f)}} q^{\alpha(f)}_{\hat{N}_i} T_2(\boldsymbol{R}^{(f)}) \ = \ 0 \mod \hat{N}_i/2 \,, \tag{341a}$$

$$\sum_{\alpha.f} q^{\alpha(f)}_{\hat{N}_i} \dim \boldsymbol{R}^{(f)} \ = \ 0 \mod \hat{N}_i/2 \,, \tag{341b}$$

for the theory including fermions with the $\boldsymbol{R}^{(f)}$ representations of the gauge group G_g and the $\mathbf{r}^{\alpha(f)}$ representations of the flavor group G, which correspond to the $Z_{\hat{N}_i}$ charges, $q^{\alpha(f)}_{\hat{N}_i}$. Note that the fermion fields with the d_α-dimensional representation $\mathbf{r}^\alpha$ contribute on these anomalies, $q^{\alpha(f)}_{\hat{N}_i} T_2(\boldsymbol{R}^{(f)})$ and $q^{\alpha(f)}_{\hat{N}_i} \dim \boldsymbol{R}^{(f)}$, but not $d_\alpha q^{\alpha(f)}_{\hat{N}_i} T_2(\boldsymbol{R}^{(f)})$ and $d_\alpha q^{\alpha(f)}_{\hat{N}_i} \dim \boldsymbol{R}^{(f)}$. If these conditions are satisfied for all of conjugacy classes of G, the full non-Abelian symmetry G is free from anomalies. Otherwise, the non-Abelian symmetry is broken by quantum effects. As we see as follows, in concrete examples, the above anomaly-free conditions often lead to the same conditions between different conjugacy classes. Note, when $\hat{N}_i = 2$, the symmetry is always free from the mixed gravitational anomalies. We study explicitly more for concrete groups.

- $\mathbf{D_4}$

We study anomalies of D_4. As shown in appendix D.1, the D_4 group has the four singlets, $\mathbf{1}_{\pm\pm}$ and one doublet $\mathbf{2}$. All of the D_4 elements can be written as products of two elements, Z and C. Their determinants on $\mathbf{2}$ are obtained as $\det(Z) = -1$ and $\det(C) = -1$. Similarly, we can obtain determinants of Z and C on four singlets, $\mathbf{1}_{\pm\pm}$. Indeed, four singlets are classified by values of $\det(Z)$ and $\det(C)$, that is, $\det(Z) = 1$ for $\mathbf{1}_{+\pm}$, $\det(Z) = -1$ for $\mathbf{1}_{-\pm}$, $\det(C) = 1$ for $\mathbf{1}_{\pm+}$ and $\det(C) = -1$ for $\mathbf{1}_{\pm-}$. Those

	$\mathbf{1}_{++}$	$\mathbf{1}_{+-}$	$\mathbf{1}_{-+}$	$\mathbf{1}_{--}$	$\mathbf{2}$
$\det(Z)$	1	1	-1	-1	-1
$\det(C)$	1	-1	1	-1	-1

Table 12: Determinants on D_4 representations

determinants are summarized in Table 12. That implies that two Z_2 symmetries can be anomalous. One Z_2 corresponds to Z and the other Z_2' corresponds to C. Under these $Z_2 \times Z_2'$ symmetry, each representation has the following behavior,

$$Z_2 \text{ even} \quad : \quad \mathbf{1}_{+\pm}, \tag{342}$$

$$Z_2 \text{ odd} \quad : \quad \mathbf{1}_{-\pm}, \quad \mathbf{2}, \tag{343}$$

$$Z_2' \text{ even} \quad : \quad \mathbf{1}_{\pm+}, \tag{344}$$

$$Z_2' \text{ odd} \quad : \quad \mathbf{1}_{\pm-}, \quad \mathbf{2}. \tag{345}$$

Then, the anomaly-free conditions are written as

$$\sum_{\mathbf{1}_{-\pm}} \sum_{\boldsymbol{R}^{(f)}} T_2(\boldsymbol{R}^{(f)}) + \sum_{\mathbf{2}} \sum_{\boldsymbol{R}^{(f)}} T_2(\boldsymbol{R}^{(f)}) \ = \ 0 \mod 1\ , \tag{346}$$

for the $Z_2 - G_g - G_g$ anomaly and

$$\sum_{\mathbf{1}_{\pm-}} \sum_{\boldsymbol{R}^{(f)}} T_2(\boldsymbol{R}^{(f)}) + \sum_{\mathbf{2}} \sum_{\boldsymbol{R}^{(f)}} T_2(\boldsymbol{R}^{(f)}) \ = \ 0 \mod 1\ , \tag{347}$$

for the $Z_2' - G_g - G_g$ anomaly.

- $\boldsymbol{\Delta}(\mathbf{27})$

Similarly, we can study anomalies of $\Delta(27)$. As shown in section D.2, the $\Delta(27)$ group has nine singlets, $\mathbf{1}_{rs}$ and two triplets, $\mathbf{3}$ and $\bar{\mathbf{3}}$. All elements $\Delta(27)$ can be written by products of Z, C. On all of triplet representations, their determinants are obtained as $\det(Z) = \det(C) = 1$. Only anomaly coefficients come from the nine singlets fields. These results are shown in Table 13. That implies that two independent Z_3 symmetries can be anomalous. One corresponds to Z and the other corresponds to C. For the Z_3 symmetry corresponding to Z, each representation has the following Z_3 charge q_3,

$$q_3 = 0 \quad : \quad \mathbf{1}_{0s}, \quad \mathbf{3}, \bar{\mathbf{3}} \tag{348}$$

$$q_3 = 1 \quad : \quad \mathbf{1}_{1s}, \tag{349}$$

$$q_3 = 2 \quad : \quad \mathbf{1}_{2s}, \tag{350}$$

	$\mathbf{1}_{rs}$	$\mathbf{3}$	$\bar{\mathbf{3}}$
$\det(Z)$	ω^r	1	1
$\det(C)$	ω^s	1	1

Table 13: Determinants on $\Delta(27)$

while for Z_3' symmetry corresponding to C, each representation has the following Z_3 charge q_3',

$$q_3' = 0 \quad : \quad \mathbf{1}_{r0}, \quad \mathbf{3}, \bar{\mathbf{3}} \tag{351}$$
$$q_3' = 1 \quad : \quad \mathbf{1}_{r1}, \tag{352}$$
$$q_3' = 2 \quad : \quad \mathbf{1}_{r2}. \tag{353}$$

Then, the anomaly-free conditions are written as

$$\sum_{\mathbf{1}_{1s}} \sum_{\boldsymbol{R}^{(f)}} T_2(\boldsymbol{R}^{(f)}) + 2 \sum_{\mathbf{1}_{2s}} \sum_{\boldsymbol{R}^{(f)}} T_2(\boldsymbol{R}^{(f)}) \ = \ 0 \mod 3/2 \ , \tag{354}$$

for the $Z_3 - G_g - G_g$ anomaly and

$$\sum_{\mathbf{1}_{1s}} \sum_{\boldsymbol{R}^{(f)}} \dim \boldsymbol{R}^{(f)} + 2 \sum_{\mathbf{1}_{2s}} \sum_{\boldsymbol{R}^{(f)}} \dim \boldsymbol{R}^{(f)} \ = \ 0 \mod 3/2 \ , \tag{355}$$

for the Z_3-gravity-gravity anomaly. Similarly, for the Z_3' symmetry, the anomaly-free conditions are written as

$$\sum_{\mathbf{1}_{r1}} \sum_{\boldsymbol{R}^{(f)}} T_2(\boldsymbol{R}^{(f)}) + 2 \sum_{\mathbf{1}_{r2}} \sum_{\boldsymbol{R}^{(f)}} T_2(\boldsymbol{R}^{(f)}) \ = \ 0 \mod 3/2 \ , \tag{356}$$

for the $Z_3' - G_g - G_g$ anomaly and

$$\sum_{\mathbf{1}_{r1}} \sum_{\boldsymbol{R}^{(f)}} \dim \boldsymbol{R}^{(f)} + 2 \sum_{\mathbf{1}_{r2}} \sum_{\boldsymbol{R}^{(f)}} \dim \boldsymbol{R}^{(f)} \ = \ 0 \mod 3/2 \ , \tag{357}$$

for the Z_3'-gravity-gravity anomaly.

- $\boldsymbol{\Delta(54)}$

Finally, we also show anomalies of $\Delta(54)$. As shown in section D.3, the $\Delta(54)$ group has two singlets, $\mathbf{1}_{1,2}$ and four doublets, $\mathbf{2}_{1,2,3,4}$ and four triplets $\mathbf{3}_{1,2}$ and $\bar{\mathbf{3}}_{1,2}$. All elements $\Delta(54)$ can be written by products of Z, C and P. First of all, we obtain $\det(Z) = \det(C) = 1$. This implies that the only anomaly is arising the symmetries of P which is Z_2 symmetry. The determinants for each representation of P are summarized in Table 14. Then, the anomaly-free condition is given by

$$\sum_{\mathbf{1}_2} \sum_{\boldsymbol{R}^{(f)}} T_2(\boldsymbol{R}^{(f)}) + \sum_{\mathbf{2}_{1,2,3,4}} \sum_{\boldsymbol{R}^{(f)}} T_2(\boldsymbol{R}^{(f)}) + \sum_{\mathbf{3}_1, \bar{\mathbf{3}}} \sum_{\boldsymbol{R}^{(f)}} T_2(\boldsymbol{R}^{(f)}) \ = \ 0 \mod 1 \ , \tag{358}$$

	$\mathbf{1}_1$	$\mathbf{1}_2$	$\mathbf{2}_1$	$\mathbf{2}_2$	$\mathbf{2}_3$	$\mathbf{2}_4$	$\mathbf{3}_1$	$\bar{\mathbf{3}}_1$	$\mathbf{3}_2$	$\bar{\mathbf{3}}_2$
$\det(P)$	1	-1	-1	-1	-1	-1	-1	-1	1	1

Table 14: Determinants on $\Delta(54)$

for the $Z_2 - G_g - G_g$ anomaly.

Similarly, we can analyze on anomalies for other non-Abelian discrete symmetries.

6.3 Other anomalies in string models

In this section, we also introduce other interesting anomalies for discrete symmetries. Here the discrete symmetries we discuss are discrete R-symmetries for heterotic orbifold models. It is widely assumed that superstring theory leads to anomaly-free effective theories. In fact the anomalous $U(1)$ symmetries are restored by the GS mechanism [43, 44, 45]. For this mechanism to work, the mixed anomalies between the anomalous $U(1)$ and other continuous gauge symmetries have to satisfy a certain set of conditions, the GS conditions, at the field theory level. In particular, in heterotic string theory the mixed anomalies between the anomalous $U(1)$ symmetries and other continuous gauge symmetries must be universal for different gauge groups up to their Kac-Moody levels [46, 47]. Therefore stringy-originated discrete symmetries are strongly constrained due to stringy consistency, and it is phenomenologically and theoretically important to study anomalies of discrete symmetries, as it is pointed out in [106] and the example of T-duality shows. We shall investigate the mixed anomalies between the discrete R-symmetries and the continuous gauge symmetries in concrete orbifold models. We will also study relations between the discrete R-anomalies, one-loop beta-function coefficients (scale anomalies).

In orbifold models, the 6D compact space is chosen to be 6D orbifold. A 6D orbifold is a division of 6D torus T^6 by a twist θ, while the torus T^6 is obtained as R^6/Λ^6, where Λ^6 is 6D lattice. Eigenvalues of the twist θ are denoted as $e^{2\pi i v_1}, e^{2\pi i v_2}$ and $e^{2\pi i v_3}$ in the complex basis Z_i $(i = 1, 2, 3)$.

It is convenient to bosonize right-moving fermionic strings. Here we write such bosonized fields by H^t $(t = 1, \cdots, 5)$. Their momenta p_t are quantized and span the SO(10) weight lattice. Space-time bosons correspond to SO(10) vector momenta, and space-time fermions correspond to SO(10) spinor momenta. The 6D compact part, i.e. the SO(6) part, p_i $(i = 1, 2, 3)$ is relevant to our study. All of $\mathbf{Z}_N$ orbifold models have three untwisted sectors, U_1, U_2 and U_3, and their massless bosonic modes have the following SO(6) momenta,

$$U_1 : (1, 0, 0), \qquad U_2 : (0, 1, 0), \qquad U_3 : (0, 0, 1). \tag{359}$$

On the other hand, the twisted sector T_k has shifted $SO(6)$ momenta, $r_i = p_i + kv_i$. Table 15 and Table 16 show explicitly H-momenta r_i of massless bosonic states. That implies

v_i	$\mathbf{Z}_3$ $(1,1,-2)/3$	$\mathbf{Z}_4$ $(1,1,-2)/4$	$\mathbf{Z}_6$-I $(1,1,-2)/6$	$\mathbf{Z}_6$-II $(1,2,-3)/6$	$\mathbf{Z}_7$ $(1,2,-3)/7$
T_1	$(1,1,1)/3$	$(1,1,2)/4$	$(1,1,4)/6$	$(1,2,3)/6$	$(1,2,4)/7$
T_2	—	$(2,2,0)/4$	$(2,2,2)/6$	$(2,4,0)/6$	$(2,4,1)/7$
T_3	—	—	$(3,3,0)/6$	$(3,0,3)/6$	—
T_4	—	—	—	$(4,2,0)/6$	$(4,1,2)/7$

Table 15: H-momenta for $\mathbf{Z}_3$, $\mathbf{Z}_4$, $\mathbf{Z}_6$-I, $\mathbf{Z}_6$-II and $\mathbf{Z}_7$ orbifolds

v_i	$\mathbf{Z}_8$-I $(1,2,-3)/8$	$\mathbf{Z}_8$-II $(1,3,-4)/8$	$\mathbf{Z}_{12}$-I $(1,4,-5)/12$	$\mathbf{Z}_{12}$-II $(1,5,-6)/12$
T_1	$(1,2,5)/8$	$(1,3,4)/8$	$(1,4,7)/12$	$(1,5,6)/12$
T_2	$(2,4,2)/8$	$(2,6,0)/8$	$(2,8,2)/12$	$(2,10,0)/12$
T_3	—	$(3,1,4)/8$	$(3,0,9)/12$	$(3,3,6)/12$
T_4	$(4,0,4)/8$	$(4,4,0)/8$	$(4,4,4)/12$	$(4,8,0)/12$
T_5	$(5,2,1)/8$	—	—	$(5,1,6)/12$
T_6	—	—	$(6,0,6)/12$	$(6,6,0)/12$
T_7	—	—	$(7,4,1)/12$	—
T_8	—	—	—	—
T_9	—	—	$(9,0,3)/12$	—
T_{10}	—	—	—	$(10,2,0)/12$

Table 16: H-momenta for $\mathbf{Z}_8$-I, $\mathbf{Z}_8$-II, $\mathbf{Z}_{12}$-I and $\mathbf{Z}_{12}$-II orbifolds

their $SO(6)$ H-momenta are obtained as

$$r_i = |kv_i| - \mathrm{Int}[|kv_i|], \tag{360}$$

where Int$[a]$ denotes an integer part of fractional number a. This relation is not available for the untwisted sectors, and r_i is obtained as Eq. (359).

The gauge sector can also be broken and gauge groups smaller than $E_8 \times E_8$ are obtained. Matter fields have some representations under such unbroken gauge symmetries.

Massless modes for 4D space-time bosons correspond to the following vertex operator [107, 10],

$$V_{-1} = e^{-\phi} \prod_{i=1}^{3} (\partial Z_i)^{\mathcal{N}_i} (\partial \bar{Z}_i)^{\bar{\mathcal{N}}_i} e^{ir_t H^t} e^{iP^I X^I} e^{ikX} \sigma_k, \tag{361}$$

in the (-1)-picture, where ϕ is the bosonized ghost, kX corresponds to the 4D part and $P^I X^I$ corresponds to the gauge part. Oscillators of the left-mover are denoted by ∂Z_i and $\partial \bar{Z}_i$, and $\mathcal{N}_i$ and $\bar{\mathcal{N}}_i$ are oscillator numbers, which are included in these massless modes. In addition, σ_k denotes the twist field for the T_k sector. Similarly, we can write the vertex

operator for 4D space-time massless fermions as

$$V_{-\frac{1}{2}} = e^{-\frac{1}{2}\phi} \prod_{i=1}^{3} (\partial Z_i)^{N_i} (\partial \bar{Z}_i)^{\bar{N}_i} e^{ir_t^{(f)} H_t} e^{iP^I X^I} e^{ikX} \sigma_k, \tag{362}$$

in the $(-1/2)$-picture. The H-momenta for space-time fermion and boson, $r_i^{(f)}$ and r_i in the same supersymmetric multiplet are related each other as

$$r_i = r_i^{(f)} + (1,1,1)/2. \tag{363}$$

We need vertex operators V_0 with the 0-picture when we compute generic n-point couplings. We can obtain such vertex operators V_0 by operating the picture changing operator, Q, on V_{-1}, [107],

$$Q = e^{\phi}(e^{-2\pi i r_i^v H_i} \bar{\partial} Z_i + e^{2\pi i r_i^v H_i} \bar{\partial} \bar{Z}_i), \tag{364}$$

where $r_1^v = (1,0,0)$, $r_2^v = (0,1,0)$ and $r_3^v = (0,0,1)$.

Next we briefly review on $\mathbf{Z}_N \times \mathbf{Z}_M$ orbifold models [108]. In $\mathbf{Z}_N \times \mathbf{Z}_M$ orbifold models, we introduce two independent twists θ and ω, whose twists are represented by $e^{2\pi i v_i^1}$ and $e^{2\pi i v_i^2}$, respectively in the complex basis. Two twists are chosen such that each of them breaks 4D N=4 SUSY to 4D N=2 SUSY and their combination preserves only N=1 SUSY. Thus, eigenvalues v_i^1 and v_i^2 are chosen as

$$v_i^1 = (v^1, -v^1, 0), \qquad v_i^2 = (0, v^2, -v^2), \tag{365}$$

where $v^1, v^2 \neq$ integer. In general, $\mathbf{Z}_N \times \mathbf{Z}_M$ orbifold models have three untwisted sectors, U_1, U_2 and U_3, and their massless bosonic modes have the same $SO(6)$ H-momenta r_i as Eq. (359). In addition, there are $\theta^k \omega^\ell$-twisted sectors, and their $SO(6)$ H-momenta are obtained as

$$r_i = |kv_i^1| + |\ell v_i^2| - \mathrm{Int}[|kv_i^1| + |\ell v_i^2|]. \tag{366}$$

Vertex operators are also constructed in a similar way. Recently, non-factorizable $\mathbf{Z}_N \times \mathbf{Z}_M$ orbifold models have been studied [109]. The above aspects are the same for such non-factorizable models.

6.3.1 Discrete R-symmetries

Here we define R-charges. We consider n-point couplings including two fermions. Such couplings are computed by the following n-point correlation function of vertex operators,

$$\langle V_{-1} V_{-1/2} V_{-1/2} V_0 \cdots V_0 \rangle. \tag{367}$$

They must have the total ghost charge -2, because the background has the ghost number 2. When this n-point correlation function does not vanish, its corresponding n-point coupling in effective theory is allowed. That is, selection rules for allowed n-point correlation functions in string theory correspond to symmetries in effective theory.

The vertex operator consists of several parts, the 4D part e^{kX}, the gauge part e^{iPX}, the 6D twist field σ_k, the 6D left-moving oscillators ∂Z_i and the bosonized fermion e^{irH}. Each part has its own selection rule for allowed couplings. For the 4D part and the gauge part, the total 4D momentum $\sum k$ and the total momentum of the gauge part $\sum P$ should be conserved. The latter is nothing but the requirement of gauge invariance. The selection rule for 6D twist fields σ_k is controlled by the space group selection rule [10, 118].

Similarly, the total H-momenta can be conserved

$$\sum r_i = 1. \tag{368}$$

Here we take a summation over the H-momenta for scalar components, using the fact that the H-momentum of fermion component differs by $-1/2$. Another important symmetry is the twist symmetry of oscillators. We consider the following twist of oscillators,

$$\begin{aligned} \partial Z_i &\to e^{2\pi i v_i} \partial Z_i, \qquad & \partial \bar{Z}_i &\to e^{-2\pi i v_i} \partial \bar{Z}_i, \\ \bar{\partial} Z_i &\to e^{2\pi i v_i} \bar{\partial} Z_i, \qquad & \bar{\partial} \bar{Z}_i &\to e^{-2\pi i v_i} \bar{\partial} \bar{Z}_i. \end{aligned} \tag{369}$$

Allowed couplings may be invariant under the above Z_N twist.

Indeed, for 3-point couplings corresponding to $\langle V_{-1} V_{-1/2} V_{-1/2} \rangle$, we can require H-momentum conservation and Z_N twist invariance of oscillators independently. However, we have to compute generic n-point couplings through picture changing, and the picture changing operator Q includes non-vanishing H-momenta and right-moving oscillators $\bar{\partial} Z_i$ and $\bar{\partial} \bar{Z}_i$. Consequently, the definition of the H-momentum of each vertex operator depends on the choice of the picture and so its physical meaning remains somewhat obscure. We therefore use a picture independent quantity as follows,

$$R_i \equiv r_i + \mathcal{N}_i - \bar{\mathcal{N}}_i, \tag{370}$$

which can be interpreted as an R-charge [3]. This R-symmetry is a discrete surviving symmetry of the continuous $SU(3)$ ($\subset SU(4)$) R-symmetry under orbifolding. Here we do not distinguish oscillator numbers for the left-movers and right-movers, because they have the same phase under Z_N twist. Indeed, physical states with -1 picture have vanishing oscillator number for the right-movers, while the oscillator number for the left-movers can be non-vanishing. Thus, hereafter $\mathcal{N}_i$ and $\bar{\mathcal{N}}_i$ denote the oscillator number for the left-movers, because we study the physical states with -1 picture from now. For simplicity, we use the notation $\Delta \mathcal{N}_i = \mathcal{N}_i - \bar{\mathcal{N}}_i$. Now, we can write the selection rule due to R-symmetry as

$$\sum R_i = 1 \mod N_i, \tag{371}$$

where N_i is the minimum integer satisfying $N_i = 1/\hat{v}_i$, where $\hat{v}_i = v_i + m$ with any integer m. For example, for Z_6-II orbifold, we have $v_i = (1, 2, -3)/6$, and $N_i = (6, 3, 2)$. Thus, these are discrete symmetries. Note that the above summation is taken over scalar components.

Discrete R symmetry itself is defined as the following transformation,

$$|R_i\rangle \to e^{2\pi i v_i R_i} |R_i\rangle, \tag{372}$$

	R_i
gaugino	$(1/2, 1/2, 1/2)$
U_1	$(1/2, -1/2, -1/2)$
U_2	$(-1/2, 1/2, -1/2)$
U_3	$(-1/2, -1/2, 1/2)$
T_k	$kv_i - \mathrm{Int}[kv_i] - 1/2 + \Delta\mathcal{N}_i$

Table 17: Discrete R-charges of fermions in $\mathbf{Z}_N$ orbifold models

for states with discrete R-charges, which are defined mod N_i. For later convenience, we show discrete R-charges for fermions in Table 17. As shown there, gaugino fields always have R-charge $(1/2, 1/2, 1/2)$.

6.3.2 Discrete R-anomalies

Let us study anomalies of discrete R-symmetry. Under the R-transformation like Eq. (372), the anomaly coefficients $A^{R_i}_{G_a}$ are obtained as

$$A^{R_i}_{G_a} = \sum R_i T(\mathbf{R}_{G_a}), \tag{373}$$

where $T(\mathbf{R}_{G_a})$ is the Dynkin index for $\mathbf{R}_{G_a}$ representation under G_a.

By use of our discrete R charge, the anomaly coefficients are written as

$$A^{R_i}_{G_a} = \frac{1}{2}C_2(G_a) + \sum_{\text{matter}} (r_i - \frac{1}{2} + \Delta\mathcal{N}_i) T(\mathbf{R}_{G_a}), \tag{374}$$

where $C_2(G_a)$ is quadratic Casimir. Note that r_i denotes the SO(6) shifted momentum for bosonic states. The first term in the right hand side is a contribution from gaugino fields and the other is the contribution from matter fields.

If these anomalies are canceled by the Green-Schwarz mechanism, these mixed anomalies must satisfy the following condition,

$$\frac{A^{R_i}_{G_a}}{k_a} = \frac{A^{R_i}_{G_b}}{k_b}, \tag{375}$$

for different gauge groups, G_a and G_b, where k_a and k_b are Kac-Moody levels. In the simple orbifold construction, we have the Kac-Moody level $k_a = 1$ for non-abelian gauge groups. Note again that anomalies are defined modulo $N_i T(\mathbf{R}^{(f)}_{G_a})$. The above GS condition has its meaning mod $N_i T(\mathbf{R}^{(f)}_{G_a})/k_a$.

As illustrating examples, let us study explicitly one Z_3 model and one Z_4 model. Their gauge groups and massless spectra are shown in Table 18 and Table 19.[22] First, we study

[22] See for explicit massless spectra Ref. [110], where a typographical error is included in the U_3 sector of the Z_4 orbifold model. It is corrected in Table 19.

gauge group	$E_6 \times SU(3) \times E_6 \times SU(3)$
sector	massless spectrum
U_1	(27,3;1,1)+ (1,1;27,3)
U_2	(27,3;1,1)+ (1,1;27,3)
U_3	(27,3;1,1)+ (1,1;27,3)
T_1	$27(1,\bar{3};1,\bar{3})$

Table 18: Massless spectrum in a $\mathbf{Z}_3$ orbifold model

gauge group	$SO(10) \times SU(4) \times SO(12) \times SU(2) \times U(1)$
sector	massless spectrum
U_1	$(16_c, 4; 1, 1) + (1, 1; 32_c, 1) + (1, 1; 12_v, 2)$
U_2	$(16_c, 4; 1, 1) + (1, 1; 32_c, 1) + (1, 1; 12_v, 2)$
U_3	$(10_v, 6; 1, 1) + (1, 1; 32_c, 2) + 2(1, 1, ; 1, 1)$
T_1	$16(1, 4; 1, 2)$
T_2	$16(10_v, 1; 1, 1) + 16(1, 6; 1, 1)$

Table 19: Massless spectrum in a $\mathbf{Z}_4$ orbifold model

R-anomalies in the Z_3 orbifold model. Since $v_i = (1, 1, -2)/3$, we have $N_i = 3$. For both E_6, mixed R-anomalies are computed as

$$A^{R_i}_{E_6} = \frac{3}{2} + 9n^i_{E_6}, \tag{376}$$

where $n^i_{E_6}$ is integer. The second term in the right hand side appears because anomalies are defined modulo $N_i T(27)$ with $N_i = 3$ and $T(27) = 3$ for E_6. Similarly, mixed R-anomalies for $SU(3)$ are computed as

$$A^{R_i}_{SU(3)} = -12 + \frac{3}{2} n^i_{SU(3)}, \tag{377}$$

where $n^i_{SU(3)}$ is integer. The second term in the right hand side appears through $N_i T(3)$ with $N_i = 3$ and $T(3) = 1/2$ for $SU(3)$. Thus, in this model, mixed R-anomalies satisfy

$$A^{R_i}_{E_6} = A^{R_i}_{SU(3)} \qquad (\text{mod } 3/2). \tag{378}$$

Next, we study R-anomalies in the Z_4 orbifold model with the gauge group $SO(10) \times SU(4) \times SO(12) \times SU(2) \times U(1)$. Since the Z_4 orbifold has $v_i = (1, 1, -2)/4$, we have $N_i = (4, 4, 2)$. Mixed anomalies between $R_{1,2}$ and $SO(10)$ are computed as

$$A^{R_{1,2}}_{SO(10)} = 1 + 4n^{1,2}_{SO(10)}, \tag{379}$$

with integer $n^{1,2}_{SO(10)}$, where the second term appears through $N_i T(\mathbf{R}_a)$ with $N_i = 4$ and $T(10) = 1$ for $SO(10)$. Similarly, mixed anomalies between R_3 and $SO(10)$ is computed as

$$A^{R_3}_{SO(10)} = -9 + 2n^3_{SO(10)}, \tag{380}$$

with integer $n^3_{SO(10)}$. Furthermore, mixed R-anomalies for other non-abelian groups are obtained as

$$\begin{aligned}
A^{R_{1,2}}_{SU(4)} &= -7 + 2n^{1,2}_{SU(4)}, \qquad & A^{R_3}_{SU(4)} &= -9 + n^3_{SU(4)}, \\
A^{R_{1,2}}_{SO(12)} &= 1 + 4n^{1,2}_{SO(12)}, \qquad & A^{R_3}_{SO(12)} &= 3 + 2n^3_{SO(12)}, \\
A^{R_{1,2}}_{SU(2)} &= -15 + 2n^{1,2}_{SU(2)}, \qquad & A^{R_3}_{SU(2)} &= 3 + n^3_{SU(2)},
\end{aligned} \tag{381}$$

with integer $n^i_{G_a}$, where the second terms appear through $N_i T(\mathbf{R}_a)$ with $N_i = (4, 4, 2)$, and $T(12) = 1$ for $SO(12)$, $T(4) = 1/2$ for $SU(4)$ and $T(2) = 1/2$ for $SU(2)$. These anomalies satisfy the GS condition,

$$\begin{aligned}
A^{R_{1,2}}_{SO(10)} = A^{R_{1,2}}_{SU(4)} = A^{R_{1,2}}_{SO(12)} = A^{R_{1,2}}_{SU(2)} \qquad &(\text{mod } \ 2), \\
A^{R_3}_{SO(10)} = A^{R_3}_{SU(4)} = A^{R_3}_{SO(12)} = A^{R_3}_{SU(2)} \qquad &(\text{mod } \ 1).
\end{aligned} \tag{382}$$

The GS condition is satisfied in the above models without Wilson lines. However, it is not satisfied in explicit models with Wilson lines for naively defined R-charges [111]. Anomalies for discrete shifts are important.

6.3.3 Relation with beta-function

Here we study the relation between discrete R anomalies and one-loop beta-functions. We find

$$\sum_{i=1,2,3} r_i = 1, \tag{383}$$

from Eqs. (360) and (366) as well as Table 15 and Table 16. By using this, we can write the sum of R-anomalies as

$$\begin{aligned}
A^R_{G_a} &= \sum_{i=1,2,3} A^{R_i}_{G_a} \\
&= \frac{3}{2} C_2(G_a) + \sum_{\text{matter}} T(\mathbf{R}_{G_a})(-\frac{1}{2} + \sum_i \Delta\mathcal{N}_i).
\end{aligned} \tag{384}$$

Thus, when $\sum_i \Delta\mathcal{N}_i = 0$, the total anomaly $A^R_{G_a}$ is proportional to the one-loop beta-function coefficient, i.e. the scale anomaly, b_{G_a},

$$b_{G_a} = 3C_2(G_a) - \sum_{\text{matter}} T(\mathbf{R}_{G_a}). \tag{385}$$

When we use the definition of R charge $\tilde{R}_i = 2R_i$, we would have $A^{\tilde{R}}_{G_a} = b_{G_a}$. It is not accidental that $A^R_{G_a}$ is proportional to b_{G_a} [112, 113]. The sum of the R-charges $\sum_{i=1,2,3} R_i$ of a supermultiplet is nothing but the R-charge (up to an overall normalization) associated with the R-current which is a bosonic component of the supercurrent [114], when the R-charge is universal for all of matter fields, i.e. $\sum_i \Delta\mathcal{N}_i = 0$. Using the supertrace identity

[115] it is in fact possible to show [113] that $A^R_{G_a}$ is proportional to b_{G_a} to all orders in perturbation theory.

In explicit models, non-abelian groups except $SU(2)$ have few massless matter fields with non-vanishing oscillator numbers, while massless matter fields with oscillators can appear as singlets as well as $SU(2)$ doublets. Thus, in explicit models the total R-anomaly $A^R_{G_a}$ is related with the one-loop beta-function coefficient b_{G_a},

$$2A^R_{G_a} = b_{G_a}, \tag{386}$$

modulo $N_i T(\mathbf{R}_a)$ for most of non-abelian groups. Since the total R-anomalies satisfy the GS condition, $A^R_{G_a} = A^R_{G_b}$, the above relation between $A^R_{G_a}$ and b_{G_a} leads to

$$b_{G_a} = b_{G_b}, \tag{387}$$

modulo $2N_i T(\mathbf{R}_a)$.

For example, the explicit Z_3 orbifold model and Z_4 orbifold model in Table 18 and Table 19 have only non-oscillated massless modes except singlets. The Z_3 orbifold model has the following total R-anomalies and one-loop beta-function coefficient,

$$\begin{aligned} A^R_{E_6} &= \frac{9}{2} + 9n_{E_6}, \qquad b_{E_6} = 9, \\ A^R_{SU(3)} &= -36 + \frac{3}{2}n_{SU(3)}, \qquad b_{SU(3)} = -72. \end{aligned} \tag{388}$$

Hence, this model satisfy $2A^R_{G_a} = b_{G_a}$ and its one-loop beta-function coefficients satisfy

$$b_{E_6} = b_{SU(3)} \qquad (\text{mod } 3). \tag{389}$$

Similarly, the Z_4 orbifold model in Table 19 has the total R-anomalies and one-loop beta-function coefficients as,

$$\begin{aligned} A^R_{SO(10)} &= -7 + 2n_{SO(10)}, \qquad b_{SO(10)} = -14 \\ A^R_{SU(4)} &= -23 + n_{SU(4)}, \qquad b_{SU(4)} = -46 \\ A^R_{SO(12)} &= 5 + 2n_{SO(10)}, \qquad b_{SO(12)} = 10 \\ A^R_{SU(2)} &= -27 + n_{SU(2)}, \qquad b_{SU(2)} = -54. \end{aligned} \tag{390}$$

Thus, this model also satisfies $2A^R_{G_a} = b_{G_a}$ and its one-loop beta-function coefficients satisfy

$$b_{SO(10)} = b_{SU(4)} = b_{SO(12)} = b_{SU(2)} \qquad (\text{mod } 2). \tag{391}$$

6.3.4 Relation with T-duality anomaly

Here we study the relation between R-anomalies and T-duality anomalies. The relation between R-symmetries and T-duality has also been studied in Ref. [116]. The T-duality anomalies are obtained as [48, 49]

$$A^{T_i}_{G_a} = -C_2(G_a) + \sum_{\text{matter}} T(\mathbf{R}_{G_a})(1 + 2n_i), \tag{392}$$

where n_i is the modular weight of matter fields for the i-th torus. The modular weight is related with r_i as

$$\begin{aligned} n_i &= -1 \quad \text{for} \quad r_i = 1, \\ &= 0 \quad \text{for} \quad r_i = 0, \\ &= r_i - 1 - \Delta \mathcal{N}_i \quad \text{for} \quad r_i \neq 0, 1. \end{aligned} \tag{393}$$

Note that $n_i = -r_i$ for $r_i = 0, 1/2, 1$. Thus, in the model, which includes only matter fields with $r_i = 0, 1/2, 1$, the T-duality anomalies and R-anomalies are proportional to each other,

$$A^{T_i}_{G_a} = -2A^{R_i}_{G_a}. \tag{394}$$

In generic model, such relation is violated, but T-duality anomalies and R-anomalies are still related with each other as

$$A^{T_i}_{G_a} = -2A^{R_i}_{G_a} - 2 \sum_{r_i \neq 0,1/2,1} (2r_i - 1). \tag{395}$$

T-duality should also satisfy the GS condition,

$$\frac{A^{T_i}_{G_a}}{k_a} = \frac{A^{T_i}_{G_b}}{k_b}, \tag{396}$$

for the i-th torus, which does not include the N=2 subsector. Thus, the requirement that T-duality anomalies and R-anomalies should satisfy the GS condition, leads to a similar condition for

$$\Delta^i_a = 2 \sum_{r^b_i \neq 0,1/2,1} (2r^b_i - 1). \tag{397}$$

For the i-th torus, which includes N=2 subsector, T-duality anomalies can be canceled by the GS mechanism and T-dependent threshold correction [117]. Thus, for such torus, the T-duality anomalies has no constrain from the GS condition. However, even for such torus, R-anomaly should satisfy the GS condition.

For example, the Z_4 orbifold model in Table 19 has the following T-duality anomalies,

$$\begin{aligned} &A^{T_{1,2}}_{SO(10)} = -2, \qquad A^{T_3}_{SO(10)} = 18, \\ &A^{T_{1,2}}_{SU(4)} = -2, \qquad A^{T_3}_{SU(4)} = 18, \\ &A^{T_{1,2}}_{SO(12)} = -2, \qquad A^{T_3}_{SO(12)} = -6, \\ &A^{T_{1,2}}_{SU(2)} = -2, \qquad A^{T_3}_{SU(2)} = -6. \end{aligned} \tag{398}$$

They satisfy the GS condition,

$$A^{T_{1,2}}_{SO(10)} = A^{T_{1,2}}_{SU(4)} = A^{T_{1,2}}_{SO(12)} = A^{T_{1,2}}_{SU(2)}. \tag{399}$$

On the other hand, for the third torus, T-duality anomalies $A^{T_3}_{G_a}$ do not satisfy the GS condition, that is, anomalies $A^{T_3}_{G_a}$ are not universal, because there is the N=2 subsector and

one-loop gauge kinetic functions depend on the T_3 moduli with non-universal coefficients [117]. However, they satisfy

$$A^{T_3}_{SO(10)} = -2A^{R_3}_{SO(10)}, \qquad A^{T_3}_{SU(4)} = -2A^{R_3}_{SU(4)},$$
$$A^{T_3}_{SO(12)} = -2A^{R_3}_{SO(12)}, \qquad A^{T_3}_{SU(2)} = -2A^{R_3}_{SU(2)}, \tag{400}$$

because this model has only massless modes with $r_3 = 0, 1/2, 1$. Indeed, all of Z_4 orbifold models include only massless modes with $r_3 = 0, 1/2, 1$. Furthermore, all of Z_N orbifold models with $v_i = 1/2$ have only massless modes with $r_i = 0, 1/2, 1$. Thus, the above relation (394) holds true in such Z_N orbifold models. That is also true for R_1-anomalies in $Z_2 \times Z_M$ orbifold models with $v_1 = (1/2, -1/2, 0)$ and $v_2 = (0, v_2, -v_2)$.

Such relation between T-duality anomalies and R-anomalies (394) would be important, because the GS condition on R-anomalies leads to a certain condition on the T-duality anomalies even including the N=2 subsector. For example, in the above Z_4 orbifold model, the following condition is required

$$A^{T_3}_{SO(10)} = A^{T_3}_{SU(4)} = A^{T_3}_{SO(12)} = A^{T_3}_{SU(2)} \qquad (\text{mod } 2). \tag{401}$$

6.3.5 Symmetry breaking of the discrete R-symmetries

- Non-perturbative breaking

If the discrete R-symmetries are anomalous, they are broken by non-perturbative effects at low-energy. This is because, for the GS mechanism to take place, the axionic part of the dilaton S should transform non-linearly under the anomalous symmetry. This means that a term like e^{-aS} with a constant a has a definite charge R_i^S under the anomalous symmetry.

Non-perturbative effects can therefore induce terms like $e^{-aS}\Phi^1 \cdots \Phi^n$ with matter fields Φ^a, where the total charge satisfies the condition for allowed couplings, i.e. $R_i^S + \sum_a R_i^a = 1$ (mod N_i). This implies that below the scale of the vacuum expectation value (VEV) of S, such non-invariant terms can appear in a low-energy effective Lagrangian. The canonical dimension of the non-invariant operator $e^{-aS}\Phi^1 \cdots \Phi^n$ that can be generated by the non-perturbative effects depends of course on the R charge R^S. If the smallest dimension is lager than four, they will be suppressed by certain powers of the string scale. However, the operator can produce non-invariant mass terms like $m\Phi\Phi'$, because some of the chiral superfields may acquire VEVs. One should worry about such cases. Needless to say that small higher dimensional terms would be useful in phenomenological applications such as explaining fermion masses.

In the case that the smallest dimension is smaller than three, the anomalous discrete R symmetry has less power to constrain the low-energy theory.

- Spontaneous breaking

In the discussion above, we have considered R-symmetry breaking by non-perturbative effects when R-symmetries are anomalous. Here we comment on another type of symmetry breaking; they can be broken spontaneously by the VEVs of scalar fields in the form $U(1) \times R \to R'$. That is, we consider a spontaneous symmetry breaking, where some scalar fields with non-vanishing $U(1)$ and R charges develop their VEVs and they break $U(1)$ and R symmetries in such a way that an unbroken R' symmetry remains intact. (Its order is denoted by N' below.) Even in such symmetry breaking, we can obtain the GS condition for the unbroken R' from the GS condition for the $U(1)$ and R-anomalies. Suppose that we have the GS condition for the $U(1)$ symmetry as

$$TrQT(\mathbf{R}_{G_a})/k_a = TrQT(\mathbf{R}_{G_b})/k_b, \tag{402}$$

where Q is the $U(1)$ charge. Since the unbroken R' charge is a linear combination of R_i and Q, the mixed anomalies for R' should also satisfy the GS condition,

$$TrR'T(\mathbf{R}_{G_a})/k_a = TrR'T(\mathbf{R}_{G_b})/k_b. \tag{403}$$

Here the anomaly coefficients $TrR'T(\mathbf{R}_{G_a})$ are defined modulo $N'T(\mathbf{R}^{(f)}_{G_a})$.

Through the symmetry breaking $U(1) \times R \to R'$, some matter fields may gain mass terms like

$$W \sim m\Phi\bar{\Phi}. \tag{404}$$

Such a pair of the matter fields Φ and $\bar{\Phi}$ should form a vector-like representation of G_a and have opposite R' charges of the unbroken R' symmetry. The heavy modes of this type have therefore no contribution to the mixed anomalies between the gauge symmetry G_a and the unbroken R' symmetry. This implies that the above GS condition for the unbroken R' remains unchanged even after the spontaneous symmetry breaking. The symmetry breaking $U(1) \times R \to R'$ also allows Majorana mass terms like

$$W \sim m\Phi\Phi. \tag{405}$$

This type of Majorana mass terms can appear for an even order N' of the R' symmetry if the R' charge of Φ is $N'/2$ and Φ is in a real representation $\mathbf{R}_{G_a}$ of the unbroken gauge group G_a. The field Φ contributes to the anomaly coefficient as $\frac{N'}{2}T(\mathbf{R}_{G_a})$. That however may change only the modulo-structure of the anomaly coefficients. For $SU(N)$ gauge group, this contribution is obtained as $\frac{N'}{2} \times$ (integer). Thus, the modulo-structure does not change, that is, the anomaly coefficients $TrR'T(\mathbf{R}_{G_a})$ are defined modulo $N'/2$. However, for other gauge groups, the modulo-structure of the anomaly coefficients may change.

- Gravity-induced supersymmetry and Gauge symmetry breaking

The most important difference of the discrete R-symmetries compared with T-duality in phenomenological applications comes from the fact that (for the heterotic orbifold string models) the moduli and dilaton superfields have vanishing R-charges. The VEVs of their

bosonic components do not therefore violate the discrete R-symmetries in the perturbation theory. (We have discussed above the non-perturbative effects due to the VEV of the dilaton, which may be small in a wide class of models.) However, the F-components of the moduli and dilaton superfields have non-zero R-charges. Therefore, since the VEVs of these F-components generate soft-supersymmetry breaking (SSB) terms at low-energy, the SSB terms do not have to respect the discrete R-symmetries. [23] Fortunately, in the visible sector, the scale of the R-symmetry breaking must be of the same order as that of supersymmetry breaking. If the order of the discrete R-symmetry is even, the VEVs of these F-components break the discrete R-symmetry down to its subgroup Z_2, an R-parity. That is an interesting observation because it may be an origin of the R-parity of the MSSM.

Gauge symmetry breaking can be achieved by VEVs of chiral supermultiplets in a non-trivial representation of the gauge group or by non-trivial Wilson lines. Clearly, if the chiral supermultiplets have vanishing R-charges and only their scalar components acquire VEVs, the discrete R-symmetries remain unbroken. Similarly, the Wilson lines do not break the discrete R-symmetries because gauge fields have no R charge. As a consequence, the discrete R-symmetries have a good chance to be intact at low-energy if the non-perturbative effects are small.

6.3.6 Constraints on low-energy beta-functions

Only anomaly-free discrete R-symmetries remain as intact symmetries in a low-energy effective theory. Obviously, the model with anomaly-free discrete R-symmetries corresponds to $A^{R_i}_{G_a} = 0 \pmod{N_i T(\mathbf{R}^{(f)}_{G_a})}$. Consider for instance $SU(N)$ gauge groups for which $T(\mathbf{R}^{(f)}_{G_a}) = 1/2$ is usually satisfied. Then in models, which have no oscillator mode in a non-trivial representations of $SU(N)$, the relation between R-anomalies and beta-function coefficients lead to

$$b_a = 2A_{G_a} = 0, \tag{406}$$

mod N_i for any gauge group G_a. For example, the Z_3 orbifold model with anomaly-free R-symmetries leads to $b_a = 3n_a$ with integer n_a, while the Z_4 orbifold model with anomaly-free R-symmetries leads to $b_a = 2n_a$. Similarly, $b_a = 1$ would be possible in Z_6-II orbifold models because $N_i = (6, 3, 2)$ as one can see from Table 1.

Even for anomalous discrete R-symmetries, the GS condition for R-anomalies and the relation between beta-function coefficients (375), (386), (387) would have phenomenological implications. As discussed at the beginning in this section, the non-perturbative effects can generate operators like $e^{-aS}\Phi^1 \cdots \Phi^n$. If its canonical dimension is larger than four, its contribution to low-energy beta-functions may be assumed to be small. [24]

As for the MSSM we find $b_3 = -3$ and $b_2 = 1$ for $SU(3)$ and $SU(2)$, respectively. That is, we have $b_2 - b_3 = 4$, implying the MSSM can not be realized, e.g. in Z_3 orbifold models,

[23] Whether the non-perturbative effects due to the VEV of the dilaton do play an important roll in the SSB sector depends on the R charge of the dilaton, and one has to check it explicitly for a given model.

[24] If the operator produces non-invariant mass terms like $M\Phi\Phi'$ with M larger than the low-energy scale, the low-energy spectrum may change. Then the power of the discrete R-symmetries decreases.

because Z_3 orbifold models require $b_a - b_b = 0 \mod 3$ if the effects of the symmetry breaking of the discrete R-symmetries can be neglected. Similarly, the model with $b_2 - b_3 = 4$ can not be obtained in the Z_6-I, Z_7 or Z_{12}-I orbifold models.

Finally, we comment on the symmetry breaking effects by quantum effect. When a discrete (flavor) symmetry is anomalous, breaking terms can appear in Lagrangian, e.g. by instanton effects, such as $\frac{1}{M^n}\Lambda^m \Phi_1 \cdots \Phi_k$, where Λ is a dynamical scale and M is a typical (cut-off) scale. Within the framework of string theory discrete anomalies as well as anomalies of continuous gauge symmetries can be canceled by the GS mechanism unless discrete symmetries are accidental. In the GS mechanism, dilaton and moduli fields, i.e. the so-called GS fields Φ_{GS}, transform non-linearly under anomalous transformation. The anomaly cancellation due to the GS mechanism imposes certain relations among anomalies. (See e.g. Ref. [111].) Stringy non-perturbative effects as well as field-theoretical effects induce terms in Lagrangian such as $\frac{1}{M^n} e^{-a\Phi_{GS}} \Phi_1 \cdots \Phi_k$. The GS fields Φ_{GS}, i.e. dilaton/moduli fields are expected to develop non-vanishing vacuum expectation values and above terms correspond to breaking terms of discrete symmetries.

7 Conclusion

Here we conclude by summarizing the results of this thesis and considering the future prospects.

In this thesis we have studied ten dimensional N=1 super Yang-Mills theory on various types of compactifications. These results can be also applied in lower dimensions as $D = 6, 8$. In the theory we considered field theoretical approach is possible to obtain the chiral fermion coupled under non-abelian gauge symmetries and also calculate matter spectrums, Yukawa couplings and other couplings related to the low-energy physics. It is quite interesting for phenomenology to survey a successful string compactifications. Although the torus compactifications with magnetic flux is one of simple background configurations, one can calculate explicitly the form of wavefunctions and Yukawa couplings. We have extended these analysis to other more complicated compactifications like orbifold background, toron background with non-Abelian Wilson line. We have seen in such constructions there are many interesting features for low-energy physics and the set up of these studies may apply in general Calabi-Yau compactifications in principle. It enables us to survey more widely range of the theory.

In section 3, we studied low-energy effective action namely superpotential and Kahler potential. Yukawa couplings itself are important to link the SM and high energy UV completion underlying theory. Following the analysis of the three wavefunction overlap, we have obtained generic n-point couplings. We have found that higher order couplings are written as products of three-point couplings. This behavior is the same as higher order amplitudes of CFT, that is, higher order amplitudes are decomposed as products of three-point amplitudes in intersecting D-brane models. Our results on higher order couplings would be useful in phenomenological applications. Numerical analysis on higher order couplings is also possible.

In section 4, We have shown the non-abelian flavor symmetries can appear dynamically in the couplings. Because these are constrained by coupling selection rule as well as heterotic orbifold models and they are easily understood geometrically. We have found that D_4, $\Delta(27)$ and other $Z_g \ltimes (Z_g \times Z_g)$ flavor symmetries can appear from magnetized brane models with non-vanishing Wilson lines. Matter fields with several representations of these discrete flavor symmetries can appear. When we consider vanishing Wilson lines, these flavor symmetries are enhanced like $D_4 \times Z_2$, $\Delta(54)$, etc. They propovided a realization of the *co-existence* of the different types of the flavor symmetries in GUT type models. These results are interesting for model building of realistic quark/lepton mass matrices and mixings.

For the purposes to survey the low-energy effective theory, it is important to study other background. Using the field theoretical approaches one can study the widely range of the background. In section 5, we studied the orbifolding with flux background which is one of the explicit examples of the non-trivial background. Even in a simple construction, i.e. T^2/Z_2 orbifold, it has a rich structure. Odd modes can have zero-modes and couplings are controlled by the orbifold periodicity of wavefunctions. We have also discussed the flavor symmetry breaking on the orbifold background.

It is important to study anomalies of non-abelian flavor symmetries. If string theory leads to anomaly-free effective low-energy theories including discrete symmetries, anomalies of discrete symmetries must be canceled by the Green-Schwarz mechanism. In section 6 we study those discrete anomalies within the framework of heterotic orbifold models in [111], and it was shown that discrete anomalies can be canceled by the Green-Schwarz mechanism. We found the important relations of discrete R-anomalies with U(1) anomalies and others. Furthermore we have studied the possible anomaly of discrete flavor symmetries come from several types of string models e.g. heterotic orbifold models and D-brane models. In addition, there are many constraints from the stringy consistency conditions. The most important consistency condition for string theory model with D-branes is the RR charge cancellation condition. This condition arises as a consequence of Gauss law constraint of the internal space. Since the globally defined string model must satisfy above conditions, several constraints on D-brane configurations are obtained. As a result of this constraint, it allows us to know all the spectrums including chiral and non-chiral multiplets and remaining gauge symmetry. Therefore it is quite important to investigate globally the string compactification models.

To distinguish string vacuum it is rather important to study the moduli parameters. Since $\mathcal{N} = 1$ supersymmetry must be broken in a certain scale we have discussed the soft supersymmetry breaking terms. Even in the type IIB theory the soft supersymmetry breaking terms are dominated u moduli contributions, soft supersymmetry terms still have constraint from this kind of symmetries. Actually it was found explicitly that certain models which have discrete flavor symmetries prohibit dangerous FCNC [89].

It is also interesting to study the flavor structure in other background. There are already many kinds of explicit construction of wavefunctions, for example, sphere background, warped compactification. It is possible to survey more the flavor structure in such a background. It is also important for the phenomenological view point. It may give some hints to derive the realistic pattern of Yukawa couplings and help to construct realistic vacua. In addition, we can discuss the phenomenological aspects of the flavor sector. Once if we have a mechanism to break low-energy supersymmetry, the relevant soft supersymmetry breaking terms would be also related to flavor structures. Thus we can analyze the low-energy spectrum including the super particle for future collider experiments.

Another application of the moduli field is the inflation. It is a challenging issue to realize a successful scenario of inflation within the framework of high energy underlying theory. Some of moduli fields have naturally flat directions due to the supersymmetry and they could be naturally candidates of the scalar fields responsible for inflation, inflaton. There are many studies for the natural inflation potential in particle physics of string theory. The scale of inflation might be the same magnitude of the scale of the low-energy supersymmetry breaking and such models could be implemented to the connection between underlying theory and cosmology or phenomenology. Indeed cosmological observation is predicted in a certain model of the moduli potential. It is quite interesting to investigate the moduli stabilization mechanism and low-energy supersymmetry breaking, in which we can also discuss about flavor phenomenology. All the above topics are left for near future.

Acknowledgment

I would like to thank my supervisor Tatsuo Kobayashi for fruitful discussions, collaboration and leading me during my doctor course. I would like to be grateful to H. Abe, H. Aoyama, K.-S. Choi, T. Eguchi, M. Fukuma, S. Hashimoto, H. Hata, K. Izawa, E. Itou, T. Kaneko, H. Kawai, T. kugo, M. Kurachi, H. Matsufuru, J. Noaki, Y. Omura, T. Onogi, S. Sasakura, R. Takahashi, M. Tanimoto, T. Uematsu, K. Sugiyama, H. Kunitomo, S. Terashima, K. Yoshioka, K. Yoshida, N. Yamada and T. Yamazaki for fruitful discussions and study meeting. The author is supported in part by the Grant-in-Aid for Scientific Research No. 21·897 from the Ministry of Education, Culture, Sports, Science and Technology of Japan.

A Dimensional reduction and the low-energy effective action

Here we construct the effective four dimensional super Yang-Mills theory. We start with ten dimensional $\mathcal{N} = 1$ super Yand-Mills theory which is the low-energy limit of the DBI action,

$$S = \frac{1}{g^2}\int d^{10}x \mathrm{Tr}\left(-\frac{1}{4}F_{MN}F^{MN} + \frac{i}{2}\bar{\lambda}\Gamma^M D_M\lambda\right), \tag{407}$$

where g^2 can be related to the string theory as $g^2 = 4\pi e^{\phi_{10}}(2\pi\sqrt{\alpha'})^6$. We take the gauge groups $U(N)$ and the generators are divided into two parts, the Cartan parts U_a and off diagonal elements e_{ab}

$$(U_a)_{ij} = \delta_{ai}\delta_{aj}, \quad (e_{ab})_{ij} = \delta_{ai}\delta_{bj}. \tag{408}$$

The gauge fields are consist of

$$A_M = B_M + W_M = B^a_M U_a + W^{ab}_M e_{ab} \tag{409}$$

and gaugino fields are also expanded in the same way. We also expand the gauge fields as background configurations as

$$\begin{aligned} B^a_i &= \langle B^a_i(y^i)\rangle + b^a_i(x,y) \\ W^{ab}_i &= \Phi^{ab}_i(x,y). \end{aligned} \tag{410}$$

In the following we will not rewrite the entire action in terms of the fields introduced above, but we will only write the relevant terms, namely the quadratic terms involving the scalar and fermion fields and the trilinear terms involving a scalar and two fermions: we will derive the Kähler metrics from the former and the Yukawa couplings from the latter. We will also restrict our considerations to toroidal compactifications.

The quadratic terms for the fields $\Phi^{ab}_M(x^\mu, y^i)$ are followings

$$\mathcal{L}_2^{(\Phi)} = -\frac{1}{2g^2}\mathrm{tr}\left[D_\mu\Phi_i D^\mu\Phi^i + \tilde{D}_i\Phi_j\tilde{D}^i\Phi^j - \tilde{D}_i\Phi_j\tilde{D}^j\Phi^i - iG_{ij}[\Phi^i, \Phi^j]\right] \tag{411}$$

where

$$D_\mu\Phi_j = \partial_\mu\Phi_j - i[B_\mu + W_\mu, \Phi_j], \tilde{D}_i\Phi_j = \partial_i\Phi_j - i[\langle B_i\rangle, \Phi_j], \tag{412}$$

$$G_{ij} \equiv \partial_i\langle B\rangle_j - \partial_j\langle B\rangle_i \tag{413}$$

where G_{ij} is the field strength obtained from the background field B. By using the properties of Lie algebra U and e one can express the above quadratic terms as

$$\begin{aligned}\mathcal{L}_2^{(\Phi)} =& -\frac{1}{2g^2}\left[(D_\mu\Phi_i)^{ab}(D^\mu\Phi^i)^{ba} + (\tilde{D}_i\Phi_j)^{ab}(\tilde{D}^i\Phi^j)^{ba} - (\tilde{D}_i\Phi_j)^{ab}(\tilde{D}^j\Phi^i)^{ba}\right] \\ & + \frac{i}{2g^2}\Phi^{i,ab}(G^a_{ij} - G^b_{ij})\Phi^{j,ba}\end{aligned} \tag{414}$$

where $(D_\mu\Phi_i)^{ab} = \partial_\mu\Phi_i - i(B^a_\mu - B^b_\mu)\Phi^{ab}_i - i(W^{ac}_\mu\Phi^{cb}_i - \Phi^{ac}_i W^{cb}_\mu)$. Taking integration by part for $(\tilde{D}_i\Phi_j)^{ab}(\tilde{D}^i\Phi^j)^{ba}$, we obtain

$$(\tilde{D}_i\Phi_j)^{ab}(\tilde{D}^i\Phi^j)^{ba} = -\Phi^{ab}_j(\tilde{D}_i\tilde{D}^i)\Phi^{j,ba}, \tag{415}$$

and similarly we obtain

$$\begin{aligned}(\tilde{D}_i\Phi_j)^{ab}(\tilde{D}^j\Phi^i)^{ba} &= -\Phi^{ab}_j(\tilde{D}_i\tilde{D}^j\Phi^i)^{ba} \\ &= -\Phi^{ab}_j([\tilde{D}_i, \tilde{D}^j] + \tilde{D}^j\tilde{D}_j)\Phi^{i,ba} \\ &= -\Phi^{ab}_j([\tilde{D}_i, \tilde{D}^j])\Phi^{i,ba},\end{aligned} \tag{416}$$

where we use the gauge fixing condition $\tilde{D}_i\Phi^i = 0$. The commutator $[\tilde{D}_i, \tilde{D}_j]$ is given by $[\tilde{D}_i, \tilde{D}_j] = -i(G^a_{ij} - G^b_{ij})$. Then we combine these results to rewrite the Lagrangian,

$$\mathcal{L}_2^{(\Phi)} = \frac{1}{2g^2}\left[\Phi^{ab}_j(D_\mu)^2\Phi^{j,ba} + \Phi^{ab}_j(\tilde{D}_i\tilde{D}^i)\Phi^{j,ba} + 2i\Phi^{ab}_j(G^j{}_i{}^{,a} - G^j{}_i{}^{,b})\Phi^{j,ba}\right]. \tag{417}$$

Thus, we obtain the equation of motion for Φ^{ab}_j as followings

$$\tilde{D}^2\Phi^{ab}_j + 2i(F^i{}_j{}^{,a} - F^i{}_j{}^{,b})\Phi^{ab}_i = -m^2\Phi^{ab}_j, \tag{418}$$

where $-m^2$ means the eigenvalue for the operator defined in left hand side. Therefore zero-mode wavefunctions are corresponding to the solution with vanishing m^2. We use the usual Kaluza-Klein expansions for the field Φ as

$$\Phi^{ab}_i(x, y) = \sum_n \varphi^{ab}_{n,i}(x^\mu) \otimes \phi^{ab}_n(y^i) \ \ ; \ \ \Psi^{ab}(x, y) = \sum_n \psi^{ab}_n(x^\mu) \otimes \eta^{ab}_n(y^i)\ . \tag{419}$$

The spectrum of the Kaluza-Klein states and their wavefunctions along the compact directions are obtained by solving the eigenvalue equations for the six-dimensional Laplace and Dirac operators:

$$- \tilde{D}_k \tilde{D}^k \phi_n^{ab} = m_n^2 \phi_n^{ab} \quad , \quad i\gamma^i_{(6)} \tilde{D}_i \eta_n^{ab} = \lambda_n \, \eta_n^{ab} \tag{420}$$

with the correct periodicity conditions along the compactified directions.

Inserting Eq. (419) and the first equation in (420) in Eq. (411) and using the coordinates z and $\bar{z}$ for describing the torus T^2, one gets scalar mass terms for six dimensions. We see that there are two towers of Kaluza-Klein states for each torus, with masses given by:

$$m_n^2 = \frac{1}{(2\pi R)^2} \left[\sum_{s=1}^{3} \frac{2\pi |M_{ab}^s|}{\mathcal{A}^{(s)}} (2N_s + 1) \pm \frac{4\pi I_{ab}^r}{\mathcal{A}^{(r)}} \right] \tag{421}$$

where N_s is an integer given by the oscillator number operator. The presence of the oscillator number is a consequence of the fact that the Laplace operator can be written in terms of the creation and annihilation operators of an harmonic oscillator. One can have a massless state only if the following condition is satisfied for $I_r > 0$ or $I_r < 0$

$$\sum_{s=1}^{3} \frac{2\pi |I_s|}{\mathcal{A}^{(s)}} - \frac{4\pi |I_r|}{\mathcal{A}^{(r)}} = 0 \Longrightarrow \frac{1}{2} \sum_{s=1}^{3} \frac{|I_s|}{\mathcal{A}^{(s)}} - \frac{|I_r|}{\mathcal{A}^{(r)}} = 0 \ . \tag{422}$$

In this case one keeps $\mathcal{N} = 1$ supersymmetry because there is a massless scalar that is in the same chiral multiplet as a fermion that we will study later. If one of the I_r's is vanishing and the other two are equal, then we have an additional massless excitation corresponding to an extended $\mathcal{N} = 2$ supersymmetry.

The SUSY conditions given in Eq. (422) show that only one of the two scalars is massless. In particular, by choosing in such equation $r = 1$ and $I_1 > 0$, we see that $\varphi_{1,-}$ is the massless scalar. The corresponding internal wave-function has been determined in Ref. [52] and is the product of three eigenfunctions. Instead, by taking $r = 1$ and $I_1 < 0$ we have that $\varphi_{1,+}$ becomes the massless mode. It is useful to notice that $(\phi_{r,+}^{ab;n_r})^\dagger = \phi_{r,-}^{ba;n_r}$, and furthermore, the reality of the scalar action implies:

$$\phi_0^{ba} = (\phi_0^{ab})^*. \tag{423}$$

In conclusion, by performing the Kaluza-Klein reduction of the low-energy world-volume action of a stack of D9 branes on $R^{3,1} \times T^2 \times T^2 \times T^2$, we have found two towers of Kaluza-Klein states for each of the scalar fields $\varphi_{r,\pm}$ for $r = 1, 2, 3$. In general, only the lowest state of one of the two towers and for a particular value of r (say $r = 1$ if Eq. (422) is satisfied for $r = 1$) is massless, depending on the sign of I_1. We have now all the elements for computing the Kähler metric of the scalars $\varphi_\pm$.

B Models

Here we give two examples of models, whose family numbers of bulk modes differ from three. That is, one model has two bulk families and the other has eighteen bulk families. We start with the ten-dimensional $U(N)$ super Yang-Mills theory on the background $R^{3,1} \times T^6/(Z_2 \times Z_2')$. We consider the trivial orbifold projections $P = P' = 1$.

In the first model, we introduce the following magnetic flux,

$$\begin{aligned}
F_{45} &= \begin{pmatrix} 0 \times \mathbf{1}_{N_a \times N_a} & & 0 \\ & -2 \times \mathbf{1}_{N_b \times N_b} & \\ 0 & & 2 \times \mathbf{1}_{N_c \times N_c} \end{pmatrix}, \\
F_{67} &= \begin{pmatrix} 0 \times \mathbf{1}_{N_a \times N_a} & & 0 \\ & -1 \times \mathbf{1}_{N_b \times N_b} & \\ 0 & & 1 \times \mathbf{1}_{N_c \times N_c} \end{pmatrix}, \\
F_{89} &= \begin{pmatrix} 0 \times \mathbf{1}_{N_a \times N_a} & & 0 \\ & -1 \times \mathbf{1}_{N_b \times N_b} & \\ 0 & & 1 \times \mathbf{1}_{N_c \times N_c} \end{pmatrix}.
\end{aligned} \tag{424}$$

This magnetic flux satisfies the condition (34) and breaks the gauge group $U(N) \to U(N_a) \times U(N_b) \times U(N_c)$, although the orbifold projections are trivial $P = P' = 1$. Then, we can analyze the zero-modes as section 3.4. The result is shown in Table 4. This model has two bulk families, when we consider λ^{ab} and λ^{ca} as left-handed and right-handed matter fields. This flavor number is not realistic. However, in orbifold models it is possible to assume that one family appears on one of fixed points.

	I^i_{ef}	chirality	wavefunction	the total number of zero-modes
λ^{ab}	$(2,1,1)$	$\lambda^{ab}_{+,+,+}$	$\Theta^{j_1}_{\text{even}}\Theta^{j_2}_{\text{even}}\Theta^{j_3}_{\text{even}}$	2
λ^{ca}	$(2,1,1)$	$\lambda^{ca}_{+,+,+}$	$\Theta^{j_1}_{\text{even}}\Theta^{j_2}_{\text{even}}\Theta^{j_3}_{\text{even}}$	2
λ^{cb}	$(4,2,2)$	$\lambda^{cb}_{+,+,+}$	$\Theta^{j_1}_{\text{even}}\Theta^{j_2}_{\text{even}}\Theta^{j_3}_{\text{even}}$	12

Table 20: Two-family model from the bulk.

We give another example. We use the same orbifold projections, i.e. $P = P' = 1$. We

introduce the following magnetic flux,

$$
\begin{aligned}
F_{45} &= \begin{pmatrix} 0\times \mathbf{1}_{N_a\times N_a} & & 0 \\ & -6\times \mathbf{1}_{N_b\times N_b} & \\ 0 & & 6\times \mathbf{1}_{N_c\times N_c} \end{pmatrix}, \\
F_{67} &= \begin{pmatrix} 0\times \mathbf{1}_{N_a\times N_a} & & 0 \\ & -3\times \mathbf{1}_{N_b\times N_b} & \\ 0 & & 3\times \mathbf{1}_{N_c\times N_c} \end{pmatrix}, \\
F_{89} &= \begin{pmatrix} 0\times \mathbf{1}_{N_a\times N_a} & & 0 \\ & -3\times \mathbf{1}_{N_b\times N_b} & \\ 0 & & 3\times \mathbf{1}_{N_c\times N_c} \end{pmatrix}.
\end{aligned} \tag{425}
$$

We study the spinor fields λ^{ab}, in whose Dirac equations the difference of magnetic fluxes $I^i_{ab} = (6,3,3)$ appears. Their zero-modes correspond to $\lambda^{ab}_{+,+,+}$, which transform $\lambda^{ab}_{+,+,+}(x,y_m,y_n) \to \lambda^{ab}_{+,+,+}(x,-y_m,y_n)$ for both Z_2 and Z'_2 actions. These boundary conditions are satisfied with the wavefunctions $\Theta^{j_1}_{\rm even}(y_4,y_5)\Theta^{j_2}_{\rm even}(y_6,y_7)\Theta^{j_3}_{\rm even}(y_8,y_9)$ and $\Theta^{j_1}_{\rm odd}(y_4,y_5)\Theta^{j_2}_{\rm odd}(y_6,y_7)\Theta^{j_3}_{\rm odd}(y_8,y_9)$. The number of zero-modes corresponding to the former wavefunctions is given by the product of $I^1_{ab({\rm even})} = 4$, $I^2_{ab({\rm even})} = 2$ and $I^3_{ab({\rm even})} = 2$, while the zero-mode number corresponding to the latter is given by the product of $I^1_{ab({\rm odd})} = 2$, $I^2_{ab({\rm odd})} = 1$ and $I^3_{ab({\rm odd})} = 1$. Thus, the total number of λ^{ab} zero-modes is equal to $18(=16+2)$. Similarly, we can analyze zero-modes for λ^{bc} and λ^{ca}. The result is shown in Table 5. For these zero-modes, only two forms of wavefunctions are allowed, that is, one is $\Theta^{j_1}_{\rm even}(y_4,y_5)\Theta^{j_2}_{\rm even}(y_6,y_7)\Theta^{j_3}_{\rm even}(y_8,y_9)$ and the other is $\Theta^{j_1}_{\rm odd}(y_4,y_5)\Theta^{j_2}_{\rm odd}(y_6,y_7)\Theta^{j_3}_{\rm odd}(y_8,y_9)$. The numbers of zero-modes corresponding to the former and latter are shown in the third and fourth columns. Six-dimensional chirality of all zero-modes correspond to $\lambda_{+,+,+}$ and they are omitted in the table.

This model has 18 families. It seems that this family number is too large. However, we can reduce the light family number if we assume anti-families of $(\bar{N}_a, N_b)$ and $(N_a, \bar{N}_c)$ matter fields on fixed points and their mass terms with the above families of matter fields. Such mass terms are possible for zero-modes corresponding to $\Theta^{j_1}_{\rm even}(y_4,y_5)\Theta^{j_2}_{\rm even}(y_6,y_7)\Theta^{j_3}_{\rm even}(y_8,y_9)$. Thus, when we assume n anti-families, the number of light families reduces to $(18-n)$. This type of models has an interesting aspect, that is, some families of matter fields correspond to $\Theta^{j_1}_{\rm even}(y_4,y_5)\Theta^{j_2}_{\rm even}(y_6,y_7)\Theta^{j_3}_{\rm even}(y_8,y_9)$ and other families of matter fields correspond to $\Theta^{j_1}_{\rm odd}(y_4,y_5)\Theta^{j_2}_{\rm odd}(y_6,y_7)\Theta^{j_3}_{\rm odd}(y_8,y_9)$. In general, other combinations of wavefunctions can appear in zero-modes of matter fields. Such asymmetry appears in this type of models. Thus, their flavor structure is rich.

C Possible patterns of Yukawa matrices

In this appendix, we show explicitly all of possible Yukawa matrices for 15 classes of models in Table 9 except the models with $I^{(1)}_{bc} = 0$ and the model without zero-modes for the Higgs fields.

	I^i_{ef}	No. of zero-modes $\Theta^{j_1}_{\rm even}\Theta^{j_2}_{\rm even}\Theta^{j_3}_{\rm even}$	No. of zero-modes $\Theta^{j_1}_{\rm odd}\Theta^{j_2}_{\rm odd}\Theta^{j_3}_{\rm odd}$	the total number of zero-modes
λ^{ab}	$(6,3,3)$	16	2	18
λ^{ca}	$(6,3,3)$	16	2	18
λ^{cb}	$(12,6,6)$	112	20	132

Table 21: Eighteen-family model from the bulk.

C.1 (Even-Even-Even) wavefunctions

Here, we study the patterns of Yukawa matrices in the models, where zero-modes of left, right-handed matter fields and Higgs fields correspond to even, even and even functions, respectively.

C.1.1 4-4-8 model

Let us study the model with $(|I^{(1)}_{ab}|, |I^{(1)}_{ca}|, |I^{(1)}_{bc}|) = (4,4,8)$. The following table shows zero-mode wavefunctions of left, right-handed matter fields and Higgs fields.

	$L_i(\lambda^{ab})$	$R_j(\lambda^{ca})$	$H_k(\lambda^{bc})$
0	$\Theta^{0,4}$	$\Theta^{0,4}$	$\Theta^{0,8}$
1	$\frac{1}{\sqrt{2}}\left(\Theta^{1,4}+\Theta^{3,4}\right)$	$\frac{1}{\sqrt{2}}\left(\Theta^{1,4}+\Theta^{3,4}\right)$	$\frac{1}{\sqrt{2}}\left(\Theta^{1,8}+\Theta^{7,8}\right)$
2	$\Theta^{2,4}$	$\Theta^{2,4}$	$\frac{1}{\sqrt{2}}\left(\Theta^{2,8}+\Theta^{6,8}\right)$
3	-	-	$\frac{1}{\sqrt{2}}\left(\Theta^{3,8}+\Theta^{5,8}\right)$
4	-	-	$\Theta^{4,8}$

This model has five zero-modes for the Higgs fields. Yukawa couplings $Y_{ijk}L_iR_jH_k$ are given by

$$Y_{ijk}H_k = \begin{pmatrix} y_aH_0+y_eH_4 & y_fH_3+y_bH_1 & y_cH_2 \\ y_fH_3+y_bH_1 & \frac{1}{\sqrt{2}}(y_a+y_e)H_2+y_c(H_0+H_4) & y_bH_3+y_dH_1 \\ y_cH_2 & y_bH_3+y_dH_1 & y_eH_0+y_aH_4 \end{pmatrix},$$

where

$$\begin{aligned} y_a &= \eta_0+2\eta_{32}+\eta_{64}, & y_b &= \eta_4+\eta_{28}+\eta_{36}+\eta_{60}, \\ y_c &= \eta_8+\eta_{24}+\eta_{40}+\eta_{56}, & y_d &= \eta_{12}+\eta_{20}+\eta_{44}+\eta_{52}, \\ y_e &= 2\eta_{16}+2\eta_{48}, \end{aligned}$$

in the short notation η_N defined in Eq. (295) with $M = M_1M_2M_3 = 128$.

C.1.2 4-5-9 model

Here we show the model with $(|I^{(1)}_{ab}|, |I^{(1)}_{ca}|, |I^{(1)}_{bc}|) = (4,5,9)$. The following table shows zero-mode wavefunctions of left, right-handed matter fields and Higgs fields.

	$L_i(\lambda^{ab})$	$R_j(\lambda^{ca})$	$H_k(\lambda^{bc})$
0	$\Theta^{0,4}$	$\Theta^{0,5}$	$\Theta^{0,9}$
1	$\frac{1}{\sqrt{2}}\left(\Theta^{1,4}+\Theta^{3,4}\right)$	$\frac{1}{\sqrt{2}}\left(\Theta^{1,5}+\Theta^{4,5}\right)$	$\frac{1}{\sqrt{2}}\left(\Theta^{1,9}+\Theta^{8,9}\right)$
2	$\Theta^{2,4}$	$\frac{1}{\sqrt{2}}\left(\Theta^{2,5}+\Theta^{3,5}\right)$	$\frac{1}{\sqrt{2}}\left(\Theta^{2,9}+\Theta^{7,9}\right)$
3	-	-	$\frac{1}{\sqrt{2}}\left(\Theta^{3,9}+\Theta^{6,9}\right)$
4	-	-	$\frac{1}{\sqrt{2}}\left(\Theta^{4,9}+\Theta^{5,9}\right)$

This model has five zero-modes for Higgs fields. Yukawa couplings $Y_{ijk}L_iR_jH_k$ are given by

$$Y_{ijk}H_k = y^0_{ij}H_0 + y^1_{ij}H_1 + y^2_{ij}H_2 + y^3_{ij}H_3 + y^4_{ij}H_4,$$

where

$$y^0_{ij} = \begin{pmatrix} \eta_0 & \sqrt{2}\eta_{36} & \sqrt{2}\eta_{72} \\ \sqrt{2}\eta_{45} & \eta_9+\eta_{81} & \eta_{27}+\eta_{63} \\ \eta_{90} & \sqrt{2}\eta_{54} & \sqrt{2}\eta_{18} \end{pmatrix},$$

$$y^1_{ij} = \begin{pmatrix} \frac{1}{\sqrt{2}}(\eta_{20}+\eta_{40}) & \eta_4+\eta_{76} & \eta_{32}+\eta_{68} \\ \eta_5+\eta_{85} & \frac{1}{\sqrt{2}}(\eta_{31}+\eta_{41}+\eta_{49}+\eta_{59}) & \frac{1}{\sqrt{2}}(\eta_{13}+\eta_{23}+\eta_{67}+\eta_{77}) \\ \sqrt{2}\eta_{50} & \eta_{44}+\eta_{64} & \eta_{22}+\eta_{58} \end{pmatrix},$$

$$y^2_{ij} = \begin{pmatrix} \frac{1}{\sqrt{2}}(\eta_{20}+\eta_{40}) & \eta_{44}+\eta_{64} & \eta_8+\eta_{28} \\ \eta_{35}+\eta_{55} & \frac{1}{\sqrt{2}}(\eta_1+\eta_{19}+\eta_{71}+\eta_{89}) & \frac{1}{\sqrt{2}}(\eta_{17}+\eta_{37}+\eta_{53}+\eta_{73}) \\ \sqrt{2}\eta_{10} & \eta_{26}+\eta_{46} & \eta_{62}+\eta_{82} \end{pmatrix},$$

$$y^3_{ij} = \begin{pmatrix} \frac{1}{\sqrt{2}}(\eta_{60}+\eta_{80}) & \eta_{24}+\eta_{84} & \eta_{12}+\eta_{48} \\ \eta_{15}+\eta_{75} & \frac{1}{\sqrt{2}}(\eta_{21}+\eta_{39}+\eta_{51}+\eta_{69}) & \frac{1}{\sqrt{2}}(\eta_3+\eta_{33}+\eta_{57}+\eta_{87}) \\ \sqrt{2}\eta_{30} & \eta_6+\eta_{26} & \eta_{42}+\eta_{78} \end{pmatrix},$$

$$y^4_{ij} = \begin{pmatrix} \frac{1}{\sqrt{2}}(\eta_{60}+\eta_{80}) & \eta_{16}+\eta_{56} & \eta_{52}+\eta_{88} \\ \eta_{25}+\eta_{65} & \frac{1}{\sqrt{2}}(\eta_{11}+\eta_{29}+\eta_{61}+\eta_{79}) & \frac{1}{\sqrt{2}}(\eta_7+\eta_{43}+\eta_{47}+\eta_{83}) \\ \sqrt{2}\eta_{70} & \eta_{34}+\eta_{74} & \eta_2+\eta_{38} \end{pmatrix},$$

in the short notation η_N defined in Eq. (295) with $M = M_1M_2M_3 = 180$.

C.1.3 4-5-1 model

Here we show the model with $(|I^{(1)}_{ab}|, |I^{(1)}_{ca}|, |I^{(1)}_{bc}|) = (4, 5, 1)$. The following table shows zero-mode wavefunctions of left, right-handed matter fields and Higgs field.

	$L_i(\lambda^{ab})$	$R_j(\lambda^{ca})$	$H_k(\lambda^{bc})$
0	$\Theta^{0,4}$	$\Theta^{0,5}$	$\Theta^{0,1}$
1	$\frac{1}{\sqrt{2}}\left(\Theta^{1,4}+\Theta^{3,4}\right)$	$\frac{1}{\sqrt{2}}\left(\Theta^{1,5}+\Theta^{4,5}\right)$	
2	$\Theta^{2,4}$	$\frac{1}{\sqrt{2}}\left(\Theta^{2,5}+\Theta^{3,5}\right)$	

This model has a single zero-modes for the Higgs field. Yukawa couplings $Y_{ijk}L_iR_jH_k$ are given

$$Y_{ijk}H_k = \begin{pmatrix} \eta_0 & \sqrt{2}\eta_4 & \sqrt{2}\eta_8 \\ \sqrt{2}\eta_5 & (\eta_1+\eta_9) & (\eta_3+\eta_7) \\ \eta_{10} & \sqrt{2}\eta_6 & \sqrt{2}\eta_2 \end{pmatrix} H_0.$$

Here we have used the short notation η_N defined in Eq. (295) with the omitted value $M = M_1M_2M_3 = 20$.

C.1.4 5-5-10 model

Here we show the model with $(|I_{ab}^{(1)}|, |I_{ca}^{(1)}|, |I_{bc}^{(1)}|) = (5, 5, 10)$. The following table shows zero-mode wavefunctions of left, right-handed matter fields and Higgs fields.

	$L_i(\lambda^{ab})$	$R_j(\lambda^{ca})$	$H_k(\lambda^{bc})$
0	$\Theta^{0,5}$	$\Theta^{0,5}$	$\Theta^{0,10}$
1	$\frac{1}{\sqrt{2}}(\Theta^{1,5}+\Theta^{4,5})$	$\frac{1}{\sqrt{2}}(\Theta^{1,5}+\Theta^{4,5})$	$\frac{1}{\sqrt{2}}(\Theta^{1,10}+\Theta^{9,10})$
2	$\frac{1}{\sqrt{2}}(\Theta^{2,5}+\Theta^{3,5})$	$\frac{1}{\sqrt{2}}(\Theta^{2,5}+\Theta^{3,5})$	$\frac{1}{\sqrt{2}}(\Theta^{2,10}+\Theta^{8,10})$
3	-	-	$\frac{1}{\sqrt{2}}(\Theta^{3,10}+\Theta^{7,10})$
4	-	-	$\frac{1}{\sqrt{2}}(\Theta^{4,10}+\Theta^{6,10})$
5	-	-	$\Theta^{5,10}$

This model has six zero-modes for Higgs fields. Yukawa couplings $Y_{ijk}L_iR_jH_k$ are obtained as

$$Y_{ijk}H_k$$
$$= \begin{pmatrix} y_aH_0+y_eH_5 & y_bH_1+y_eH_4 & y_cH_2+y_dH_3 \\ y_bH_1+y_eH_4 & y_cH_0+\frac{1}{\sqrt{2}}(y_aH_2+y_fH_3)+y_dH_5 & \frac{1}{\sqrt{2}}(y_dH_1+y_eH_2+y_bH_3+y_cH_4) \\ y_cH_2+y_dH_3 & \frac{1}{\sqrt{2}}(y_dH_1+y_eH_2+y_bH_3+y_cH_4) & y_bH_0+\frac{1}{\sqrt{2}}(y_fH_1+y_aH_4)+y_aH_5 \end{pmatrix}.$$

$$\begin{aligned} y_a &= \eta_0+2\eta_{50}+2\eta_{100}, & y_b &= \eta_5+\eta_{45}+\eta_{55}+\eta_{95}+\eta_{105}, \\ y_c &= \eta_{10}+\eta_{40}+\eta_{60}+\eta_{90}+\eta_{110}, & y_d &= \eta_{15}+\eta_{35}+\eta_{65}+\eta_{85}+\eta_{115}, \\ y_e &= \eta_{20}+\eta_{30}+\eta_{70}+\eta_{80}+\eta_{120}, & y_f &= 2\eta_{25}+2\eta_{75}+\eta_{125}, \end{aligned}$$

in the short notation η_N defined in Eq. (295) with $M = M_1M_2M_3 = 250$.

C.2 (Even-Odd-Odd) wavefunctions

Here, we study the patterns of Yukawa matrices in the models, where zero-modes of left, right-handed matter fields and Higgs fields correspond to even, odd and odd functions, respectively.

C.2.1 4-7-11 model

Here we show the model with $(|I_{ab}^{(1)}|, |I_{ca}^{(1)}|, |I_{bc}^{(1)}|) = (4, 7, 11)$. The following table shows zero-mode wavefunctions of left, right-handed matter fields and Higgs fields.

	$L_i(\lambda^{ab})$	$R_j(\lambda^{ca})$	$H_k(\lambda^{bc})$
0	$\Theta^{0,4}$	$\frac{1}{\sqrt{2}}(\Theta^{1,7} - \Theta^{6,7})$	$\frac{1}{\sqrt{2}}(\Theta^{1,11} - \Theta^{10,11})$
1	$\frac{1}{\sqrt{2}}(\Theta^{1,4} + \Theta^{3,4})$	$\frac{1}{\sqrt{2}}(\Theta^{2,7} - \Theta^{5,7})$	$\frac{1}{\sqrt{2}}(\Theta^{2,11} - \Theta^{9,11})$
2	$\Theta^{2,4}$	$\frac{1}{\sqrt{2}}(\Theta^{3,7} - \Theta^{4,7})$	$\frac{1}{\sqrt{2}}(\Theta^{3,11} - \Theta^{8,11})$
3	-	-	$\frac{1}{\sqrt{2}}(\Theta^{4,11} - \Theta^{7,11})$
4	-	-	$\frac{1}{\sqrt{2}}(\Theta^{5,11} - \Theta^{6,11})$

This model has five zero-modes for the Higgs fields. Yukawa couplings $Y_{ijk}L_iR_jH_k$ are given by

$$Y_{ij}^k H_k = y_{ij}^0 H_0 + y_{ij}^1 H_1 + y_{ij}^2 H_2 + y_{ij}^3 H_3 + y_{ij}^4 H_4,$$

where

$$\begin{aligned}
y_{ij}^0 &= \frac{1}{\sqrt{2}} \begin{pmatrix} \sqrt{2}(\eta_4 - \eta_{136}) & \sqrt{2}(\eta_{92} - \eta_{48}) & \sqrt{2}(\eta_{128} - \eta_{40}) \\ \eta_{81} - \eta_{59} - \eta_{95} + \eta_{73} & \eta_{139} - \eta_{29} - \eta_{125} + \eta_{15} & \eta_{51} - \eta_{117} - \eta_{37} + \eta_{103} \\ \sqrt{2}(\eta_{150} - \eta_{18}) & \sqrt{2}(\eta_{62} - \eta_{16}) & \sqrt{2}(\eta_{26} - \eta_{114}) \end{pmatrix}, \\
y_{ij}^1 &= \frac{1}{\sqrt{2}} \begin{pmatrix} \sqrt{2}(\eta_{80} - \eta_{52}) & \sqrt{2}(\eta_8 - \eta_{36}) & \sqrt{2}(\eta_{96} - \eta_{124}) \\ \eta_3 - \eta_{25} - \eta_{129} + \eta_{151} & \eta_{85} - \eta_{113} - \eta_{41} + \eta_{69} & \eta_{135} - \eta_{107} - \eta_{47} + \eta_{19} \\ \sqrt{2}(\eta_{74} - \eta_{102}) & \sqrt{2}(\eta_{146} - \eta_{118}) & \sqrt{2}(\eta_{58} - \eta_{30}) \end{pmatrix}, \\
y_{ij}^2 &= \frac{1}{\sqrt{2}} \begin{pmatrix} \sqrt{2}(\eta_{144} - \eta_{32}) & \sqrt{2}(\eta_{76} - \eta_{120}) & \sqrt{2}(\eta_{12} - \eta_{100}) \\ \eta_{87} - \eta_{109} - \eta_{45} + \eta_{67} & \eta_1 - \eta_{111} - \eta_{43} + \eta_{153} & \eta_{89} - \eta_{23} - \eta_{131} + \eta_{65} \\ \sqrt{2}(\eta_{10} - \eta_{122}) & \sqrt{2}(\eta_{78} - \eta_{34}) & \sqrt{2}(\eta_{142} - \eta_{54}) \end{pmatrix}, \\
y_{ij}^3 &= \frac{1}{\sqrt{2}} \begin{pmatrix} \sqrt{2}(\eta_{148} - \eta_{104}) & \sqrt{2}(\eta_{148} - \eta_{104}) & \sqrt{2}(\eta_{72} - \eta_{16}) \\ \eta_{171} - \eta_{115} - \eta_{39} + \eta_{17} & \eta_{83} - \eta_{27} - \eta_{127} + \eta_{71} & \eta_5 - \eta_{61} - \eta_{13} + \eta_{149} \\ \sqrt{2}(\eta_{94} - \eta_{38}) & \sqrt{2}(\eta_6 - \eta_{50}) & \sqrt{2}(\eta_{82} - \eta_{138}) \end{pmatrix}, \\
y_{ij}^4 &= \frac{1}{\sqrt{2}} \begin{pmatrix} \sqrt{2}(\eta_{24} - \eta_{108}) & \sqrt{2}(\eta_{64} - \eta_{20}) & \sqrt{2}(\eta_{152} - \eta_{68}) \\ \eta_{53} - \eta_{31} - \eta_{123} + \eta_{101} & \eta_{141} - \eta_{57} - \eta_7 + \eta_{13} & \eta_{79} - \eta_{145} - \eta_9 + \eta_{75} \\ \sqrt{2}(\eta_{130} - \eta_{46}) & \sqrt{2}(\eta_{90} - \eta_{134}) & \sqrt{2}(\eta_2 - \eta_{86}) \end{pmatrix},
\end{aligned}$$

in the short notation η_N defined in Eq. (295) with $M = M_1M_2M_3 = 308$.

C.2.2 4-7-3 model

Here we show the model with $(|I_{ab}^{(1)}|, |I_{ca}^{(1)}|, |I_{bc}^{(1)}|) = (4, 7, 3)$. The following table shows zero-mode wavefunctions of left, right-handed matter fields and Higgs fields.

	$L_i(\lambda^{ab})$	$R_j(\lambda^{ca})$	$H_k(\lambda^{bc})$
0	$\Theta^{0,4}$	$\frac{1}{\sqrt{2}}(\Theta^{1,7} - \Theta^{6,7})$	$\frac{1}{\sqrt{2}}(\Theta^{1,3} - \Theta^{2,3})$
1	$\frac{1}{\sqrt{2}}(\Theta^{1,4} + \Theta^{3,4})$	$\frac{1}{\sqrt{2}}(\Theta^{2,5} - \Theta^{5,7})$	-
2	$\Theta^{2,4}$	$\frac{1}{\sqrt{2}}(\Theta^{3,5} - \Theta^{4,5})$	-

This model has a single zero-modes for Higgs fields. Yukawa couplings $Y_{ijk}L_iR_jH_k$ are obtained as

$$Y_{ij}^k H_k = \frac{1}{\sqrt{2}} H_0 \begin{pmatrix} \sqrt{2}(\eta_4 - \eta_{32}) & \sqrt{2}(\eta_{20} - \eta_8) & \sqrt{2}(\eta_{40} - \eta_{16}) \\ \eta_{17} + \eta_{25} - \eta_{11} - \eta_{31} & \eta_1 + \eta_{41} - \eta_{13} - \eta_{29} & \eta_{19} + \eta_{23} - \eta_5 - \eta_{37} \\ \sqrt{2}(\eta_{38} - \eta_{10}) & \sqrt{2}(\eta_{22} - \eta_{34}) & \sqrt{2}(\eta_2 - \eta_{26}) \end{pmatrix},$$

in the short notation η_N defined in Eq. (295) with $M = M_1M_2M_3 = 84$.

C.2.3 4-8-12 model

Here we show the model with $(|I_{ab}^{(1)}|, |I_{ca}^{(1)}|, |I_{bc}^{(1)}|) = (4, 8, 12)$. The following table shows zero-mode wavefunctions of left, right-handed matter fields and Higgs fields.

	$L_i(\lambda^{ab})$	$R_j(\lambda^{ca})$	$H_k(\lambda^{bc})$
0	$\Theta^{0,4}$	$\frac{1}{\sqrt{2}}(\Theta^{1,8} - \Theta^{7,8})$	$\frac{1}{\sqrt{2}}(\Theta^{1,12} - \Theta^{11,12})$
1	$\frac{1}{\sqrt{2}}(\Theta^{1,4} + \Theta^{3,4})$	$\frac{1}{\sqrt{2}}(\Theta^{2,8} - \Theta^{6,8})$	$\frac{1}{\sqrt{2}}(\Theta^{2,12} - \Theta^{10,12})$
2	$\Theta^{2,4}$	$\frac{1}{\sqrt{2}}(\Theta^{3,8} - \Theta^{5,8})$	$\frac{1}{\sqrt{2}}(\Theta^{3,12} - \Theta^{9,12})$
3	-	-	$\frac{1}{\sqrt{2}}(\Theta^{4,12} - \Theta^{8,12})$
4	-	-	$\frac{1}{\sqrt{2}}(\Theta^{5,12} - \Theta^{7,12})$

This model has five zero-modes for the Higgs fields. Yukawa couplings $Y_{ijk}L_iR_jH_k$ are given by

$$Y_{ij}^k H_k = y_{ij}^0 H_0 + y_{ij}^1 H_1 + y_{ij}^2 H_2 + y_{ij}^3 H_3 + y_{ij}^4 H_4,$$

where

$$y_{ij}^0 = \begin{pmatrix} y_b & 0 & -y_l \\ 0 & \frac{1}{\sqrt{2}}(y_e - y_i) & 0 \\ -y_f & 0 & y_h \end{pmatrix}, \quad y_{ij}^1 = \begin{pmatrix} 0 & y_c - y_k & 0 \\ \frac{1}{\sqrt{2}}(y_b - y_h) & 0 & \frac{1}{\sqrt{2}}(y_f - y_l) \\ 0 & 0 & 0 \end{pmatrix},$$

$$y_{ij}^2 = \begin{pmatrix} -y_j & 0 & y_d \\ 0 & \frac{1}{\sqrt{2}}(y_a - y_m) & 0 \\ y_d & 0 & -y_j \end{pmatrix}, \quad y_{ij}^3 = \begin{pmatrix} 0 & 0 & 0 \\ \frac{1}{\sqrt{2}}(y_f - y_l) & 0 & \frac{1}{\sqrt{2}}(y_b - y_h) \\ 0 & y_c - y_k & 0 \end{pmatrix},$$

$$y_{ij}^4 = \begin{pmatrix} y_h & 0 & -y_f \\ 0 & \frac{1}{\sqrt{2}}(y_e - y_i) & 0 \\ -y_l & 0 & y_b \end{pmatrix},$$

and

$$\begin{aligned} y_a &= \eta_0 + \eta_{96} + \eta_{192} + \eta_{96}, & y_b &= \eta_4 + \eta_{100} + \eta_{188} + \eta_{92}, \\ y_c &= \eta_8 + \eta_{104} + \eta_{184} + \eta_{88}, & y_d &= \eta_{12} + \eta_{108} + \eta_{180} + \eta_{84}, \\ y_e &= \eta_{16} + \eta_{112} + \eta_{176} + \eta_{80}, & y_f &= \eta_{20} + \eta_{116} + \eta_{172} + \eta_{76}, \\ y_g &= \eta_{24} + \eta_{120} + \eta_{168} + \eta_{72}, & y_h &= \eta_{28} + \eta_{124} + \eta_{164} + \eta_{68}, \\ y_i &= \eta_{32} + \eta_{128} + \eta_{160} + \eta_{64}, & y_j &= \eta_{36} + \eta_{132} + \eta_{156} + \eta_{60}, \\ y_k &= \eta_{40} + \eta_{136} + \eta_{152} + \eta_{56}, & y_l &= \eta_{44} + \eta_{140} + \eta_{148} + \eta_{52}, \\ y_m &= \eta_{48} + \eta_{144} + \eta_{144} + \eta_{48}, \end{aligned}$$

in the short notation η_N defined in Eq. (295) with $M = M_1M_2M_3 = 384$.

C.2.4 4-8-4 model

Here we show the model with $(|I^{(1)}_{ab}|, |I^{(1)}_{ca}|, |I^{(1)}_{bc}|) = (4, 8, 4)$. The following table shows zero-mode wavefunctions of left, right-handed matter fields and Higgs fields.

	$L_i(\lambda^{ab})$	$R_j(\lambda^{ca})$	$H_k(\lambda^{bc})$
0	$\Theta^{0,4}$	$\frac{1}{\sqrt{2}}(\Theta^{1,8} - \Theta^{7,8})$	$\frac{1}{\sqrt{2}}(\Theta^{1,4} - \Theta^{3,4})$
1	$\frac{1}{\sqrt{2}}(\Theta^{1,4} + \Theta^{3,4})$	$\frac{1}{\sqrt{2}}(\Theta^{2,7} - \Theta^{6,7})$	-
2	$\Theta^{2,4}$	$\frac{1}{\sqrt{2}}(\Theta^{3,7} - \Theta^{5,7})$	-

This model has a single zero-modes for Higgs fields. Yukawa couplings $Y_{ijk}L_iR_jH_k$ are obtained as

$$Y^k_{ij}H_k = H_0 \begin{pmatrix} y_b & 0 & -y_c \\ 0 & \frac{1}{\sqrt{2}}(y_a - y_d) & 0 \\ -y_c & 0 & y_b \end{pmatrix},$$

where

$$\begin{aligned} y_a &= \eta_0 + 2\eta_{32} + \eta_{64}, & y_b &= \eta_4 + \eta_{28} + \eta_{36} + \eta_{60}, \\ y_c &= \eta_{12} + \eta_{20} + \eta_{44} + \eta_{52}, & y_d &= 2\eta_{16} + 2\eta_{48}, \end{aligned}$$

in the short notation η_N defined in Eq. (295) with $M = M_1M_2M_3 = 128$.

C.2.5 5-7-12 model

Here we show the model with $(|I^{(1)}_{ab}|, |I^{(1)}_{ca}|, |I^{(1)}_{bc}|) = (5, 7, 12)$. The following table shows zero-mode wavefunctions of left, right-handed matter fields and Higgs fields.

	$L_i(\lambda^{ab})$	$R_j(\lambda^{ca})$	$H_k(\lambda^{bc})$
0	$\Theta^{0,5}$	$\frac{1}{\sqrt{2}}(\Theta^{1,7} - \Theta^{6,7})$	$\frac{1}{\sqrt{2}}(\Theta^{1,12} - \Theta^{11,12})$
1	$\frac{1}{\sqrt{2}}(\Theta^{1,5} + \Theta^{4,5})$	$\frac{1}{\sqrt{2}}(\Theta^{2,7} - \Theta^{5,7})$	$\frac{1}{\sqrt{2}}(\Theta^{2,12} - \Theta^{10,12})$
2	$\frac{1}{\sqrt{2}}(\Theta^{2,5} + \Theta^{3,5})$	$\frac{1}{\sqrt{2}}(\Theta^{3,7} - \Theta^{4,7})$	$\frac{1}{\sqrt{2}}(\Theta^{3,12} - \Theta^{9,12})$
3	-	-	$\frac{1}{\sqrt{2}}(\Theta^{4,12} - \Theta^{8,12})$
4	-	-	$\frac{1}{\sqrt{2}}(\Theta^{5,12} - \Theta^{7,12})$

This model has five zero-modes for the Higgs fields. Yukawa coupling $Y_{ijk}L_iR_jH_k$ are given by

$$Y_{ijk}H_k = y^0_{ij}H_0 + y^1_{ij}H_1 + y^2_{ij}H_2 + y^3_{ij}H_3 + y^4_{ij}H_4,$$

where

$$y^0_{ij} = \frac{1}{\sqrt{2}} \begin{pmatrix} \sqrt{2}(\eta_5 - \eta_{65}) & \sqrt{2}(\eta_{185} - \eta_{115}) & \sqrt{2}(\eta_{55} + \eta_{125}) \\ \eta_{173} - \eta_{103} - \eta_{187} + \eta_{163} & \eta_{67} - \eta_{137} - \eta_{53} + \eta_{17} & \eta_{113} - \eta_{43} - \eta_{127} + \eta_{197} \\ \eta_{79} - \eta_{149} - \eta_{19} + \eta_{89} & \eta_{101} - \eta_{31} - \eta_{199} + \eta_{151} & \eta_{139} - \eta_{209} - \eta_{41} + \eta_{29} \end{pmatrix},$$

$$y^1_{ij} = \frac{1}{\sqrt{2}} \begin{pmatrix} \sqrt{2}(\eta_{170} - \eta_{110}) & \sqrt{2}(\eta_{10} - \eta_{130}) & \sqrt{2}(\eta_{190} + \eta_{50}) \\ \eta_2 - \eta_{142} - \eta_{58} + \eta_{82} & \eta_{178} - \eta_{38} - \eta_{122} + \eta_{158} & \eta_{62} - \eta_{202} - \eta_{118} + \eta_{22} \\ \eta_{166} - \eta_{26} - \eta_{194} + \eta_{94} & \eta_{74} - \eta_{206} - \eta_{46} + \eta_{94} & \eta_{106} - \eta_{34} - \eta_{134} + \eta_{146} \end{pmatrix},$$

$$y^2_{ij} = \frac{1}{\sqrt{2}} \begin{pmatrix} \sqrt{2}(\eta_{75} - \eta_{135}) & \sqrt{2}(\eta_{165} - \eta_{45}) & \sqrt{2}(\eta_{15} - \eta_{195}) \\ \eta_{177} - \eta_{33} - \eta_{117} + \eta_{93} & \eta_3 - \eta_{207} - \eta_{123} + \eta_{87} & \eta_{183} - \eta_{27} - \eta_{57} + \eta_{153} \\ \eta_9 - \eta_{201} - \eta_{51} + \eta_{81} & \eta_{171} - \eta_{39} - \eta_{129} + \eta_{81} & \eta_{69} - \eta_{141} - \eta_{111} + \eta_{99} \end{pmatrix},$$

$$y^3_{ij} = \frac{1}{\sqrt{2}} \begin{pmatrix} \sqrt{2}(\eta_{100} - \eta_{140}) & \sqrt{2}(\eta_{80} - \eta_{200}) & \sqrt{2}(\eta_{160} - \eta_{20}) \\ \eta_{68} - \eta_{208} - \eta_{128} + \eta_{152} & \eta_{172} - \eta_{32} - \eta_{52} + \eta_{88} & \eta_8 - \eta_{148} - \eta_{188} + \eta_{92} \\ \eta_{184} - \eta_{44} - \eta_{124} + \eta_{164} & \eta_4 - \eta_{136} - \eta_{116} + \eta_{164} & \eta_{176} - \eta_{104} - \eta_{64} + \eta_{76} \end{pmatrix},$$

$$y^4_{ij} = \frac{1}{\sqrt{2}} \begin{pmatrix} \sqrt{2}(\eta_{145} - \eta_{205}) & \sqrt{2}(\eta_{95} - \eta_{25}) & \sqrt{2}(\eta_{85} - \eta_{155}) \\ \eta_{107} - \eta_{37} - \eta_{47} + \eta_{23} & \eta_{73} - \eta_{143} - \eta_{193} + \eta_{157} & \eta_{167} - \eta_{97} - \eta_{13} + \eta_{83} \\ \eta_{61} - \eta_{131} - \eta_{121} + \eta_{11} & \eta_{179} - \eta_{109} - \eta_{59} + \eta_{11} & \eta_1 - \eta_{71} - \eta_{181} + \eta_{169} \end{pmatrix},$$

in the short notation η_N defined in Eq. (295) with $M = M_1 M_2 M_3 = 420$.

C.2.6 5-8-13 model

Here we show the model with $(|I^{(1)}_{ab}|, |I^{(1)}_{ca}|, |I^{(1)}_{bc}|) = (5, 8, 13)$. The following table shows zero-mode wavefunctions of left, right-handed matter fields and Higgs fields.

	$L_i(\lambda^{ab})$	$R_j(\lambda^{ca})$	$H_k(\lambda^{bc})$
0	$\Theta^{0,5}$	$\frac{1}{\sqrt{2}}(\Theta^{1,8} - \Theta^{7,8})$	$\frac{1}{\sqrt{2}}(\Theta^{1,13} - \Theta^{12,13})$
1	$\frac{1}{\sqrt{2}}(\Theta^{1,5} + \Theta^{4,5})$	$\frac{1}{\sqrt{2}}(\Theta^{2,8} - \Theta^{6,8})$	$\frac{1}{\sqrt{2}}(\Theta^{2,13} - \Theta^{11,13})$
2	$\frac{1}{\sqrt{2}}(\Theta^{2,5} + \Theta^{3,5})$	$\frac{1}{\sqrt{2}}(\Theta^{3,8} - \Theta^{5,8})$	$\frac{1}{\sqrt{2}}(\Theta^{3,13} - \Theta^{10,13})$
3	-	-	$\frac{1}{\sqrt{2}}(\Theta^{4,13} - \Theta^{9,13})$
4	-	-	$\frac{1}{\sqrt{2}}(\Theta^{5,13} - \Theta^{8,13})$
5	-	-	$\frac{1}{\sqrt{2}}(\Theta^{6,13} - \Theta^{7,13})$

This model has six zero-modes for the Higgs fields. Yukawa couplings $Y_{ijk} L_i R_j H_k$ are given by

$$Y^k_{ij} H_k = y^0_{ij} H_0 + y^1_{ij} H_1 + y^2_{ij} H_2 + y^3_{ij} H_3 + y^4_{ij} H_4 + y^5_{ij} H_5,$$

where

$$y_{ij}^0 = \frac{1}{\sqrt{2}}\begin{pmatrix} \sqrt{2}(\eta_5-\eta_{125}) & \sqrt{2}(\eta_{190}-\eta_{70}) & \sqrt{2}(\eta_{135}-\eta_{255}) \\ \eta_{203}+\eta_{213}-\eta_{83}-\eta_{187} & \eta_{122}-\eta_{138}+\eta_{18}-\eta_{242} & \eta_{73}-\eta_{57}+\eta_{177}-\eta_{47} \\ \eta_{109}-\eta_{21}+\eta_{99}-\eta_{229} & \eta_{86}-\eta_{174}+\eta_{226}-\eta_{34} & \eta_{239}-\eta_{151}+\eta_{31}-\eta_{161} \end{pmatrix},$$

$$y_{ij}^1 = \frac{1}{\sqrt{2}}\begin{pmatrix} \sqrt{2}(\eta_{205}-\eta_{75}) & \sqrt{2}(\eta_{10}-\eta_{250}) & \sqrt{2}(\eta_{185}-\eta_{55}) \\ \eta_{3}+\eta_{237}-\eta_{133}-\eta_{107} & \eta_{198}-\eta_{62}+\eta_{132}-\eta_{152} & \eta_{127}-\eta_{257}+\eta_{23}-\eta_{153} \\ \eta_{211}-\eta_{179}+\eta_{101}-\eta_{29} & \eta_{114}-\eta_{146}+\eta_{94}-\eta_{166} & \eta_{81}-\eta_{49}+\eta_{231}-\eta_{159} \end{pmatrix},$$

$$y_{ij}^2 = \frac{1}{\sqrt{2}}\begin{pmatrix} \sqrt{2}(\eta_{115}-\eta_{245}) & \sqrt{2}(\eta_{210}-\eta_{50}) & \sqrt{2}(\eta_{15}-\eta_{145}) \\ \eta_{197}+\eta_{137}-\eta_{67}-\eta_{93} & \eta_{2}-\eta_{258}+\eta_{102}-\eta_{158} & \eta_{193}-\eta_{63}+\eta_{223}-\eta_{167} \\ \eta_{11}-\eta_{141}+\eta_{219}-\eta_{171} & \eta_{206}-\eta_{54}+\eta_{106}-\eta_{154} & \eta_{119}-\eta_{249}+\eta_{89}-\eta_{41} \end{pmatrix},$$

$$y_{ij}^3 = \frac{1}{\sqrt{2}}\begin{pmatrix} \sqrt{2}(\eta_{85}-\eta_{45}) & \sqrt{2}(\eta_{110}-\eta_{150}) & \sqrt{2}(\eta_{135}-\eta_{255}) \\ \eta_{123}+\eta_{163}-\eta_{253}-\eta_{227} & \eta_{202}-\eta_{58}+\eta_{98}-\eta_{162} & \eta_{7}-\eta_{137}+\eta_{97}-\eta_{33} \\ \eta_{189}-\eta_{59}+\eta_{19}-\eta_{149} & \eta_{6}-\eta_{254}+\eta_{214}-\eta_{46} & \eta_{201}-\eta_{71}+\eta_{111}-\eta_{241} \end{pmatrix},$$

$$y_{ij}^4 = \frac{1}{\sqrt{2}}\begin{pmatrix} \sqrt{2}(\eta_{235}-\eta_{155}) & \sqrt{2}(\eta_{90}-\eta_{170}) & \sqrt{2}(\eta_{105}-\eta_{25}) \\ \eta_{77}+\eta_{157}-\eta_{53}-\eta_{27} & \eta_{118}-\eta_{142}+\eta_{222}-\eta_{38} & \eta_{207}-\eta_{183}+\eta_{103}-\eta_{233} \\ \eta_{131}-\eta_{259}+\eta_{181}-\eta_{51} & \eta_{194}-\eta_{66}+\eta_{14}-\eta_{246} & \eta_{1}-\eta_{129}+\eta_{209}-\eta_{79} \end{pmatrix},$$

$$y_{ij}^5 = \frac{1}{\sqrt{2}}\begin{pmatrix} \sqrt{2}(\eta_{35}-\eta_{165}) & \sqrt{2}(\eta_{230}-\eta_{30}) & \sqrt{2}(\eta_{95}-\eta_{225}) \\ \eta_{243}+\eta_{43}-\eta_{147}-\eta_{173} & \eta_{82}-\eta_{178}+\eta_{22}-\eta_{238} & \eta_{113}-\eta_{17}+\eta_{217}-\eta_{87} \\ \eta_{69}-\eta_{61}+\eta_{139}-\eta_{251} & \eta_{126}-\eta_{134}+\eta_{186}-\eta_{74} & \eta_{199}-\eta_{191}+\eta_{9}-\eta_{121} \end{pmatrix},$$

in the short notation η_N defined in Eq. (295) with $M = M_1M_2M_3 = 520$.

C.2.7 5-8-3 model

Here we show the model with $(|I_{ab}^{(1)}|, |I_{ca}^{(1)}|, |I_{bc}^{(1)}|) = (5, 8, 3)$. The following table shows zero-mode wavefunctions of left, right-handed matter fields and Higgs fields.

	$L_i(\lambda^{ab})$	$R_j(\lambda^{ca})$	$H_k(\lambda^{bc})$
0	$\Theta^{0,5}$	$\frac{1}{\sqrt{2}}(\Theta^{1,8}-\Theta^{7,8})$	$\frac{1}{\sqrt{2}}(\Theta^{1,3}-\Theta^{2,3})$
1	$\frac{1}{\sqrt{2}}(\Theta^{1,5}+\Theta^{4,5})$	$\frac{1}{\sqrt{2}}(\Theta^{2,8}-\Theta^{6,8})$	-
2	$\frac{1}{\sqrt{2}}(\Theta^{2,5}+\Theta^{3,5})$	$\frac{1}{\sqrt{2}}(\Theta^{3,8}-\Theta^{5,8})$	-

This model has a single zero-mode for the Higgs field. Yukawa couplings $Y_{ijk}L_iR_jH_k$ are given by

$$Y_{ij}^k H_k = \frac{1}{\sqrt{2}}\begin{pmatrix} \sqrt{2}(\eta_5-\eta_{35}) & \sqrt{2}(\eta_{50}-\eta_{10}) & \sqrt{2}(\eta_{25}-\eta_{55}) \\ \eta_{43}-\eta_{37}-\eta_{13}+\eta_{53} & \eta_{2}-\eta_{38}-\eta_{58}+\eta_{22} & \eta_{47}-\eta_{7}-\eta_{17}+\eta_{23} \\ \eta_{29}-\eta_{11}-\eta_{59}+\eta_{19} & \eta_{46}-\eta_{34}-\eta_{14}+\eta_{26} & \eta_{1}-\eta_{41}-\eta_{31}+\eta_{49} \end{pmatrix},$$

in the short notation η_N defined in Eq. (295) with $M = M_1M_2M_3 = 120$.

C.3 (Odd-Odd-Even) wavefunctions

Here, we study the patterns of Yukawa matrices in the models, where zero-modes of left, right-handed matter fields and Higgs fields correspond to odd, odd and even functions, respectively.

C.3.1 7-7-14 model

Here we show the model with $(|I_{ab}^{(1)}|, |I_{ca}^{(1)}|, |I_{bc}^{(1)}|) = (7, 7, 14)$. This model is studied in the subsections 5.4.2 and 5.4.3 in detail. The zero-mode wavefunctions of left, right-handed matter fields and Higgs fields are shown in Table 10.

This model has eight zero-modes for the Higgs fields. Yukawa couplings $Y_{ijk}L_jR_jH_k$ are obtained as

$$Y_{ijk}H_k \quad = \quad y_{ij}^0 H_0 + y_{ij}^1 H_1 + y_{ij}^2 H_2 + y_{ij}^3 H_3 + y_{ij}^4 H_4 + y_{ij}^5 H_5 + y_{ij}^6 H_6 + y_{ij}^7 H_7,$$

where y_{ij}^k is shown in Eq. (296) with $M = M_1M_2M_3 = 686$.

C.3.2 7-8-15 model

Here we show the model with $(|I_{ab}^{(1)}|, |I_{ca}^{(1)}|, |I_{bc}^{(1)}|) = (7, 8, 15)$. The following table shows zero-mode wavefunctions of left, right-handed matter fields and Higgs fields.

	$L_i(\lambda^{ab})$	$R_j(\lambda^{ca})$	$H_k(\lambda^{bc})$
0	$\frac{1}{\sqrt{2}}\left(\Theta^{1,7} - \Theta^{6,7}\right)$	$\frac{1}{\sqrt{2}}\left(\Theta^{1,8} - \Theta^{7,8}\right)$	$\Theta^{0,15}$
1	$\frac{1}{\sqrt{2}}\left(\Theta^{2,7} - \Theta^{5,7}\right)$	$\frac{1}{\sqrt{2}}\left(\Theta^{2,8} - \Theta^{6,8}\right)$	$\frac{1}{\sqrt{2}}\left(\Theta^{1,15} + \Theta^{14,15}\right)$
2	$\frac{1}{\sqrt{2}}\left(\Theta^{3,7} - \Theta^{4,7}\right)$	$\frac{1}{\sqrt{2}}\left(\Theta^{3,7} - \Theta^{5,8}\right)$	$\frac{1}{\sqrt{2}}\left(\Theta^{2,15} + \Theta^{13,15}\right)$
3	-	-	$\frac{1}{\sqrt{2}}\left(\Theta^{3,15} + \Theta^{12,15}\right)$
4	-	-	$\frac{1}{\sqrt{2}}\left(\Theta^{4,15} + \Theta^{11,15}\right)$
5	-	-	$\frac{1}{\sqrt{2}}\left(\Theta^{5,15} + \Theta^{10,15}\right)$
6	-	-	$\frac{1}{\sqrt{2}}\left(\Theta^{6,15} + \Theta^{9,15}\right)$
7	-	-	$\frac{1}{\sqrt{2}}\left(\Theta^{7,15} + \Theta^{8,15}\right)$

This model has eight zero-modes for the Higgs fields. Yukawa couplings $Y_{ijk}L_iR_jH_k$ are given by

$$Y_{ij}^k H_k \quad = \quad y_{ij}^0 H_0 + y_{ij}^1 H_1 + y_{ij}^2 H_2 + y_{ij}^3 H_3 + y_{ij}^4 H_4 + y_{ij}^5 H_5 + y_{ij}^6 H_6 + y_{ij}^7 H_7,$$

where

$$y^0_{ij} = \begin{pmatrix} \eta_{225}-\eta_{15} & \eta_{330}-\eta_{90} & \eta_{405}-\eta_{195} \\ \eta_{345}-\eta_{135} & \eta_{390}-\eta_{30} & \eta_{285}-\eta_{75} \\ \eta_{375}-\eta_{255} & \eta_{270}-\eta_{150} & \eta_{165}-\eta_{45} \end{pmatrix},$$

$$y^1_{ij} = \frac{1}{\sqrt{2}}\begin{pmatrix} \eta_{113}-\eta_{97}-\eta_{127}+\eta_{337} & \eta_{218}-\eta_{202}-\eta_{22}+\eta_{398} & \eta_{323}-\eta_{307}-\eta_{83}+\eta_{293} \\ \eta_{233}-\eta_{23}-\eta_{247}+\eta_{383} & \eta_{338}-\eta_{82}-\eta_{142}+\eta_{278} & \eta_{397}-\eta_{187}-\eta_{37}+\eta_{173} \\ \eta_{353}-\eta_{143}-\eta_{367}+\eta_{263} & \eta_{382}-\eta_{38}-\eta_{262}+\eta_{158} & \eta_{277}-\eta_{67}-\eta_{157}+\eta_{53} \end{pmatrix},$$

$$y^2_{ij} = \frac{1}{\sqrt{2}}\begin{pmatrix} \eta_{1}-\eta_{209}-\eta_{239}+\eta_{391} & \eta_{106}-\eta_{314}-\eta_{134}+\eta_{286} & \eta_{211}-\eta_{419}-\eta_{29}+\eta_{181} \\ \eta_{121}-\eta_{89}-\eta_{359}+\eta_{271} & \eta_{226}-\eta_{194}-\eta_{254}+\eta_{166} & \eta_{331}-\eta_{299}-\eta_{149}+\eta_{61} \\ \eta_{241}-\eta_{31}-\eta_{361}+\eta_{151} & \eta_{346}-\eta_{74}-\eta_{374}+\eta_{46} & \eta_{389}-\eta_{179}-\eta_{269}+\eta_{59} \end{pmatrix},$$

$$y^3_{ij} = \frac{1}{\sqrt{2}}\begin{pmatrix} \eta_{111}-\eta_{321}-\eta_{351}+\eta_{279} & \eta_{6}-\eta_{414}-\eta_{246}+\eta_{174} & \eta_{99}-\eta_{309}-\eta_{141}+\eta_{69} \\ \eta_{9}-\eta_{201}-\eta_{369}+\eta_{159} & \eta_{114}-\eta_{306}-\eta_{366}+\eta_{54} & \eta_{219}-\eta_{411}-\eta_{261}+\eta_{51} \\ \eta_{129}-\eta_{81}-\eta_{249}+\eta_{39} & \eta_{234}-\eta_{186}-\eta_{354}+\eta_{66} & \eta_{339}-\eta_{291}-\eta_{381}+\eta_{171} \end{pmatrix},$$

$$y^4_{ij} = \frac{1}{\sqrt{2}}\begin{pmatrix} \eta_{223}-\eta_{407}-\eta_{377}+\eta_{167} & \eta_{118}-\eta_{302}-\eta_{358}+\eta_{62} & \eta_{13}-\eta_{197}-\eta_{253}+\eta_{43} \\ \eta_{103}-\eta_{313}-\eta_{257}+\eta_{47} & \eta_{2}-\eta_{418}-\eta_{362}+\eta_{58} & \eta_{107}-\eta_{317}-\eta_{373}+\eta_{163} \\ \eta_{17}-\eta_{193}-\eta_{137}+\eta_{73} & \eta_{122}-\eta_{298}-\eta_{242}+\eta_{178} & \eta_{227}-\eta_{403}-\eta_{347}+\eta_{283} \end{pmatrix},$$

$$y^5_{ij} = \frac{1}{\sqrt{2}}\begin{pmatrix} \eta_{335}-\eta_{295}-\eta_{265}+\eta_{55} & \eta_{230}-\eta_{190}-\eta_{370}+\eta_{50} & \eta_{125}-\eta_{85}-\eta_{365}+\eta_{155} \\ \eta_{215}-\eta_{415}-\eta_{145}+\eta_{65} & \eta_{110}-\eta_{310}-\eta_{250}+\eta_{170} & \eta_{5}-\eta_{205}-\eta_{355}+\eta_{275} \\ \eta_{95}-\eta_{305}-\eta_{25}+\eta_{185} & \eta_{10}-\eta_{410}-\eta_{130}+\eta_{290} & \eta_{115}-\eta_{325}-\eta_{235}+\eta_{395} \end{pmatrix},$$

$$y^6_{ij} = \frac{1}{\sqrt{2}}\begin{pmatrix} \eta_{393}-\eta_{183}-\eta_{153}+\eta_{57} & \eta_{342}-\eta_{78}-\eta_{258}+\eta_{162} & \eta_{237}-\eta_{27}-\eta_{363}+\eta_{267} \\ \eta_{327}-\eta_{303}-\eta_{33}+\eta_{177} & \eta_{222}-\eta_{198}-\eta_{138}+\eta_{282} & \eta_{117}-\eta_{93}-\eta_{243}+\eta_{387} \\ \eta_{207}-\eta_{417}-\eta_{87}+\eta_{297} & \eta_{102}-\eta_{318}-\eta_{18}+\eta_{402} & \eta_{3}-\eta_{213}-\eta_{123}+\eta_{333} \end{pmatrix},$$

$$y^7_{ij} = \frac{1}{\sqrt{2}}\begin{pmatrix} \eta_{281}-\eta_{71}-\eta_{41}+\eta_{169} & \eta_{386}-\eta_{34}-\eta_{146}+\eta_{274} & \eta_{349}-\eta_{139}-\eta_{251}+\eta_{379} \\ \eta_{401}-\eta_{191}-\eta_{79}+\eta_{289} & \eta_{334}-\eta_{86}-\eta_{26}+\eta_{394} & \eta_{229}-\eta_{19}-\eta_{131}+\eta_{341} \\ \eta_{319}-\eta_{311}-\eta_{199}+\eta_{409} & \eta_{214}-\eta_{206}-\eta_{94}+\eta_{326} & \eta_{109}-\eta_{101}-\eta_{11}+\eta_{221} \end{pmatrix},$$

in the short notation η_N defined in Eq. (295) with $M = M_1M_2M_3 = 840$.

C.3.3 7-8-1 model

Here we show the model with $(|I^{(1)}_{ab}|, |I^{(1)}_{ca}|, |I^{(1)}_{bc}|) = (7, 8, 1)$. The following table shows zero-mode wavefunctions of left, right-handed matter fields and Higgs fields.

	$L_i(\lambda^{ab})$	$R_j(\lambda^{ca})$	$H_k(\lambda^{bc})$
0	$\frac{1}{\sqrt{2}}(\Theta^{1,7}-\Theta^{6,7})$	$\frac{1}{\sqrt{2}}(\Theta^{1,8}-\Theta^{7,8})$	$\Theta^{0,1}$
1	$\frac{1}{\sqrt{2}}(\Theta^{2,7}-\Theta^{5,7})$	$\frac{1}{\sqrt{2}}(\Theta^{2,8}-\Theta^{6,8})$	-
2	$\frac{1}{\sqrt{2}}(\Theta^{3,7}-\Theta^{4,7})$	$\frac{1}{\sqrt{2}}(\Theta^{3,8}-\Theta^{5,8})$	-

This model has a single zero-mode for the Higgs field. Yukawa couplings $Y_{ijk}L_iR_jH_k$ are given by

$$Y^k_{ij}H_k = \frac{1}{\sqrt{2}}H_0\begin{pmatrix} \sqrt{2}(\eta_{5}-\eta_{35}) & \sqrt{2}(\eta_{50}-\eta_{10}) & \sqrt{2}(\eta_{25}-\eta_{55}) \\ \eta_{43}-\eta_{37}-\eta_{13}+\eta_{53} & \eta_{2}-\eta_{38}-\eta_{58}+\eta_{22} & \eta_{47}-\eta_{7}-\eta_{17}+\eta_{23} \\ \eta_{29}-\eta_{11}-\eta_{59}+\eta_{19} & \eta_{46}-\eta_{34}-\eta_{14}+\eta_{26} & \eta_{1}-\eta_{41}-\eta_{31}+\eta_{49} \end{pmatrix},$$

in the short notation η_N defined in Eq. (295) with $M = M_1 M_2 M_3 = 56$.

C.3.4 8-8-16 model

Here we show the model with $(|I_{ab}^{(1)}|, |I_{ca}^{(1)}|, |I_{bc}^{(1)}|) = (8, 8, 16)$. The following table shows zero-mode wavefunctions of left, right-handed matter fields and Higgs fields.

	$L_i(\lambda^{ab})$	$R_j(\lambda^{ca})$	$H_k(\lambda^{bc})$
0	$\frac{1}{\sqrt{2}}(\Theta^{1,8} - \Theta^{7,8})$	$\frac{1}{\sqrt{2}}(\Theta^{1,8} - \Theta^{7,8})$	$\Theta^{0,16}$
1	$\frac{1}{\sqrt{2}}(\Theta^{2,8} - \Theta^{6,8})$	$\frac{1}{\sqrt{2}}(\Theta^{2,8} - \Theta^{6,8})$	$\frac{1}{\sqrt{2}}(\Theta^{1,16} + \Theta^{15,16})$
2	$\frac{1}{\sqrt{2}}(\Theta^{3,8} - \Theta^{5,8})$	$\frac{1}{\sqrt{2}}(\Theta^{3,8} - \Theta^{5,8})$	$\frac{1}{\sqrt{2}}(\Theta^{2,16} + \Theta^{14,16})$
3	-	-	$\frac{1}{\sqrt{2}}(\Theta^{3,16} + \Theta^{13,16})$
4	-	-	$\frac{1}{\sqrt{2}}(\Theta^{4,16} + \Theta^{12,16})$
5	-	-	$\frac{1}{\sqrt{2}}(\Theta^{5,16} + \Theta^{11,16})$
6	-	-	$\frac{1}{\sqrt{2}}(\Theta^{6,16} + \Theta^{10,16})$
7	-	-	$\frac{1}{\sqrt{2}}(\Theta^{7,16} + \Theta^{9,16})$
8	-	-	$\Theta^{8,16}$

This model has eight zero-modes for the Higgs fields. Yukawa couplings $Y_{ijk} L_i R_j H_k$ are obtained as

$$Y_{ij}^k H_k = y_{ij}^0 H_0 + y_{ij}^1 H_1 + y_{ij}^2 H_2 + y_{ij}^3 H_3 + y_{ij}^4 H_4 + y_{ij}^5 H_5 + y_{ij}^6 H_6 + y_{ij}^7 H_7 + y_{ij}^8 H_8,$$

where

$$y_{ij}^0 = \begin{pmatrix} -y_g & 0 & 0 \\ 0 & -y_e & 0 \\ 0 & 0 & -y_g \end{pmatrix}, \qquad y_{ij}^1 = \frac{1}{\sqrt{2}} \begin{pmatrix} 0 & -y_d & 0 \\ -y_d & 0 & -y_f \\ 0 & -y_f & 0 \end{pmatrix},$$

$$y_{ij}^2 = \frac{1}{\sqrt{2}} \begin{pmatrix} y_a & 0 & -y_e \\ 0 & 0 & 0 \\ -y_e & 0 & y_i \end{pmatrix}, \qquad y_{ij}^3 = \frac{1}{\sqrt{2}} \begin{pmatrix} 0 & y_b & 0 \\ y_b & 0 & y_h \\ 0 & y_h & 0 \end{pmatrix},$$

$$y_{ij}^4 = \frac{1}{\sqrt{2}} \begin{pmatrix} 0 & 0 & y_c + y_g \\ 0 & y_a + y_i & 0 \\ y_c + y_g & 0 & 0 \end{pmatrix}, \qquad y_{ij}^5 = \frac{1}{\sqrt{2}} \begin{pmatrix} 0 & y_h & 0 \\ y_h & 0 & y_b \\ 0 & y_b & 0 \end{pmatrix},$$

$$y_{ij}^6 = \frac{1}{\sqrt{2}} \begin{pmatrix} y_i & 0 & -y_e \\ 0 & 0 & 0 \\ -y_e & 0 & y_a \end{pmatrix}, \qquad y_{ij}^7 = \frac{1}{\sqrt{2}} \begin{pmatrix} 0 & -y_f & 0 \\ -y_f & 0 & -y_d \\ 0 & -y_d & 0 \end{pmatrix},$$

$$y_{ij}^8 = \begin{pmatrix} -y_c & 0 & 0 \\ 0 & -y_e & 0 \\ 0 & 0 & -y_c \end{pmatrix},$$

and

$$
\begin{aligned}
y_a &= \eta_0 + 2(\eta_{128} + 2\eta_{256} + 2\eta_{384}) + \eta_{512}, \\
y_b &= \eta_8 + \eta_{120} + \eta_{136} + \eta_{248} + \eta_{264} + \eta_{376} + \eta_{392} + \eta_{504}, \\
y_c &= \eta_{16} + \eta_{112} + \eta_{144} + \eta_{240} + \eta_{272} + \eta_{368} + \eta_{400} + \eta_{496}, \\
y_d &= \eta_{24} + \eta_{104} + \eta_{156} + \eta_{232} + \eta_{280} + \eta_{360} + \eta_{408} + \eta_{488}, \\
y_e &= \eta_{32} + \eta_{96} + \eta_{164} + \eta_{224} + \eta_{288} + \eta_{352} + \eta_{416} + \eta_{480}, \\
y_f &= \eta_{40} + \eta_{88} + \eta_{172} + \eta_{216} + \eta_{296} + \eta_{344} + \eta_{424} + \eta_{472}, \\
y_g &= \eta_{48} + \eta_{80} + \eta_{180} + \eta_{208} + \eta_{304} + \eta_{336} + \eta_{432} + \eta_{464}, \\
y_h &= \eta_{56} + \eta_{72} + \eta_{188} + \eta_{200}, + \eta_{312} + \eta_{328} + \eta_{440} + \eta_{456}, \\
y_i &= 2(\eta_{64} + \eta_{192} + \eta_{320} + \eta_{448}),
\end{aligned}
$$

in the short notation η_N defined in Eq. (295) with $M = M_1 M_2 M_3 = 1024$.

D Non-Abelian discrete symmetries

In this appendix the group theoretical aspects of the some discrete symmetries are explained.

D.1 D_4

Here, we give a examples of D_4 which can appear in the models containing at least two flavors.

The D_4 is the symmetry of a square, which is generated by the $\pi/4$ rotation A and the reflection B, where they satisfy $A^4 = e$, $B^2 = e$ and $BAB = A^{-1}$. Indeed, the D_4 consists of the eight elements, which are represented by $(-1)^t Z^r C^s$ with $t, r, s = 0, 1$. They are related each other by $A = ZC$, $B = Z$ where Z and C are defined by

$$
Z = \begin{pmatrix} 1 & 0 \\ 0 & -1 \end{pmatrix}, \quad C = \begin{pmatrix} 0 & 1 \\ 1 & 0 \end{pmatrix}. \tag{426}
$$

The D_4 has the following five conjugacy classes,

$$
\begin{array}{rcl}
C_1 : & \{e\}, & h = 1 \\
C_1^{(1)} : & \{-e\}, & h = 2 \\
C_2^{(0,1)} : & \{C, -C\}, & h = 2 \\
C_2^{(1,0)} : & \{Z, -Z\}, & h = 2 \\
C_2^{(1,1)} : & \{ZC, -ZC\}, & h = 4,
\end{array}
$$

where h denotes the order of the elements.

	h	$\chi_{1_{++}}$	$\chi_{1_{+-}}$	$\chi_{1_{-+}}$	$\chi_{1_{--}}$	χ_2
C_1	1	1	1	1	1	2
$C_1^{(1)}$	2	1	1	1	1	-2
$C_2^{(0,1)}$	2	1	-1	1	-1	0
$C_2^{(1,0)}$	2	1	1	-1	-1	0
$C_2^{(1,1)}$	4	1	-1	-1	1	0

Table 22: Characters of D_4 representations

The D_4 has four singlets, $\mathbf{1}_{++}$, $\mathbf{1}_{+-}$, $\mathbf{1}_{-+}$ and $\mathbf{1}_{--}$, and one doublet $\mathbf{2}$. The characters are shown in Table 22. The tensor products are obtained as

$$\begin{aligned} \begin{pmatrix} x_1 \\ x_2 \end{pmatrix}_{\mathbf{2}} \otimes \begin{pmatrix} y_1 \\ y_2 \end{pmatrix}_{\mathbf{2}} &= (x_1y_1 + x_2y_2)_{\mathbf{1}_{++}} + (x_1y_1 - x_2y_2)_{\mathbf{1}_{+-}} \\ &\quad + (x_1y_2 + x_2y_1)_{\mathbf{1}_{-+}} + (x_1y_2 - x_2y_1)_{\mathbf{1}_{--}} , \end{aligned}$$

$$\begin{aligned} (x)_{\mathbf{1}_{++}} \times \begin{pmatrix} y_1 \\ y_2 \end{pmatrix}_{\mathbf{2}} &= \begin{pmatrix} xy_1 \\ xy_2 \end{pmatrix}_{\mathbf{2}}, \qquad & (x)_{\mathbf{1}_{+-}} \times \begin{pmatrix} y_1 \\ y_2 \end{pmatrix}_{\mathbf{2}} &= \begin{pmatrix} xy_1 \\ -xy_2 \end{pmatrix}_{\mathbf{2}}, \\ (x)_{\mathbf{1}_{-+}} \times \begin{pmatrix} y_1 \\ y_2 \end{pmatrix}_{\mathbf{2}} &= \begin{pmatrix} xy_2 \\ xy_1 \end{pmatrix}_{\mathbf{2}}, \qquad & (x)_{\mathbf{1}_{--}} \times \begin{pmatrix} y_1 \\ y_2 \end{pmatrix}_{\mathbf{2}} &= \begin{pmatrix} xy_2 \\ -xy_1 \end{pmatrix}_{\mathbf{2}}. \end{aligned}$$

D.2 $\Delta(27)$

The elements g of $\Delta(27)$ are summarized as $g = \omega^t Z^r C^s$, $(r, s, t = 0, 1, 2)$. The elements Z and C are defined

$$Z = \begin{pmatrix} 1 & 0 & 0 \\ 0 & \omega & 0 \\ 0 & 0 & \omega^2 \end{pmatrix}, \ C = \begin{pmatrix} 0 & 1 & 0 \\ 0 & 0 & 1 \\ 1 & 0 & 0 \end{pmatrix}, \tag{427}$$

where ω is the cubic root of 1. Therefore the order of this group is 27. The elements Z and C satisfy the following algebra

$$C^3 = Z^3 = e, \quad CZ = \omega ZC, \tag{428}$$

	h	$\chi_{1_{(r,s)}}$	χ_{3}	$\chi_{\bar{3}}$
C_1	1	1	3	3
$C_1^{(1)}$	3	1	3ω	$3\omega^2$
$C_1^{(2)}$	3	1	$3\omega^2$	3ω
$C_3^{(0,1)}$	3	ω^s	0	0
$C_3^{(0,2)}$	3	ω^{2s}	0	0
$C_3^{(1,p)}$	3	ω^{r+sp}	0	0
$C_3^{(2,p)}$	3	ω^{2r+sp}	0	0

Table 23: Characters of $\Delta(27)$

where e denotes the identity matrix. The conjugacy classes of $\Delta(27)$ are obtained as

$$\begin{array}{rcl}
C_1: & \{e\}, & h=1 \\
C_1^{(1)}: & \{\omega\}, & h=3 \\
C_1^{(2)}: & \{\omega^2\}, & h=3 \\
C_3^{(0,1)}: & \{C,\omega C,\omega^2 C\}, & h=3 \\
C_3^{(0,2)}: & \{C^2,\omega C^2,\omega^2 C^2\}, & h=3 \\
C_3^{(1,0)}: & \{Z,\omega Z,\omega^2 Z\}, & h=3 \\
C_3^{(1,1)}: & \{ZC,\omega ZC,\omega^2 ZC\}, & h=3 \\
C_3^{(1,2)}: & \{ZC^2,\omega ZC^2,\omega^2 ZC^2\}, & h=3 \\
C_3^{(2,0)}: & \{Z^2,\omega Z^2,\omega^2 Z^2\}, & h=3 \\
C_3^{(2,1)}: & \{Z^2C,\omega Z^2C,\omega^2 Z^2C\}, & h=3 \\
C_3^{(2,2)}: & \{Z^2C^2,\omega Z^2C^2,\omega^2 Z^2C^2\}, & h=3
\end{array}$$

The $\Delta(27)$ has nine singlets $\mathbf{1}_{r,s}$ $(r,s=0,1,2)$ and two triplets, $\mathbf{3}$ and $\bar{\mathbf{3}}$. The characters are shown in Table 23.

Tensor products between triplets are obtained as

$$\begin{pmatrix} x_1 \\ x_2 \\ x_3 \end{pmatrix}_{\mathbf{3}} \otimes \begin{pmatrix} y_1 \\ y_2 \\ y_3 \end{pmatrix}_{\mathbf{3}} = \begin{pmatrix} x_1y_1 \\ x_2y_2 \\ x_3y_3 \end{pmatrix}_{\bar{\mathbf{3}}} + \begin{pmatrix} x_1y_2 \\ x_2y_3 \\ x_3y_1 \end{pmatrix}_{\bar{\mathbf{3}}} + \begin{pmatrix} x_1y_3 \\ x_2y_1 \\ x_3y_2 \end{pmatrix}_{\bar{\mathbf{3}}} \tag{429}$$

$$\begin{pmatrix} x_1 \\ x_2 \\ x_3 \end{pmatrix}_{\bar{\mathbf{3}}} \otimes \begin{pmatrix} y_1 \\ y_2 \\ y_3 \end{pmatrix}_{\bar{\mathbf{3}}} = \begin{pmatrix} x_1y_1 \\ x_2y_2 \\ x_3y_3 \end{pmatrix}_{\mathbf{3}} + \begin{pmatrix} x_1y_2 \\ x_2y_3 \\ x_3y_1 \end{pmatrix}_{\mathbf{3}} + \begin{pmatrix} x_1y_3 \\ x_2y_1 \\ x_3y_2 \end{pmatrix}_{\mathbf{3}} \tag{430}$$

$$\begin{pmatrix} x_1 \\ x_2 \\ x_3 \end{pmatrix}_{\mathbf{3}} \otimes \begin{pmatrix} y_1 \\ y_2 \\ y_3 \end{pmatrix}_{\bar{\mathbf{3}}} = \begin{pmatrix} x_1y_1 \\ x_2y_2 \\ x_3y_3 \end{pmatrix}_{\mathbf{3}} + \begin{pmatrix} x_1y_2 \\ x_2y_3 \\ x_3y_1 \end{pmatrix}_{\mathbf{3}} + \begin{pmatrix} x_1y_3 \\ x_2y_1 \\ x_3y_2 \end{pmatrix}_{\mathbf{3}} \tag{431}$$

$$\begin{pmatrix} x_1 \\ x_2 \\ x_3 \end{pmatrix}_{\mathbf{3}} \otimes \begin{pmatrix} y_1 \\ y_2 \\ y_3 \end{pmatrix}_{\bar{\mathbf{3}}} = \sum_r (x_1 y_1 + +\omega^r x_2 y_2 + \omega^{2r} x_3 y_3)_{\mathbf{1}_{(0,r)}} + \sum_r (x_1 y_3 + +\omega^r x_2 y_1 + \omega^{2r} x_3 y_2)_{\mathbf{1}_{(1,r)}} + \sum_r (x_1 y_2 + +\omega^r x_2 y_3 + \omega^{2r} x_3 y_1)_{\mathbf{1}_{(2,r)}} \quad (432)$$

D.3 $\Delta(54)$

The elements g of $\Delta(54)$ are summarized as $g = \omega^t Z^r C^s P^u$, $(r, s, t = 0, 1, 2, u = 0, 1)$. The elements Z and C are same as $\Delta(27)$ and P is defined by

$$P = \begin{pmatrix} 1 & 0 & 0 \\ 0 & 0 & 1 \\ 0 & 1 & 0 \end{pmatrix}. \quad (433)$$

The order of $\Delta(54)$ is 54. These elements satisfy the following algebra as

$$P^2 = e, \quad PC = C^{-1}P, \quad PZ = Z^{-1}P. \quad (434)$$

The conjugacy classes of $\Delta(54)$ are obtained as

$$\begin{array}{rcr}
C_1: & \{e\}, & h=1 \\
C_1^{(1)}: & \{\omega\}, & h=3 \\
C_1^{(2)}: & \{\omega^2\}, & h=3 \\
C_6^{(0,1)+(0,2)}: & \{Z, \omega Z, \omega^2 Z, Z^2, \omega Z^2, \omega^2 Z^2\}, & h=3 \\
C_6^{(1,0)+(2,0)}: & \{C, \omega C, \omega^2 C, C^2, \omega C^2, \omega^2 C^2\}, & h=3 \\
C_6^{(1,2)+(2,1)}: & \{C^2 Z, \omega C^2 Z, \omega^2 C^2 Z, CZ^2, \omega CZ^2, \omega^2 CZ^2\}, & h=3 \\
C_6^{(1,1)+(2,2)}: & \{CZ, \omega CZ, \omega^2 CZ, C^2 Z^2, \omega C^2 Z^2, \omega^2 C^2 Z^2\}, & h=3 \\
C_9^{(1)}: & \{P, ZP, Z^2 P, CP, C^2 P, \omega PCZ, \omega^2 PCZ^2, \omega^2 PC^2 Z, \omega PC^2 Z^2\}, & h=2 \\
C_9^{(2)}: & \{\omega P, \omega ZP, \omega Z^2 P, \omega CP, \omega C^2 P, \omega^2 PCZ, PCZ^2, PC^2 Z, \omega^2 PC^2 Z^2\}, & h=6 \\
C_9^{(3)}: & \{\omega^2 P, \omega^2 ZP, \omega^2 Z^2 P, \omega^2 CP, \omega^2 C^2 P, PCZ, \omega PCZ^2, \omega PC^2 Z, PC^2 Z^2\}, & h=6
\end{array}$$

The $\Delta(54)$ has two singlets $\mathbf{1}_1$, $\mathbf{1}_2$ and four doublets $\mathbf{2}_1$, $\mathbf{2}_2$, $\mathbf{2}_3$, $\mathbf{2}_4$ and four triplets $\mathbf{3}_1$, $\mathbf{3}_2$, $\bar{\mathbf{3}}_1$ and $\bar{\mathbf{3}}_2$. The characters are shown in Table 24.

References

[1] L. J. Dixon, J. A. Harvey, C. Vafa and E. Witten, Nucl. Phys. B **261** , 678 (1985); Nucl. Phys. B **274**, 285 (1986).

	h	χ_{1_1}	χ_{1_2}	χ_{2_1}	χ_{2_2}	χ_{2_3}	χ_{2_4}	χ_{3_1}	$\chi_{\bar{3}_1}$	χ_{3_2}	$\chi_{\bar{3}_2}$
C_1	1	1	1	2	2	2	2	3	3	3	3
$C_1^{(1)}$	3	1	1	2	2	2	2	3ω	$3\omega^2$	3ω	$3\omega^2$
$C_1^{(2)}$	3	1	1	2	2	2	2	$3\omega^2$	3ω	$3\omega^2$	3ω
$C_6^{(0,1)+(0,2)}$	3	1	1	2	-1	-1	-1	0	0	0	0
$C_6^{(1,0)+(2,0)}$	3	1	1	-1	2	-1	-1	0	0	0	0
$C_6^{(1,2)+(2,1)}$	3	1	1	-1	-1	2	-1	0	0	0	0
$C_6^{(1,1)+(2,2)}$	3	1	1	-1	-1	-1	2	0	0	0	0
$C_9^{(1)}$	2	1	-1	0	0	0	0	1	1	-1	-1
$C_9^{(2)}$	6	1	-1	0	0	0	0	ω	ω^2	$-\omega$	$-\omega^2$
$C_9^{(3)}$	6	1	-1	0	0	0	0	ω^2	ω	$-\omega^2$	$-\omega$

Table 24: Characters of $\Delta(54)$

[2] L. E. Ibáñez, H.-P. Nilles and F. Quevedo, Phys. Lett. B **187**, 25 (1987); L. E. Ibáñez, J. E. Kim, H.-P. Nilles and F. Quevedo, Phys. Lett. B **191**, 282 (1987); L. E. Ibáñez, J. Mas, H. P. Nilles and F. Quevedo, Nucl. Phys. B **301**, 157 (1988); A. Font, L. E. Ibáñez, F. Quevedo and A. Sierra, Nucl. Phys. B **331**, 421 (1990); D. Bailin, A. Love and S. Thomas, Phys. Lett. B **194**, 385 (1987); Y. Katsuki, Y. Kawamura, T. Kobayashi, N. Ohtsubo, Y. Ono and K. Tanioka, Nucl. Phys. B **341**, 611 (1990).

[3] T. Kobayashi, S. Raby and R. J. Zhang, Phys. Lett. B **593**, 262 (2004) [arXiv:hep-ph/0403065].

[4] S. Förste, H. P. Nilles, P. K. S. Vaudrevange and A. Wingerter, Phys. Rev. D **70**, 106008 (2004); S. Förste, H. P. Nilles and A. Wingerter, Phys. Rev. D **72**, 026001 (2005) [arXiv:hep-th/0504117]; Phys. Rev. D **73**, 066011 (2006) [arXiv:hep-th/0512270].

[5] W. Buchmüller, K. Hamaguchi, O. Lebedev and M. Ratz, Nucl. Phys. B **712**, 139 (2005) [arXiv:hep-ph/0412318]; K. S. Choi, S. Groot Nibbelink and M. Trapletti, JHEP **0412** (2004) 063 [arXiv:hep-th/0410232]; H. P. Nilles, S. Ramos-Sanchez, P. K. S. Vaudrevange and A. Wingerter, JHEP **0604**, 050 (2006) [arXiv:hep-th/0603086]; J. E. Kim and B. Kyae, arXiv:hep-th/0608085.

[6] T. Kobayashi, S. Raby and R. J. Zhang, Nucl. Phys. B **704**, 3 (2005) [arXiv:hep-ph/0409098].

[7] O. Lebedev, H. P. Nilles, S. Raby, S. Ramos-Sanchez, M. Ratz, P. K. S. Vaudrevange and A. Wingerter, Phys. Lett. B **645**, 88 (2007) [arXiv:hep-th/0611095]; P. K. S. Vaudrevange and A. Wingerter, Phys. Rev. D **77**, 046013 (2008) [arXiv:0708.2691 [hep-th]].

[8] J. E. Kim and B. Kyae, arXiv:hep-th/0608086.

[9] W. Buchmuller, K. Hamaguchi, O. Lebedev and M. Ratz, Phys. Rev. Lett. **96**, 121602 (2006) [arXiv:hep-ph/0511035]; arXiv:hep-th/0606187.

[10] S. Hamidi and C. Vafa, Nucl. Phys. B **279**, 465 (1987); L. J. Dixon, D. Friedan, E. J. Martinec and S. H. Shenker, Nucl. Phys. B **282**, 13 (1987).

[11] T. T. Burwick, R. K. Kaiser and H. F. Müller, Nucl. Phys. B **355**, 689 (1991); J. Erler, D. Jungnickel, M. Spalinski and S. Stieberger, Nucl. Phys. B **397**, 379 (1993).

[12] T. Kobayashi and O. Lebedev, Phys. Lett. B **566**, 164 (2003).

[13] T. Kobayashi and O. Lebedev, Phys. Lett. B **565**, 193 (2003).

[14] P. Ko, T. Kobayashi and J. h. Park, Phys. Lett. B **598**, 263 (2004); Phys. Rev. D **71**, 095010 (2005) [arXiv:hep-ph/0503029].

[15] H. Kawai, D. C. Lewellen and S. H. H. Tye, Phys. Rev. Lett. **57** (1986) 1832 [Erratum-ibid. **58** (1987) 429], Nucl. Phys. B **288** (1987) 1; I. Antoniadis, C. P. Bachas and C. Kounnas, Nucl. Phys. B **289** (1987) 87; I. Antoniadis, J. R. Ellis, J. S. Hagelin and D. V. Nanopoulos, Phys. Lett. B **231** (1989) 65.

[16] A. E. Faraggi, Phys. Lett. B **278**, 131 (1992), A. E. Faraggi, C. Kounnas, S. E. M. Nooij and J. Rizos, Nucl. Phys. B **695**, 41 (2004) [arXiv:hep-th/0403058]; A. E. Faraggi, C. Kounnas and J. Rizos, orbifold arXiv:hep-th/0606144; A. E. Faraggi, E. Manno and C. Timirgaziu, arXiv:hep-th/0610118.

[17] A. E. Faraggi, Phys. Lett. B **326** (1994) 62 [arXiv:hep-ph/9311312], Phys. Lett. B **544** (2002) 207 [arXiv:hep-th/0206165]; P. Berglund, J. R. Ellis, A. E. Faraggi, D. V. Nanopoulos and Z. Qiu, Phys. Lett. B **433** (1998) 269 [arXiv:hep-th/9803262].

[18] J. Polchinski, Phys. Rev. Lett. **75** (1995) 4724 [arXiv:hep-th/9510017].

[19] M. Berkooz, M. R. Douglas and R. G. Leigh, Nucl. Phys. B **480**, 265 (1996) [arXiv:hep-th/9606139].

[20] R. Blumenhagen, L. Goerlich, B. Kors and D. Lust, JHEP **0010**, 006 (2000) [arXiv:hep-th/0007024].

[21] C. Angelantonj, I. Antoniadis, E. Dudas and A. Sagnotti, Phys. Lett. B **489**, 223 (2000) [arXiv:hep-th/0007090].

[22] R. Blumenhagen, M. Cvetic, P. Langacker and G. Shiu, Ann. Rev. Nucl. Part. Sci. **55**, 71 (2005) [arXiv:hep-th/0502005]; R. Blumenhagen, B. Kors, D. Lust and S. Stieberger, Phys. Rept. **445**, 1 (2007) [arXiv:hep-th/0610327].

[23] G. Aldazabal, S. Franco, L. E. Ibanez, R. Rabadan and A. M. Uranga, J. Math. Phys. **42**, 3103 (2001) [arXiv:hep-th/0011073]; JHEP **0102**, 047 (2001) [arXiv:hep-ph/0011132].

[24] R. Blumenhagen, B. Kors and D. Lust, JHEP **0102**, 030 (2001) [arXiv:hep-th/0012156].

[25] M. Cvetic, G. Shiu and A. M. Uranga, intersecting brane Phys. Rev. Lett. **87**, 201801 (2001) [arXiv:hep-th/0107143]; Nucl. Phys. B **615**, 3 (2001) [arXiv:hep-th/0107166].

[26] D. Cremades, L. E. Ibanez and F. Marchesano, JHEP **0307** (2003) 038 [arXiv:hep-th/0302105].

[27] C. D. Froggatt and H. B. Nielsen, Nucl. Phys. B **147** (1979) 277.

[28] T. Kobayashi, H. P. Nilles, F. Plöger, S. Raby and M. Ratz, arXiv:hep-ph/0611020.

[29] G. Altarelli, F. Feruglio and Y. Lin, Nucl. Phys. B **775**, 31 (2007) [arXiv:hep-ph/0610165].

[30] J. P. Conlon, A. Maharana and F. Quevedo, JHEP **0809**, 104 (2008) [arXiv:0807.0789 [hep-th]].

[31] F. Marchesano, P. McGuirk and G. Shiu, JHEP **0904** (2009) 095 [arXiv:0812.2247 [hep-th]].

[32] P. G. Camara and F. Marchesano, arXiv:0906.3033 [hep-th].

[33] R. Donagi and M. Wijnholt, arXiv:0802.2969 [hep-th]; R. Donagi and M. Wijnholt, arXiv:0808.2223 [hep-th].

[34] C. Beasley, J. J. Heckman and C. Vafa, JHEP **0901**, 058 (2009) [arXiv:0802.3391 [hep-th]]; JHEP **0901**, 059 (2009) [arXiv:0806.0102 [hep-th]].

[35] G. Curio, A. Klemm, D. Lust and S. Theisen, Nucl. Phys. B **609**, 3 (2001) [arXiv:hep-th/0012213].

[36] S. Kachru, M. B. Schulz and S. Trivedi, JHEP **0310**, 007 (2003) [arXiv:hep-th/0201028].

[37] S. Kachru, R. Kallosh, A. D. Linde and S. P. Trivedi, Phys. Rev. D **68**, 046005 (2003) [arXiv:hep-th/0301240].

[38] See, e.g. ,
G. Altarelli, arXiv:0705.0860 [hep-ph]; E. Ma, arXiv:0705.0327 [hep-ph] and references therein.

[39] D. B. Kaplan and M. Schmaltz, Phys. Rev. D **49**, 3741 (1994); L.J. Hall and H. Murayama, Phys. Rev. Lett. **75**, 3985 (1995) ; C.D. Carone, L.J. Hall and H. Murayama, Phys. Rev. D **53**, 6282 (1996).

[40] K.S. Babu, T. Kobayashi and J. Kubo, Phys. Rev. D **67**, 075018 (2003); K. Hamaguchi, M. Kakizaki and M. Yamaguchi, Phys. Rev. D **68**, 056007 (2003); T. Kobayashi, J. Kubo and H. Terao, Phys. Lett. B **568**, 83 (2003); G. G. Ross, L. Velasco-Sevilla and Oscar Vives, Nucl. Phys. B **692**, 50 (2004); S. F. King and G. G. Ross, Phys. Lett. B **520**, 243 (2001); B**574,** 239 (2003); G. G. Ross and L. Velasco-Sevilla, Nucl. Phys. B **653**, 3 (2003); Ki-Y. Choi, Y. Kajiyama, J. Kubo and H.M. Lee, Phys. Rev. D **70**, 055004 (2004); N. Maekawa and T. Yamashita, JHEP **0407,** 009 (2004); K.S. Babu and J. Kubo, Phys. Rev. D **71**, 056006 (2005); T. Yamashita, hep-ph/0503265; I. de Medeiros Varzielas and G.G. Ross, hep-ph/0612220; P. Ko, T. Kobayashi, J. h. Park and S. Raby, arXiv:0704.2807 [hep-ph].

[41] L. E. Ibanez and G. G. Ross, Nucl. Phys. B **368**, 3 (1992); S. P. Martin, Phys. Rev. D **46**, 2769 (1992); H. Murayama and D.B. Kaplan, Phys. Lett. B **336**, 221 (1994); V. Ben-Hamo and Y. Nir, Phys. Lett. B **339**, 77 (1994); C.D. Carone, L.J. Hall and H. Murayama, Phys. Rev. D **53**, 6282 (1996).

[42] M. Kakizaki and M. Yamaguchi, JHEP **0206,** 032 (2002); R. Harnik, D.T. Larson, H. Murayama and M. Thormeier, Nucl. Phys. B **706**, 372 (2005); E. Itou, Y. Kajiyama and J. Kubo, Nucl. Phys. B **743**, 74 (2006).

[43] M. B. Green and J. H. Schwarz, Phys. Lett. B **149**, 117 (1984).

[44] E. Witten, Phys. Lett. B **149**, 351 (1984); M. Dine, N. Seiberg and E. Witten, Nucl. Phys. B **289**, 589 (1987); W. Lerche, B. E. W. Nilsson and A. N. Schellekens, Nucl. Phys. B **289**, 609 (1987); J. J. Atick, L. J. Dixon and A. Sen, Nucl. Phys. B **292**, 109 (1987); M. Dine, I. Ichinose and N. Seiberg, Nucl. Phys. B **293**, 253 (1987).

[45] L. E. Ibanez, R. Rabadan and A. M. Uranga, Nucl. Phys. B **542**, 112 (1999); Z. Lalak, S. Lavignac and H. P. Nilles, Nucl. Phys. B **559**, 48 (1999).

[46] A. N. Schellekens and N. P. Warner, Nucl. Phys. B **287**, 317 (1987).

[47] T. Kobayashi and H. Nakano, Nucl. Phys. B **496**, 103 (1997).

[48] J. P. Derendinger, S. Ferrara, C. Kounnas and F. Zwirner, Nucl. Phys. B **372**, 145 (1992).

[49] L. E. Ibanez and D. Lüst, Nucl. Phys. B **382**, 305 (1992).

[50] L. E. Ibanez, D. Lüst and G. G. Ross, Phys. Lett. B **272**, 251 (1991).

[51] H. Kawabe, T. Kobayashi and N. Ohtsubo, Phys. Lett. B **325**, 77 (1994); Nucl. Phys. B **434**, 210 (1995).

[52] D. Cremades, L. E. Ibanez and F. Marchesano, JHEP **0405**, 079 (2004) [arXiv:hep-th/0404229].

[53] H. Abe, K. S. Choi, T. Kobayashi and H. Ohki, arXiv:0907.5274 [hep-th].

[54] H. Abe, K. S. Choi, T. Kobayashi and H. Ohki, arXiv:1001.1788 [hep-th].

[55] K. S. Choi, T. Kobayashi, R. Maruyama, M. Murata, Y. Nakai, H. Ohki and M. Sakai, arXiv:0908.0395 [hep-ph].

[56] H. Abe, K. S. Choi, T. Kobayashi and H. Ohki, arXiv:0903.3800 [hep-th].

[57] H. Abe, K. S. Choi, T. Kobayashi and H. Ohki, arXiv:0904.2631 [hep-ph].

[58] H. Abe, T. Kobayashi and H. Ohki, JHEP **0809**, 043 (2008) [arXiv:0806.4748 [hep-th]].

[59] H. Abe, K. S. Choi, T. Kobayashi and H. Ohki, Nucl. Phys. B **814**, 265 (2009) [arXiv:0812.3534 [hep-th]].

[60] N. S. Manton, Nucl. Phys. B **193**, 502 (1981); G. Chapline and R. Slansky, Nucl. Phys. B **209**, 461 (1982); S. Randjbar-Daemi, A. Salam and J. A. Strathdee, Nucl. Phys. B **214**, 491 (1983); C. Wetterich, Nucl. Phys. B **222**, 20 (1983); P. H. Frampton and K. Yamamoto, Phys. Rev. Lett. **52**, 2016 (1984); P. H. Frampton and T. W. Kephart, Phys. Rev. Lett. **53**, 867 (1984); K. Pilch and A. N. Schellekens, Nucl. Phys. B **256**, 109 (1985).

[61] C. Bachas, arXiv:hep-th/9503030.

[62] J. Troost, Nucl. Phys. B **568**, 180 (2000) [arXiv:hep-th/9909187].

[63] G. 't Hooft, Nucl. Phys. B **153**, 141 (1979).

[64] J. Alfaro, A. Broncano, M. B. Gavela, S. Rigolin and M. Salvatori, JHEP **0701**, 005 (2007) [arXiv:hep-ph/0606070]; D. Hernandez, S. Rigolin and M. Salvatori, arXiv:0712.1980 [hep-ph].

[65] G. von Gersdorff, Nucl. Phys. B **793**, 192 (2008) [arXiv:0705.2410 [hep-th]].

[66] G. 't Hooft, Commun. Math. Phys. **81** (1981) 267; P. van Baal, Commun. Math. Phys. **94** (1984) 397; Z. Guralnik and S. Ramgoolam, Nucl. Phys. B **521**, 129 (1998) [arXiv:hep-th/9708089].

[67] A. Font and L. E. Ibanez, JHEP **0902**, 016 (2009) [arXiv:0811.2157 [hep-th]]; arXiv:0907.4895 [hep-th].

[68] J. L. Bourjaily, arXiv:0901.3785 [hep-th]; arXiv:0905.0142 [hep-th].

[69] H. Hayashi, T. Kawano, R. Tatar and T. Watari, arXiv:0901.4941 [hep-th].

[70] J. Marsano, N. Saulina and S. Schafer-Nameki, arXiv:0904.3932 [hep-th]; arXiv:0906.4672 [hep-th].

[71] R. Blumenhagen, T. W. Grimm, B. Jurke and T. Weigand, arXiv:0906.0013 [hep-th].

[72] G. F. Chapline and N. S. Manton, Phys. Lett. B **120** (1983) 105; A. H. Chamseddine, Nucl. Phys. B **185** (1981) 403.

[73] D. Mumford, "Tata Lectures on Theta, vol I, II, III," In Progress in Mathematics, Vol. 28 (1983) Birkhauser.

[74] P. Di Vecchia, A. Liccardo, R. Marotta and F. Pezzella, arXiv:0810.5509 [hep-th].

[75] T. Higaki, N. Kitazawa, T. Kobayashi and K. j. Takahashi, Phys. Rev. D **72**, 086003 (2005) [arXiv:hep-th/0504019].

[76] M. A. Virasoro, Phys. Rev. **177** (1969) 2309; J. A. Shapiro, Phys. Rev. **179** (1969) 1345; G. Veneziano, Nucl. Phys. B **74** (1974) 365.

[77] P. Koerber and A. Sevrin, JHEP **0210** (2002) 046 [arXiv:hep-th/0208044].

[78] J. Polchinski, "String Theory," vol. 1, Cambridge Univ. Press (1998).

[79] J. J. Atick, L. J. Dixon, P. A. Griffin and D. Nemeschansky, Nucl. Phys. B **298** (1988) 1.

[80] S. A. Abel and A. W. Owen, Nucl. Phys. B **682** (2004) 183 [arXiv:hep-th/0310257].

[81] K. S. Choi and T. Kobayashi, Nucl. Phys. B **797** (2008) 295 [arXiv:0711.4894 [hep-th]].

[82] M. Cvetic and I. Papadimitriou, Phys. Rev. D **68** (2003) 046001 [Erratum-ibid. D **70** (2004) 029903] [arXiv:hep-th/0303083]; S. A. Abel and A. W. Owen, Nucl. Phys. B **663** (2003) 197 [arXiv:hep-th/0303124]; V. Braun, Y. H. He and B. A. Ovrut, JHEP **0604** (2006) 019 [arXiv:hep-th/0601204]; C. M. Chen, T. Li, V. E. Mayes and D. V. Nanopoulos, Phys. Rev. D **78**, 105015 (2008) [arXiv:0807.4216 [hep-th]].

[83] T. T. Burwick, R. K. Kaiser and H. F. Muller, Nucl. Phys. B **355** (1991) 689;

[84] S. Stieberger, D. Jungnickel, J. Lauer and M. Spalinski, Mod. Phys. Lett. A **7**, 3059 (1992) [arXiv:hep-th/9204037].

[85] A. Brignole, L. E. Ibanez and C. Munoz, arXiv:hep-ph/9707209.

[86] M. Bianchi and E. Trevigne, JHEP **0508** (2005) 034 [arXiv:hep-th/0502147].

[87] I. Antoniadis and T. Maillard, Nucl. Phys. B **716** (2005) 3 [arXiv:hep-th/0412008].

[88] G. C. Branco, J. M. Gerard and W. Grimus, Phys. Lett. B **136**, 383 (1984); C. Luhn, S. Nasri and P. Ramond, J. Math. Phys. **48**, 073501 (2007) [arXiv:hep-th/0701188]; I. de Medeiros Varzielas, S. F. King and G. G. Ross, Phys. Lett. B **648**, 201 (2007) [arXiv:hep-ph/0607045]; E. Ma, Mod. Phys. Lett. A **21**, 1917 (2006) [arXiv:hep-ph/0607056]; Phys. Lett. B **660**, 505 (2008) [arXiv:0709.0507 [hep-ph]].

[89] W. Grimus and L. Lavoura, Phys. Lett. B **572**, 189 (2003); W. Grimus, A. S. Joshipura, S. Kaneko, L. Lavoura and M. Tanimoto, JHEP **0407**, 078 (2004); A. Blum, R. N. Mohapatra and W. Rodejohann, Phys. Rev. D **76**, 053003 (2007); A. Blum, C. Hagedorn and M. Lindner, Phys. Rev. D **77**, 076004 (2008) [arXiv:0709.3450 [hep-ph]]; W. Grimus, A. S. Joshipura, S. Kaneko, L. Lavoura, H. Sawanaka and M. Tanimoto, Nucl. Phys. B **713**, 151 (2005). H. Ishimori, T. Kobayashi, H. Ohki, Y. Omura, R. Takahashi and M. Tanimoto, Phys. Lett. B **662**, 178 (2008) [arXiv:0802.2310 [hep-ph]]; H. Ishimori, T. Kobayashi, H. Ohki, Y. Omura, R. Takahashi and M. Tanimoto, Phys. Rev. D **77**, 115005 (2008) [arXiv:0803.0796 [hep-ph]]; A. Adulpravitchai, A. Blum and C. Hagedorn, JHEP **0903**, 046 (2009) [arXiv:0812.3799 [hep-ph]].

[90] H. Ishimori, T. Kobayashi, H. Okada, Y. Shimizu and M. Tanimoto, arXiv:0811.4683 [hep-ph]; H. Ishimori, T. Kobayashi, H. Okada, Y. Shimizu and M. Tanimoto, JHEP **0912** (2009) 054 [arXiv:0907.2006 [hep-ph]]; J. A. Escobar and C. Luhn, J. Math. Phys. **50**, 013524 (2009) [arXiv:0809.0639 [hep-th]].

[91] H. Ishimori, T. Kobayashi, H. Ohki, H. Okada, Y. Shimizu and M. Tanimoto, arXiv:1003.3552 [hep-th].

[92] R. Blumenhagen, M. Cvetic, F. Marchesano and G. Shiu, JHEP **0503**, 050 (2005) [arXiv:hep-th/0502095].

[93] N. Haba, A. Watanabe and K. Yoshioka, Phys. Rev. Lett. **97**, 041601 (2006) [arXiv:hep-ph/0603116].

[94] T. Kobayashi, Y. Omura and K. Yoshioka, Phys. Rev. D **78**, 115006 (2008) [arXiv:0809.3064 [hep-ph]].

[95] G. Seidl, arXiv:0811.3775 [hep-ph].

[96] R. Blumenhagen, L. Gorlich and T. Ott, JHEP **0301**, 021 (2003) [arXiv:hep-th/0211059]; M. Cvetic and I. Papadimitriou, Phys. Rev. D **67**, 126006 (2003) [arXiv:hep-th/0303197]; M. Cvetic, T. Li and T. Liu, Nucl. Phys. B **698**, 163 (2004) [arXiv:hep-th/0403061].

[97] M. B. Green, J. H. Schwarz and E. Witten, "Superstring Theory. Vol. 2: Loop Amplitudes, Anomalies And Phenomenology," *Cambridge, Uk: Univ. Pr. (1987) 596 P. (Cambridge Monographs On Mathematical Physics)*

[98] L. E. Ibanez, H. P. Nilles and F. Quevedo, Phys. Lett. B **192**, 332 (1987).

[99] K. Fujikawa, Phys. Rev. Lett. **42** (1979), 1195.

[100] K. Fujikawa, Phys. Rev. **D21** (1980), 2848.

[101] L. Alvarez-Gaume and E. Witten, Nucl. Phys. **B234** (1984), 269.

[102] L. Alvarez-Gaume and P. H. Ginsparg, Ann. Phys. **161** (1985), 423.

[103] K. Fujikawa, S. Ojima, and S. Yajima, Phys. Rev. **D34** (1986), 3223.

[104] V. Rohlin, Dokl. Akad. Nauk. **128** (1959), 980 –983.

[105] C. Csaki and H. Murayama, Nucl. Phys. **B515** (1998), 114–162, [hep-th/9710105].

[106] L. E. Ibanez and G. G. Ross, Phys. Lett. B **260** (1991) 291; T. Banks and M. Dine, Phys. Rev. D **45**, 1424 (1992); L. E. Ibanez, Nucl. Phys. B **398**, 301 (1993); K. Kurosawa, N. Maru and T. Yanagida, Phys. Lett. B**512**, 203 (2001); J. Kubo and D. Suematsu, Phys. Rev. D**64**, 115014 (2001); K. S. Babu, I. Gogoladze and K. Wang, Nucl. Phys. B**660**, 332 (2003); M. Dine and M. Graesser, JHEP **0501**, 038 (2005); T. Araki, arXiv:hep-ph/0612306; H. Dreiner and M. Thormeier, Phys. Rev. D**69**, 053002 (2004); H. Dreiner, H. Murayama and M. Thormeier, Nucl. Phys. B**729**, 278 (2005); A. H. Chamseddine and H. K. Dreiner, Nucl. Phys. B **458**, 65 (1996); H. K. Dreiner, C. Luhn and M. Thormeier, Phys. Rev. D **73**, 075007 (2006); H. K. Dreiner, C. Luhn, H. Murayama and M. Thormeier, arXiv:hep-ph/0610026.

[107] D. Friedan, E. J. Martinec and S. H. Shenker, Nucl. Phys. B **271**, 93 (1986).

[108] A. Font, L. E. Ibáñez and F. Quevedo, Phys. Lett. B **217** (1989) 272.

[109] A. E. Faraggi, S. Forste and C. Timirgaziu, JHEP **0608**, 057 (2006).

[110] Y. Katsuki, Y. Kawamura, T. Kobayashi, N. Ohtsubo, Y. Ono and K. Tanioka, DPKU-8904.

[111] T. Araki, T. Kobayashi, J. Kubo, S. Ramos-Sanchez, M. Ratz and P. K. S. Vaudrevange, Nucl. Phys. B **805**, 124 (2008) [arXiv:0805.0207 [hep-th]].

[112] D.R.T Jones and L. Mezincescu, Phys. Lett. B **136**, 242 (1984); B **138**, 293 (1984); P. West, Phys. Lett. B **137**, 371 (1984); A.J. Parkes and P.C West, Phys. Lett. B **138**, 99 (1984); Nucl. Phys. B **256**, 340 (1985); A.J. Parkes, Phys. Lett. B **156**, 73 (1985); D.R.T Jones and A.J. Parkes, Phys. Lett. B **160**, 267 (1985).

[113] O. Piguet and K. Sibold, Int. Mod. Phys. A **1**, 913 (1986); Phys. Lett. B **177**, 373 (1986).

[114] S. Ferrara and B. Zumino, Nucl. Phys. B **87**, 207 (1975).

[115] O. Piguet and K. Sibold, Nucl. Phys. B **196**, 428 (1982); B **196**, 447 (1982).

[116] L. E. Ibanez and D. Lüst, Phys. Lett. B **302**, 38 (1993).

[117] L. J. Dixon, V. Kaplunovsky and J. Louis, Nucl. Phys. B **355**, 649 (1991);

[118] T. Kobayashi and N. Ohtsubo, Int. J. Mod. Phys. A **9**, 87 (1994).

[119] T. Araki, K. S. Choi, T. Kobayashi, J. Kubo and H. Ohki, Phys. Rev. D **76**, 066006 (2007) [arXiv:0705.3075 [hep-ph]].